UNIVERSITAT DE BARCELONA

Arming Oncolytic Adenoviruses with Transgenes to Engage Stroma Toxicity and Immune Stimulation as a Double Strategy Against Cancer

Marcel Arias Badia

UNIVERSITAT DE BARCELONA

FACULTAT DE FARMÀCIA I CIÈNCIES DE L'ALIMENTACIÓ

PROGRAMA DE DOCTORAT EN BIOMEDICINA

ARMING ONCOLYTIC ADENOVIRUSES WITH TRANSGENES TO ENGAGE STROMA TOXICITY AND IMMUNE STIMULATION AS A DOUBLE STRATEGY AGAINST CANCER

MARCEL ARIAS BADIA

JUNY 2017

UNIVERSITAT DE BARCELONA

FACULTAT DE FARMÀCIA I CIÈNCIES DE L'ALIMENTACIÓ

PROGRAMA DE DOCTORAT EN BIOMEDICINA

ARMING ONCOLYTIC ADENOVIRUSES WITH TRANSGENES TO ENGAGE STROMA TOXICITY AND IMMUNE STIMULATION AS A DOUBLE STRATEGY AGAINST CANCER

MARCEL ARIAS BADIA

2017

Memòria presentada per Marcel Arias Badia per optar al grau de Doctor per la Universitat de Barcelona

Dr. Ramon Alemany Bonastre	Dr. Francesc Viñals Canals	Marcel Arias Badia
Director	Tutor	Autor

Table of contents

List of abbreviations

%	Percentage
°C	Centigrade degrees
Δ24	*delta*24 mutation, deletion of 24 bp in E1A protein
µF	microfarad
µg	microgram
µL	microliter
µm	micrometer
Ω	Ohm
AAALAC	Association for Assessment and Accreditation of Laboratory Animal Care
ACK	Ammonium-chloride-potassium
Ad	Adenovirus
ADCC	Antibody-dependent cell-mediated cytotoxicity
ADP	Adenovirus Death Protein
AFP	Alpha-Fetoprotein Promoter
ALL	Acute Lymphocytic Leukemia
ANOVA	Analysis of Variance
APC	Antigen-Presenting Cell
APC	Allophycocyanin
APS	Ammonium persulfate
ATCC	American Type Cell Culture
Atox	Alpha-toxin from *Clostridium septicum*
BAC	Bacterial Artificial Chromosome
Bak	Bcl-2 homologous antagonist/killer
Bax	Bcl-2-associated X protein
BCA	Bicinchoninic Acid Assay
bp	base pairs
BPSA	Branch-point Splicing Acceptor
BSA	Bovine Serum Albumin
$CaCl_2$	Calcium chloride
CAF	Cancer-Associated Fibroblast
CAR	Coxsackievirus B and Adenovirus Receptor or Chimeric Antigen Receptor
CCE	Clarified Cell Extract
CD	Cytosine Deaminase
CD200	Cluster of differentiation 200
cDNA	complementary DNA
CE	Cell Extract
CFSE	Carboxyfluorescein diacetate succinimidyl ester
Cm	Chloramphenicol
cm	centimeter
CMV	Cytomegalovirus
CO_2	Carbon dioxide
CPE	Cytopathic effect
CRAd	Conditionally Replicative Adenovirus
CsCl	Cesium chloride
CTL	Cytotoxic T Lymphocyte
CTLA-4	Cytotoxic T-Lymphocyte-Associated Protein 4
DAB	3,3'-Diaminobenzidine

DAMP	Damage-Associated Molecular Pattern
DAPI	4',6-Diamidino-2-phenylindole dihydrochloride
DC	Dendritic cell
ddH_2O	bi-distilled water
ddDNTP	2',3' dideoxynucleotides
DMEM	Dulbecco's Modified Eagle's Medium
DMSO	Dimethyl sulfoxide
DNA	Deoxyribonucleic Acid
dNTP	Nucleoside triphosphate
DTT	Dithiothreitol
ECM	Extracellular Matrix
EDTA	Ethylenediaminetetraacetic acid
ELISA	Enzyme-Linked Immunosorbent Assay
ELISPot	Enzyme-Linked Immunospot Assay
ER	Endoplasmic Reticulum
FACS	Fluorescence Activated Cell Sorting
FAP	Fibroblast Activation Protein
FBS	Fetal Bovine Serum
FDA	Food and Drug Administration
FITC	Fluorescein isothiocyanate
FLAER	Fluorescently-labelled Aerolysin
G	Gauge
g	acceleration of gravity
g	gram
GALV	Gibbon Ape Leukaemia Virus
GM-CSF	Granulocyte Macrophage-Colony Stimulating Factor
GPI	Glycosylphosphatidylinositol
h	hour
H_2O_2	Hydrogen peroxide
HA	Hyaluronic acid or Hemagglutinin
HCl	Chloridric acid
HEPES	4-(2-hydroxyethyl)-1-piperazineethanesulfonic acid
HHV-8	Human Herpesvirus 8
HLA	Human Leukocyte Antigen
HRP	Horseradish peroxidase
HSG	Heparan-Sulphate-Glycosaminoglicans
HSP	Heat Shock Protein
HSV	Herpes Simplex Virus
IC_{50}	Inhibitory Concentration 50
IDO	Indoleamine 2,3-dioxigenase
IFN	Interferon
Ig	Immunoglobulin
IHC	Immunohistochemistry
IL	Interleukin
IT	Intratumoral
IV	Intravenous
Kan	Kanamycin
Kb	kilobase pair
KC	Kupffer Cell
KSHV	Kaposi Sarcoma Herpesvirus
L	Litre

LMP	Low Molecular Weight Protein
mA	milliampere
MCA	Methylcholanthrene
MDSC	Myeloid-derived Suppressor Cell
Mets	Metastasis
MFI	Mean Fluorescence Intensity
mg	milligram
MHC	Major Histocompatibility Complex
Min	minute
MIP	Macrophage Inflammatory Protein
mL	Milliliter
MLC	Mixed Leukocyte Culture
MLP	Major Late Promoter
MLR	Mixed Leukocyte Reaction
MLU	Major Late transcription Unit
mm	millimeter
mm^3	cubic millimeter
mM	millimolar
MM	Multiple Myeloma
MMP	Matrix Metalloprotease
MOI	Multiplicity of Infection
mRNA	Messenger Ribonucleic Acid
MTT	3-(4,5-Dimethylthiazol-2-yl)-2,5-Diphenyltetrazolium Bromide
NAbs	Neutralizing antibodies
NaCl	Sodium chloride
NaH_2PO_4	Monosodium phosphate
NaOH	Sodium hydroxide
$Na_2S_2O_3$	Sodium thiosulfate
NDV	Newcastle Disease Virus
NF-κβ	Nuclear factor Kappa-light-chain-enhancer of activated B cells
ng	nanogram
NK	Natural Killer
nm	nanometer
NPC	Nuclear Pore Complex
NSCLC	Non-Small Cell Lung Carcinoma
OCT	Optimum Cutting Temperature compound
OD	Optical Density
PAMP	Pathogen-Associated Molecular Pattern
PAGE	Polyacrylamide Gel Electrophoresis
PBS	Phosphate Buffered Saline
PBMC	Peripheral Blood Mononuclear Cell
PCR	Polymerase Chain Reaction
PD-1	Death Protein-1
PD-L1	Death Protein Ligand-1
PE	R-phycoerythrin
PFT	Pore-forming toxin
p.i.	Post-infection or post-injection
pg	picogram
pmol	picomol
PRR	Pattern Recognition Receptor

PS	Penicillin-Streptomycin
PSA	Prostate-Specific Antigen
qPCR	Quantitative PCR
Rb	Retinoblastoma
RGD	Arginine-glycine-aspartic acid
RID	Receptor Internalization and Degradation
RIG-I	Retinoic acid-inducible Gene I
RITR	Right Inverted Terminal Repeats
RNA	Ribonucleic Acid
rpm	revolutions per minute
RPMI	Roswell Park Memorial Institute
RT	Radiation Therapy or Room Temperature
RT-PCR	Real-Time PCR
SD	Standard Deviation
SDS	Sodium dodecyl sulfate
SEM	Standard Error of the Mean
SPARC	Secreted Protein Acidic and Rich in Cysteine
Strep	Streptomycin
TAA	Tumor-Associated Antigen
TAE	Tris-Acetate-EDTA
TBS	Tris-Buffered Saline
TAP	Transporter Associated to Antigen Processing
TCR	T Cell Receptor
TE	Tris-EDTA
TEMED	Tetramethylethylenediamine
TERT	Telomerase Reverse Transcriptase
TGF-β	Transforming Growth Factor-β
TIL	Tumor-Infiltrating Lymphocyte
TK	Thymidine Kinase
TLP	Tripartite Leader Peptide
TNF	Tumor Necrosis Factor
TLR	Toll-Like Receptor
TP	Terminal Protein
TRAIL	TNF-related apoptosis-inducing ligand
T_{reg}	Regulatory T cell
Tris	Tris(hydroxymethyl)aminomethane
TU	Transducing Unit
V	Volt
V	Volume
VA	Virus-Associated
VEGF	Vascular Endothelial Growth Factor
vp	viral particle
VSV	Vesicular Stomatitis Virus
WHO	World Health Organization

Amino acids

F Phe, phenylalanine	**S** Ser, serine	**Y** Tyr, tyrosine	**K** Lys, lysine	**W** Trp tryptophan
L Leu, leucine	**P** Pro, proline	**H** his, histidine	**D** Asp, aspartic acid	**R** Arg, arginine
I Ile, isoleucine	**T** Thr, threonine	**Q** Gln, glutamine	**E** Glu, glutamic acid	**G** Gly, glycine
M Met, methionine	**A** Ala, alanine	**N** Asn, asparragina	**C** Cys, cysteine	**V** Val, valine

Nucleotides

A adenine	T thymine	**G** guanine	**C** cytosine	**U** uracil

List of figures

List of tables

Resum

La viroteràpia amb Adenovirus oncolítics ha recuperat una embranzida que havia perdut fa anys amb l'aparició de noves estratègies per atacar els tumors. Entre les limitacions més importants que troba aquest tipus de teràpia es troben la immunosupressió induïda en el microambient tumoral, que evita la generació d'una resposta immune antitumoral, i la presència de barreres estromals, que dificulten la dispersió del virus dins el tumor i que conté fibroblasts, cèl·lules molt resistents a la replicació viral.

En aquesta tesi s'han adreçat aquests dos problemes en dos capítols diferents. En primer lloc, amb l'objectiu de trobar una manera d'activar les cèl·lules del sistema immune, es va generar una bateria de virus expressant versions solubles de la proteïna humana CD200, un ligand immunoinhibidor; CD200tr, una versió truncada en un domini N-terminal de la primera que té una funció antagonista amb el seu receptor; K14, una proteïna del HHV-8 amb estructura i funció homòlogues a CD200; i K14tr, una versió truncada de K14 que es va testar com a possible antagonista alternatiu a CD200R, el receptor de CD200. En el desenvolupament d'aquest projecte, es va validar la viabilitat d'aquests virus, es va detectar transgen en sobrenedants de cultius infectats, es va confirmar el paper inhibidor de CD200 i K14 i l'antagonista de CD200tr, però no es van trobar indicis que K14tr pogués actuar de la mateixa manera.

Quant a al segon projecte, es van generar virus oncolítics expressant toxines bacterianes modificades per activar-se tan sols en presència de proteases específiques de l'estroma tumoral, amb l'objectiu d'induir una mort cel·lular indiscriminada un cop activades al teixit diana. Les toxines escollides van ser l'Alpha-toxin de *Clostridium septicum* i l'aerolisina d'*Aeromonas hydrophyla*. Durant el desenvolupament del projecte es van generar i caracteritzar satisfactòriament tots els virus, es va detectar transgen en sobrenedants de cultius infectats, es va confirmar l'activitat citotòxica d'aquestes toxines en cèl·lules que expressaven les proteases a les quals havien estat dirigides, i es van fer estudis in vivo per avaluar l'eficàcia antitumoral, la toxicitat i l'efecte en l'estructura de l'estroma de les esmentades toxines. Mentre que l'Alpha-toxin no va generar resultats prometedors, els resultats obtinguts amb el virus expressant aerolisina obren la porta a considerar-lo com a un candidat clínic en tumors amb alt contingut estromal i a seguir aquesta línia de recerca.

Abstract

Oncolytic virotherapy with Adenoviruses has regained importance in the past years with the appearance of fresh and promising strategies to deal with tumors. Among the major limitations of this therapy are the immune suppression induced in the tumor microenvironment, which prevents the generation of an antitumor immune response, and the presence of stromal barriers which hinder the viral spread and also contain fibroblasts, cells which are highly resistant to viral replication.

In this thesis, both limitations have been addressed in separate chapters. Firstly, aiming to induce immune activation, a panel of viruses expressing, CD200, an immune checkpoint, CD200tr, an N-terminal truncated version of the former with antagonistic effect on its receptor (CD200R), K14, a CD200 homolog from HHV-8, and K14tr, a truncated version of K14 and hence a putative antagonist to CD200R, was generated. Throughout the development of this project, we validated the viability of these viruses, we detected the transgenes in supernatants from infected cultures, we confirmed the inhibitory role of CD200 and K14 and the antagonistic one for CD200tr, but our data did not suggest a similar function for K14tr.

As for the second project, we generated oncolytic Adenoviruses expressing bacteria-derived toxins modified in such a way they become activated only stroma-specific proteases, aiming to induce indiscriminate cell death once activated at the target tissue. Alpha-toxin from *Clostridium septicum* and aerolysin from *Aeromonas hydrophyla* were the toxins of choice. During the development of this project, we successfully generated and characterized all the viruses, we detected aerolysin in supernatants from infected cultures, we confirmed toxin-mediated cytotoxicity in cultures that expressed the activating proteases, and we performed in vivo studies to evaluate the antitumor efficacy, toxicity and the effects on the stroma of the toxins. Whilst for Alpha-toxin no promising results were obtained, the aerolysin-expressing virus increased oncolytic potency in our models, indicating that it could be considered as a potential clinical candidate in stroma-abundant tumors and encouraging to follow this research pipeline.

Acknowledgements

1 de març de 2013, kaboom, llum verda. 4 anys i mig de tesi, un parell d'experiments, tres o quatre festes, algun canvi de look, 9 predocs amb qui he compartit grup, moltíssima més gent, coneguda abans o durant aquesta tesi, que ha ballat amb mi aquest reggaeton fins a esdevenir doctor. Bé, doctor i plusmarquista. Quina trajectòria plena de dades i rècords que mai hauria assolit tot sol. Amb el permís del lector (sigui del tribunal o no), les següents línies van dedicades a aquestes persones, a aquests X-(Wo)Men que m'han fet gaudir tant d'aquest viatge.

En el segon o tercer intercanvi de correus, el Ramon em diu amb tota honestedat: "M'agrada la teva experiència però hem de parlar del teu expedient". I a partir d'aquí, rècords non-stop. Rècord de confiança dipositada professionalment en mi, de tolerància a errors comesos dissenyant oligos i transgens, de disponibilitat per parlar de tot. També de crítiques al meu estil d'escriptura poètic i a les meves diapos de powerpoint, que ens han proporcionat uns bons riures als lab meetings. Deixes els estàndards molt alts, Ramon.

Hay tres vicioatletas con los que he batido muchos récords a base de abusar del mando negro. Rafa aka W. Roncero, gran compañero en el memorable congreso de Lausanne y en el lab en general, cofriki de Nintendo; Luis Alfredo, contigo el récord de freír a la gente con bromas malas hechas en un solo día (o en una sola hora) está fuera de peligro; Betinho, récord de horas jugadas a Mario Kart 64 y de compartir nuestra filosofía barata para cambiar el mundo. Habéis sido un gran apoyo, tanto científico como, sobre todo, personal, y siempre me vais a tener dispuesto a batir mil récords más.

Janine i Martino, vaja combo de peleles. Sense que serveixi de precedent, us trameto la meva admiració per lo cracks que sou en tots els àmbits en què puc dir que us conec, potser exceptuant el pàdel (obro paraigua). Us desitjo el millor per aquests anys de tesi que us queden, i que em vegeu guanyar-vos moltes vegades més!

Tota la progènie viral és imprescindible per fer una teràpia de rècord. Amb la Cris i l'Edu vaig compartir alguns mesos i un viatge a Mallorca i només puc desitjar-los que tot els hi estigui anant genial. Marta, tieta simultània! Merci per l'acollida que em vau donar al grup. Ahmed, shokran! Contigo tenemos el récord de veces que hemos mirado la página de depositar la tesis de la UB! Gracias por ser un tío siempre positivo y un gran compañero de viaje a Zaragoza. Raúl, sin duda tú tienes el récord de "increping" que he recibido en la terraza de la Flama, pero te quiero igual! Sil, amb tu segur que tinc diversos rècords, però em quedo amb el nombre de

vegades que hem cantat “Bailando” deixant-nos la gola! Alba, como bien apuntabas en tu tesis, hemos descubierto el potencial del otro durante la tesis, pero más vale tarde! Me voy a quedar con el récord de veces que te dije que devolviéramos la maldita máscara de la Pegatina! Sabes que te quiero un montón y que te agradezco que fueras mi “sponsor” cuando entré al grupo. Sònia, quin gran encert va ser fer amb tu aquella excursió en bici a la platja del Prat, merci per escoltar amb criteri sempre! Loli, la meva recordwoman amb l’RNA, merci per tot també! Quiero mencionar también a Patri, Sara, Ana, Míriam y Ari por el (corto) tiempo compartido en el grupo y su inacabable amabilidad.

Un altre dels rècords que m’enduc d’aquest temps és el de neologismes que ara signifiquen molt, com ara astraco, camallo, xupitazo, espelecho, tavegah, esacto o bé els fantàstics conceptes “R de remolque” o “ja t’entenc”, per esmentar uns quants. Tot això ha estat possible gràcies a uns companys de laboratori irrepetibles. Mariona, amb qui comparteixo el rècord d’esmorzars al Granier després de sortir de festa i de “txapes” mútues. Per alguna cosa ets una campiona. Amb la Roser tenim un rècord de vegades que ens hem “trollejat” amb tot l’amor i carinyo que la ironia permet! Nerea, la meva mestra al microtom i la persona que segurament ha estat més vegades la meva mare adoptiva amb l’habitació que em guarden ella i el Francis sempre que la nit ho requereix. Carmen, nunca se me va a olvidar tu imitación del “cani colocao” en Torreblanca, absolutamente de récord. Sònia, l’últim fitxatge del lab (i més recentment de la sala de becaris!), espero que compartim moltes més coreos i comentaris tribuneros! Quina versatilitat! Iratxe, la bonita del norte, que ostentará el récord de veces que me recriminará haberse hecho representante de becarios, pese a que tiene carisma e inteligencia para ridiculizar a muchos Guiness. Ja saps que sempre podràs comptar amb mi per riure de les teves “L” catalanes, per ser el teu “superamic cupaire” que no sempre utilitza desodorant i per eixir a buscar l’alegria, encara que tu vagis a kalis. No vull oblidar Júlia, Nick, Elena, Samu, Sara, María, Paki, Derek, Agnès, la resta de gent del LRT1 i molts més que us hauríeu de donar per al·ludits! Gràcies a tots!

També guardo registrades algunes fites de gent que volta pel món: Eli, rècord de voltes a una illa de cases; Eric, rècord de generació de veïns molestos en una hora; Ali, rècord d’empanament adorable! Joan, l’etern rialler, prepara les torxes que Cuba ens espera. Natalia, récord de veces que me has dicho que me ibas a regalar una planta. Curro, récord de imitaciones en una sola cena. Jacko, récord de kilos de pasta cocinados para desayunar. Y un largo etcétera de personajes entrañables!

Even though it is highly unlikely that you read these lines, I would like to thank Angelica, Emma, Hannah, Jessica and all the group for their support and feedback during my stay in Uppsala!

Hi ha un grupet de biotecnòlegs encantadors que amb aquesta tesi sumaran un doctor més al grup. Ha estat un plaer haver anat comprovant en la meva pell que totes les penúries i alegries que vivíeu al doctorat... eren certes! Un petonàs a tots, estigueu a Terrassa, Girona, París, Ammersfort, Philadelphia o on sigui.

Per suposat, com a ciutadà armeni agraeixo de tot cor la companyia que els meus compatriotes m'han proporcionat durant aquests anys (per no esmentar els 20 anteriors). Sabeu que us estimo i que sempre em tindreu per aportar actitud.. i gorres!

Por último, no puedo olvidarme de mi familia, la gente que atesora más récords en lo que aguantar a mi persona concierne. Son atletas de élite y solo me han dado facilidades y ánimos a lo largo de estos años de tesis. Aunque la maquiavélica de mi hermanita Blanca haya tenido la osadía de doctorarse antes que yo siendo 2 años más joven (siempre tiene que haber una crack que te eclipsa ;D), confío que disfrutaréis conmigo este día, en el que habéis tenido mucho que ver.

El moment en què tots aquests rècords perden l'accent i esdevenen records, em sento immensament agraït per haver pogut escriure aquestes tres pàgines amb un somriure gegant als llavis.

PS: Suposo que seria parcialment hipòcrita no esmentar en aquests agraïments el personal de tots els escenaris d'on sortiran les potencialment humiliants fotos que es veuran durant el dia de la presentació. Gràcies per les múltiples nits de rècord viscudes, però jo prohibiria l'ús del flaix al vostres locals.

1 INTRODUCTION

1.1 Oncolytic virotherapy

Oncolytic virotherapy is the treatment of cancer with replication-competent viruses able to lyse tumor cells. These viruses have the capability to infect and kill selectively neoplastic cells without damaging normal tissues (Hedley et al. 2006; Kelly and Russell 2007). Viral progeny produced after the initial infection of tumor cells is released to the extracellular media in order to infect neighboring cells, thus amplifying the initial dose and, ideally, achieving the complete eradication of the tumor eventually (**Figure 1**).

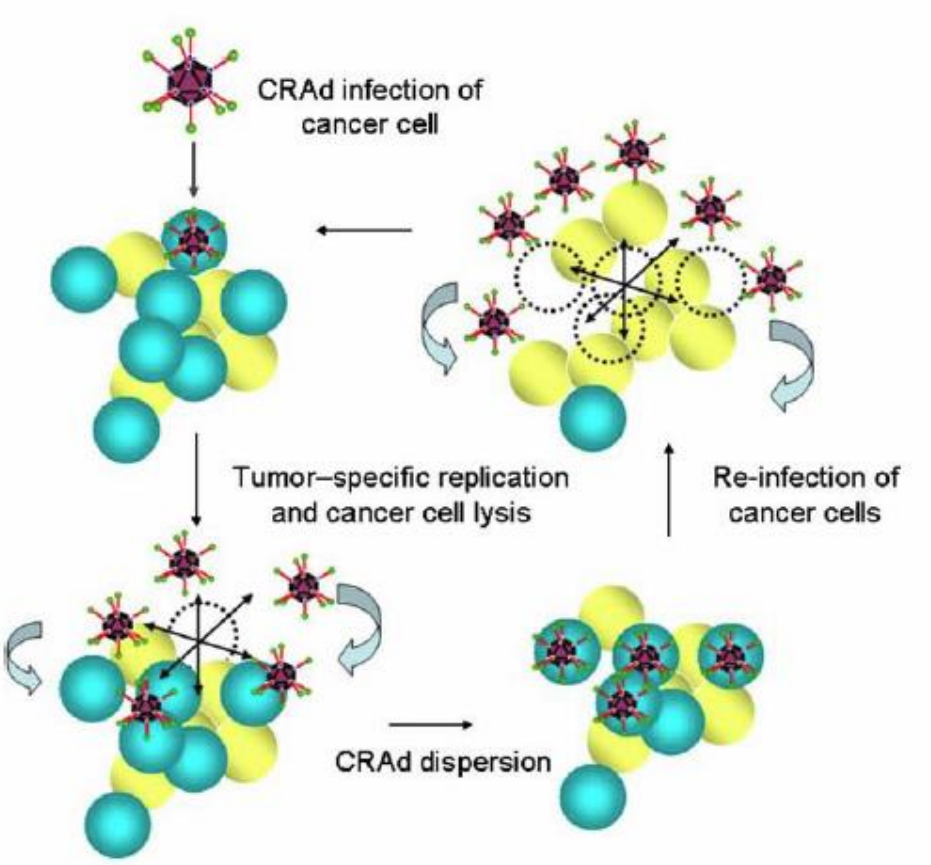

Figure 1. Oncolytic viral spread. Oncolytic viruses replicate in and kill selectively tumor cells. The self-amplification of the virus allows lateral spread in the tumor and greater tumor cell death from an initial infection of only few cells (adapted from Hedley et al. 2006). CRAd, conditionally replicative adenovirus.

In addition to the direct killing of infected cells, oncolytic viruses can mediate the killing of uninfected cancer cells by indirect mechanisms, such as destruction of tumor blood vessels, amplification of specific antitumoral immune responses, or through specific activities of transgene-encoded proteins expressed from engineered viruses (Russell, Peng, and Bell 2012).

The use of viruses to treat cancer is an old concept that has been revisited during the last two decades with genetically-modified viruses aiming for improved selectivity and potency. Soon

after the discovery of viruses, in the turn of nineteenth century, the idea to use them as anticancer agents arose. This approach came from the observation of spontaneous tumor regressions in patients that had undergone natural virus infections or which had been vaccinated (Kelly and Russell 2007; Sinkovics and Horvath 1993). Dock described in 1904 a leukemia case that went into remission after a presumed influenza infection (Dock 1904). However, it was not until 1912 when DePace associated for the first time the regression of a cervix tumor after the administration of rabies vaccine to a patient with viral-related oncolysis (DePace 1912).

In 1950s an 1960s, the advent of cell and tissue culture systems allowed *ex vivo* propagation of viruses, leading to the evaluation in human patients of the oncolytic properties of different viruses which had been previously tested in rodents (Hunter-Craig et al. 1970; R. Smith et al. 1956; Southam and Moore 1952). However, poor efficacy results combined with the pathogenicity of some viruses led to the abandonment of the field.

Nevertheless, a modern era of virotherapy started in the 1990s, thanks to the development of genetic engineering techniques that allowed the rational design of oncolytic viruses. Pioneers in this line were Martuza and colleagues, who developed a thymidine kinase-negative HSV that replicated in dividing cells but crippled in non-dividing cells. This virus showed to be active in murine glioblastoma models (Martuza et al. 1991). In 1996, McCormick improved the prospects of selectivity and efficacy by targeting defects that cause cancer with virus modifications (Bischoff et al. 1996). From that moment on, engineered oncolytic viruses from more than 10 different families have been tested in Phase I-III clinical trials, demonstrating excellent tolerability profiles. So far, strongest evidences of antitumor activity after single-agent treatment have been observed in clinical trials with talimogene laherparepvec, also known as T-Vec (nowadays owned by Amgen) or Imlygic™, which is an oncolytic Herpes Simplex Virus (HSV) encoding the granulocyte macrophage-colony stimulating factor (GM-CSF). Intratumoral administration of this virus led to complete regressions in 8 out of 50 treated patients with metastatic malignant melanoma in a phase II clinical trial (Senzer et al. 2009). More recently, a phase III clinical trial in patients with unresectable stage IIIB-IV melanoma showed an overall objective response rate of 26.4%, including 10.8% of complete responses (Bartlett et al. 2013), and improved mean survival of more than 4 months was observed in patients receiving T-Vec compared with systemic GM-CSF treatment (Andtbacka et al. 2015). Importantly, T-Vec was approved in 2015 for the treatment of melanoma.

1.1.1 Oncolytic Adenoviruses

Adenoviruses have several features that make them attractive to be used as a platform for oncolytic viruses: they are not associated to any serious disease, they have a lytic cycle, their genome can be easily modified to improve selectivity and potency traits, and they can be grown at high titers for its use in the clinical setting (Cody and Douglas 2009).

1.1.1.1 Classification of adenoviruses

Adenovirus was firstly isolated from human adenoid cells in 1953 (Rowe et al. 1953). Since then, more than 100 species have been characterized, including 57 different human serotypes, which are classified into 7 subgroups (A-G). Serotype 5 (Ad5) from subgroup C is the most widely used in the virotherapy field (Liebert, Rux, and Burnett 2004). The members of this group infect epithelial tissue from the respiratory tract, causing mild respiratory affections.

1.1.1.2 Ad structure

Adenovirus is a non-enveloped, double-stranded DNA virus. Viral DNA and associated core proteins such as pV, pVII, Mu (pX), and terminal protein (TP), are encased in an icosahedral capsid with 20 triangular faces and has a diameter of 60-90 nm. Each of the triangular faces is constituted by 12 copies of hexon trimer (polypeptide II). Complexes formed by the pentameric penton base (polypeptide III) and trimeric fiber (polypeptide IV) form the vertices. Fiber protein, which radiates from the 12 vertices of the virion, is structured in 3 domains: the N-terminal tail, that attaches to the penton base, a central *shaft*, and a C-terminal globular *knob* domain that functions as the cellular attachment site. Moreover, other minoritary proteins such as protein IIIa, VI, VIII, and IX make up the capsid, acting as cement between hexons (**Figure 2**).

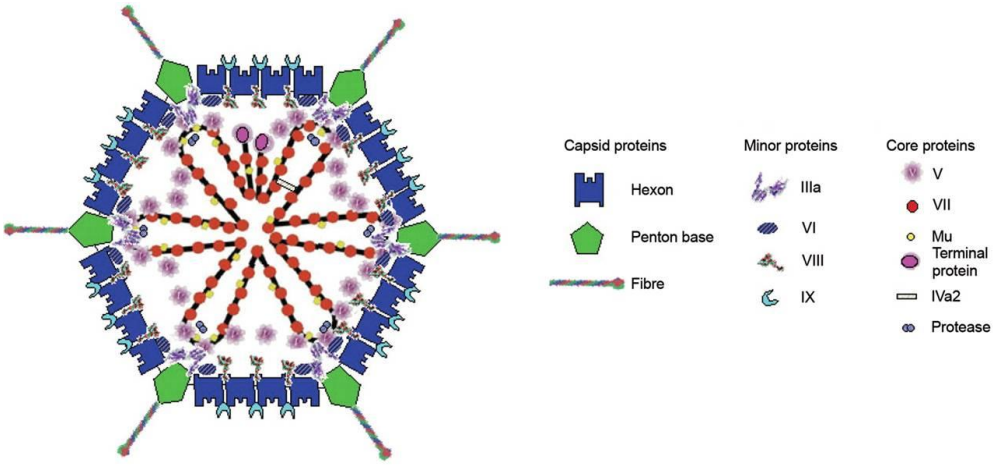

Figure 2. Adenovirus virion structure. Schematic representation of the capsid and core proteins of an adenovirus (adapted from Russell, Peng, and Bell 2012).

1.1.1.3 Ad genome

The Ad5 genome consists of a 36 Kb linear molecule of double-stranded DNA. Genetic information is organized in overlapping transcription units on both strands. Extensive splicing leads to the translation of over 50 proteins, of which 11 are structural virion proteins (I. M. Verma and Weitzman 2005). Adenoviral genes are classified in 3 groups, according to the moment in which their expression is engaged during the viral cycle: early (E1A, E1B, E2, E3, and E4), delayed (IX and Iva2), and the major late transcription unit (MLU). The latter is processed into 5 mRNAs (L1-L5) that produce all the structural proteins. Moreover, adenovirus genome also contains the viral-associated (VA) genes that generate two untranslated RNAs. At both sides of the genome there are two inverted terminal repeats (ITR), where the viral DNA replication origins are located. The packaging signal is located at 100 bp from the left ITR. It is rich in adenine and thymine and has an important role in the encapsidation of the virus. **Figure 3** depicts a schematic representation of the Ad5 genome.

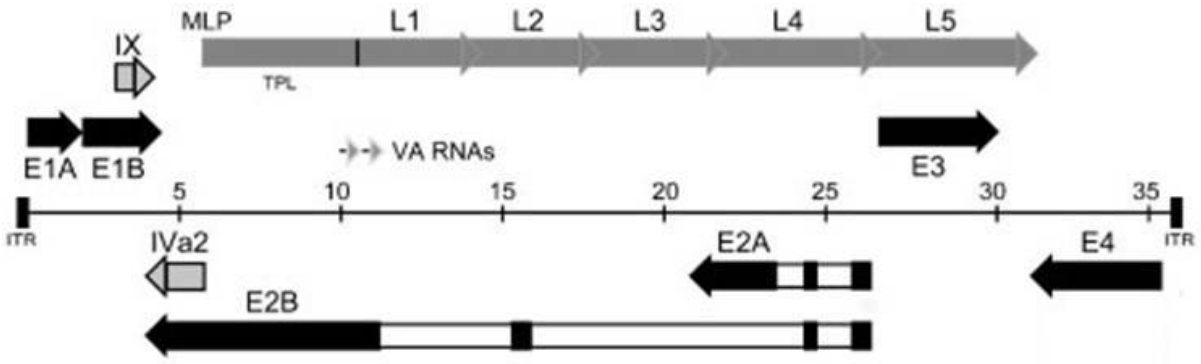

Figure 3. Adenovirus genome structure. The linear double-stranded genome is depicted in the center as a thin line, with the inverted terminal repeats (ITR) at each end: lengths are marked in kbp. Early transcription units are shown relative to their position and orientation in the Ad5 genome. Early genes are indicated by black bars and genes expressed at intermediate and late times of infection are indicated by gray bars (modified from Täuber and Dobner 2001. MLP, Major Late Promoter; TLP, Tripartite leader; VA, virus-associated.

1.1.1.4 Biology of the infectious cycle

1.1.1.4.1 Binding and entry

The first step in attachment of adenovirus type 5 (Ad5) particles to the cell membrane is the interaction between the fiber *knob* and the coxsackievirus B and adenovirus receptor (CAR). In order to achieve a successful internalization of the virus, a secondary interaction between an exposed RGD (Arg-Gly-Asp) motif located on the penton base protein and $\alpha_V\beta_3$ and $\alpha_V\beta_5$ integrins is needed (Wickham et al. 1993). Interestingly, genetically engineered Ad5 that lack CAR binding showed identical liver transduction than wild-type Ad5 after intravenous

administration in rodents and primates, evidencing alternative mechanisms of virus transduction (R. Alemany, Suzuki, and Curiel 2000; T. A. G. Smith et al. 2003). Low affinity interactions between the conserved aminoacid sequence KKTK$^{91-94}$ within the fiber *shaft* domain with heparan-sulphate-glycosaminoglicans (HSG) are described as possible mediators of Ad2 and Ad5 transduction in the absence of CAR (Bayo-Puxan et al. 2006; Dechecchi et al. 2001; Y. Zhang and Bergelson 2005).

The binding of adenovirus particles to its cellular receptors triggers virus internalization by clathrin-dependent, receptor-mediated endocytosis (Meier et al. 2002; Stewart et al. 1997). The acidic environment of endosomes induces escape of virions into the cytoplasm, where they traffic along microtubules toward the nucleous. After the dissembling of the capsid at the nuclear pore complex (NPC), viral transcriptional program starts (**Figure 4**).

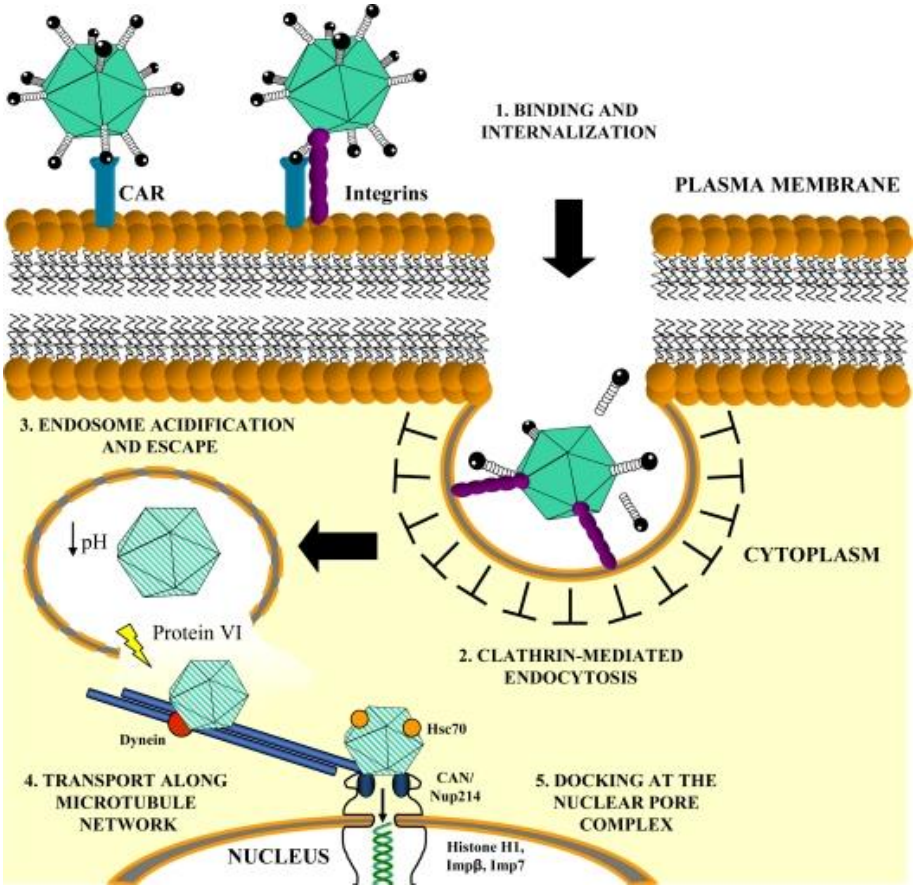

Figure 4. In vitro entry pathway of Ad5. Schematic representation of the different steps involved in the entry pathway of Ad5 in vitro (adapted from Coughlan et al. 2010).

1.1.1.4.2 Early gene expression and DNA replication

E1A is the first viral transcription unit expressed upon internalization, generating multiple mRNA and protein products by differential splicing or mRNA processing. During early infection, two transcripts are produced: 13S mRNA, encoding 289R protein, and 12S mRNA that encodes 243R protein. The main functions of E1A proteins are the engagement of phase S in order to provide an optimal environment for virus replication and the *trans*-activation of the remaining adenoviral early transcription units: E1B, E2, E3, and E4 (Berk 1986). Such activation of the cell cycle occurs by means of the interaction of the E1A products with Retinoblastoma (Rb) protein, which is a tumor suppressor that inhibits cell cycle by sequestering E2F transcription factor, thus promoting DNA replication.

Cell cycle deregulation by E1A results in the accumulation of p53 tumor suppression protein, which usually leads to apoptosis. In order to avoid this premature death of infected cells and hence maximize viral yields, adenoviral protein E1B-55K binds p53 and prevents the onset of pro-apoptotic gene expression. Additionally, E1B-19K protein contributes to this purpose by directly binding pro-apoptotic proteins such as Bak and Bax.

E2 region encodes for proteins involved in genome replication, including DNA polymerase, pre-terminal protein and the single-stranded DNA-binding protein.

Products of E3 region are responsible for the escape from the host immune response, and allow persistence of infected cells. For instance, E3-gp19K (E3-19K) is a transmembrane glycoprotein that prevents the presentation of viral antigens by the major histocompatibility complex (MHC) class I pathway, thereby avoiding the recognition and lysis of infected cells by cytotoxic T cells. This process relies on its ability to sequester either the MHC class I molecules or the Transporter Associated to antigen-Processing (TAP) in the ER.

E4 transduction unit encodes for proteins that play a role in cell cycle control and transformation. Moreover, other functions of these proteins include viral replication, stability and transport of viral mRNA, and induction of late gene expression.

Although adenoviruses excel at subduing their common host cells (human pulmonary tract in the case of Ad5) throughout evolution, there are cell types that have acquired mechanisms to impair viral replication and viral protein expression. Firstly, success in viral replication is very species-specific, which is the reason why Ad5 shows very poor replication rates in murine cells, which is a relevant issue if suitable preclinical models are sought. Also, cell populations such as fibroblasts, which are key components of the tumor stroma, have been shown to express

antiviral genes such as retinoic acid-inducible gene (RIG-I) or type I interferon related genes that interfere with viral replication and protein synthesis and facilitate the detection of viral elements by intracellular receptors (Ilkow et al. 2015). Hence, preclinical models are very challenging scenarios for the use of Ad5-based vectors, since both factors will be present in these tumors, as even though human cells can be implanted in immunosuppressed mice to facilitate Ad replication (and of course to better reproduce the real target of the treatment, which is the oncologic patient), highly virus-resistant murine stromal fibroblasts will eventually populate the tumor mass.

1.1.1.4.3 Late gene expression and virion assembly

After the onset of DNA replication, transcription from the major late promoter (MLP) is up-regulated to ensure the production of sufficient amounts of structural proteins. The MLP regulates the expression of genes from the major late transcription unit (MLU), which encodes for 15 to 20 different mRNAs derived from a single pre-mRNA by differential splicing and polyadenylation. Most adenoviral late genes are expressed from regions L1-L5, and correspond mostly to structural proteins and other players in virion assembly (Mcconnell and Imperiale 2004). Transcription of these genes starts thanks to a conformational change in the adenoviral genome structure and to the activation by IVa2 protein (H. Chen, Vinnakota, and Flint 1994). Late mRNA molecules are accumulated in the cytoplasm and become translated thanks to the tripartite leader sequence, a 5' element shared by all the mRNA produced from MLP which allows the helicase-independent transcription of these genes (J. Huang and Schneider 1991). Then, translated proteins are transported to the nucleus, where new virions are assembled. Finally, adenoviral DNA is packaged in the capsid thanks to the binding of IVa2 protein to the packaging signal (W. Zhang et al. 2001).

Cell lysis and release of progeny virions occurs approximately 30 hours after the infection. Capsids are accumulated in the nucleus and intermediate filaments are disaggregated, conferring the cell with a round shape, commonly identified as the cytopathic effect (CPE). This process also involves E3-11.6K protein or adenovirus death protein (ADP), which unlike other products of E3 region, is only produced during the late phase of infection and is transcribed from MLP rather than E3 promoter (Tollefson, Ryerse, et al. 1996; Tollefson, Scaria, et al. 1996).

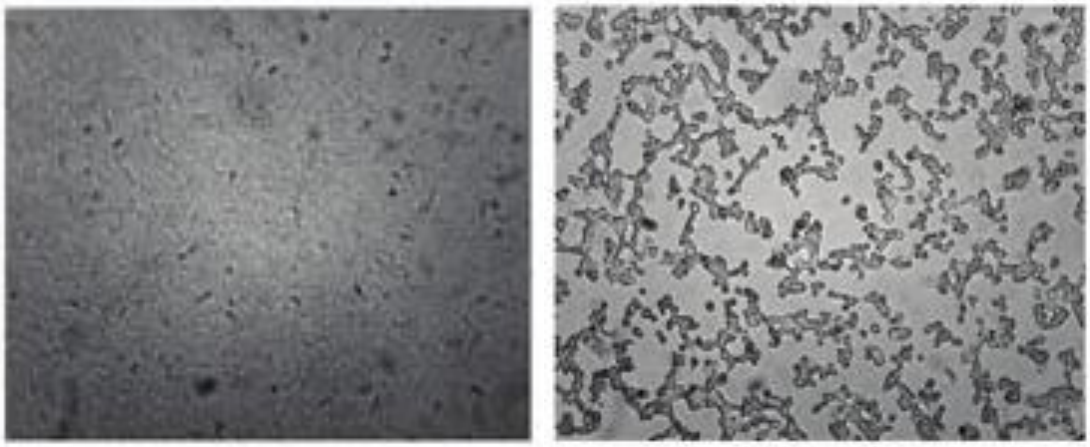

Figure 5. Cytopathic effect of Adenoviruses in A549 cells. Uninfected A549 cells (left) form monolayers on the plate surface. After 3 days of infection with Adenoviruses (right), cells show a CPE phenotype with round shape and reduced size.

1.1.1.5 Design of tumor selective oncolytic adenoviruses

Unlike other viruses such as reovirus, Newcastle disease viruses (NDV) or vesicular stomatitis virus (VSV), adenoviruses are not naturally selective for tumor cells. Therefore, genetic manipulation of the adenoviral genome is needed to achieve tumor replication selectivity. Several strategies have been used with this purpose, including the deletion of viral genes that are essential for virus propagation in healthy cells but complemented in tumor cells, the insertion of tumor-specific promoters controlling the expression of essential viral genes (transcriptional or translational targeting) or the modification of capsid proteins to achieve specific and efficient infection of tumor cells (transductional targeting). The combination of these strategies has allowed the rational design of oncolytic adenoviruses.

1.1.1.5.1 Restricted replication

It is known that adenoviral infection and oncogenic transformation induce similar signaling cascades in eukaryotic cells. Consequently, some mutant adenoviruses which showed impaired replication in normal cells are complemented for productive replication in tumor cells in which p53 and pRb pathways are deregulated. The first CRAd, proposed by Frank McCormick on 1996, called ONYX-15, contained the deletion of E1B-55K gene, whose function is to inactivate p53 protein and prevent apoptosis (Bischoff et al. 1996). Since most tumor cells already present endogenous inactivation of p53, E1B-55K turned out to be dispensable. However, E1B-55K has other functions that are not complemented in tumor cells, so viral replication becomes attenuated.

Other examples of tumor-selective replicating adenoviruses carry Δ24 and *dl922-927* mutations. These viruses contain the deletion of the conserved region CR2 of E1A, which is

responsible for sequestering Rb and thereby inducing S phase of cell cycle in normal cells. However, tumor cells usually present a defective Rb pathway. Viruses harboring this mutation are not able to impair the interaction between Rb and E2F in normal cells and present an attenuated replication in these cells while preserving oncolytic potency in tumor cells (**Figure 6**). However, the selectivity of these viruses is not fully exclusive, since other regions of E1A can also interact with pRB (Fueyo et al. 2000; Heise et al. 2000).

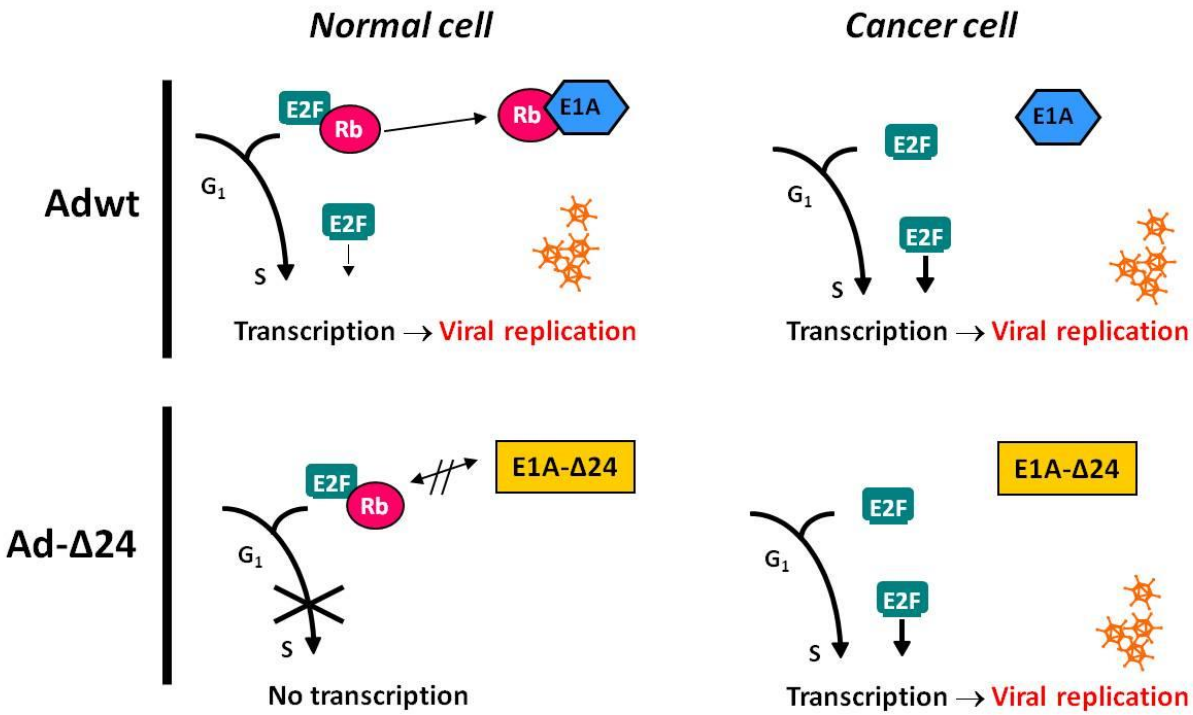

Figure 6. Δ24 selectivity mechanism. E1A protein binds and inactivates Rb to induce S phase of cell cycle and viral replication. In tumor cells this function is redundant, since Rb pathway is truncated and E2F is already free. In normal cells, Δ24 deletion avoids the dissociation of Rb and E2F and no viral replication occurs.

The deletion of the VA-RNAs genes is also described as a strategy to enable effective viral replication only in cells with activated Ras pathway or truncated interferon (IFN) pathway, which are very common defects in tumors (Cascallo et al. 2006; Cascalló et al. 2003).

1.1.1.5.2 Transcriptional and translational targeting

The second approach to confer tumor selectivity to oncolytic adenoviruses consists of the insertion of tissue- or tumor-specific promoters regulating viral gene expression, mainly E1A, due to its central role as the first transcript to be generated, but also other early genes such as E1B, E2 or E4. Transcriptional targeting of adenoviruses was firstly introduced with the use of the prostate-specific antigen promoter (PSA) to drive the expression of E1A in the adenovirus CV706 (CN706) (Rodriguez et al. 1997). Other examples of specific promoters that

have been used to target other type of tumors are the α-fetoprotein promoter (AFP) for hepatic carcinoma (Liebert et al. 1999), the melanoma-specific tyrosinase promoter (Bauerschmitz et al. 2002) or promoters that respond to hypoxia and estrogens to treat breast cancer (Hernandez-Alcoceba et al. 2002).

Since this strategy is restricted to tumors that express the corresponding tumor-specific antigens, promoters which exploit common features of tumor cells have also been chosen to broaden the range of tumor types to be targeted. In this regard, the telomerase reverse transcriptase (TERT) promoter has been used to drive E1A expression in oncolytic adenoviruses, since high telomerase activity is one of the hallmarks of tumor cell immortality (Savontaus et al. 2002). Promoters that respond to E2F transcription factor are also suitable to achieve restricted replication in a broad range of tumor cells since, as mentioned before, Rb pathway tends to be defective in cancer cells. Among others, regulation of E1A expression under E2F-1 promoter confers high potency of transcription (Cascallo et al. 2007; Johnson et al. 2002; J J Rojas et al. 2009; Tsukuda et al. 2002).

In this sense, an alternative strategy used by our group for the generation of ICOVIR-15 is the modification of the wild-type E1A promoter by inserting E2F-binding sites to redirect E1A expression toward pRb deregulation (Juan J Rojas et al. 2010). Moreover, this promoter also includes an Sp-1-binding site, since it has been described that both, E2F and Sp-1 transcription factors work together to activate transcription (Karlseder, Rotheneder, and Wintersberger 1996).

1.1.1.5.3 Transductional targeting

Transductional targeting strategies pursue preferential infection of tumor cells rather than normal cells through the modification of capsid proteins. Virus attachment proteins can be modified to use receptors that are highly or exclusively expressed on the membrane of tumor cells. Upon intravascular administration, adenovirus accumulates mostly in the liver, causing toxicity and limiting the amount of available virus to reach the tumor. Therefore, transductional strategies include both the ablation of the interaction of adenoviruses with its normal receptors, especially those implicated in hepatic transduction (detargeting), and the redirection of virion binding to tumor-associated receptors (retargeting).

In this sense, abrogation of the interactions involving the adenoviral capsid and coagulation factors or the putative previously mentioned HSG-binding domain KKTK has been strongly associated with loss of liver transduction although, in both cases, it was accompanied with

loss in tumor transduction (Bayo-Puxan et al. 2006; Nicol et al. 2004; T. A. G. Smith et al. 2003; Waddington et al. 2008).

With regard to tumor targeting, a widely used ligand to enhance tumor tropism is the RGD-4C motif (CDCRGDCFC), which targets RGD-binding integrins, usually overexpressed in tumors. The insertion of this ligand in the HI-loop allows the use of integrins as primary receptors instead of CAR, which is not highly expressed in tumor cells (Bauerschmitz et al. 2002). Other locations for different ligands have been tested, but HI-loop offers best insertion capacity with negligible losses in viral replication (Belousova et al. 2002).

The combination of hepatic tropism ablation by mutation of the KKTK domain and the insertion of targeting peptides in the HI-loop such as RGD has not proved successful, presumably due to a negative effect on the structure of the fiber (Bayo-Puxan et al. 2006; Kritz et al. 2007; Rittner et al. 2007). However, the replacement of the KKTK domain with an RGD motif described by our group (RGDK modification), significantly increased tumor cell transduction and improved the tumor-to-liver ratio *in vivo* in the context of a non-replicative adenovirus (Bayo-puxan et al. 2009).

1.1.1.6 ICOVIR-15K

ICOVIR-15K is an oncolytic adenovirus that has been developed by our group and that we currently use as a platform to incorporate novel modifications and improvements (J J Rojas et al. 2012). This virus derives from ICOVIR-15 (Juan J Rojas et al. 2010) and combines modifications corresponding to the three previously described strategies to achieve tumor selectivity. First of all, the endogenous promoter of E1A has been modified by incorporating eight extra E2F-responsive sites organized in four palindromes and one extra Sp-1-binding site. Secondly, it contains the Δ24 deletion in E1A that abrogates the interaction of this protein with pRb, so in case that leaky expression of E1A occurs, it will not be able to release E2F from pRb. Lastly, ICOVIR-15K incorporates the previously mentioned transductional targeting mutation RGDK. ICOVIR-15K has shown increased bioavailability after systemic administration and greater antitumor activity *in vivo* compared to ICOVIR-15 (**Figure 7**).

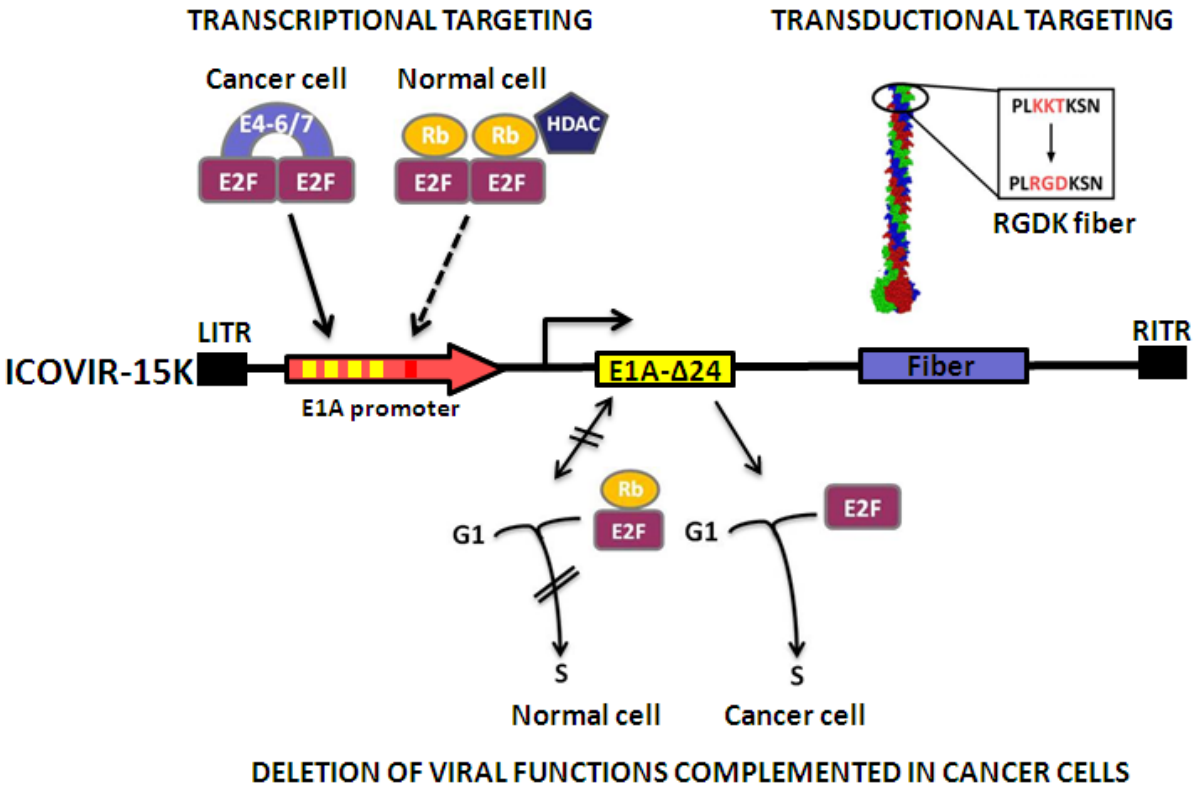

Figure 7. Schematic representation of the modifications in ICOVIR-15K genome. ICOVIR-15K contains the modified E1A promoter (including four E2F boxes and one Sp1 box) and the truncated E1A protein to confer selectivity for tumor cells. It also has the RGD motif replacing the KKTK domain in the shaft of the fiber. Picture provided by Dr. Alba Rodríguez García.

1.1.1.7 Clinical experience with oncolytic adenoviruses

Among the human Adenoviral serotypes described, Ad5 is the most frequently used in the development of oncolytic Adenoviruses. In the human population, 50% of people are seropositive for this virus, which is a clinically relevant piece of data because, combined with the fact that cancer patients are often immunosuppressed, a number of adverse effects and toxicity might be observed in such patients and, also, it adds complexity to the fate of the administered virus depending on the administration route.

The p53-selective, E1B-55K-deleted chimeric Ad2/5 Adenovirus Onyx-015 mentioned in previous sections moved rapidly to the clinic after showing good safety profiles in spite of lacking robust efficacy or even significant tumor tropism. Eighteen phase I and II clinical trials with very different administration routes and in different malignancies, from the initially treated head and neck tumors to the last colon and colorectal tumors. In general, even though side effects were generally mild, no objective responses were observed. Also, biodistribution studies in a deceased patient showed that most of the virus was in the spleen and liver hepatocytes, which reproduced the data obtained in murine models. In spite of all this, China

Sunway Biotech is ready to market its Onyx-015 version named H101. Besides lacking E1b-55K, H101 also lacks all E3 proteins, including ADP, which renders it less potent and more immunogenic, traits that may skew the therapeutic mechanism towards immunotherapy. . In a phase II trial with 50 patients and a phase III with 123 patients, all of them head and neck cancer patients, the response rate doubled when H101 was added to the conventional chemotherapy (Lu et al. 2004; Xia et al. 2004), and it was eventually approved by the China's State Food and Drug Administration.

Nowadays, the most frequent setting for treatment with replication-competent Adenoviruses implies the expression of a transgene and, with increasing frequency, the combination with chemotherapy or even radiotherapy, with which an apparent synergy has been described (R.-F. Chen et al. 2015). Previous modifications to render the viruses tumor-selective, such as the E2F-sensitive promoter or the Δ24 deletion, are generally maintained, but they have not proved successful clinical outcomes on their own. In terms of pharmacokinetics, oncolytic Adenoviruses can burst from tumors and cause delayed activity and toxicity events that are not dose-dependent, but might correlate better with the tumor load of the patient. Also, fast tumor lysis can provoke a tumor lysis syndrome (TLS) and a subsequent cytokine storm, with potential severe adverse effects on the patient's health. Thus, it has been advised to proceed from patients with low tumor burden to patients with large metastatic disease to better monitor these parameters (Alemany 2013). Also, even though the systemic delivery of the Adenoviral vectors is ideal to reach secondary or metastatic lesions, intratumoral administration, whenever feasible, is preferred to avoid unwanted secondary effects caused by the presence of Adenoviruses in the bloodstream.

OncAd	Modification	Transgene	Target	Administration	Phase	ClinicalTrials.gov identifier
ICOVIR-5	E2F-E1A Δ24 RGD		Solid tumors	Mesenchymal stem cell delivery IV	I,II	NCT0184461
LOAd703	5/3 Δ24	CD40L & 4-1BBL	Pancreatic cancer	IT	I/IIa	NCT02705196
Ad5-yCD/ mutTKSR39rep-hIL12	E1B-55K	CD/TK hIL12	Prostate cancer	Intraprostatic	I	NCT02555397
ONCOS-102 w/ cyclophosphamide	5/3 Δ24	GM-CSF	Advanced neoplasms	IV	I	NCT01598129
VCN-01 w/or w/o Abraxane® and Gemcitabine	DM-1-E2F-E1A Δ24 RGD	Hyaluronidase	Advanced solid tumors	IV	I	NCT02045602
VCN-01 w/Abraxane® and Gemcitabine	DM-1-E2F-E1A Δ24 RGD	Hyaluronidase	Advanced pancreatic cancer	IV	I	NCT02045589
CG0070	E2F-E1A	GM-CSF	Bladder cancer	IV	III	NCT02365818
CG0070	E2F-E1A	GM-CSF	Bladder cancer	IV	II/III	NCT01438112
Colo-Ad1	Ad11p/Ad3		Colon, NSCLC, bladder, renal cancer	IT, IV	I	NCT02053220
DNX-2401 w/ Temozolomide	E1A Δ24 RGD		Glioblastoma multiforme	IT	I	NCT01956734
DNX-2401 w/IFNγ	E1A Δ24 RGD		Brain tumors	IT	I	NCT02197169
Ad5-yCD/ mutTKSR39rep-ADP w/IMRT	E1B-55K	CD/TK	Prostate carcinoma	Intraprostatic	II/III	NCT00583492
OBP-301	hTERT		Hepatocellular carcinoma	IT	I/II	NCT02293850

Abbreviations: CD, cytosine deaminase; GM-CSF, granulocyte macrophage colony-stimulating factor; IFNγ, interferon γ; IMRT, intensity-modulated radiation therapy; IT, intratumoral; IV, intravenous; NSCLC, non-small cell lung cancer; TK, tyrosine kinase; w/, with; w/o, without.

Table 1. Recent completed and current clinical trials using oncolytic Adenoviruses. Adapted from (Rosewell Shaw and Suzuki 2016).

Some of the latest most advanced clinical Adenoviral candidates are shown in **Table 1**. These candidates comprise different approaches to treat several kinds of tumors. LOAd703 is a trimerized CD40L-expressing virus which is able to induce a T_H1 immune activation and reduce the aggressiveness of the tumor stroma. It is being tested in pancreatic cancer patients at Baylor College of Medicine (Emma Eriksson et al. 2017). VCN-01 is also being trialed in pancreatic patients exploiting the high proportion in Hyaluronic Acid (HA) present in such tumors. Upon the action of hyaluronidase expressed from the virus, the stroma structure is disrupted and and viral spread is significantly improved (Rodríguez-García et al. 2015). CG0070 is a GM-CSF-expressing oncolytic Adenovirus used to treat bladder cancer which has showed a tolerable safety profile and an antitumor Complete Response (CR) rate across cohorts of 48.6% and is already being tested in phase III trials after such successful outcomes (Burke et al. 2012). An antiprostate cancer Adenovirus derived from the previously mentioned Onyx-015 expressing well-known double suicide genes (CD and TK) has not only shown very mild toxicity profiles, but also sustained transgene expression, antitumor activity, broad intratumor distribution and synergy with radiation, as well as hints of antitumor immune responses in different clinical trials performed (Freytag et al. 2003; Rojas-Martínez et al. 2013).

Summing up, several oncolytic Adenoviruses have shown antitumor potential and good tolerance in varying scenarios and approaches, reinforcing the relevance this treatment could imply for many patients if further research is performed. Notwithstanding, events of striking

tumor shrinkage are relatively rare, especially in single-agent approaches. The road towards indisputable success is, therefore, still a long way to go.

1.1.1.8 Limitations of oncolytic adenoviruses

Overall, clinical data on oncolytic adenoviruses, especially after intravenous administration, point out the need of more potent and selective viruses. Beyond the difficulties of this route of administration, other hurdles for the success of virotherapy imposed by the tumor microenvironment need to be addressed (Parato et al. 2005).

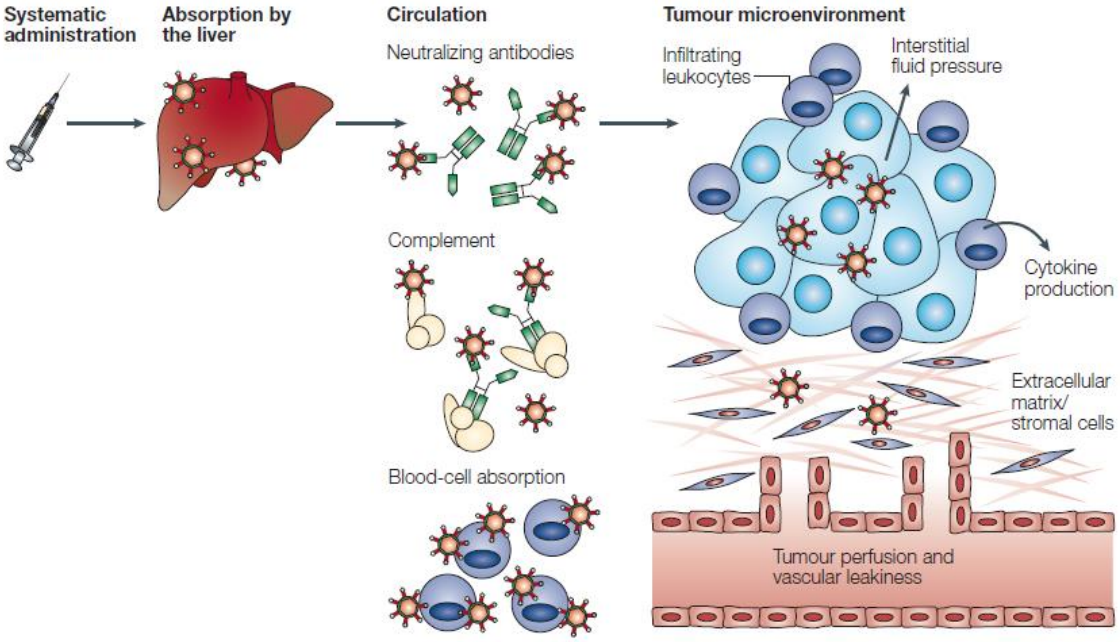

Figure 8. Barriers to intravenous delivery of oncolytic viruses *in vivo*. Within minutes after systemic administration of an oncolytic virus, most of the initial dose is retained by the liver. Moreover, oncolytic viruses can be neutralized by the interaction with blood cells, the complement or neutralizing antibodies. Finally, to enter into the tumor mass, the virus must cross the vascular endothelium against a gradient of interstitial fluid pressure. In addition, tumor stroma and infiltrating leukocytes limit the intratumoral spread of the virus (adapted from (Parato et al. 2005)).

1.1.1.8.1 Tumor targeting upon systemic administration

Although many ongoing clinical trials involving oncolytic viruses are set up with intratumoral administration, systemic delivery is crucial for metastatic disease treatment. In order to take on this challenge, current research on the field is focused on escaping virus neutralization by serum factors, minimizing liver and spleen uptake and enhancing permeability within tumor vasculature.

Since adenoviruses are not blood-borne viruses, they are cleared from the circulation fairly quickly, with a half-life of less than 2 minutes in mice (R. Alemany, Suzuki, and Curiel 2000) and 10 minutes in humans (Reid, Warren, and Kirn 2002). Intravascular delivery of adenoviruses leads to a complex series of interactions with blood components such as coagulation factors, complement, blood cells, and neutralizing antibodies. Moreover, the loss

of virus through vascular fenestrations of spleen and liver and subsequent uptake of adenovirus particles by Kupffer cells (KC) in the liver contribute to this clearance. Opsonization of viral particles with natural antibodies and complement, together with unspecific interaction with scavenger receptors, are responsible for the uptake by KCs (J. Smith et al. 2008).

Some strategies involving genetic modifications of capsid proteins to improve tumor targeting and reduce liver transduction have been discussed in section 1.1.1.5.3 (transductional targeting). Insertion of an albumin-binding domain in the HI loop of the Hypervariable Region 1 has proved to allow viral escape from neutralizing antibodies in preimmunized mice (L. A. Rojas et al. 2016).

1.1.1.8.2 Stromal barriers

The self-amplifying ability of oncolytic adenoviruses within tumors is one of the advantages of virotherapy compared to conventional therapies, since the initial dose is enhanced until the complete lysis of the tumor. However, tumors are heterogeneous organs cemented by variable amounts of a dense stroma containing extracellular matrix (ECM) proteins such as collagen, fibronectin, laminin, fibrin and sparc-osteonectin, polysaccharides such as proteoglycan glycosaminoglycans (heparin, chondroitin, keratin-sulfates) or non-proteoglycan glycosaminoglycans (hyaluronan), and cells such as fibroblasts or inflammatory cells. In turn, besides hampering virus arrival to the tumors via vasculature, the tumor stroma also halts intratumoral virus spread, since adenoviruses neither cross barriers imposed by extracellular matrix nor replicate in non-tumor cells such as stromal fibroblasts, as has been described in previous sections.

Several strategies to improve intratumoral spread of oncolytic adenoviruses are currently being explored. Arming oncolytic viruses with ECM-degrading enzymes is a commonly exploited strategy to enhance viral penetration of solid tumors (Smith *et al.*, 2011). In our group, a hyaluronidase-expressing oncolytic virus, ICOVIR-17K, was developed recently and is currently in clinical trials (Sonia Guedan et al. 2010; Rodríguez-García et al. 2015). A number of proteins that modulate the configuration of ECM have been used to increase viral spread and antitumor efficacy in different tumor models. For instance, small molecules such as relaxin and decorin have been expressed from oncolytic adenoviruses, aiming to inhibit collagen production and upregulate the expression of matrix metalloproteases (MMP) that participate in the degradation of this connective tissue protein (Ganesh et al. 2007; Kim et al. 2006). Depletion of the stromal scaffold decreases the interstitial fluid pressure inside the tumors

with a subsequent increase in vascular permeability, thereby favouring the penetration of the virus to the tumor core (Eikenes et al. 2005; Pillwein et al. 1998; K. J. Smith et al. 1997).

Strategies to improve virus replication in stromal fibroblasts are also being developed. One approach is the restriction of E1a expression under the control of specific promoters, such as the SPARC (a stroma-abundant protein) promoter, that allow for virus replication in tumor and stromal cells (Lopez et al. 2012). Alternatively, our group recently described that the truncation of the i-leader adenoviral protein enhanced the release and cytotoxicity of the virus in cancer-associated fibroblasts (CAFs) *in vitro* and increased its antitumor activity *in vivo* (C Puig-Saus et al. 2014; C Puig-Saus et al. 2012).

Activatable toxins (zymoxins) with protease-cleavable linkers separating the catalytic and inhibitory domains have also been traditionally the chosen approach as safely targeted drugs to induce toxicity when specific pathological conditions are met at the target tissue. Similarly, in this work, an adenovirus expressing aerolysin, a pore-forming toxin from *Aeromonas hydrophyla*, with an MMP-9-sensitive linker in its propeptide form has been designed. MMP-9 is commonly overexpressed in tumors and is highly associated with malignant processes such as tumor angiogenesis, metastasis and tissue remodeling (U B Hofmann et al. 1999; R. P. Verma and Hansch 2007). More exhaustive details about this approach will be provided in section 1.3.

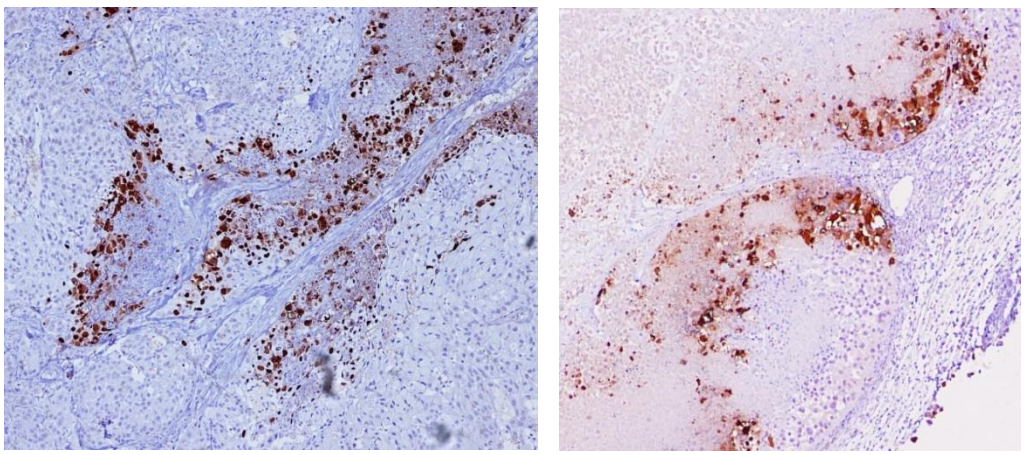

Figure 9. Stromal barriers in oncolytic virotherapy. Immunohistochemical of anti-E1a viral protein staining tumors slides from subcutaneous A549 tumors developed in athymic nude mice. Virus localization (brown) is clearly detained within regions determined by fibroblast septa and broad spread of the virus within the tumor cannot be achieved. Images provided by Dr. Luis Rojas.

1.1.1.8.3 Antiviral immune responses

Intravenous administration of adenoviruses leads to a strong innate immune response, mediated by neutrophils, macrophages, natural killer (NK) cells, and soluble factors such as complement and inflammatory cytokines.

Interaction of adenoviruses with preexisting anti-adenovirus antibodies in the bloodstream, and the activation of the classical route of the complement pathway with the consequent opsonization of viral particles, lead to virus neutralization and facilitate its rapid blood clearance by cellular elements of the innate immune response, including KCs and other cells of the reticulo-endothelial system.

Once captured by innate immune cells, response against adenoviruses is launched with the recognition of pathogen-associated molecular patterns (PAMPs) mediated by pattern recognition receptors (PRRs) such as Toll-like receptors (TLRs). This effect is strongly associated with the expression of inflammatory cytokines or chemokines such as IL-6, TNF-α, MIP-2, MIP-1α, and type I IFNs (Hartman, Appledorn, and Amalfitano 2008). All these cytokines recruit initially neutrophils and NK cells to the site of infection, and later monocytes and T cells. Moreover, they also activate trafficking of DCs to draining lymph nodes and their maturation to engage adaptive and memory immune responses that rapidly eliminate infected cells (Alemany and Cascallo 2009).

The immune system can be regarded as an ally or as a foe for virotherapy. From the "virocentric" point of view, the immunosuppression exerted within the tumor is beneficial for the treatment with oncolytic viruses, since it might allegedly translate into increased tolerance to viral replication. Although adenoviruses have acquired through evolution several mechanisms to counteract the effect of the immune system, they are not enough to evade immune responses.

Other strategies have been explored to evade the immune system. Preimmunity against adenovirus 5 in humans, which is highly prevalent, can be counteracted by the genetic engineering or chemical modification of the adenoviral capsid, as mentioned in section 1.1.1.5.3. Capsid pseudotyping with less prevalent serotypes, chemical coating or the use of tumor-homing cell carriers are alternative approaches when aiming for immune escape of the adenovirus (Bunuales et al. 2012; Nakashima, Kaur, and Chiocca 2010). Finally, genetic engineering of oncolytic viruses to express genes with immunosuppressive functions has been

explored to achieve enhanced antitumor activity (Altomonte et al. 2009; Haralambieva et al. 2007).

In contrast, from the "immunocentric" perspective, immunogenicity of oncolytic viruses is regarded as a disruption of the local immunosuppression in tumors, thus favoring the generation of specific antitumor immune responses and improving the outcome of virotherapy. Importantly, one of the hurdles for this strategy is that the strong immune response generated against viruses might mask specific responses against tumor antigens (Alemany and Cascallo 2009). Attempts to try to overcome this viral immunodominance have been made, usually by removing the most immunogenic viral epitopes from the capsid, at the expense of viral potency but aiming for an increased presentation of tumoral epitopes and, hence, the mounting of an antitumoral immune response. This last particular concept will be treated in the following section.

1.2 Cancer immunology

The idea that the immune system can behave against tumors has been discussed for over a century. In the early 1900s, Paul Ehrlich was the first author to suggest that tumor development can be suppressed by the immune system. A more comprehensive understanding of the immune system and the discovery of tumor antigens resurfaced this idea 50 years later. These advances led to the proposal of the immunosurveillance hypothesis by Burnet and Thomas, which postulates that adaptive immunity is responsible for preventing cancer development in immunocompetent hosts (Burnet 1957). This hypothesis was supported by the discovery of the role of IFN-γ in promoting immunological induced rejection of transplanted tumor cells (Dighe et al. 1994). Moreover, it was observed that immunodeficient mice lacking IFN-γ responsiveness or adaptive immunity were more susceptible to carcinogen-induced and spontaneous neoplasia than immunocompetent mice (Kaplan et al. 1998; Shankaran et al. 2001). Furthermore, a relatively high percentage of tumors (40%) of methylcholanthrene (MCA) carcinogen-induced sarcomas derived from immunodeficient mice were spontaneously rejected when transplanted into wild-type mice. In contrast, tumors derived in immunocompetent mice grew normally after its transplantation into wild-type syngenic mice (Shankaran et al. 2001). These evidences strongly suggested that tumors formed in immunocompetent recipients can undergo an “editing” process in order to become less immunogenic than those developed in the absence of an intact immune system (Schreiber, Old, and Smyth 2011).

This immunoediting of tumors comprises three distinct phases known as “elimination”, “equilibrium”, and “escape” represented in **Figure 10** (G P Dunn et al. 2002). The elimination phase is an updated version of cancer immunosurveillance, in which innate and adaptive immune systems work together to detect the presence of a developing tumor and eliminate it before it becomes clinically conspicuous. Such antitumor activity may involve many key players interacting with immunostimulatory receptors, like ‘danger signals’ (type I IFN), damage-associated molecular patterns (DAMPs) from damaged cells, or stress ligands commonly expressed on tumor cells. Additionally, expression of tumor antigens is needed to propagate $CD4^+$ and $CD8^+$ T cells. After this, tumor cell variants may survive and enter into the equilibrium phase, in which tumor cells remain functionally dormant and clinically unapparent (Koebel et al. 2007). This latency can be interrupted by several mechanisms which take the tumor to the escape phase, in which immune recognition is circumvented and clinically visible tumors are developed.

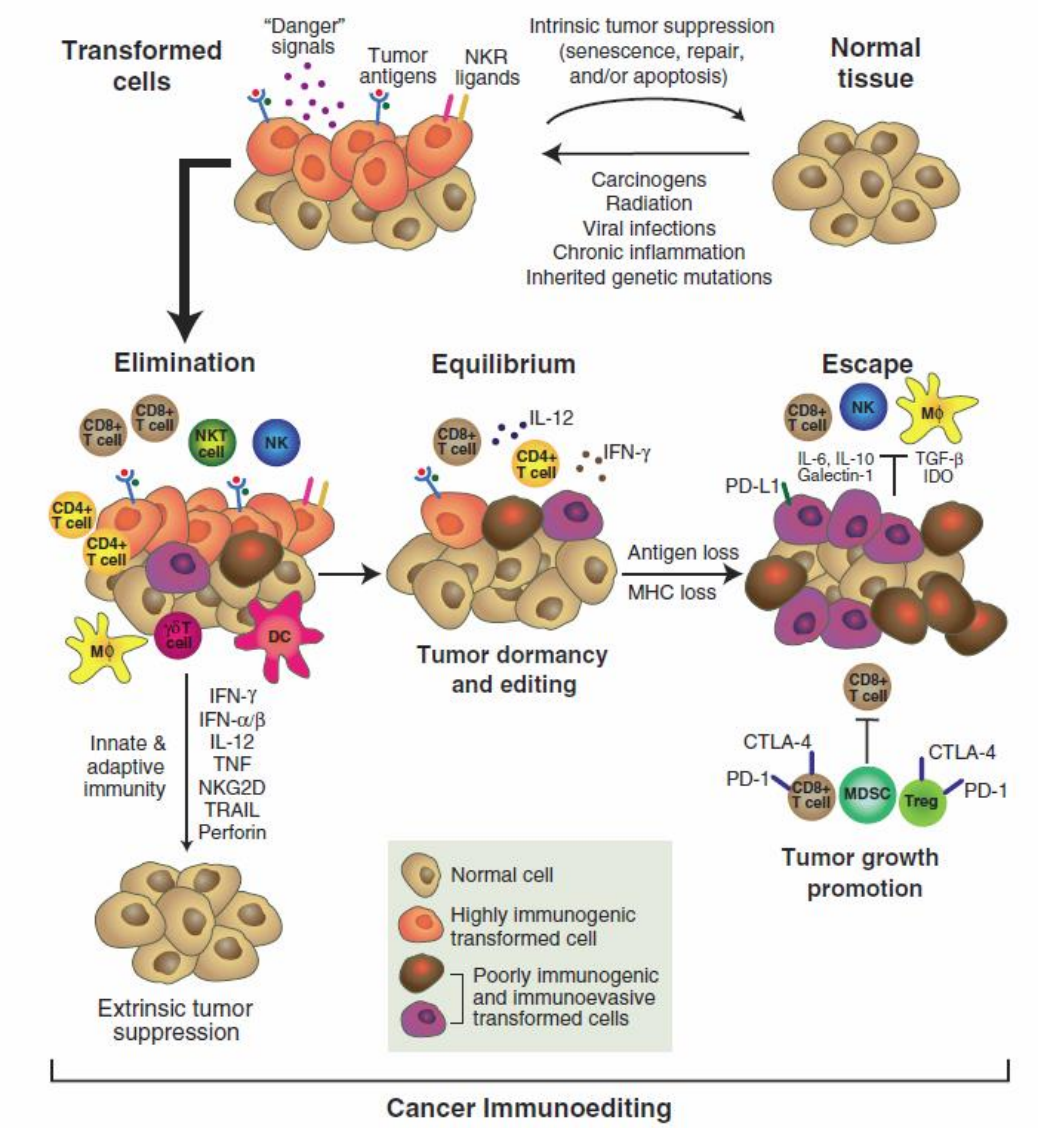

Figure 10. Cancer immunoediting. Cancer immunoediting consists of three sequential phases: elimination, equilibrium, and escape. In the elimination phase, innate and adaptive immunity destroy developing tumors before they become clinically apparent. If a rare cancer cell variant is not destroyed in the elimination phase, it may then enter the equilibrium phase, in which its outgrowth is prevented by immunologic mechanisms. Editing of tumor immunogenicity occurs in the equilibrium phase. Tumor cell variants may enter the escape phase, in which their outgrowth is no longer blocked by immunity. These tumor cells emerge to cause clinically apparent disease (Schreiber, Old, and Smyth 2011).

1.2.1 Antitumor immune response

Analysis of the tumor microenvironment in patients with a variety of cancer types including colorectal cancer, breast cancer, renal cell carcinoma, ovarian cancer, melanoma, and gastrointestinal stromal tumors, has revealed that the presence of tumor-infiltrating lymphocytes (TILs) is strongly associated with a positive prognostic and a favorable clinical outcome (Galon et al. 2006; Pages et al. 2005).

Innate immune activation triggered by stress-associated signals or DAMPs may constitute a bridge toward adaptive immunity that can allow some patients to spontaneously develop specific antitumor $CD8^+$ T cell responses.

The initiation of antitumor immunity begins with the capture by DCs of antigens derived from tumors, which process them for presentation or cross-presentation on MHC class I and II molecules. Tumor-antigen-loaded DCs migrate to draining lymph nodes where, under stimulating conditions, will prime antitumor effector T-cell responses by antigen presentation and costimulatory signaling. Then, activated T cells might enter the tumors and display their cytotoxic potential specifically onto tumor cells that present the tumor antigen against which they were selected (Mellman, Coukos, and Dranoff 2014) (**Figure 11**). Production of cytokines and activation of $CD4^+$ T cells are also required to generate a potent and sustained response.

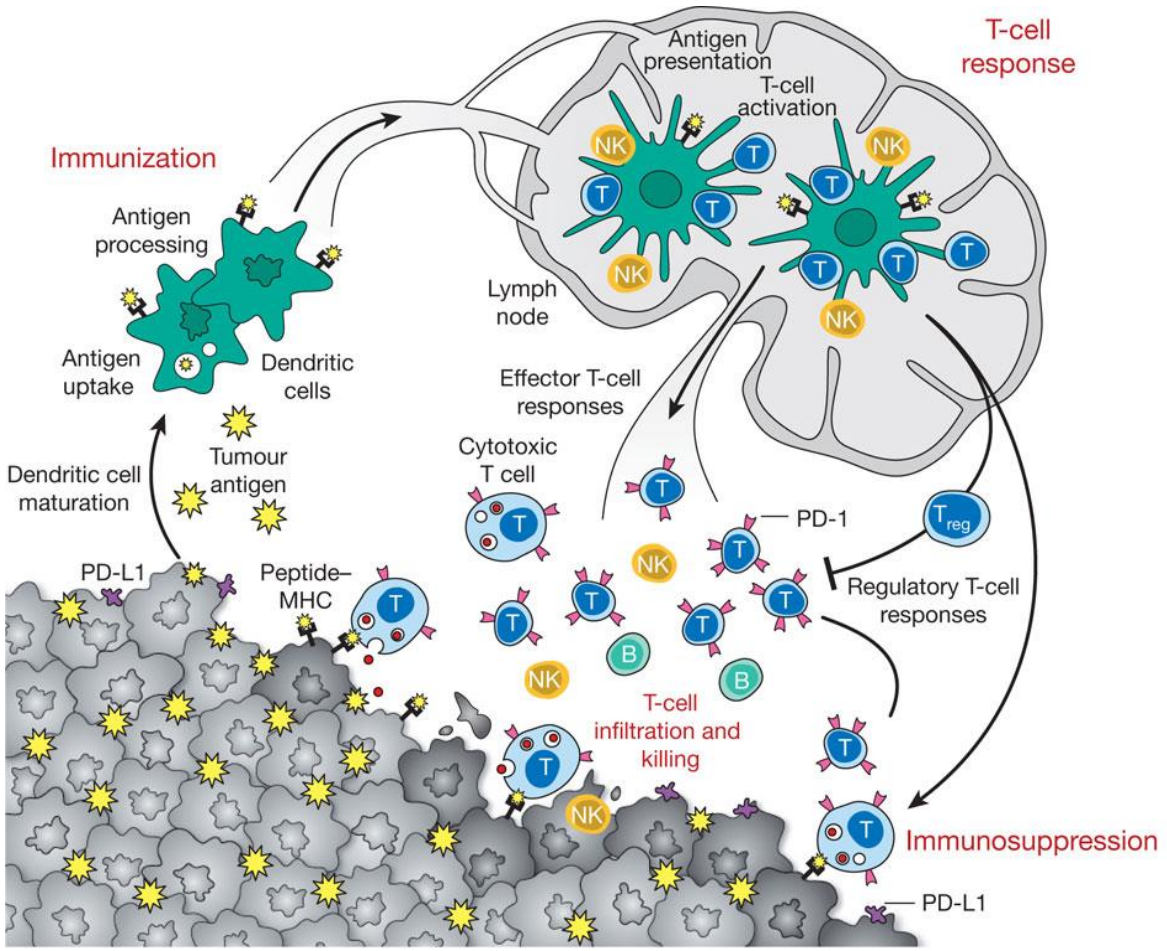

Figure 11. Generation and regulation of antitumor immunity. Antitumor immune responses start with the capture and processing of tumor-associated antigens by DCs for presentation on MHC class II or cross-presentation on class I molecules. Then, DCs migrate to draining lymph nodes where, in the presence of an immunogenic stimulus, will elicit anticancer effector T-cell responses in the lymph node. On the contrary, without such stimulus, dendritic cells will induce tolerance. In the lymph node, antigen presentation to T cells will elicit a response depending on the type of dendritic cell maturation stimulus received and on the interaction of T-cell co-stimulatory molecules with their surface receptors on dendritic cells. Antigen-educated T cells will exit the lymph node and enter the tumor bed, where immunosuppressive defense mechanisms produced by tumors oppose effector T-cell function (obtained from (Mellman, Coukos, and Dranoff 2014)).

1.2.2 Tumor-induced immune evasion

As hinted previously, tumors can undergo changes at the cell or microenvironment level in order to escape from immune surveillance. These mechanisms range from reducing the exposure of TAAs to the immune system receptors up to generating central or peripheral tolerance, that is, inducing anergy on T cells recognizing tumor epitopes.

1.2.2.1 Impaired presentation machinery and TAA loss

Tumor cells can acquire defects in antigen processing and presentation pathways, leading to evasion from adaptive immune recognition. Loss of different components of MHC class I pathway such as TAP, MHC class I molecules, β2m, immunoproteasome subunits (LMP2, LMP7, and LMP10), or chaperones have been detected in many different tumor types (Gavin P Dunn, Koebel, and Schreiber 2006; Leone et al. 2013). In our group, we demonstrated that reduced presentation of exogenous antigens due to TAP deficiency in tumor cells can be circumvented by fusing tumor epitopes to the viral protein E3-19K, which shows ER localization, and therefore TAP-independent presentation of such antigens can take place (Rodriguez-Garcia et al. 2015).

Genetic instability of tumor cells can also account for the loss of tumor antigens, turning tumor cells invisible to antigen-specific $CD8^+$ T cells. Similarly, tumor cells can cease to express ligands for the NK cell effector molecule NKG2D (Stern-Ginossar et al. 2008) or downregulate proinflammatory danger signals and thereby impair DC maturation (Wang et al. 2004).

1.2.2.2 Resistance to immune-mediated apoptosis

Tumor cells can upregulate anti-apoptotic molecules such as FLIP (Kataoka et al. 1998) or express inactive forms of death receptors including TRAIL, DR5, and Fas (Shin et al. 2001; Takahashi et al. 2006) in order to minimize the cytotoxic effects of immune cell attacks.

1.2.2.3 Immunosuppressive milieu

Tumor cells can express on its surface immune-inhibitory ligands that even recognized by immune cells inhibit its cytotoxic actions in a cell-contact mediated manner. Some famous examples are PD-1, PD-L1 (B7-H1) or PD-L2 (B7-DC), whose receptors are highly expressed in TILs (Dong et al. 2002).

Tumor cells, and even stromal fibroblasts, can also produce immunosuppressive cytokines that inhibit DCs function such as vascular endothelial growth factor (VEGF) (Gabrilovich et al. 1999), transforming growth factor-β (TGF-β), which also inhibits T and NK cell function (Wrzesinski, Wan, and Flavell 2007), or IL-10, that can also bias T cell responses toward a type 2 immune response (T_H2) that favors tumor progression (Aruga et al. 1997). Further on, galectin impedes T cell activity and survival (Rubinstein et al. 2004), and expression of indoleamine 2,3-dioxigenase (IDO) enzyme by tumor cells metabolizes tryptophan to generate kynurenines and inhibits $CD8^+$ T cell proliferation and promotes $CD4^+$ T cell apoptosis (Uyttenhove et al. 2003). Recruitment of regulatory immune cells such as regulatory T cells

(T_{reg} cells) and myeloid-derived suppressor cells (MDSCs) can also suppress immune responses. Both cell types are leukocyte populations that play key roles in inhibiting host-protective antitumor responses. T_{reg} cells inhibit tumor-specific T lymphocytes by producing IL-10 and TGF-β, by expressing inhibitory molecules like CTLA-4, PD-1, and PD-L1, and by consuming IL-2, a critical cytokine for cytotoxic T lymphocyte (CTL) function (Terabe and Berzofsky 2004). MDSCs inhibit lymphocyte function by promoting T_{reg} cells (B. Huang et al. 2006), producing TGF-β, depleting arginine, tryptophan, or cysteine, required for T cell function (Srivastava et al. 2010), or by nitrosilation of T cell receptors (TCR) or chemokine receptors on tumor-specific T cells (Nagaraj et al. 2008). Also, the T_H2-biased immune response is highly associated to the differentiation of tumor-attracted monocytes into an M2 macrophage phenotype, which reinforces the production of anti-inflammatory cytokines such as IL-10, TGF-β or IL-12, that eventually cause a reduction in immune-mediated toxicity by effector cells and antigen presentation by APCs. This subset of tumor-associated macrophages (TAMs), opposed to the pro-inflammatory M1 subset, is strongly linked to tumor progression due to its role in tissue repair and immunosuppression, which protect the tumor (Allavena and Mantovani 2012). All these mechanisms lead to a dormant immune system within the tumor that is not able to fight its proliferative status.

1.2.2.3.1 Immune checkpoints

T cell-mediated immunity relies on a balance between activating and inhibitory stimuli which determines the neat outcome of the response. On one hand, co-stimulatory proteins such as CD80 or CD86, expressed in APCs, provide the critical signal for efficient T cell clonal expansion and cytokine release. On the other hand, epithelial cells or even immune cells can express inhibitory molecules, also known as immune checkpoints, which counter the co-stimulatory signals. When these checkpoints outnumber the activating signals, potentially effector T cells enter in an unresponsive state or anergy, and eventually undergo apoptosis or differentiate into tolerance-inducing T cells (T_{regs}) (Mellman, Coukos, and Dranoff 2014; Merelli et al. 2014).

In physiological conditions, these checkpoints play a crucial role in preventing autoimmune responses in healthy tissues. They can also be involved in processes such as brain and bone homeostasis, transplantation or pregnancy, where sustained immune tolerance is essential (Holmannová et al. 2012; L. Lee et al. 2006). In the context of tumors, however, upregulation of these checkpoints has been widely associated as an ‘adaptive resistance’ mechanism adopted by tumor cells upon an immune attack (Mellman, Coukos, and Dranoff 2014).

Among the abundant number of checkpoints identified in the past years, PD-1/PD-L1 and CTLA-4 are the most investigated ones for their potential in cancer immunotherapy approaches, and many efforts are being made to bring targeted therapies against these two markers to the clinic (Merelli et al. 2014). In this work, the targeting of another immunological checkpoint, CD200 (also OX-2), which exerts its function mainly at the myeloid level, unlike the two previously mentioned exclusive T cell inhibitors, is to be discussed.

1.2.2.3.1.1 The tricky CD200:CD200R axis

Both ligand CD200 and receptor CD200R are highly conserved type I transmembrane-anchored glycoproteins belonging to the Immunoglobulin superfamily due to the presence of C-type and V-type regions at their extracellular N-terminal domains (Holmannová et al. 2012). CD200 was firstly identified in the early 80s (Barclay 1981), and the receptor was described by the same group two decades later (G J Wright et al. 2000). Both proteins share their extracellular and transmembrane domains, but differ at their cytosolic C-terminal domains, since CD200 is unable to transduce any kind of signal, whereas CD200R1, the main CD200 receptor, presents tyrosine receptor features that allow it to transduce downstream immune inhibitory signals, essentially through the PI3K and MAPK pathways. However, another human CD200 receptor (CD200RLa) and others in rodents have been characterized with alternative signal transducing structures and with controversial roles of activating and inhibitory roles (Akkaya et al. 2013; Jenmalm et al. 2006; Gavin J Wright et al. 2003).

In terms of expression patterns, CD200 is more ubiquitous and can be found in many cell types such as lymphocytes, dendritic cells, endothelial cells, retina, central nervous system or hair follicle cells. This broad gamut of $CD200^{+}$ population is very illustrative of the pivotal role CD200 may have as a tolerance inducer. In contrast, CD200R is mainly restricted to cells from the myeloid lineage, such as dendritic cells and macrophages, but it has also been described in subsets of T and NK cells (Reginald M Gorczynski 2012), specially as an indicator for T cell exhaustion in chronically inflamed tumors, that is, CD200 and CD200R expression seems enhanced in CTLs when compared to naïve T cells (Caserta et al. 2012; Coles et al. 2011).

It has been shown in a number of studies that CD200-mediated signaling results in the inhibition of the myeloid function by the induction of regulatory cytokines like IL-10 or TGFβ or the activation of IDO and the subsequent reduction of proinflammatory cytokine release. One of the first hints about this regulation was the inhibition of xenograft rejection in mice administered with a soluble version of CD200 (R M Gorczynski et al. 1999). Also, inhibition of mast cell degranulation and proinflammatory cytokine release was observed in the presence

of CD200 (S. Zhang et al. 2004). As for its role in cancer, it was firstly associated with tumor progression when the addition of soluble CD200 and CD200R$^+$ macrophages to C57/BL6 mice carrying bone marrow tumor challenges allowed the growth of tumors, whereas they were rejected in non-administered mice (R. M. Gorczynski et al. 2001). Later on, CD200 expression, both the full-length form and a soluble version lacking the transmembrane and cytosolic domains, was linked to tumor progression, poor prognosis and reduced antitumor immune responses in parallel studies, both in solid and liquid tumors (Colmont et al. 2013; Kretz-rommel et al. 2007; Rygiel et al. 2012; Stumpfova et al. 2010; Wong et al. 2010). A clear shift from T_H1 to T_H2 responses was observed in Mixed Leukocyte Reaction (MLR) assays where CD200$^+$ ovarian and melanoma cells were cocultured with myeloid cells, and CD200R antagonists rescued the T_H1 profile (Siva et al. 2008). Also, induction of T_{reg} differentiation has also been linked recentliy to CD200 expression (Curry et al. 2017). Finally, CD200 expression has been observed in cancer stem cells and it has been hypothesized that this subset of immune-privileged cells might be the founding population of tumors (Kawasaki and Farrar 2008).

Altogether, and even though it is still a not fully elucidated axis, a relevant tumor adaptative immunoregulatory function for CD200:CD200R has been described and has been highlighted as a possible target for cancer immunotherapy.

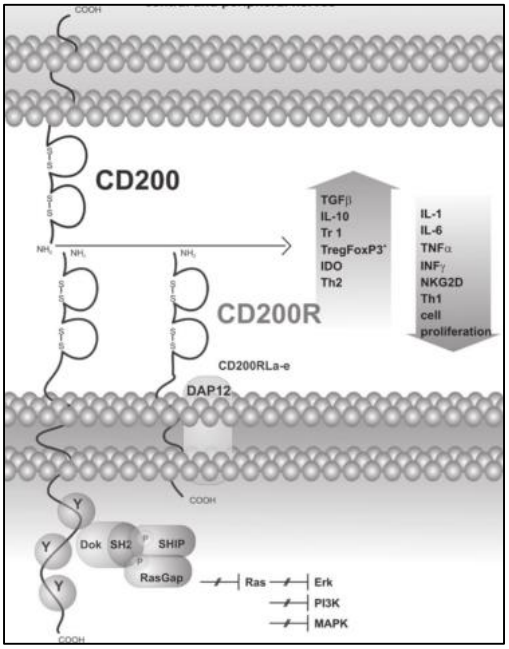

Figure 12. CD200:CD200R interaction and downstream effects. CD200 and CD200R are members of the Ig superfamily. Upon binding of CD200, found in many cell types, to the main receptor CD200R (left) or the alternate receptor founds in other species (right, CD200RLa-e), expressed mainly in myeloid cells, inhibitory signals are transduced are immunotolerance is induced. Adapted from (Holmannová et al. 2012).

1.2.3 Cancer immunotherapy

Taking into account the different mechanisms of tumor escape to the immune system and thanks to recent advances in molecular and cellular immunology, several immunotherapeutic treatments have been proposed to overcome this acquired resistance. Different approaches involve the use of anti-TAA antibodies like bevacizumab against VEGF or the BiTE™ technology, based on bispecific antibodies that enable an immunological synapse between the TAA-expressing cell and the surrounding $CD8^+$ effector T cell. Others involve adoptive T cell therapy, a very promising field, especially on the liquid tumor context, based on the manipulation of autologous immune cells, mainly T cells, to target a specific tumor epitope, so that they can be reinfused to the patient in search of an antitumoral response. Therapeutic cancer vaccines, with over 400 products in clinical trials, or immune checkpoint blockade, with successful examples in the clinic such as the anti-PD1:PD-L1 pembrolizumab, nivolumab or atezolizumab or the anti-CTLA4 ipilimumab, are also the big players around. In this work, focus will be made on anti-CD200 treatment from an 'immunocentric' point of view, due to its relevance for the results presented in the following sections.

1.2.3.1 Targeting CD200:CD200R

Even though, as explained before, the CD200:CD200R axis presents a number of challenges to deal with, ranging from the polymorphic degree of CD200R to the uncertainty around the precise mechanism of inhibition it exerts, its continuous appearance as a hurdle for immunotherapy in many kinds of tumors has encouraged researchers to seek drugs that can efficiently block this immune checkpoint.

1.2.3.1.1 Monoclonal anti-CD200 antibodies

Since CD200 and all CD200R variants show membrane localization and are expressed in systemically available tumors like B cell Chronic Lymphocytic Leukemia (B-CLL), Multiple Myeloma (MM) or Acute Myeloid Leukemia (AML) (Coles et al. 2015; Conticello et al. 2013), the generation of monoclonal antibodies against these proteins seems a logical step forward. In this sense, efforts have been made to antagonize CD200R, the inhibitory mediator of myeloid function upon binding with CD200, which has no signal transducing domains. In spite of the obstacles that a polymorphic receptor such as CD200R poses when trying to find a fully antagonizing antibody, preclinical studies in NOD/SCID humanized mice harboring human CD200-expressing tumors and treatment of those with human PBMCs in the presence or absence or differently engineered anti-CD200 antibodies have yielded interesting data. It has

been shown that the inhibition exerted by CD200:CD200R in the PBMCs can be suppressed by either antibody-dependent cell-mediated cytotoxicity (ADCC), achieved with IgG1-containing antibodies, or by specific inhibition of the signaling cascade, mediated by hybrid IgG2-G4 antibodies, which ensures a safer action, since ADCC might affect adjacent effector antitumoral T cells or healthy $CD200^+$ cells (Akkaya et al. 2013; Kretz-rommel et al. 2007). A thorough screening of diverse anti-hCD200 candidates has been performed, and this knowledge is protected under the patents US8075884 and US8709415.

1.2.3.1.2 Truncated CD200

Despite the efforts to find efficient blockade of the CD200 pathway, there is actually a naturally-occurring CD200R antagonist. In detail, a splice variant from CD200 lacking 43 aa from exon 2, which belongs to the V-type Ig domain of its N-terminal region, was detected in lymphoid tissue from immunized BALB/c mice (Borriello et al. 1998). The role of this splice variant, named CD200tr, was further analyzed for the murine and human versions and, interestingly, it showed specific binding to hCD200R and an antagonist behavior compared to CD200 in MLRs, in terms of TNFα secretion and human target cell lysis (Z. Chen et al. 2008). Antibodies against CD200tr and uses thereof are protected under the patent US20040054145. Allegedly, hCD200tr would be a natural competitor for CD200R binding (it binds with the same affinity than the full-length version) but would not engage signaling upon binding, thus acting as a positive regulator of the myeloid function. These data are in line with other studies in which 15-mer peptides derived from the extracellular domains of CD200 were shown to already compete for CD200R binding, but were not able to induce the immune suppression mediated by full-length CD200:CD200R interaction (D. X. Chen, He, and Gorczynski 2005; Reg Gorczynski, Boudakov, and Khatri 2008).

In deeper studies looking for the regulation of the human CD200:CD200tr ratio, it has been shown that both viral infections and tumors promote a biased splicing pattern favoring CD200 at the expense of CD200tr, allegedly with the aim of inducing a tolerant microenvironment. Interestingly, total transcription levels of the CD200 mRNA do not vary, but splicing mediators SF2/ASF, which allow exon 2 inclusion in the final protein through an Exonic Splicing Enhancer (ESE), are increased in the full-length CD200-favoring conditions (Z. Chen et al. 2010; Reginald M Gorczynski 2012). Notwithstanding, such immune evading mechanisms are not the only tools at hand of pathogens. Another way to trick the immune system will be explained in the following lines due to its relevance for the oncolytic virotherapy approach shown in this work.

1.2.3.1.3 K14, a viral CD200 orthologue

Pathogens have been successfully overcoming the human immune system for millions of years. They have mastered their multiple abilities to evade recognition by the innate immune cells and to delay or attenuate the antigen-specific adaptive responses, as has been introduced in the previous section. For the case of paired receptors such as human CD200:CD200R, the 'counterbalance theory' suggests that pathogens target inhibitory receptors in host immune cells and therefore acquire inhibitory ligands, such as CD200, to prevent their elimination. Hence, host activating receptors would be evolutionary responses to such pathogenic mechanisms, by means of gene duplication resulting in extracellularly almost identical receptors lacking the ability to transduce inhibitory signals upon binding to their ligands (Akkaya and Barclay 2013).

There are nowadays 26 viral CD200 homologs from 3 virus types (Herpes, Pox and Adenoviruses) described in the literature (Cameron et al. 2005; Estep et al. 2014; Farré et al. 2017; Foster-Cuevas et al. 2011), among which K14 from Human Herpesvirus 8 (HHV-8) is the most characterized one. K14 shows 40% sequence identity to human CD200, yet it completely shares the double Ig-like domain structure of CD200. It is expressed bicistronically together with ORF74, another immune inhibitory protein, once the lytic phase of HHV-8 is engaged, and has been shown to bind CD200R with identical kinetics than endogenous CD200 and to reversibly decrease TNFα secretion in myeloid cells, clearly indicating an immune evading mechanism to favor viral spread (Foster-cuevas et al. 2004; Kirshner et al. 1999; J. Zhang et al. 2005). However, there are also reports indicating an immune activating role for K14 in promoting HHV-8-mediated sarcoma, also known as Kaposi Sarcoma. In such studies, release of IFNγ, TNFα and IL-1β is associated to K14 expression, and an uncontrolled angioproliferative response mediated by infiltrating lymphocytes upon myeloid activation for the development of KS is proposed (Chung et al. 2002).

In this work, we hypothesize that a truncation of the HHV-8 K14 protein, which we named K14tr, in a parallel manner to that of CD200tr, might result in an unprecedented viral-derived CD200R antagonist, as the majority of literature we found would suggest. In order to test this, soluble versions of hCD200, hCD200tr, K14 and K14tr lacking the natural transmembrane and intracellular domains were cloned into adenoviral vectors.

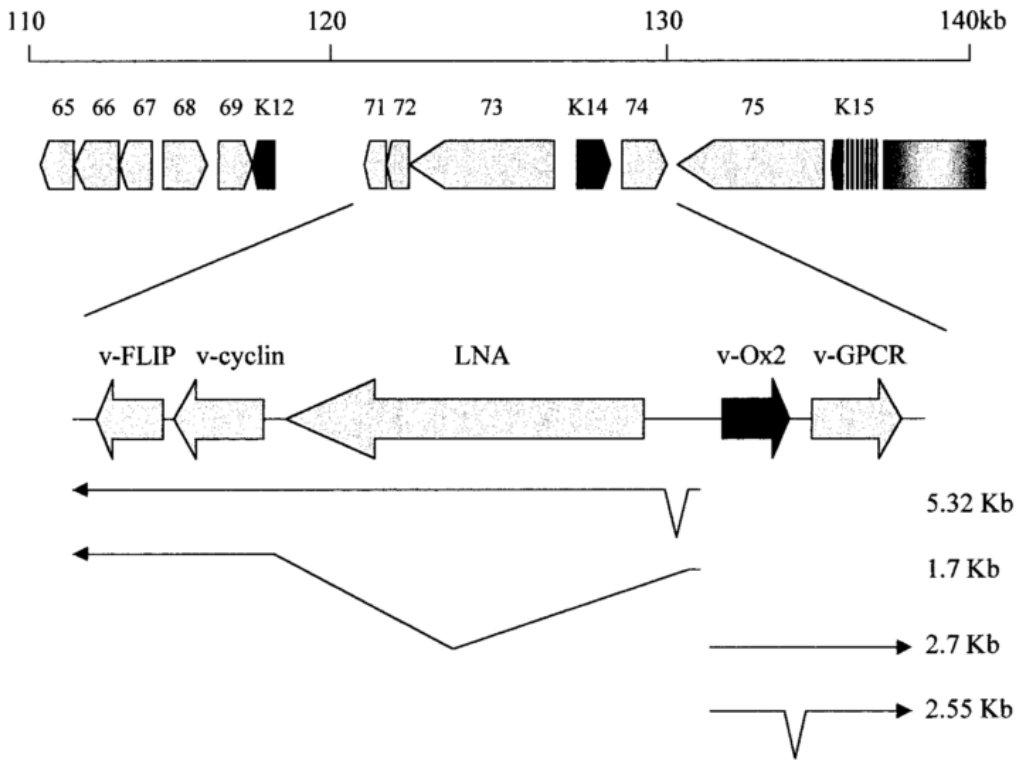

Figure 13. Genomic organisation of the right end of the HHV-8 genome. ORFs 71 (K13)–74 encoding K14 (v-Ox2), and v-GPCR (also ORF74), among others, are shown. Splicing patterns is indicated by arrows. The expression of K14 is restricted to the lytic phase of HHV-8, when immunotolerance against viral epitopes is critical to ensure secondary infections of the new viral progeny. Adapted from (Talbot et al. 1999).

1.2.3.2 Oncolytic adenoviruses and immunotherapy

The immunocentric perspective was not acquired by oncolytic virotherapy until the last decade, when inflammation in tumors treated with oncolytic Adenoviruses was associated to immunological processes related to the release of PAMPs by lysing cells, which compromises the tumor-induced tolerance (Hemminki 2014) and can prime adaptive antitumor immune responses. Later, the generation of danger signals by the activation of the TLR-9 pathway was elucidated. Moreover, the characterization of tumor-infiltrated lymphocytes (TILs) whose inhibition can be reverted in order to mount an antitumor immune response added interest to this emerging field.

From this revealing studies, several Adenoviruses carrying immunomodulating transgenes have been developed. Some of them already appeared in section 1.1.1.7, like LOAd703, a CD40L-expressing virus currently in clinical trials which induces strong immunostimulation and proliferation of CTLs (Eriksson et al. 2017; E Eriksson et al. 2017), or CG0070, a GM-CSF-expressing Adenovirus with promising outcomes observed in clinical trials (Burke et al. 2012). Expression of immunostimulatory cytokines such as IFNα, IFNγ, GM-CSF, IL-12, IL-18, TNFα or

costimulatory molecules like B7-1 has been chosen in many cases, even in dual strategies (I.-K. Choi et al. 2011; K.-J. Choi et al. 2006, 2012) to disrupt the immune tolerance induced by tumors in the microenvironment (Chang et al. 2009; Hirvinen et al. 2015; Y. S. Lee et al. 2006; Shashkova et al. 2007; Su et al. 2006; Zheng et al. 2010). Other approaches include the combination of OAds and radiation to produce enhanced immune responses (Kim et al. 2011), the augmentation of TLR9 signaling through the insertion of CpG sequences in the adenoviral genome seeking the same outcome (Cerullo et al. 2012), the expression of Heat-Shock Porteins (HSP) to improve the efficiency of peptide transportation into MHC molecules (X. F. Huang et al. 2003), the combination of DCs and OAds to enhance the presentation of TAA to effector cells (J.-H. Huang et al. 2010). Also, endeavors towards personalized antitumor gene therapy have been made, with Adenoviruses displaying TAAs from the patient's tumor in the viral capsid (Capasso et al. 2016).

In our group, an oncolytic Adenovirus expressing a Bispecific T cell engager (BiTE) was developed, with which effective retargeting of T cells towards Epidermial Growth Factor Receptor (EGFR) was demonstrated (Fajardo et al. 2017). Other similar approaches are also being developed with other target tumor epitopes.

In the recent years, with the blossom of immunotherapy but also the report of resistance to immune checkpoint blockade, some strategies combining OAds and immunotherapeutic drugs, such as immune checkpoint inhibitors have been engaged, in search of an additive or synergistic immunostimulatory effect of both the Adenovirus itself and the already proven inhibitors. In this sense, a chimeric 5/3 Adenovirus expressing an anti-CTLA-4 antibody proved to induce higher IFNγ and IL-2 levels in PBMCs from oncologic patient samples (Dias et al. 2012). Checkpoint combination with virotherapy, specifically anti-PD1 and anti-PD-L1 antibodies with different OAds, is also ongoing in separate administration in four different clinical trials (NCT02636036, NCT02798406, NCT03003676, NCT02798406).

Interestingly, Woller and colleagues demonstrated that an Adenovirus with a modified E1a protein under the control of the TERT promoter could overcome resistance to PD1 immunotherapy by broadening the neoepitope repertoire against which CTL were amplified, achieving a sustained CD8 response (Woller et al. 2015).

In general, immune stimulation and antitumor immune responses have been achieved in many of these approaches. However, clear and long lasting antitumor efficacy still needs to be harnessed in order to consider OAds as possible first line immunotherapeutic treatments.

1.2.3.2.1 An oncolytic adenovirus targeting the CD200:CD200R axis

Research in the oncolytic adenoviral therapy field has yielded a fruitful technological platform to address the eradication of tumors from multiple perspectives. ICOVIR-15 constituted a real door-opener, since its significantly reduced genome, thanks to the insertion of the E2F-responsive boxes, allowed for the first time the insertion of transgenes into the adenoviral genome without impairing its encapsidation step, and consequently, its viability (Juan J Rojas et al. 2010).

From then on, in our group, several adenoviruses carrying transgenes with very diverse functions have been developed: degradation of the extracellular matrix (Guedan et al. 2010), cell fusion and formation of sincytia (Guedan et al. 2012), and, more recently, activation of cytotoxic T lymphocytes against a tumor epitope (Fajardo et al. 2017). In most of these approaches, significant advantages from the insert-virus combination have been observed in terms of antitumor efficacy, which has encouraged the group to enhance the number of transgene-based approaches.

In this thesis, we propose the insertion of immune modulating transgenes within the ICOVIR-15K genome in order to test their ability to interfere in the myeloid function through the CD200:CD200R inhibitory pathway. In our ideal scenario, the TLR9-mediated activation elicited by the virus added to the CD200 inhibition mediated by our truncated proteins CD200tr or K14tr will result in an enhanced T cell activation, which, in the context of a real tumor, could collaborate in mounting an antitumoral adaptive immune response through the activation of anti-TAA CTLs and completely eradicate the tumor burden. Also, since the Ad5 serotype does not infect DCs or T cells efficiently, these populations would render unaffected from the oncolytic process. Of course, the immunodominance of the viral epitopes is an issue that could bias these responses but is not addressed in this work. However, an important advantage derived from this approach is that, by the initial inhibition of CD200 and the generation of a strong immune response, premature clearance of the virus by the immune system could be a negligible problem if a sustained antitumoral response has also been started, provoking a long-term antitumor effect caused by these OAds even when they are not there anymore.

1.3 Activatable drugs for the treatment of cancer

Some decades ago, cancer researchers and medical professionals realized that the successful cure for many malignancies, especially solid tumors, required approaches beyond conventional non-selective anticancer drugs, which have not only showed modest results in

several tumor types, but also cause notorious side effects in most of the patients. Trying to overcome both limitations, cancer targeting appeared as a promising field where specific tumor-associated antigens or proteases become the triggers of the treatment. In this line, huge amounts of monoclonal antibodies, specific inhibitors or metabolism-targeted drugs have been developed (Dubowchik and Walker 1999).

Denmeade and Isaacs used the term 'molecular grenade' to describe a combination of a non-selective toxin with an inhibition system to render it tumor-specific, that is, the inhibition system should be targeted so that it becomes unlocked only when the drug enters the tumor microenvironment. The main advantages of this approach are the feasibility of increasing the administrated dose, the reduction of the secondary effects and the unspecific bystander effect caused by the 'detonation' of the cytotoxic agent. To maximize the effectiveness of this strategy, the toxin must be highly cell penetrating, highly toxic to affected cells, and it must allow conjugation with an inhibitory peptide (Denmeade and Isaacs 2012). Examples of such approach are peptide hormone conjugates to treat bombesin receptor-expressing tumors, or protease-activated conjugates like a glucuronidase-sensitive doxorubicin (P. S. Huang and Oliff 2001). The tumor stroma appears to be a fruitful target for this approaches due to the abundant number of specific proteases that are overexpressed in it. In this line, a thapsigargin (toxin of plant origin)-derived conjugate which is activated when it encounters the Fibroblast Activation Protein (FAP) expressed in tumor fibroblasts has been developed with promising results (Brennen et al. 2012, 2014).

Avoiding unwanted activation of the prodrug is an important concern, as well as achieving full action upon release of the inhibition system. Taking this into account, bacterial-derived toxins have attracted attention due to their convenience to meet the above mentioned requirements. In the following pages, more detail about the toxins chosen for this work will be provided, as well as about the design and the advantages that their expression from an oncolytic adenovirus might imply.

1.3.1 Pore-forming toxins (PFTs)

Bacterial pathogens are highly opportunistic in nature. Such feature can only be explained by the evolutionary development of effective virulence agents able to cause severe damage to eukaryotic cells. In the 1960s, the term 'hemolysin' was initially coined as a general name for these factors, since they were basically discovered by their ability to lyse erythrocytes *in vitro* (G. van der Goot 2001). After decades of research, proteins secreted as water-soluble molecules able to bind membranes, oligomerize and generate pores in target eukaryotic cells

have been classified into PFTs, which represent the 30% of all known bacterial proteins. There are many criteria in the literature to classify them. According to the structure with which they eventually cross the cell membrane, α-PFTs (helical) and β-PFTs (barrel) can be found. One of the traits that makes them attractive for targeted therapies is that, naturally, some PFTs must be cleaved by host proteases to activate their lytic functions (Iacovache, van der Goot, and Pernot 2008). Two related toxins meeting this last point were chosen in this work for their cloning into the genome of an oncolytic adenovirus.

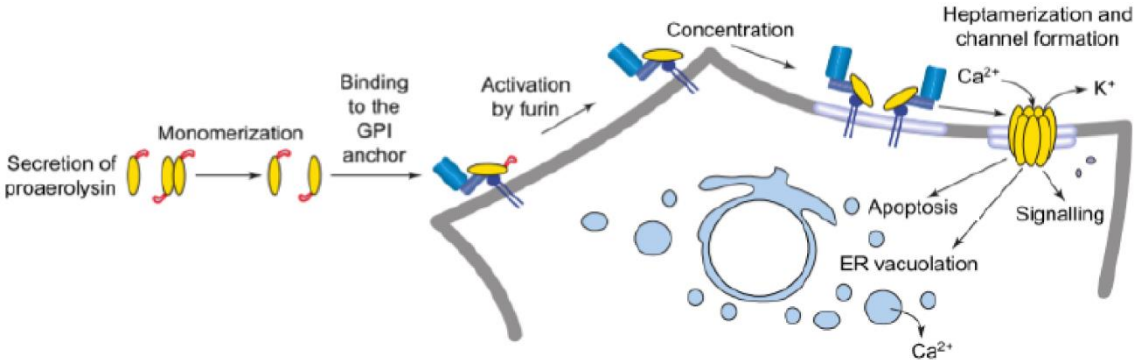

Figure 14. Schematic representation of the pore formation process of PFTs. Aerolysin is a paradigmatic example of PFTs. The proaerolysin monomer (or dimer) binds to the glycan of GPI-anchored proteins on mammalian cells and is then processed to aerolysin by furin. The mature form of the toxin heptamerizes and loses its water solubility. Eventually, a pore is formed in the membrane which selectively permeabilizes it to small ions. As consequences, calcium is released from the ER, vacuolation is observed and varying apoptotic pathways are triggered. Adapted from (Abrami, Fivaz, and Van Der Goot 2000).

1.3.1.1 Aerolysin from Aeromonas hydrophyla

Aerolysin is a 54-kDa protein secreted by *Aeromonas hydrophyla,* a water-borne Gram-negative bacterium responsible for a number of malignancies, from gastroinstestinal and wound infections to septicemia. It was firstly associated to human pathogenicity in the 80s (Daily et al. 1981) and firstly characterized in the 90s (Parker et al. 1994; Tucker et al. 1990). Aerolysin is secreted as a water-soluble monomeric or dimeric protoxin (Howard and Buckley 1985) which then binds glycophosphatidil-inositol (GPI)-anchored proteins, preferably Thy-1 (Kim L. Nelson, Raja, and Buckley 1997), on eukaryotic cell membranes and becomes activated by furin, which recognizes the sequence K^{427}VRRAR^{432} and cleaves a 18-aa long C-terminal peptide that prevents premature oligomerisation of the toxin (Abrami et al. 1998). Once activated, it stabilizes at the outer membrane thanks to its interaction with lipid rafts, builds up a heptamer that undergoes a conformational change and eventually forms a pore on the cell membrane by the insertion of two concentric β-barrel in a piston-like fashion (Abrami,

Fivaz, and Van Der Goot 2000; Iacovache et al. 2016). This aggression results in an osmotic imbalance of calcium and potassium, endoplasmatic reticulum (ER) vacuolation and engagement of proapoptotic and necrotic signaling pathways. Altogether, and even though cells can remain alive for several hours, aerolysin-mediated effects lead to increased cell permeability and cell lysis (Knapp, Stiles, and Popoff 2010).

A modified aerolysin carrying a PSA-sensitive linker HSSKLQ instead of the natural furin-sensitive one has already shown selective cytotoxicity and antitumor effect in PSA-expressing cell lines and tumor models, respectively (Williams et al. 2007), setting an appealing precedent for targeted drug therapies with this toxin.

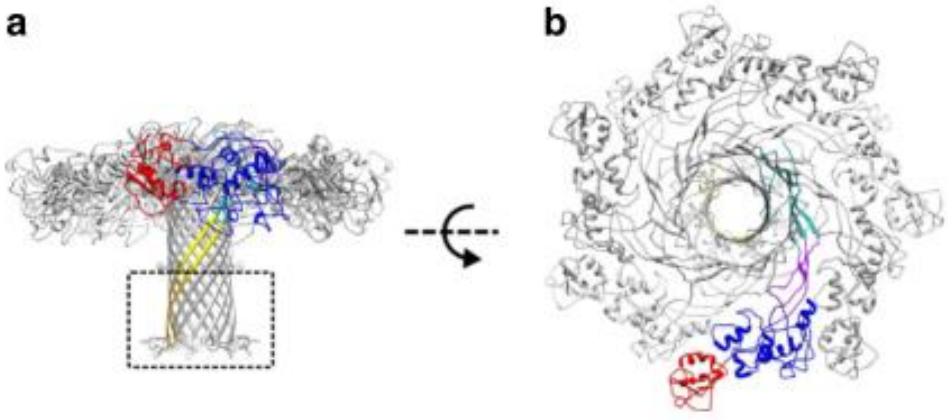

Figure 15. Quasipore heptameric structure of aerolysin. Side (a) and top (b) views of a heptameric aerolysin complex in the pore formation process. Receptor binding domains of a single monomer are colored in red and blue. Adapted from Iacovache et al. 2016.

1.3.1.2 Alpha-toxin from Clostridium septicum

Alpha-toxin (atox) is the main virulent factor from the anaerobic Gram-positive bacterium *Clostridium septicum,* responsible for gas gangrene and myonecrosis of the intestinal mucosa in humans. Atox, with a size of 47.5 kDa, belongs to the aerolysin-like family of PFTs and was isolated in the early 90s (Ballard et al. 1992). Even though it shares only 27% of the aminoacid sequence with aerolysin, they are very closely related structure-wise. Similarly to aerolysin, it is secreted as a protoxin from the bacterial cell, binds GPI-anchored proteins such as Thy-1 or Folate Receptor (hFR), oligomerizes after the furin-mediated cleavage of a 45-aa long C-terminal inhibitory peptide and forms a pore on the cell membrane by a parallel mechanism to aerolysin (Knapp et al. 2010; Popoff and Bouvet 2009). Unlike for aerolysin, it has been shown that the atox inhibitory peptide also acts as an intramolecular chaperone, therefore being crucial for the correct folding of the protein until the oligomerization process begins

(Sellman and Tweten 1997). Consequences at the cellular level are very similar to aerolysin-mediated cytotoxicity: osmotic imbalance, ER vacuolation, activation of proapoptotic and necrotic signaling pathways with the common fate of cell lysis (Knapp et al. 2010).

1.3.2 Oncotargeting of PFTs

PFTs gather a number of features that, in combination, make them appealing for targeted therapies. Firstly, they bind membrane proteins that are ubiquitous among tissues. Secondly, they are potent cytotoxic agents on affected cells, inducing necrosis in short times. Finally, they are secreted as protoxins (also called 'zymoxins'), that is, they are actually naturally-occurring prodrugs that become activated by the cleavage of determined proteases. Luckily enough, many tumoral processes such as invasion, angiogenesis or metastasis, involve the action of specific proteases which are not expressed in healthy tissues. Among those cancer-specific proteases, matrix metalloproteases (MMPs), a large family of calcium-dependent zinc-containing endopeptidases with more than 25 members in humans, possess central roles to pave the way for the establishment and progression of tumors due to their interaction with the extracellular matrix, and their inhibition has been pursued as cancer treatment for a long time (Mannello, Tonti, and Papa 2005; R. P. Verma and Hansch 2007). Specifically, MMP-2 and MMP-9, also called gelatinases A and B, respectively, named after their main substrates and with overlapping functions and structures, have been widely linked to poor prognosis in breast cancer and melanoma, to name a couple (Uta B. Hofmann et al. 2000; Ranuncolo et al. 2003). It has been shown that these two soluble MMPs, secreted by stromal fibroblasts, collaborate in triggering the angiogenic switch in tumors, that is, the formation of new vessels from the invasive front of the tumor, mainly by inducing the release of VEGF from adjacent endothelial cells (Bergers et al. 2000).

MMP-2/9-sensitive linkers have already been tested even in the oncolytic virotherapy field: retroviral capsid proteins have been engineered to become activated upon cleavage of MMP-2/9 and thus render the virus oncoselective (Schneider et al. 2003), and the adenoviral fiber gene has been modified to be transduction-competent only upon cleavage of an MMP-2/9-sensitive peptide linker, AKGLYK (Szécsi et al. 2006), that releases an inhibitory domain (José et al. 2014). This linker was chosen in this work to substitute the natural furin-cleavable linker present in aerolysin so as to render it stroma-activatable.

Another interesting tumor-specific protease in the zymoxin field is Fibroblast Activation Protein-α (FAP). This 95 kDa protease is a member of the dipeptydil peptidase 4 (DPP4) family and has been highly associated to wound healing processes in tumors by inhibiting plasmin, a

major effector of fibrinolysis, but also to immunosuppression and invasiveness, since it is a collagenolytic enzyme. It is also expressed almost exclusively in stromal fibroblasts, particularly at the invasive front, of most of epithelial cancers, even though preclinical studies have shown reduced expression of FAP in healthy proliferative tissues in mice (Garin-Chesa, Oldt, and Rettigt 1990; Hamson et al. 2014; Huber et al. 2003).

The best available example of FAP-mediated prodrug activation is the one mentioned previously in this section involving thapsigargin (Brennen et al. 2012, 2014). The same group had initially developed a FAP-activatable melittin toxin, from the honeybee, which had already shown FAP-dependent cytotoxicity *in vitro* (LeBeau et al. 2009). There are some FAP-sensitive linkers described in the literature. In this work, linkers from collagen I and a tyrosine kinase receptor named SPROUTY2 (Spry2), with aminoacid sequences DRGETGPS and GSSFSSGPSVDS respectively, were chosen to substitute the natural furin-linker linker in atox as a stroma-targeting strategy (Aggarwal et al. 2008; C. H. Huang et al. 2011).

The smart combination of cancer-specific protease activity and zymoxin activation derived from the lines above has produced promising data, and several parallel endeavors are already on the run. In this work, synergy with the already efficient oncolytic adenovirus ICOVIR-15K by inserting these genes into its genome is to be tested.

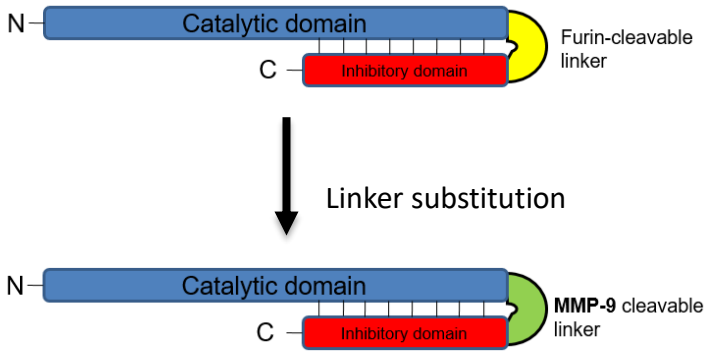

Figure 16. Oncotargeting of PFTs. Schematic representation of linker substitution strategy in aerolysin. The resulting modified toxin will be activated in solution by MMP-9, an ECM-degrading enzyme expressed selectively in the tumor stroma by stromal cells.

1.3.2.1 Oncolytic viruses expressing stroma-targeted PFTs

The advantages brought by the generation of adenoviruses expressing stroma-targeted PFTs comprise, in the first place, the already mentioned oncolytic effects at the tumor site, that is, cell lysis and localized transgene expression in cyclic and exponentially increasing

rounds. But mainly, the novelty brought about by this approach is the unspecific, rapid and potent cytotoxicity caused by the PFTs upon their activating cleavage. Unlike previous strategies, the cytotoxic span of PFTs includes not only tumor cells, since both aerolysin and atox bind GPI-anchored proteins, present in all eukaryotic cells, and will form pores in all of them. Provided that, stromal fibroblasts, traditionally a huge obstacle for the efficient viral spread within the tumor and eventually tumor eradication, as reviewed in section 1.1.1.8.2, will, for the first time, become a target of the oncolytic approach, and any advance in harming them will be extraordinary valuable.

In order to achieve the best possible outcomes, however, optimal conditions for the configuration of such viruses are uncertain. In the atox approach, the traditional insert region after the L5 gene was chosen, with the presence of the IIIa splicing acceptor and the 5' kozak CCACC sequence to maximize transgene yields. For the aerolysin-expressing virus, however, a more distant insertion was performed, between adenoviral E4 locus and the RITR. This time, a stronger splicing acceptor was chosen (BPSA) and Kozak was also included. Insertion in this region has been shown to render transgene expression less leaky than in other sites, while not impairing virus viability (Jin, Kretschmer, and Hermiston 2005; Quirin et al. 2011). For both cases, human-biased codon-optimization was performed, and eukaryotic signal peptides were added at the N-terminal site of the transgenes. ICOVIR-15K was chosen as the adenoviral platform for these viruses, since liver detargeting looks primordial in order to minimize unwanted off-site effects from these very potent toxins (J J Rojas et al. 2012).

2 OBJECTIVES

Oncolytic virotherapy has overcome numerous difficulties on its way towards clinical efficacy. Still today, and even though many efforts have been made, some of those hurdles look challenging to defeat. In this work, we have addressed two of them. Firstly, we have generated a panel of oncolytic Adenoviruses carrying both CD200R agonists, that induce immunosuppressive microenvironments, and potential CD200R antagonists, in search of a 'break release' in the immune system that could eventually turn into an antitumor immune response. Secondly, we have generated another panel of oncolytic Adenoviruses expressing pore-forming toxins, modified in such a way that become activated exclusively by proteases present in the tumor stroma. This way, we expect the toxins to induce potent unspecific cytotoxicity only in the tumor burden, affecting both tumor cells and fibroblasts, which are very resistant to virus replication and which generally constitute an obstacle for the success of this therapy.

The general objective of this thesis was to evaluate the feasibility of the above mentioned viruses for clinical application. Also, specific objectives were set for each chapter:

Oncolytic adenoviruses carrying soluble versions of human CD200, CD200tr, the viral homolog K14 and K14tr

- To generate and characterize oncolytic Adenoviruses expressing soluble versions of the human CD200, CD200tr, the viral protein K14 and a truncated K14tr.
- To evaluate the immunoregulatory effect of the different viruses in contact with immune cells.
- To find a suitable model in which the CD200:CD200R pathway can be adequately studied.

Oncolytic adenoviruses expressing stroma-activatable toxins

- To generate and characterize oncolytic Adenoviruses expressing stroma-activatable Alpha-toxin and aerolysin.
- To test the functionality and specificity of the modified toxins in suitable in vitro assays.
- To evaluate the antitumor efficacy of the toxin-expressing viruses in preclinical models.
- To evaluate the disruption of the tumor stroma mediated by the modified toxins in the preclinical models.

3 MATERIALS AND METHODS

3.1 Handling of bacteria

In order to obtain sufficient amounts of plasmid DNA for easy manipulation, its amplification in bacteria was required. For this reason, the plasmid should have a replication origin that allows its replication on the desired strain and a gene that confers resistance to an antibiotic in order to select the bacteria and avoid contaminations. In this work, the *Escherichia coli* strain DH5α has been used to this purpose. Moreover, the SW102 strain has been used to perform homologous recombination.

3.1.1 Preparation of competent bacteria

The bacteria stock was conserved at -80°C with 15% glycerol. In order to induce competence, the glycerinate was scratched with a sterile pipette tip into 10 mL of LB (1% Tryptone, 0.5% Yeast Extract, 0.5% NaCl) and it was grown overnight at 37°C in a 50 mL Falcon tube under agitation. Next day, the 10 mL preculture was grown in 1 L of LB at 37°C in agitation until the culture reached an OD of 0.6-0.7 at 600 nm. The bacterial solution was distributed in 250 mL bottles (suitable for centrifugation in a SORVALL centrifuge) and kept 40 minutes on ice in order to stop bacterial growth. Further manipulation of bacteria was carried out at 4°C. Next, bacteria were centrifuged 15 minutes at 4000 *g* and 4°C in a SORVALL centrifuge, supernatant was discarded and the pellet was washed with cold bi-distilled (dd)H_2O water (4°C). This centrifugation/washing process was repeated 3 times and in the last wash the pellet was resuspended in 45 mL of water with 10% glycerol. Bacteria were centrifuged one more time and, finally, resuspended in 3 mL of water containing 10% glycerol. Next, OD at 600 nm was measured from a 1:100 dilution of the suspension. OD value should be close to 1 (which equals $2.5x10^8$ bacteria/mL). Finally, the bacterial suspension was distributed in 50 µL aliquots that were immediately frozen in carbon dioxide and stored at -80°C.

3.1.2 Transformation of competent bacteria by electroporation

Bacteria aliquots stored at -80°C were thawed on ice and an amount of plasmid DNA between 10 pg and 25 ng was added in a final volume of 2 µL. The mixture was incubated 5 minutes on ice and added to previously cooled electroporation cuvettes. Then, bacteria were electroporated with the Electro Cell Manipulator™ ECM 630 at the following conditions: 50 µF, 1500 V and 125 Ω. Pulses lower than 5 miliseconds were considered correct. Immediately, bacteria were resuspended in 300 µL of LB and incubated for 1 hour in agitation at 37°C. The

suspension was plated on LB plates containing the corresponding selection antibiotic for each plasmid.

3.1.3 Obtaining plasmidic DNA from bacterial cultures

In this work, plasmidic DNA was obtained from saturated *E.coli* cultures which grew in LB with antibiotic according to protocols based on an alkaline lysis with SDS. DNA was prepared at small and large scale.

3.1.3.1 Small scale DNA preparations

DNA minipreparations were performed following an adapted protocol described by (Bimboim and Doly 1979), which allows the obtaining of 20-50 µg DNA preparations. The procedure is detailed below.

First of all, a colony grown in a LB-antibiotic dish was inoculated in 2 mL of LB+antibiotic and incubated overnight. Then an aliquot of 1.5 mL was taken and centrifuged at 13000 rpm 1 minute. Then the pellet was resuspended in 200 µL of pre-cooled solution 1 (25 mM Tris-HCl pH 8, 10 mM EDTA, 50 mM glucose). 200 µL of freshly prepared solution 2 (SDS 1%, NaOH 0.2 M) were added and the mixture was blended by inversion. Finally, 200 µL of pre-cooled solution 3 (3 M potassium acetate, 11.5% acetic acid) were added and the mixture was blended again by inversion until a white precipitate appears. The mixture was incubated 5 minutes on ice and centrifuged 15 minutes at 15000 *g*. Next, the clear supernatant was collected without taking the white pellet that corresponds to cellular DNA, proteins and SDS, and 2 volumes of ethanol were added. The mixture was incubated 15 minutes at room temperature (RT) and plasmidic DNA was precipitated by centrifugation 10 minutes at 15000 *g*, supernatant was discarded and the pellet was washed with 70% ethanol. It was centrifuged again 5 minutes at 15000 *g*, supernatant was discarded and the pellet was air-dried. Finally, plasmidic DNA was resuspended in 50 µL of TE with RNAse (10 mM Tris-HCl, 1 mM EDTA, 0.1 mg/mL RNAse).

3.1.3.2 Large scale DNA preparations

DNA maxipreparations allow obtaining large amounts of highly pure plasmidic DNA (≥100 µg). Maxipreps were prepared from 200 mL of saturated bacteria culture using the Invitrogen commercial kit "PureLink™ HiPure Plasmid Filter Purification Kits", following manufacturer's instructions.

3.1.4 Positive-negative selection homologous recombination in bacteria

Most of the homologous recombinations performed in this work have been conducted in bacteria because of the high efficiency of the system developed by Richard Stanton, who kindly gave us the plasmid pAdZ5-CV5-E3^{+} in SW102 strain of *E.coli*, which has the adenovirus genome type 5 (E1^{-}) as a bacterial artificial chromosome (BAC) and with chloramphenicol (Cm) resistance. This system works using phage *λ* genes Red*γβα* under the control of a temperature-sensitive promoter which is repressed at 32◦C and activated by incubating bacteria at 42◦C.

Resistance genes SacB and Ampicilline (Amp) were replaced by the more efficient system rpsL-neo in the original plasmid. The modification was done in two phases, and for each of them a fragment of DNA or insert was constructed. In the first phase or positive selection, we selected bacteria cells that have incorporated the inserted DNA. This first fragment had homology regions (about 40 bp) with the site we wanted to modify on each end. Moreover, this fragment includes rpsL-neo genes, so after the first transformation recombinant clones with Kanamycin (Kan) resistance provided by neo gene were selected. In the second phase or negative selection, susceptibility to Streptomycin (Strep) provided by rpsL gene (since SW102 strain is naturally resistant to Strep) was lost. The second fragment had the same homology arms but, in this case, it included the modification that we wanted to insert. After the second transformation, recombinant clones were those that had incorporated the inserted DNA and had lost the rpsL-neo fragment.

Plasmid pAdZ5-CV5-E3^{+} was modified in order to obtain pAdZ-ICOVIR-15K plasmid, the backbone that has been used to introduce the modifications described in this thesis.

The procedure that has been followed to perform recombinations is described next. First of all, glycerinates of the bacteria that contain the plasmid to be modified were scratched with a sterile pipette tip, inoculated in 5 mL of LB media including Cm + Strep antibiotics (12.5 µg/mL, and 1 mg/mL, respectively) and incubated overnight at 32◦C with constant agitation. Then 25 mL of LB Cm + Strep were inoculated with 0.5 mL of the previous culture and incubated at 32◦C with agitation until it reached an OD of 0.5-0.6 at 600 nm. At this moment, culture was split into two Falcon tubes with equal volumes. One of them was induced by incubation during 15 minutes at 42◦C and then cultures were incubated on ice for 15 minutes. From that moment, manipulation was done at 4◦C in order to ensure transformation efficiency. Both cultures (induced and non-induced) were centrifuged 5 minutes at 3220 *g* at 4◦C and supernatant was discarded. Bacteria pellet was resuspended in 12 mL of cold ddH_2O water and centrifugation

was repeated. In the same way, two more washes were performed and in the last one the pellet was resuspended in the remaining water (≤300 µL). Afterwards, 50 µL aliquots of bacteria (both from the induced and non-induced cultures) were transformed with 100-200 ng of DNA (the fragment which contains rpsL-neo). Bacteria were recovered in 1 mL of LB and incubated 70 minutes at 32°C. Finally, they were plated into LB plates containing Cm and Kan (12.5 µg/mL, and 15 µg/mL, respectively) and incubated overnight at 32°C. About 20-24 hours later, colonies should be grown and the ratio between the colonies obtained in the induced culture (recombinant) and the non-induced one (control) were compared in order to assess recombination efficiency. Then, colonies were picked, minipreparations of DNA were made and restriction patterns of different clones were checked. Finally, the correct clone was frozen as a glycerinate.

A similar procedure was followed for the second phase, in which the clones obtained in the previous step were inoculated in 5 mL of LB Cm+Kan and cultured overnight at 32°C. Next day, the bacteria were made competent for its transformation by electroporation as described previously. Again, 100-200 ng of DNA (insert containing the desired modification) were transformed. After the recovery incubation, 100 µL from a 1:25 dilution were plated in LB agar Cm+Strep plates and were incubated overnight at 32°C. 24 hours later, colonies were picked, minipreparations of DNA were obtained and clones were checked by the analysis of restriction pattern and/or sequencing of the recombinant region.

3.2 Cell culture

3.2.1 HEK293

Human Embryonic Kidney 293 (HEK293) cells derive from human primary embryonic kidney cells. This cell line has been transformed with a fragment of the Ad5 genome including the E1A gene. 293 cells are highly permissive for the generation and replication of adenoviruses and are easily transfectable by the calcium phosphate method. This cell line has been used for the generation and functional titration of the oncolytic adenoviruses.

3.2.2 Cell lines

Cell lines used in the *in vitro* and *in vivo* experiments and their origins (mainly tumoral or tumor-associated) are summarized in the following table:

Cell line	Tissue of origin	Origin species
A549	Lung adenocarcinoma	Human
Skmel-28	Melanoma	
HPAC	Pancreatic adenocarcinoma	
MiaPaca2		
U87	Primary glioblastoma	
HT1080	Fibrosarcoma	
A431	Cervix cancer	
SW872	Liposarcoma	
293-hFAP	Human embryonic kidney	
293-mFAP		
CAF	Cancer-associated fibroblasts	
NIH-3T3	Embryo fibroblasts	Mouse
CHO-hCD200	Ovary	Hamster

Table 2. Cell lines used in this work.

A549 cell line has been used to amplify the different oncolytic adenoviruses due to its high efficiency to produce virus. CHO-hCD200 were kindly provided by Dr. Cristina Costa (IDIBELL, Barcelona). NIH-3T3 cells were kindly provided by Ellen Puré (UPenn, USA). 293-hFAP and 293-mFAP were kind gifts from Eric Tran (UPenn, USA). A431 cells were kindly provided by Dr. Josep Balart (IDIBELL, Barcelona). Human CAFs were provided by Varda Rotter (Weizmann Institute of Science, Israel). The rest of the cell lines had been obtained at the American Type Cell Culture (ATCC). All cell lines were maintained in Dulbecco's modified Eagle's medium (DMEM) supplemented with 10% fetal bovine serum (FBS, Invitrogen Carlsbad, CA, USA) previously inactivated by heating at 56°C for 30 minutes and penicillin-streptomycin (PS, Gibco-BRL, Barcelona, Spain) (100 U/mL and 100 µg/mL, respectively) at 37°C and 5% CO_2. B16CAR were maintained with 0.5 mg/mL hygromycin (Invivogene, San Diego, CA).

3.2.3 PBMCs

Human peripheral blood mononuclear cells were obtained by Ficoll™ (Lonza) gradient protocol from either blood collection tubes or buffy coats kindly provided by Banc de Sang i Teixits (Barcelona). Then, PBMCs were cultured in RPMI medium supplemented with 10% FBS and penicillin-streptomycin (100 U/mL and 100 µg/mL, respectively).

3.2.3.1 T cells

CD14-negative cells were typically obtained from PBMC cultures by letting the cells rest for a minimum of 2h and collecting the non-adherent fraction of the culture.

3.2.3.2 Monocytes and DCs

Monocytes were isolated from PBMC cultures using the magnetic bead-based kit CD14 Microbeads (Miltenyi). From CD14 immature monocytes, DC differentiation was performed by incubating the monocytes (1M/ml) with IL-4 and GM-CSF (50 ng/µl and 150 ng/ul, respectively) for 7 days at 37ºC and 5% CO_2.

3.2.4 Mycoplasma test

All cell lines were routinely tested for mycoplasma contamination by PCR using the following oligonucleotides:

Oligonucleotide	Sequence
MICO-1	5'- GGCGAATGGGTGAGTAACACG-3'
MICO-2	5'-CGGATAACGCTTGCGACTATG-3'

Table 3. Oligonucleotides used for the detection of mycoplasma contamination.

As a template for the PCR, medium from cells that had been in overconfluence and absence of antibiotics for at least 5 days was used. If the result was positive, cells were treated with Plasmocin™ at 25 µg/mL for 2 weeks, and then the cells were tested again.

3.2.5 Cell counting

To determine cell concentrations, manual or automatic methods were performed, using in both cases trypan blue dying exclusion test. Adherent cells were detached by incubating them with Trypsin-EDTA 0.05% (GIBCO RBL) and were resuspended in fresh medium supplemented with FBS. For the manual counting, a dilution in which 30 to 100 cells could be counted in each quadrant of the Neubauer chamber was made. Viable cells in each quadrant were counted and the mean was calculated. The number of cells per mL was calculated according to the following formula:

$$Number\ of\ \frac{cells}{mL} = Mean\ number\ of\ viable\ cells\ per\ quadrant \times Dilution\ factor \times 10^4$$

The automatic counting was performed with the TC20™ cell counter (Bio-Rad) according to the manufacturer's instructions.

3.2.6 Cell freezing and cryopreservation

Cells were counted as explained above and resuspended in cold freezing medium (90% FBS plus 10% DMSO) at a final concentration of 5-10x10^6 cells/mL depending on the cell line. Cell

suspension was distributed in cryotubes at 1 mL/tube and placed in a container filled with 2-propanol for its freezing at -80°C during 24 hours. Then the cryotubes were stored in a liquid nitrogen tank. For cell thawing, cells were rapidly moved from the liquid nitrogen to a water bath at 37°C. Then the cells were diluted in pre-warmed medium and trespassed to a 15 mL Falcon tube. They were centrifuged at 1000 *g* for 5 minutes and the pellet was resuspended in fresh medium and plated at high confluence to optimize the recovery.

3.3 Construction of recombinant adenoviruses

3.3.1 Generation of recombinant vectors

Human adenovirus serotype 5 (Adwt) was obtained from ATCC, and AdwtRGDK, AdTL, ICOVIR-15K have been previously described (Bayo-puxan et al. 2009; J J Rojas et al. 2009).

In order to allow the insertion of transgenes after the viral fiber gene of ICOVIR-15K, the rpsLNeo cassette was introduced in that location after restriction of pJet-rpsLNeo (Genscript) with EcoRV and subsequent homologous recombination into the ICOVIR-15K backbone. This way, ICOVIR-15K-rpsLNeo was generated prior to this work.

In a parallel way, in order to insert transgenes between the E4 and RITR regions of the adenoviral genome, ICOVIR-15K-E4-rpsLNeo was generated by, firstly, amplifying rpsLNeo from the pJet vector with E4itrrpslF and E4itrrpslR primers, and then performing homologous recombination into the ICOVIR-15K backbone. This was done as part of the work in this thesis.

It is worth mentioning that an E1-deleted adenoviral vector was also generated during this work from ICOVIR-15K, in order to have a non-replicative transgene-expressing tool at hand. However, recombination with CD200 and K14 inserts did never yield viable vectors, so no data was produced in this line.

Following, the details of the construction of the recombinant vectors successfully generated in this work are described.

3.3.1.1 ICOVIR-15K-shCD200 and ICOVIR-15K-shCD200tr

The first step to generate these vectors was to amplify human CD200 (GenBank AY048814.1) from pCR2.1-hCD200, kindly provided by Dr. Cristina Costa (IDIBELL, Barcelona). To do that, primers 3ASHCD200F and 3ASHCD200R were used to generate a ready-to-recombine fragment containing a soluble version of human CD200. In order to generate the truncated

version of CD200, 3ASHCD200F+HTRCD200R and 3ASHCD200R+HTRCD200F were used separately to amplify the N-terminal and C-terminal regions of CD200tr, which shared an overlapping sequence at their 3' and 5' ends, respectively. Then, a cross-over PCR using 3ASHCD200F and 3ASHCD200R was performed to generate a ready-to-recombine fragment containing the truncated version of CD200.

3.3.1.2 ICOVIR-15K-sK14 and ICOVIR-15K-sK14tr

A pUC57 containing a full-length codon-optimized K14 (GenBank U75698.1, ORF K14) and the corresponding after-fiber homology regions was acquired from GenScript. In order to clone sK14, 3AF and 3ASK14R were used to generate a ready-to-recombine fragment from the pUC57 plasmid as template. In order to generate the truncated version of K14, an equivalent strategy to CD200 was followed by means of the primers TRK14F and TRK14R.

3.3.1.3 ICOVIR-15K-ATOX-colagI and ICOVIR-15K-ATOX-spryl

A pUC57 containing a codon-optimized native atox with the corresponding after-fiber homology regions was purchased from GenScript. In order to substitute the natural linker of atox, primer pairs L6F+COLAGR or L6F+SPRY2LR were used to amplify the N-terminal region of atox, whilst MMP2LF and L6R2 were used to generate the C-terminal region of both variants, harboring a shared sequence with the N-terminal region at its 5' end. Finally, cross-over PCRs were performed with primers L6F and L6R2 to generate both ready-to-recombine fragments.

3.3.1.4 ICOVIR-15K-AERO

A pUC57 containing a codon-optimized aerolysin with a MMP-9 sensitive linker and with homology arms for E4 region was purchased from GenScript. Double digestion with SmaI and ScaI-HF (NEB) was performed and its 1636 bp product was purified and recombined into ICOVIR-15K-E4-rpsLNeo.

Oligonucleotide	SEQUENCE (5'→3')
E4itrrpslF	TTCCTCAAATCGTCACTTCCGTTTTCCCACGTTACGTCACGGCCTGGTGATG ATG
E4itrrpslR	GAGTAACTTGTATGTGTTGGGAATTGTAGTTTTCTTAAAATGTCAGAAGAA CTCGTCA
3ASHCD200F	CAATTGGTACTAAGCGGTGATGTTTCTGATCAGCCACCATGGAGAGGCTG GTGATC
3ASHCD200R	GACTTGAAATTTTCTGCAATTGAAAAATAAAGTTTATTACTTGTCGTCGTCG TCCTTGTAATCTCCTTTGTTGACGGTTTG
HTRCD200F	GAAAACATGGTCACCTTCAGC
HTRCD200R	GCTGAAGGTGACCATGTTTTCTGCTGTGCACAGCACCAC
3AF	CAATTGGTACTAAGCGGTG
3ASK14R	GACTTGAAATTTTCTGCAATTGAAAAATAAAGTTTATTACTTGTCGTCGTCG TCCTTGTAATCCGCGGGAAGGTCATGG
TRK14F	GTAAACGTCGCCACGTAC
TRK14R	GTACGTGGCGACGTTTACACCCCCAACCGCGCCAAG
L6F	CAATTGGTACTAAGCGGTG
L6R2	GACTTGAAATTTTCTGCAATTG
MMP2LF	CTGGACGCAAGACTGCAG
COLAGLR	CTGCAGTCTTGCGTCCAGAGAATCTACTGAGGGGCCGGTCTCGCCTCTGTC TTTCTTGTCAGGCAGGGGA
SPRY2LR	CTGCAGTCTTGCGTCCAGAGAATCTACTGAGGGGCCGGAGGAAAAGGAG GAGCCTTTCTTGTCAGGCAGGGGA

Table 4. Oligonucleotides used to generate the different transgenes described in this thesis.

3.3.2 Adenovirus generation by calcium phosphate transfection

Once the desired modifications have been incorporated into the viral genome included in a plasmid, this recombinant viral DNA needs to be introduced into packaging cells to generate the adenovirus. To this aim, we used HEK293 cells (F.L. Graham 1977), which were transfected with the viral DNA by the calcium phosphate-based method. PAdZ plasmids incorporate a self-excising system by which once it enters the cell, endonuclease I-*Sce*I is expressed and releases the viral genome. This system increases the efficiency of the transfection, since circular DNA is transfected more efficiently than linear DNA. After the transfection, the viral cycle begins, and after several rounds of replication (about 7 days post-transfection), foci of cytopathic effect are clearly identified.

For transfection, HEK293 cells seeded in 6-well plates and at a confluence of 60-80% were used. For each plasmid to be transfected, the following mixture was prepared in a 1.5 mL tube:

- 19.5 µL of $CaCl_2$ 2 M
- 3 µg of DNA

- ddH_2O up to a final volume of 162 µL

This solution was mixed up softly for 10 seconds, and another 1.5 mL tube containing 162 µL of HBS 2X (NaCl 274 mM, HEPES 50 mM, and NaH_2PO_4 1.5 mM in H_2O, pH adjusted to 6.95 – 7.05 with NaOH) was prepared. Then, the solution containing the DNA was added drop by drop to the tube containing the HBS while air was being bubbled with a pipette. The mixture was incubated for 1 minute at RT and added to the cells while shaking the plate softly to allow a homogenous distribution. 2 hours later the precipitates became visible and 16 hours post-transfection the medium was exchanged by fresh medium.

When the foci of cytophatic effect were visible, the cells were collected together with the supernatant (cell extract, CE) and underwent through 3 rounds of freeze (-80°C) and thaw (37°C) to completely release the viral particles from the cells. This way, the first viral lysate (passage 0, CEp0) was obtained.

3.3.3 Clone isolation by plaque purification assay

In order to have a homogenous stock of each generated recombinant adenovirus, clone isolation by plaque purification assay was performed with the initial viral lysate (CEp0). This assay was performed in A549 cells in order to avoid the possible homologous recombination between the modified E1 region of the adenovirus and the wild-type E1 region of the packaging HEK293 cells. Once isolated, the clones were characterized and those which were correct were amplified for its subsequent use in *in vitro* and *in vivo* assays. The plaque formation assay is based on the infection of cell monolayers with a bank of serial dilutions made from the CEp0 of the different adenoviruses. Then, the infected cells are covered with an agarose overlay that allows nutrient and gas exchange with the medium but does not allow diffusion of the viral progeny. Therefore, viral particles released from the cells are only able to infect neighboring cells, leading to the formation, after several rounds of replication, of viral plaques within the cellular monolayer.

First, serial dilutions ranging from 10^{-1} to 10^{-7} were prepared from the CEp0 in DMEM 5% FBS. Each well of the 6-well plate, which contains A549 cells at an 80% of confluence, was infected with 100 µL of each viral dilution during 4 hours at 37°C. Then, cells were covered with 3 mL of a 1:1 solution of DMEM 5% FBS and 1% agarose previously prepared at 56°C. Once solidified, 2 mL of fresh medium was added over the agarose matrix. Plates were incubated at 37°C until plaques appeared at day 5-8 post-infection. At that moment, the medium was removed

carefully and the plaques were picked through the agarose overlay using a pipette tip. The aspirated agarose/medium was resuspended in 500 µL of DMEM 5% FBS.

3.3.4 Amplification and purification of adenoviruses

Amplification and purification processes allowed the obtainment of sufficient amounts of the recombinant adenoviruses and in the appropriate formulation to be used for *in vitro* and *in vivo* assays. The amplification of the adenovirus is based on the propagation of the viral vector through culture plates of larger sizes at each passage and in bigger amounts. The purification of the adenovirus is based on its separation from the cell debris by an ultracentrifugation in a cesium chloride gradient. Both processes are described in the following sections.

3.3.4.1 Amplification of recombinant adenoviruses

Taking into account that HEK293 cells contained in its genome the wild-type E1 region of the adenoviral genome, and that our conditionally replicative viruses have a modified E1 region, the amplification of all the oncolytic adenoviruses has been carried out in A549 cells to avoid undesirable recombinations.

The starting material for the amplification of the adenoviruses was the plaque obtained from the plaque isolation assay. 250 µL of the medium containing the isolated clone were used to infect a well from a 6-well plate of A549. When the cytopathic effect (CPE) was complete, cells were harvested together with the supernatant (CE) and underwent 3 rounds of freeze and thaw to release the viral particles from the cells. With the CE obtained from the 6-well plate (CEp1), 2 plates of 10 cm were infected. Again, when CPE was complete (around 72 hours post-infection) the CE was collected (CEp2). One of these plates was used to obtain viral DNA by Hirt's method (detailed in following sections) and the second one was used to infect 3 plates of 15 cm and continue with the amplification process. The CE from one of these 15 cm plates contains sufficient amount of virus to perform *in vitro* studies and was kept at -80ºC for this use. In order to purify the virus for *in vivo* administration, with the CE from the other 2 plates, 20 more 15 cm plates of A549 were infected. For the final amplification step, the CE was collected when the CPE was evident in 90-100% of the cells but they were not completely detached from the plate, since the purification process is carried out with cell pellets and the virus present in the supernatant will be lost. At that moment, the cells and the supernatant were collected in 50 mL Falcon tubes and centrifuged 5 minutes at 1000 *g*. The supernatant was discarded (except from 40 mL that were kept at -80ºC to be used in the purification

process) and the cells from each tube were carefully resuspended in the remaining supernatant and joined into one Falcon tube in an approximate volume of 10 mL. This CE was kept at -80°C until the moment of purification.

3.3.4.2 Purification of recombinant adenoviruses

The purification of the adenoviruses is performed in order to have a viral stock with the appropriate formulation and concentration to be administered in mice by systemic injection.

The method used in this work for the purification of adenovirus is based on a cesium chloride (CsCl) density gradient combined with ultracentrifugation to separate viral particles from the rest of the CE components (cell debris, empty viral capsids, etc.) and to concentrate them. The buffer exchange was performed by dialysis.

In order to release the viral particles from the cells, pellets obtained in the amplification step were subject to 3 freeze/thaw cycles. The viral extract was centrifuged 5 minutes at 1000 *g* and the supernatant containing the virus, which is called clarified cell extract (CCE), was collected. The pellet was resuspended in 10 mL of supernatant that was kept from the amplification process and centrifuged again under the same conditions. This step was repeated 3 times until a volume of 42 mL of CCE was obtained. This CCE was then loaded onto the CsCl gradients. The CsCl gradients were prepared in ultracentrifugation tubes (Beckman Coulter) using 3 solutions at different concentrations. First, 0.5 mL of a 1.5 g/mL CsCl solution was layered in the bottom of 6 tubes. The second and third layers consisted of 2.5 mL of CsCl solutions at respective concentrations of 1.35 g/mL and 1.25 g/mL. These layers were added drop by drop in order not to disturb the formed gradient. Finally, 7 mL of the CCE were carefully loaded onto each tube containing the gradients. Then the tubes were ultracentrifuged 2 hours at 10°C and 150000 *g* (35000 rpm, SW40 Ti rotor, Beckman). At these conditions, viral particles are separated from cell debris and appear as 2 bluish-white bands at the interface between 1.25 and 1.35 g/mL layers. The upper band corresponds to empty viral capsids and was removed by suction. Then, the band of interest was carefully collected and placed on ice in a 50 mL Falcon tube. For further purification, a second centrifugation step using a continuous CsCl gradient was necessary. The solution containing the virus was brought up to 24 mL with the CsCl solution at 1.35 g/mL and distributed into 2 ultracentrifuge tubes. The second centrifugation was carried out overnight at the same conditions. After this centrifugation, the solution above the white band was discarded by suction and the band corresponding to the virus was collected in the smallest possible volume (in order to keep the

virus at high concentration) and introduced into a dialysis membrane. Three steps of 2 hour-dialysis (each at 4°C) were carried out in 1 L Tris buffer (Tris-HCl 20 mM, NaCl 2 mM, and glycerol 2.5%).

3.3.5 Titration of adenoviruses

3.3.5.1 Determination of physical viral particles by spectrophotometry

This method allows the quantification of the viral particles (vp) from a purified adenovirus stock without discrimination between infective or defective particles, and is based on the determination of the absorbance of viral DNA at a wavelength of 260 nm.

Three different dilutions (1:5, 1:10, and 1:20) of the purified viral stock were prepared in lysis buffer (Tris 10 mM, EDTA 1 mM, 0.1% SDS, pH 8.0) and incubated for 5 minutes at 56°C. Then, OD was measured at 260 nm and 280 nm with a spectrophotometer. Final concentration of the virus could be calculated by the following formula, taking into account that the extinction coefficient of adenoviruses is 1.1×10^{12} per OD unit:

$$vp/mL = OD_{260\,nm} \times sample\ dilution \times 1.1 \times 10^{12}$$

The ratio between the absorbance at 260 nm and 280 nm gives an idea of the integrity of the purified sample, and should be around 1.4.

3.3.5.2 Determination of functional viral particles by anti-hexon staining

This method is based on the detection of positive cells for the immunodetection of the viral hexon protein in monolayers of infected HEK293 cells. This technique allows the determination of functional transducing units (TU) in purified stocks as well as in cell extract samples.

Serial 1:10 dilutions of the viral stock were prepared in triplicate in 96-well plates in a total volume of 100 µL per well of DMEM 5% FBS. Then, a cell suspension at 10^5 cells/well was added and the plates were incubated for 36 hours at 37°C. After this time, the medium was removed by suction and the cells were left to dry for 5 minutes at RT. 100 µL of cold methanol were added to each well in order to fix the cells and they were incubated 10 minutes at -20°C. The methanol was removed and the wells were washed twice with PBS^{++} 1% BSA. Next, the cells were incubated with a primary antibody against the hexon protein of the capsid obtained from the hybridoma 2Hx-2 (ATCC, Manasas, VA, USA), diluted 1:5 during 1 hour at 37°C.

Afterwards, the cells were washed three times more and incubated with an anti-mouse secondary antibody, conjugated with the dye Alexa-488 (Invitrogen), diluted 1:500 during 1 hour. Finally, the cells were washed thrice and the viral titer was determined by the counting of stained cells using an inverted fluorescence microscope. To calculate the number of transducing units per mL the following formula was used:

$$TU/mL = \frac{Mean\ of\ positive\ cells}{100\ \mu L} \times Dilution\ factor \times 1000\ \mu L$$

3.3.6 Characterization of recombinant adenoviruses

3.3.6.1 Methods for obtaining viral DNA

In this work, viral DNA has been obtained from two different sources: infected cells or purified virus stocks. The methods used in each case are detailed in the following lines.

3.3.6.1.1 Obtaining viral DNA from infected cells (Hirt's)

This method has been used for the analysis and validation of the clones obtained in the plaque formation assay.

The cell extract of infected cells was harvested and centrifuged 5 minutes at 1000 *g*. The supernatant was discarded and the pellet resuspended in 1 mL of PBS. The cell suspension was pelleted again by centrifugation and resuspended in 350 µL of ddH_20. 350 µL of Hirt's solution 2X (10 mM Tris pH 8.0, 20 mM EDTA, 1.2% SDS, and 200 µg/mL of proteinase K) were added to the cell suspension. The sample was mixed up and incubated for 1 hour at 56°C. Next, 200 µL of NaCl 5 M were added drop by drop to the mixture while vortexing and it was incubated at 4°C for 8-16 hours until a white precipitate, corresponding to cellular DNA, appeared. In order to eliminate this cellular DNA, the suspension was centrifuged for 30 minutes at 15000 *g* and 4°C and the clear supernatant containing the viral DNA was collected. This supernatant was incubated with RNAse at a final concentration of 100 µg/µL for 1 hour at 37°C. Then, a phenol:chloroform DNA extraction was performed and the DNA was precipitated with ethanol containing 2% of sodium acetate. Finally, the pellet corresponding to the viral DNA was resuspended in 25 µL of ddH_2O or TE pH 8.0.

3.3.6.1.2 Obtaining viral DNA from purified virus stocks

This method has been used to verify the identity of each generated virus purified stock. Usually, the starting material has been a 50 µL aliquot of purified virus, containing approximately $2x10^{10}$ vp, corresponding to 1 µg of viral DNA.

To this aliquot, we added:

- EDTA pH 8.0 (16 µL 0.5 M)
- SDS (20 µL 10%)
- Proteinase K (8 µL, 10 mg/mL)
- TE pH 8.0 up to 400 µL

The mixture was incubated for 2 hours at 56°C and as in the method above, phenol:chloroform extraction and precipitation of DNA with ethanol 2% sodium acetate were performed. Finally, the pellet corresponding to the viral DNA was resuspended in 25 µL of ddH_2O or TE pH 8.0.

3.3.6.2 Characterization of the viral genome by enzyme restriction, PCR and sequencing

All three techniques have been used to confirm the identity of the generated adenoviruses using DNA from both infected cells and purified stocks.

3.3.6.2.1 Digestion of DNA with restriction enzymes

As starting material for the digestion of viral DNA with restriction enzymes, 500-800 ng of DNA were used. To this amount of DNA, 1 unit of the enzyme, the appropriate buffer to each one (provided by the manufacturer at 10X), and ddH_2O up to the desired final volume were added. The mixture was incubated normally for 2 hours in a water-bath at 37°C and then the samples were resolved in a 1% agarose electrophoresis gel prepared in Tris-Acetate-EDTA (TAE) buffer, together with a molecular weight marker. The restriction enzymes used in this work to assess the integrity of the viral genome were *Nhe*I, *Bst*XI, *Xba*I, *Bsr*GI, *Xma*I, *Kpn*I, *Hind*III, *Spe*I, *Nde*I, *Rsr*II, *Xmn*I, *Afl*II, *EcoR*I, and *EcoR*V.

3.3.6.2.2 PCR detection of transgene inserts

PCR amplification of inserts was performed as a complementary tool to DNA restriction for the validation of recombinant clones. Typically, 50 µl reactions were set up using PrimeSTAR polymerase (Clontech) with 10 ng of template DNA obtained from mini- or midipreparations. Primers used for the different genome locations are described in **Table 5**. In general, such

primers were combined with primers which would anneal to sequences present only in the inserts, such as the ones in **Table 4**, in order to achieve recombinant-specific amplification.

Span	Oligonucleotide	SEQUENCE (5'→3')
Fiber	FiberUp	CAAACGCTGTTGGATTTATG
	FiberDown2	GGCTATACTACTGAATGAA
E4	Ad35566F	CACCACTCGACACGGCACCA
	Ad35825R	GGGCGGAGTAACTTGTATG
E1	Oligo11	GTGTTACTCATAGCGCGTAA
	3634R	CTTCCATCAAACGAGTTGG

Table 5. Oligonucleotides used for insert sequencing.

3.3.6.2.3 Sequencing viral DNA

Sequencing of viral DNA was performed using 100 ng of DNA to which 5 µL of the sequencing mix 3.1 (Applied Biosystems) containing dNTPs and ddDNTPs marked with different fluorochroms, 5 µL of 5X sequencing buffer, 3.2 pmols of the corresponding oligonucleotide, and ddH_2O up to 10 µL. The conditions of the sequencing reaction were 24 cycles consisting on: 30 seconds at 96°C, 15 seconds at 50°C, and 4 minutes at 60°C. Primers in **Table 5** were generally chosen for sequencing reactions. The sequencing reactions were analyzed with an automatic sequentiator at the "Servei de Seqüenciació I Genòmica dels Serveis Científics de la Universitat de Barcelona".

3.4 Viral production assays

To perform viral production assays, typically, $2 \cdot 10^5$ tumor cells were seeded into 24-well plates in order to have 80% confluence at the moment of infection. Then, each cell line was infected per triplicate at an MOI sufficient to guarantee 80 to 100% of infection. A549 were infected at 20 TU/cell, Skmel-28 at 30 TU/cell, and SW872 and HPAC at 50 TU/cell. 4 hours later, infection media was removed, cells were washed thrice with PBS and incubated with fresh medium. At indicated time points (24, 48, and 72 hours post infection), cells and medium (CE) were harvested and subjected to 3 rounds of freeze-thaw lysis.

After the freeze-thaw cycles the cell extracts were centrifuged 5 minutes at 5000 *g* to separate cell debris and viral titers were determined in triplicate according to the anti-hexon staining-based method, described previously.

3.5 Cytotoxicity assays

Cytotoxicity analysis *in vitro* is based on the evaluation of cell viability after the exposure of tumor cells to serial (1/3 or 1/5) dilutions of the different adenoviruses. Such analysis was performed by the quantification of total protein content by the bicinchoninic acid assay (BCA, Pierce Biotechnology, Rockford, IL, USA). This assay combines the reduction of Cu^{2+} to Cu^{1+} by proteins in an alkaline medium with the highly sensitive and selective colorimetric detection of the cuprous cation (Cu^{1+}) by bicinchoninic acid. The reaction of two molecules of BCA with one Cu^{1+} resulted in an intense purple-colored product that exhibits a strong linear absorbance at 540 nm with increasing protein concentrations. Some assays were also read by MTT protocols, described elsewhere (Mosmann 1983).

Cytotoxicity assays were performed by seeding 40000 Skmel-28 cells, 30000 A549, A431, U87, 293, 293-hFAP, 293-mFAP, SW872, HPAC, B16, TRAMPC2 or HT1080 cells, 15000 MiaPaCa-2, CAF, NIH-3T3, NIH-3T3-hFAP or NIH-3T3-mFAP cells per well in 96-well plates in DMEM with 5% FBS. Cells were infected with serial dilutions starting with 600 TU/cell for SW872, HT1080, CAF, 3T3, B16, TRAMPC2 cells, or 200 TU/cell for the rest of cell lines. For the cytotoxicity assays performed with supernatants, cells were treated with serial dilutions of concentrated supernatants from infected cultures, harvested at 72h post-infection. Such concentration was achieved by centrifuging the supernatants in Amicon 30K devices (Millipore) for 10 minutes at 4000 rpm, RT. Typical concentration values were 10 to 15-fold. At day 5 to 7 post-infection, plates were washed with PBS and incubated with 200 µL of BCA reagent during 30 minutes at 37°C. Absorbance was quantified at 540 nm and the TU/cell required to produce 50% of inhibition (IC_{50} value) was estimated from dose-response curves by standard nonlinear regression (GraphPad 6 Software Inc., CA, USA).

3.6 *In vivo* assays with recombinant adenoviruses

3.6.1 Animals and conditions

All the animal studies were performed at the IDIBELL facility (AAALAC unit 1155) and approved by the IDIBELL's Ethical Committee for Animal Experimentation.

For the realization of this work, athymic nude mice have been used for antitumor efficacy studies. In all cases, 6-8 week-old mice with a body weight between 20 and 30 g were used.

Animals were housed at a temperature between 22 and 24°C under an artificial circadian 12 hours light/dark cycle and received *ad libitum* standard diet and water.

3.6.2 Tumor implantation and monitoring

3.6.2.1 Subcutaneous tumors

Tumor cells for the implantation of tumors were maintained in 15 cm plates at standard conditions *in vitro*. At the moment of implantation, cells were trypsinized, resuspended with DMEM 5% FBS, centrifuged for 5 minutes at 1000 *g*, washed with PBS, and counted. Finally, they were resuspended in an appropriate volume of PBS in order to have a final volume of 200 µL for each tumor. The number of cells per tumor varied depending on the cell line and ranged from $3x10^6$ to $5x10^6$ cells/tumor. Mice were anesthetized with isofluorane 2.5% before the implantation of the tumors. The subcutaneous injections were carried out with 29 G hypodermic needles. After tumor implantation, the appearance of the tumors was monitored by palpation, and when they reached a measurable volume, they were measured with a caliper. Tumor volume was calculated according to the following equation:

$$V\ (mm^3) = \frac{\pi}{6} \times L \times W^2$$

where W and L stand for width and length of the tumor, respectively.

The percentage of growth was calculated according to the following formula:

$$\%\ of\ tumor\ growth = \frac{V - V_0}{V_0} \times 100$$

where V_0 is the tumor volume on day 0.

When tumors reached a mean volume of 130-200 mm^3, animals were randomized into experimental groups and were treated accordingly.

3.6.2.2 Orthotopic pancreatic tumors

Cryopreserved TP5 clone fragments from a patient with pancreatic ductal adenocarcinoma previously perpetuated during 5 passages in athymic mice were implanted in isofluorane-anesthetized athymic nude animals orthotopically in the pancreas and were allowed to grow for 3-4 weeks, in which palpation was performed as a monitoring tool. Once tumors reached 600 mm^3, intravenous administrations were performed. Measurement of the tumors, both

pre- and post-administration, was done by externalizing the visceral mass, identifying the tumor burden and with use of a caliper. Calculations were performed as shown previously.

3.6.3 Adenovirus administration

Viral solutions for the administration *in vivo* were prepared by diluting the purified viral stocks in PBS. For the systemic administration of adenoviruses in mice, dilutions at a concentration of $4\text{-}5\cdot10^{10}$ vp in a final volume of 200 µL per animal were prepared. The injection was performed with hypodermic 29G needles via tail vein.

3.6.3.1 Organ collection

Tumors were obtained from sacrificed animals and washed with a saline solution. Then, tumors were split into pieces and fixed in formaldehyde 4% for 16 hours to be included in paraffin, frozen in OCT, or frozen directly in order to extract RNA and protein. In the case of the orthotopic pancreatic model, tumors were weighted at endpoint.

3.6.3.2 Paraffin inclusion

Fixation of tissues in formaldehyde was followed by washing them with water in order to eliminate the fixative agent. Next, tissues underwent a battery of alcohols of crescent graduation in order to dehydrate them and allow the penetration of paraffin. Tissues were submerged for 1 hour in ethanol 70%, for 2 hours in ethanol 96%, and then in new 96% ethanol overnight. Next day, tissues went through another battery consisting of 3 absolute ethanol rounds (1.5 hours each) and then were submerged into xylol for 1.5 hours. Finally, they were submerged into liquid paraffin at 65°C overnight and the next day they were included in blocks.

3.6.3.2.1 OCT inclusion

OCT inclusion was performed directly after collecting the sample. Tumors were placed in *Criomold* (Tissue-Tek Sakura) molds in which a cryoprotective matrix of OCT (Tissue-Tek Sakura) was previously added. Included tissues were frozen immediately in dry ice and stored at -80°C.

3.7 Histology

3.7.1 Immunohistochemistry in paraffinized sections

Paraffin-embedded blocks were cut into 5-µm thick sections with a microtome and deposited into poly-L-lysine treated slides. Sections were deparaffinized by subjecting them to a battery of 4 xylols (10 minutes each), 3 absolute ethanol, 3 96% ethanol, 1 70% ethanols, and 1 50% ethanol (5 minutes each). Finally the sections were rehydrated by submerging them in ddH_2O. Next, endogenous peroxidase activity was blocked by incubation for 10 minutes in 0.3 % H_2O_2. Antigens masked during routine fixation were retrieved by submerging the slides in sodium citrate solution (pH 6.0) and heating during 12 minutes. Then, sections were washed thrice with ddH_2O during 5 minutes and then once in PBS for 5 minutes. Sections were blocked in order to reduced unspecific binding with Normal Goat Serum diluted 1:5 in PBS 1% BSA for 1 hour at RT. All the incubations were performed in a humidity chamber. Primary antibody incubation was performed using an anti-E1A adenovirus-2/5 (sc-430, Santa Cruz) diluted 1:200 or a rabbit anti-αSMA (RB-9010-P, Thermo) diluted 1:100 overnight at 4°C. After washing thrice with PBS 0.2% Triton-X100 for 5 minutes, the sections were covered with anti-mouse Envision$^+$-System-HRP (Dako Laboratories, Glostrup, Denmark) and incubated 1 hour at RT. Next, slides were washed 3 times more with PBS 0.2% Triton X-100 and developed by covering the sections with the chromogenic substrate DAB+ (EnVision™ Kit, Dako Cytomation K3468) during approximately 30 seconds, until a brown precipitated appeared. The reaction was stopped by rinsing the slides with tap water for 10 minutes. Finally, the sections were rehydrated and mounted with Vectashield™ (Vectorlabs).

3.7.2 In situ zymography

OCT preserved samples at -80°C were cut into 5-µm thick sections with a cryostat that maintained the samples at -20°C. The sections were deposited at RT into poly-L-lysine treated slides and kept at -80°C until their processing.

In this work, in situ zymography has been performed in frozen sections of tumors in order to detect MMP-9 activity in the tumor milieu. To this aim, DQ gelatin (EnzCheck™ Gelatinase/Collagenase Assay Kit, Molecular Probes) was used according to the manufacturer's instructions.

The images were taken with a fluorescence microscope Olympus BX60 and a digital camera Olympus U-RFL-T, using the SPOT Advanced 3.2.4 software (Diagnostic instruments).

3.8 Flow cytometry

Generally, cells were seeded in 24 or 96-well plates and, in the case of adherent cells, were detached at the moment of the staining, either with trypsin-EDTA, cell dissociation buffer (Gibco) or Accutase™ (Gibco), and resuspended in FACS buffer (PBS 1% BSA 0.01% sodium azide). Cells were pelleted by centrifugation for 5 minutes at 1000 *g* and 4°C in either 96-well plates or eppendorf tubes, washed twice with FACS buffer and incubated with the corresponding primary antibodies or fluorescent reagents, such as viability stains Live&Dead (Molecular Probes) or 7-Aminoactinomycin D (Enzo), or other reagents like FLAER™ (Fluorescent-Labelled AERolysin) or 5(6)-carboxyfluorescein (CFSE). Incubations were carried out for 30 minutes at RT or 4°C and in a final volume of 100 µl. In the case of FLAER, optimized conditions described elsewhere were used (Brodsky et al. 2000; Dahmani et al. 2016). After the incubation, 3 washes were performed with FACS buffer and, if needed, further incubations of 30 minutes at 4°C in a final volume of 100 µL with an appropriate secondary antibody was performed. Finally, samples were washed again 3 times with FACS buffer, resuspended in 300 µL of final volume, and analyzed by flow cytometry. The staining reagents used and their corresponding dilutions are summarized in **Table 6**.

Antibody	Antigen	Species	Dilution	Manufacturer
H-155	Human CD200	Mouse	1:50	Santa Cruz
OX-104 PE	Human CD200	Mouse	1:50	Abcam
OX-109 A647	Human CD200R	Mouse	1:50	Abcam
CRL-2733 F19 Hybridoma	Human FAP	Mouse	1:100	ATCC
73.3	Murine FAP	Rabbit	1:100	ATCC
SK7 PerCP	Human CD3	Mouse	1:250	Biolegend
RPA-T8 APC	Human CD8	Mouse	1:250	Biolegend
GHI/61 BV421	Human CD163	Mouse	1:200	Biolegend
L243 PerCP	Human HLA-DR	Mouse	1:200	Biolegend
63D3 PE	Human CD14	Mouse	1:250	Biolegend
ICRF44 APC	Human CD11b	Mouse	1:200	Biolegend
HI149 APC	Human CD1a	Mouse	1:200	Biolegend
HB15e APC	Human CD83	Mouse	1:200	Biolegend
P67.6 PE	Human CD33	Mouse	1:200	Biolegend
CMV-tetramer PE	HLA-A*02:01 CMVpp65-specific TCR		1:1000	Mobitec

FLAER A488	GPI-anchored proteins		1:100	Cedarlane
DIA-900	His Tag	Mouse	1:1000	Dianova
Anti-mouse A488	Mouse IgG1	Goat	1:500	Life Technologies

Table 6. Primary and secondary antibodies used for flow cytometry detections.

For every staining, the corresponding isotype control or irrelevant tetramer was included in the analysis to validate the technique and to avoid false positive results.

In the case of cytotoxicity assays analyzed with the cytometer, CountBright™ microbeads (Life Technologies) have been used as stop-and-save event counting criteria, typically with values of 2,000-5,000. Fixed volumes of beads were added to samples right before running them through the cytometer.

A Gallios™ (Beckman Coulter) cytometer was used for the analysis at IDIBELL, whereas a Canto™ (Beckton-Dickinson) was used for data produced at Uppsala Universitet. Typically, no less than 10,000 events were analyzed for each sample and FlowJo vX.0.7 (Tree Star, Inc.) software was used for data analysis.

3.9 ELISA

In the present work, ELISA kits shown in **Table 7** have been used according to the manufacturer's instructions. Samples were obtained from supernatants of cell cultures and quantified for protein concentration:

ELISA kit	Antigen	Manufacturer
RAB0083	Human CD200	Sigma
440707	Human MMP-9	Biolegend
3420-1HP	Human IFNγ	Mabtech
3445-1HP	Human IL-2	Mabtech

Table 7. ELISA kits used in this work.

3.10 Mixed Leukocyte Reaction (MLR)

Allogeneic reactions were induced by mixing populations of PBMCs from two different donors at a ratio of 1:1 in 24-well plates, typically $5 \cdot 10^5$ cells from each donor, in the presence or absence of $2.5 \cdot 10^5$ CD200-expressing SKMel-28 cells. Positive controls for stimulation were treated with phorbol-myristate-acetate (PMA) at 15 ng/mL plus ionomycin at 250 ng/mL. After 4h of incubation at 37ºC, Amicon-concentrated supernatants from cultures infected with different viruses were added (100 µl). After 2-5 days, supernatants were collected and

concentration of IFNγ or IL-2 was measured by ELISA. This protocol was based on the work done by other groups trying to impair the CD200:CD200R pathway (Siva et al. 2008).

3.11 Monocyte-tumor cell cocultures

Typically, $5 \cdot 10^5$ CD14+ cells obtained by magnetic separation were seeded in 24-well plates in RPMI media in the presence or absence of tumor cells, either A549 or SKMel-28, infected with the different viruses at an MOI of 20 (30 for SKMel-28) at a ratio of 1:1. Cultures were incubated at 37ºC and at days 3 and 5 cells were trypsinized and stained for the detection of CD14, CD33, CD163, HLA-DR or CD200R in the flow cytometer.

3.12 Inhibition of CMV-specific CTLs

PBMCs obtained from CMV^+ donors were initially assessed for the presence of CD8+ CTLs recognizing the CMV-derived peptide pp65 (NLVPMVATV) by flow cytometry. On the other hand, magnetically-purified CD14+ cells from the same donors were differentiated into mature DCs as described previously. After 7 days, expression of DC markers CD1a and CD83 was verified in the cytometer and cells were infected with the different viruses at an MOI of 1000. The following day, DCs were washed with PBS and pulsed with 0.01 µg CMV pp65 peptide and 1 µg β_2-microglobulin for 4h at 37ºC. Positive controls for stimulation were treated with TNFα and poly(I:C) at 40 ng/ml and 30 µg/ml, respectively. Then, cells were washed twice with PBS and resuspended in RPMI and were brought to 10^5 cells/ml. At the same time, CD14- cells were thawed and diluted to 10^6 cells/ml. Both populations were mixed at a CD14- responders-to-CD14+ stimulators ratio of 10:1 in 12-well plates and cultured at 37ºC for 11 days. Then, T cells were harvested and stained for CD3, CD8 and HLA-A*02:01 CMV pp65-specific TCRs. Samples were run through the flow cytometer and triple-positive populations were quantified.

3.13 Activation of aerolysin in supernatants by recombinant MMP-9

Supernatants from 10-cm plates of A549 cells infected with different viruses were harvested after 72h of incubation at 37ºC and concentrated with Amicon™ 30K tubes up to 30-fold. Then, they were incubated in the presence or absence of 1 ng/ml recombinant MMP-9 (Calbiochem) for 1h at 37ºC in eppendorf tubes. Afterwards, 100 µl of each tube were added to target cells (HT1080, A431, CAFs, HPAC, NIH-3T3 mainly), previously seeded at, generally, $3 \cdot 10^4$ cells/well in 96-well plates. Plates were incubated at 37ºC for 36h and then cells were harvested. After this, viability and cell concentration were analyzed via flow cytometry.

3.14 Bystander effect assays

A549 cells were infected at an MOI of 20 with the different viruses and were incubated at 37º C for 4h. After this, they were washed with PBS twice and they were seeded in 96-well plates at a density of $3 \cdot 10^4$ cells/well. On the other hand, target tumoral cells (HT1080, A431, CAFs, HPAC and NIH-3T3 mainly) were stained with CFSE 2 µM for 30 minutes at RT, after which they were washed with PBS and were also seeded together with A549 at the same density (ratio of 1:1). After 48-72h, cultures were harvested and viability and cell concentration were analyzed through flow cytometry.

3.15 Quantitative PCR

RNA and DNA material was obtained from tumor lysates with the AllPrep DNA/RNA/Protein kit from Qiagen (ref. 80004) and quantified at the Nanodrop. Further qPCR assays were performed with each kind of sample in a LightCycler 480 from Roche. In all cases, the LC480 software was used to analyze the outcoming data. Samples were always run at least in duplicate.

3.15.1 Adenoviral genomes in tumors by SYBR Green

Viral DNA from tumors was analyzed by qPCR by the SYBR Green-based approach using two primers spanning the hexon protein: Ad18852 (CTTCGATGATGCCGCAGTG) and Ad19047R (ATGAACCGCAGCGTCAAACG). SYBR Green 2X Master Mix from Applied Biosystems was used. 100 ng of total DNA were loaded in every well. A standard curve with known Adenoviral particle concentration was included in every run.

3.15.2 Murine FAP expression in tumors by TaqMan

1 µg RNA from tumor lysates was firstly retrotranscribed with the High Capacity cDNA Retrotranscription kit from Thermo (ref. 4368814). The resulting cDNA was analyzed for murine FAP expression with the TaqMan Gene Expression Assay ref. Mm01329177_m1 from Thermo. Murine B-actin cDNA was quantified as a housekeeping reference gene by means of the TaqMan Gene Expression Assay ref. Hs99999903_m1 (Thermo) in separate wells. Murine FAP-expressing cell line HT1080-mFAP was included in every run as positive control. Human FAP-expressing cell line HT1080-hFAP was also included alongside with water as negative controls.

3.16 Statistical analysis

The graphs and statistic tests were performed with GraphPad Prism v6 software (GraphPad Software, Inc.). Unpaired two-tailed Student's *t*-test was used for the comparison of means between two groups. When more than two groups were compared, one-way ANOVA test with Tukey or Kruskal-Wallis post-hoc tests were used according to the data types.

Survival curves were obtained with the same software and *logrank* Mantel-Cox test was used to determine statistically significant differences.

The statistical significance was defined at a *p* value lower than 0.05.

4 RESULTS

4.1 Oncolytic adenoviruses carrying soluble versions of human CD200, CD200tr, the viral homolog k14 and k14tr

4.1.1 Generation and characterization of OAds expressing shCD200, shCD200tr, sK14 and sK14tr

CD200 is an increasingly studied immune checkpoint due to its potential role in tumor-induced tolerance, which it exerts by inhibition of myeloid cells and by shifting immune responses from T_H1 to T_H2 profiles (Jenmalm et al. 2006; Koning et al. 2010; S. Zhang et al. 2004). The expression of CD200 ligand is broadly distributed among cell types, whereas CD200R expression is highly restricted to cells from myeloid origin (Holmannová et al. 2012; Lorvik et al. 2013; Minas and Liversidge 2008). There is a naturally-occurring CD200R antagonist has consisting of a truncated splice variant of CD200, called CD200tr, lacking 43 aa at its N-terminal V-type Immunoglobulin-like domain, which is allegedly involved in receptor binding (Z. Chen et al. 2008). Such truncation does not, however, impair CD200tr affinity towards CD200R, and it has been hypothesized that a CD200-favoring and CD200tr-decreasing splicing bias may be a tolerance-inducing mechanism used by tumors to induce immune tolerance, which constitutes a hurdle for immunotherapy (Holmannová et al. 2012).

Human Herpesvirus 8 (HHV-8) encodes a human CD200 homolog called K14 as an evolutionary mechanism to evade the immune system (Foster-cuevas et al. 2004). In this work, we hypothesize that a truncated K14 (K14tr) could emulate CD200tr in antagonizing CD200R and thus revert immune blockade. In the context of oncolytic virotherapy with Adenoviruses, a soluble K14tr released from infected tumor cells would easily reach dormant antitumoral T lymphocytes within the tumor and would help reverting the immune suppression exerted by the tumor microenvironment and eventually mount a sustained immune response against tumor epitopes. To this end, viruses expressing soluble versions of hCD200, hCD200tr, K14 and K14tr, shown in **Figure 17**, were designed.

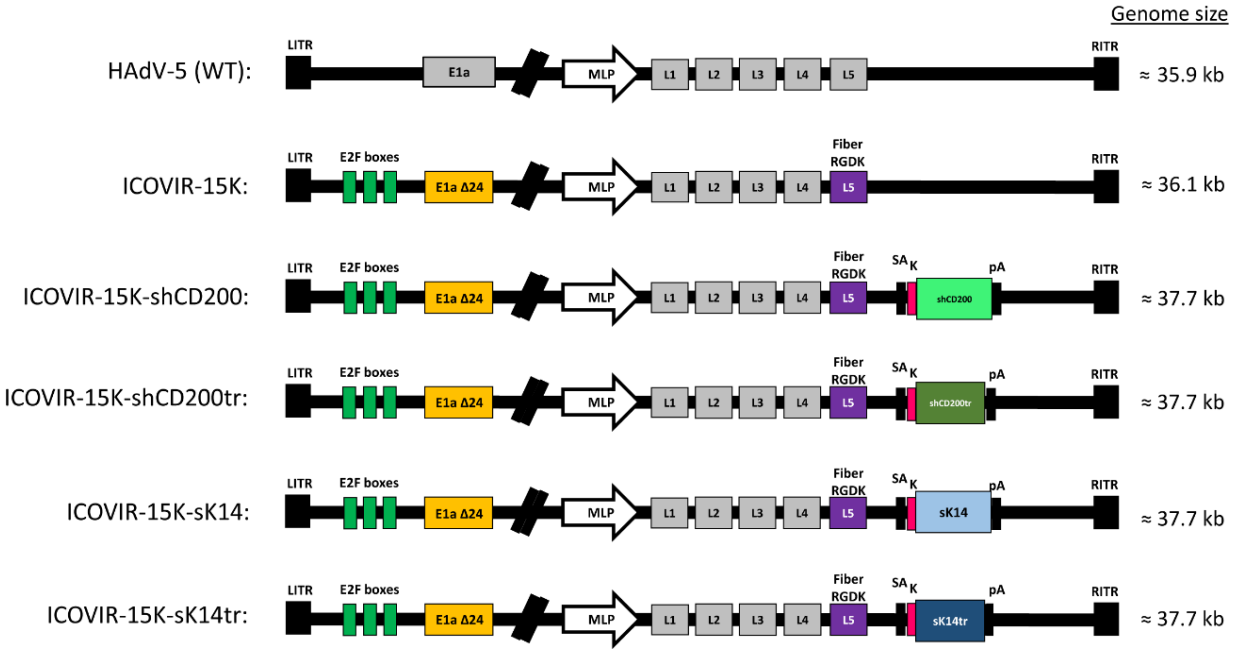

Figure 17. CD200 viruses. Schematic representation of the OAds used in this chapter. WT virus is the human Ad5 wild type virus. ICOVIR-15K is the backbone containing the main genetic oncotargeting modifications in which recombinations were performed to generate the transgene-carrying viruses. These modifications are the modified E1a promoter, the truncated E1a protein and the RGD insertion in the fiber shaft substituting the KKTK domain. In the transgene-carrying viruses, the IIIa splicing acceptor site and the Kozak sequence are located at the 5'-end of the transgenes so that efficient translation can be achieved under the regulation of the Major Late Promoter (MLP).

All the viruses shown in **Figure 17** were generated by homologous recombination in bacteria and further amplified in A549 cells. After such amplification, viruses were purified by ultracentrifugation for their use in in vitro and in vivo assays. Reference viral physical and functional titers are shown in **Table 8**. All physical/functional ratios are within the same range, as well as the viral production yields shown in **Figure 18**, which means that the insertion of the transgenes did not translate into a loss of replication efficiency.

Virus	Physical titer (vp/ml)	Functional titer (TU/ml)	Ratio
ICOVIR-15K	$5{,}7 \cdot 10^{12}$	$3'4 \cdot 10^{11}$	16,76
ICOVIR-15K-shCD200	$1{,}57 \cdot 10^{13}$	$3{,}58 \cdot 10^{11}$	43,87
ICOVIR-15K-shCD200tr	$1{,}3 \cdot 10^{13}$	$5 \cdot 10^{11}$	25,98
ICOVIR-15K-sK14	$5{,}16 \cdot 10^{12}$	$1{,}8 \cdot 10^{11}$	28,64
ICOVIR-15K-sK14tr	$1{,}3 \cdot 10^{13}$	$3{,}47 \cdot 10^{11}$	37,49

Table 8. Physical and functional viral titers. Ratio values are expressed in vp/TU. In general, in vitro assays are based on functional titers, whereas in vivo assays are based on physical values due to toxicity normalizing grounds.

Figure 18. Viral production assay in A549 cells. Viral yields in TU/cell from all the viruses were obtained by anti-hexon staining after 72h of infection in A549, an Adenovirus-permissive cell line. No significant differences were observed between viruses. One-way ANOVA and Tukey post-hoc test were applied on these data.

Transgene expression was measured for shCD200 and shCD200tr viruses by ELISA on concentrated supernatant samples, as shown in **Figure 19**. Both full-length CD200 and CD200tr were successfully detected by the ELISA antibody, whereas no background signal was observed either in uninfected supernatants or supernatants infected with the control virus.

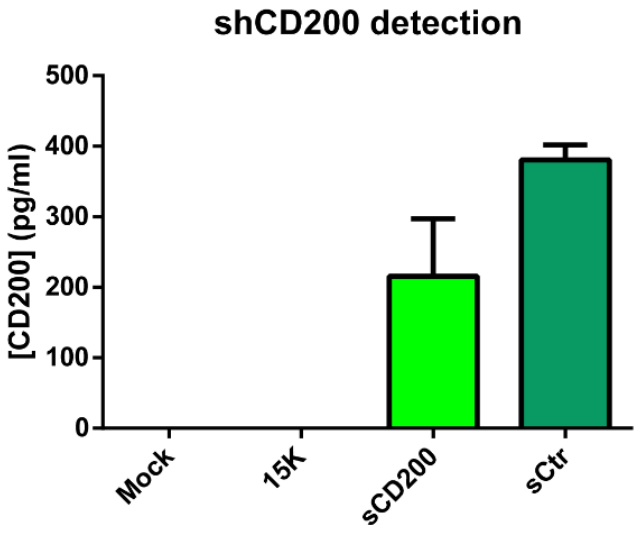

Figure 19. Detection of soluble human CD200 by ELISA. Concentrated supernatants from either uninfected (Mock) or infected cells were analysed by ELISA after 72h infection.

Cytotoxic features of the recombinant viruses were tested in the permissive cell lines A549 and SK-Mel-28, a $CD200^+$ melanoma-derived cell line. IC_{50} values from curves in **Figure 20** are shown in **Table 9**. The maximum loss of cytotoxic potency was observed in SK-Mel-28 for the shCD200-expressing virus (2,34x), whereas, interestingly, the maximum gain was observed in A549 cells for the same virus (11x). However, no significant differences were detected in any

case between measures of individual time points, meaning that the transgene-expressing viruses could retain the cytotoxic traits of their parental 15K virus.

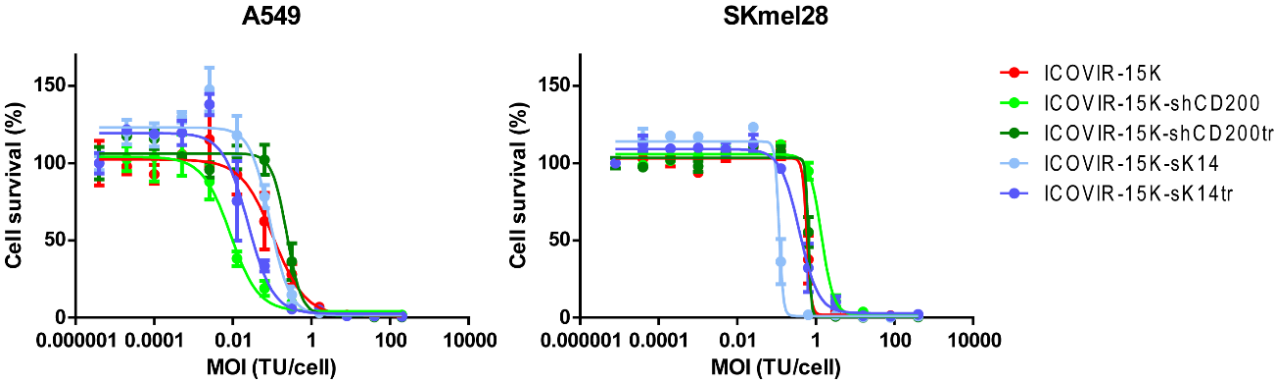

Figure 20. Cytotoxic curves of recombinant viruses in two permissive models. Cells were infected in 96-well plates with the different viruses at gradually decreasing MOIs, starting at 200, and were incubated at 37ºC for 5-7 days, ideally until half of the plate presented complete CPE. Viability was then assessed by a BCA standard protocol and IC_{50} values were calculated with non-infected samples as reference.

Virus	IC50 in A549	IC50 in SKM28	Fold vs 15K A549	Fold vs 15K SK-Mel-28
ICOVIR-15K	0,11	0,59	1	1
ICOVIR-15K-shCD200	0,01	1,38	0,09	2,34
ICOVIR-15K-shCD200tr	0,24	0,65	2,18	1,1
ICOVIR-15K-sK14	0,09	0,12	0,82	0,2
ICOVIR-15K-sK14tr	0,02	0,38	0,18	0,64

Table 9. IC_{50} values of recombinant viruses in A549 and SK-Mel-28 cell lines. IC_{50} values are expressed in TU/ml. Regarding fold values, <1 means increased potency, and vice versa.

4.1.2 Assessment of immune modulation exerted by recombinant CD200 and K14 viruses

4.1.2.1 Mixed Leukocyte Reaction (MLR)

Assays involving stimulator and responder populations are often used to assess immune modulation in different settings. In the case of CD200:CD200R, either MLRs combining either differentiated DCs and T cells, or simply two hPBMCs populations from different donors have been used in the literature (D. X. Chen, He, and Gorczynski 2005; Gorczynski et al. 2004). MLRs are based on the generation of an allogeneic reaction between populations from the different donors which induces basal immune activation upon which immune regulation is studied. The degree of activation is donor-dependent. In particular, CD200 expression in a panel of cell lines, including SK-Mel-28, correlated with myeloid inhibition as described by Siva and collaborators in terms of IFN-γ and IL-2 expression (Siva et al. 2008). In other cases, CD200-mediated inhibition in MLRs could be reverted in the presence of anti-CD200 antibodies.

In order to reproduce the above mentioned data from other researchers and in search of the most adequate method, MLR were performed by either mixing T cells and differentiated DCs or just different PBMC populations in the presence or absence of CD200-expressing CHO-hCD200 or SK-Mel-28 cells, as shown in **Figure 23**. CD200 expression from both cell lines was confirmed by flow cytometry (**Figure 21**). Whilst SK-Mel-28 showed a unique positive peak, CHO-hCD200 cells showed two populations, one of which clearly positive for CD200 (87,4% of the total). CD200 and CD200R levels in the MLR populations were also analyzed by flow cytometry prior to engaging the MLR (**Figure 22**). As described in the literature, differentiated DCs presented high CD200R levels and moderate CD200 levels, compared to the CD200R$^-$ T cells, which also presented moderate CD200 levels, as expected from naïve cells.

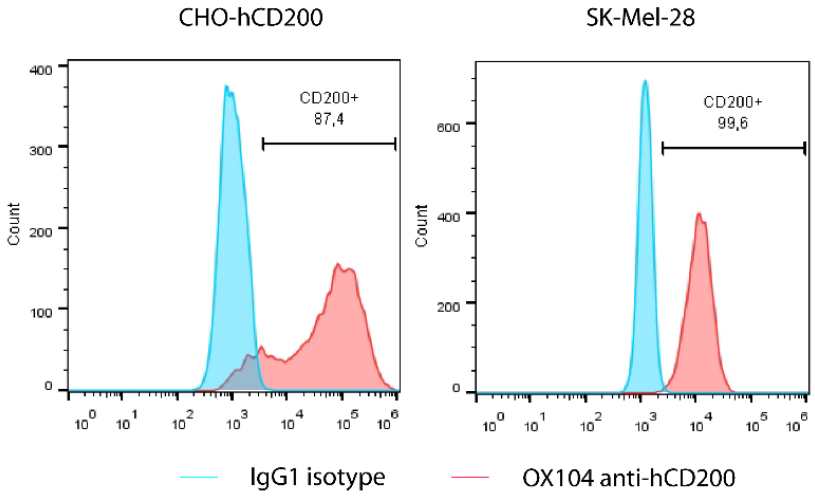

Figure 21. CD200 expression in modified CHO and in non-modified SK-Mel-28 cell lines. CD200 levels were in line with what was described for SK-Mel-28 in the literature (Siva et al. 2008). CHO-hCD200 cells were mainly positive, with a small negative population (12,6%). A minimum of 10^4 events were obtained for analysis.

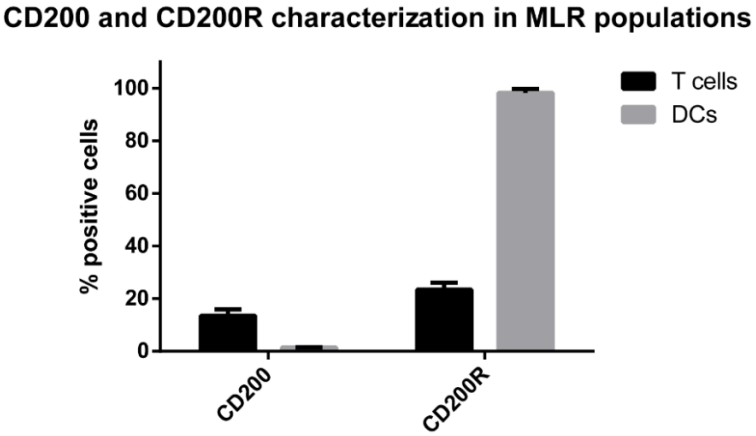

Figure 22. CD200 and CD200R levels on MLR populations. Prior to engaging MLR, T cells and differentiated DCs from monocytes from different donors were stained for both CD200 and CD200R. A minimum of 10^4 events were acquired for analysis.

In both MLR configurations, only the presence of SK-Mel-28 cells provided a significant and even complete reduction of IFN-γ release when compared to the non-treated condition, which yielded the basal allogeneic reaction values. These results led us to use the hPBMCs mix for further assays.

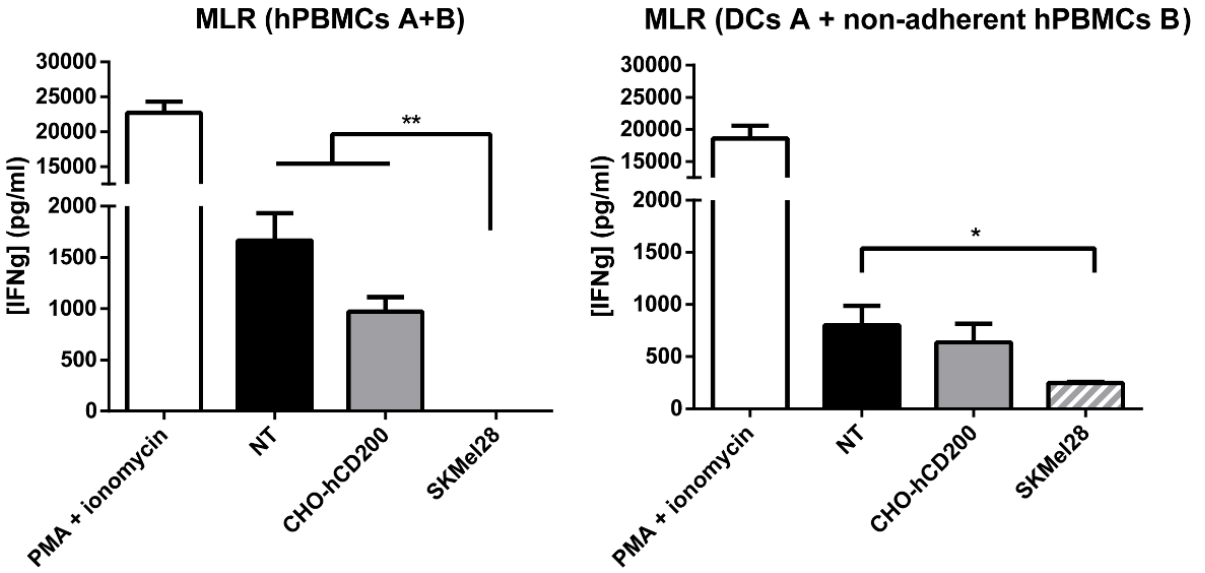

Figure 23. MLR optimization in CD200⁻ and CD200⁺ conditions. In the case of hPBMC mix (left), 1:1 mixes were added to 24-well plates, whereas 10:1 responder:stimulator ratios were used for the T+DC setting (right). CHO-hCD200 and SK-Mel-28 cells were added at a ratio of 1:4 versus total PBMCs in the first setting, and 2:1 versus stimulators (DCs) in the T+DC setting. PMA and ionomycin were used as the stimulation positive control. All MLRs were read after 3-5 days of incubation, when cytokine release was analysed by ELISA on supernatants. One-way ANOVA with Tukey post-hoc test was applied on these data: * p<0,05, ** p<0,01.

In order to test the viruses and the ability of the soluble transgenes to modulate IFN-γ release, MLRs were performed by adding concentrated supernatants from infected cultures to the leukocyte mix in the presence or absence of CD200⁺ SK-Mel-28 cells. Without SKmel28 cells, the CD200 or K14 expressed from the corresponding viruses should inhibit IFN secretion in the MLR. The truncated forms should not inhibit IFN secretion. The results (**Figure 24,** black bars) show that the untreated basal condition induced a level of IFNγ of almost 4000 pg/ml. The control virus, ICOVIR-15K, increased IFNγ levels up to 6000 pg/ml, presumably due to immunogenicity of the virus. The inhibitory or immune suppressor role of CD200 and K14 was confirmed since the ICOVIR15K-shCD200 and ICOVIR15K-K14 supernatants reduced IFNγ secretion. As expected, the truncated form of CD200 did not inhibit IFNγ secretion. However, K14tr showed the same inhibitory activity on IFNγ secretion as the full length K14. This result was against our hypothesis that the truncation of K14 could block the CD200-CD200 inhibitory pathway.

SK-Mel-28 cells are a source of CD200 to bind to CD200R on myeloid cells and inhibit IFNγ secretion in the MLR. In these conditions CD200 and K14 would not further inhibit IFNγ secretion, but the truncated forms should prevent the SK-mel28-mediated inhibition of IFNγ secretion. . The results show (**Figure 24**, gray bars) reduced IFN-γ levels in all MLR conditions, Of note, supernatants with soluble CD200tr were not able to rescue the levels of IFNγ, suggesting that the level of CD200tr expressed by ICOVIR15K-shCD200tr were insufficient to overcome the CD200-mediated inhibition by SK-Mel28 cells.

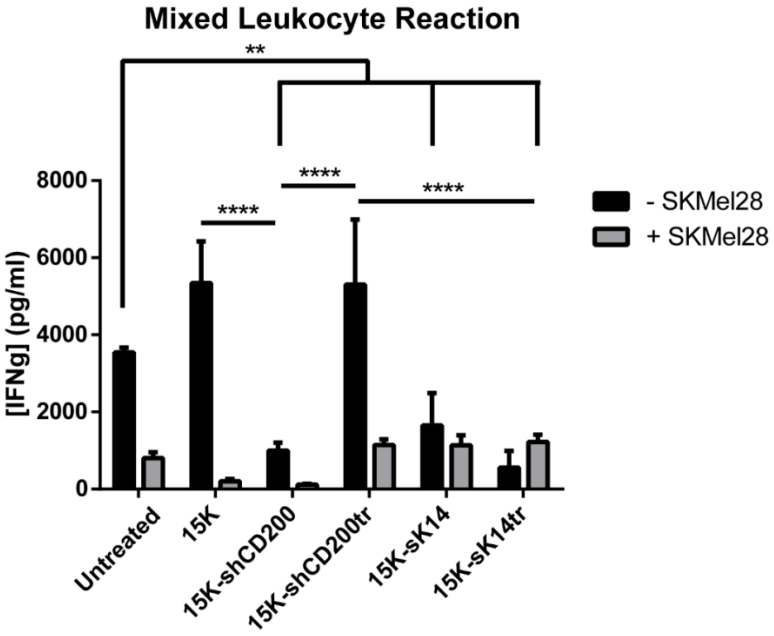

Figure 24. MLR in the presence of the transgenes. MLRs were set up by mixing 1:1 PBMCs populations from different donors in the presence or absence of 1:4 SK-Mel-28 cells versus total PBMCs in 24-well plates. Concentrated supernatants from infected cultures were added to MLRs and IFN-γ concentration was measured by ELISA after 3 days of incubation at 37ºC. Two-way ANOVA and Tukey post-hoc test were applied on these data: ** p<0,01, **** p<0,0001.

4.1.2.2 Monocyte-tumor cocultures

As an alternative method to evaluate the CD200 pathway we used cocultures of undifferentiated monocytes with tumor cells (SKmel28 as CD200+, and A549 as $CD200^-$ control). Interaction of CD200 with monocytes leads to macrophage M2 or MDSC differentiation and increases CD200R expression in such a differentiated monocytes, as described (Belkin et al. 2013; Koning et al. 2010; Moertel et al. 2014). To set up this assay prior to the analysis of virus-produced transgenes, the expression of the M2 marker CD163, the MDSC marker CD33, or the loss of HLA-DR and gain of CD200R as a monocyte differentiation markers were measured after the coculture of monocytes and tumor cells. Results are shown in **Figure 25**, in which no significant increase of M2 or MDSC markers CD163, CD33 were detected in the coculture with $CD200^+$ SkMel28 cells. Only CD163 showed increase in the presence of SK-Mel-28 cells at day 5 compared to the day 3 value but it was not significant. On the other hand loss of HLA-DR was observed to the same extent regardless of the cell line used ($CD200^+$ or $CD200^-$) and, contrary to the expected, CD200R decreased upon coculture of monocytes with both cell lines. In conclusion, in our hands the monocyte coculture with CD200-expressing tumor cells did not lead to M2/MDSC differentiation and we discarded this assay for further studies with the viruses.

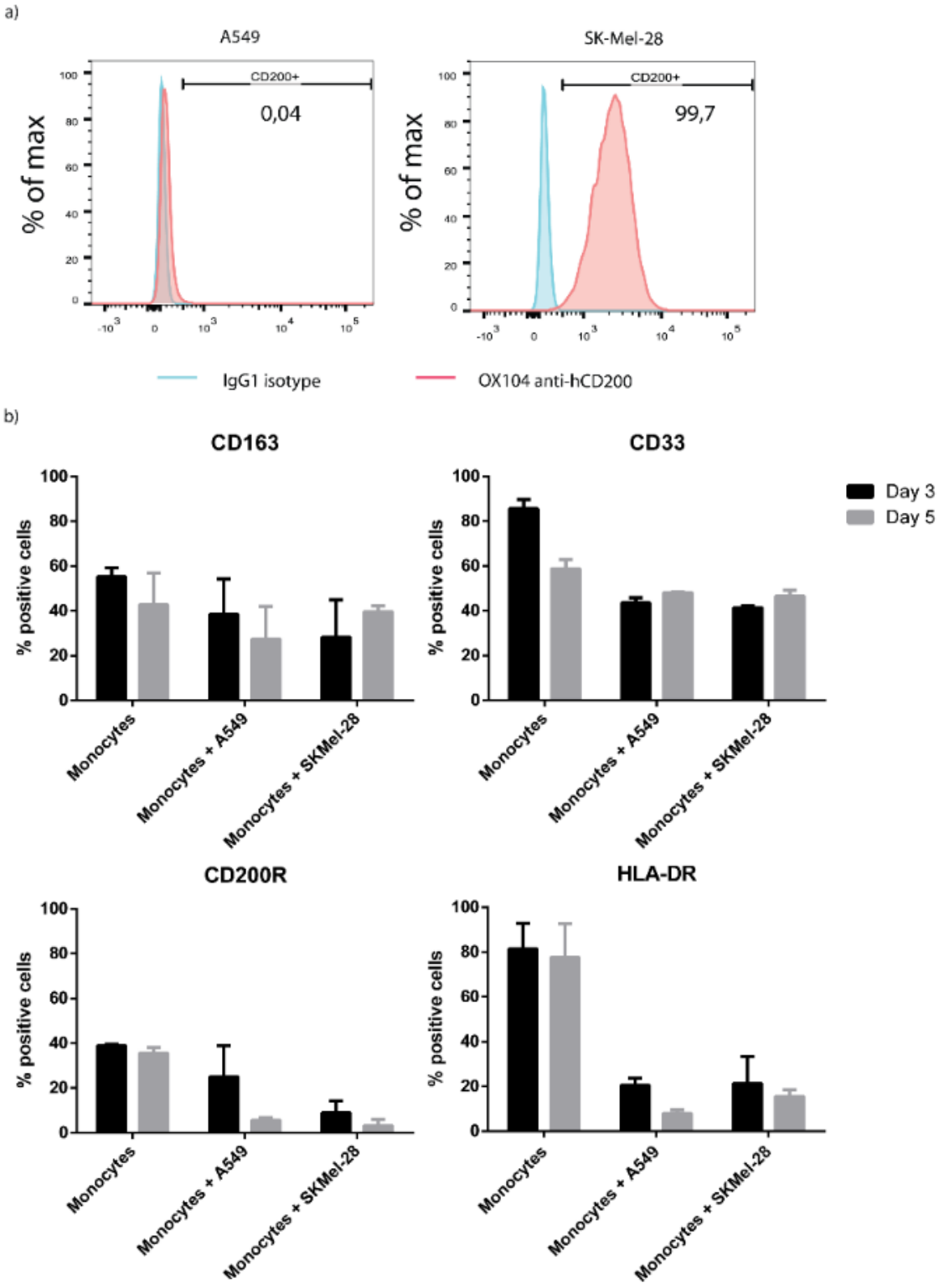

Figure 25. Monocyte-tumor cell cocultures. a) CD200 expression in A549 and SK-Mel-28 cells was assessed by flow cytometry. 10^4 events were acquired for analysis per sample b) CD14+ undifferentiated monocytes were purified from PBMCs and cocultured at 1:1 ratio with either A549 or SK-Mel-28 cells, or alone in 24-well plates. At days 3 and 5, expression of the different markers was analysed by flow cytometry. 105 events were acquired per sample for analysis.

4.1.2.3 CMV-specific CTL proliferation

In order to assess a the effect of the transgenes on antigen-driven adaptive immune amplifications, T cells and peptide-pulsed DCs from CMV-reactive donors were cocultured in the presence of the different viruses, and proliferation of specific CTLs for the pulsed peptide was quantified. In theory, the inhibitory transgenes CD200 and K14 should bind CD200R on DCs and eventually block T cell activation and proliferation, whereas the truncated proteins should prevent this inhibition of the system and allow efficient T cell proliferation. As results show in **Figure 26**, the only significantly CTL-proliferated population was the positive control (black). No transgene-carrying virus could achieve similar levels compared to the control ICOVIR-15K virus (red), which resembled the untreated culture (white) with ~5% proliferation values. Even though an inhibitory role for CD200 and K14 seems consistent, no immunostimulatory or CD200R antagonistic effect was observed for any of the truncated proteins, which was especially unexpected for CD200tr, which had shown CD200R antagonism fashion in previous experiments.

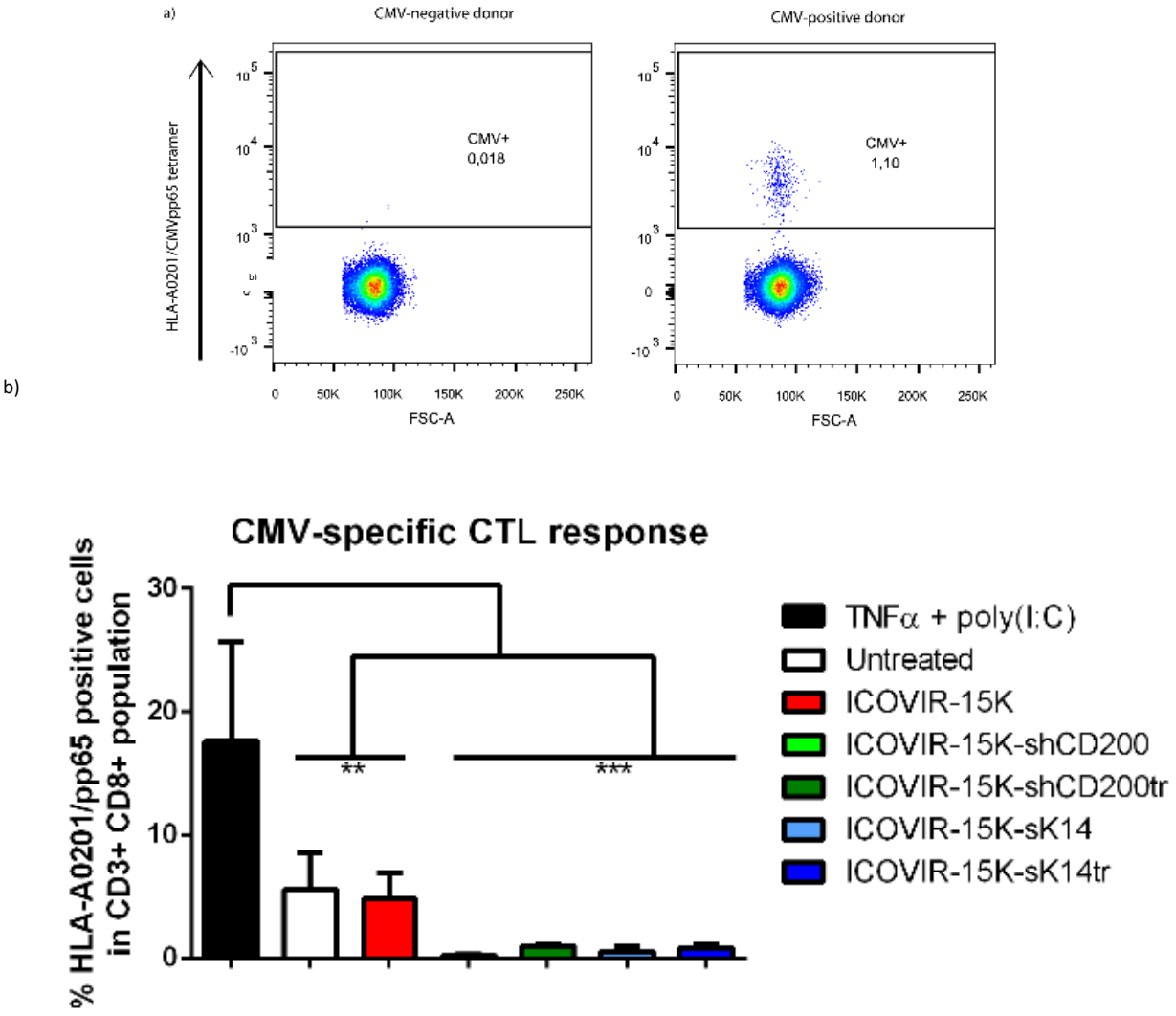

Figure 26. CMV-specific CTL proliferation. a) PBMCs from buffy coats were analyzed by flow cytometry to select CMV-reactive donors for the experiments. In both graphs, CD3+ CD8+ gated cells are shown. Donors with >1% of tetramer-positive lymphocytes were chosen for the experiments. 106 total events per sample were acquired for total PBMC analysis **b)** Differentiated DCs pulsed with CMV-pp65 peptide were cocultured with autologous T cells at a respective 1:10 ratio in 24-well plates in the presence of the different treatments or viruses and were left for 11 days at 37ºC. Then, tetramer binding of the CD3+ CD8+ population in all wells was analysed by flow cytometry. 105 events per sample were acquired for analysis. One-way ANOVA and Tukey post-hoc test were applied on these data: ** p<0,01, *** p<0,001.

Adding up all results from this chapter, we came to realize nothing was even slightly leading us to think that K14tr could behave as a CD200R antagonist in any in vitro setup. This, coupled to the fact that we were having a lot of variability in our assays, made us find no basis to move on to in vivo studies, which were already intrinsically complicated for this project, since they would have probably implied either the use of immunocompetent murine models or the humanization of immunodeficient murine models. Thus, this project was stopped at this point.

4.2 Oncolytic adenoviruses expressing stroma-activatable toxins

4.2.1 Generation of OAds expressing stroma-activated toxins

Alpha-toxin (atox) and aerolysin are bacterial pore-forming toxins from the same family. They show many common features, including binding to GPI-anchored proteins on cell membrane, specific activating cleavage sites and fast and potent induction of cell necrosis by means of hampering cell homeostasis due to the pores they form on the cell membrane once the oligomerize (Abrami, Fivaz, and van der Goot 2000; van der Goot 2001). Many of their traits are highly appealing for the stroma-targeting approach presented in this work. Firstly, because their zymoxin initial status allows for engineered stroma-specific protease activation by the substitution of their natural linker, which keeps the catalytic and inhibitory toxin domains bound until its cleavage. Secondly, because their unspecific toxicity upon activation allows killing of stromal fibroblasts, which are not affected by OAd infection.

Altogether, we propose the combination of oncolytic virotherapy with Adenoviruses and the targeted toxicity provided by these engineered toxins in the form of recombinant viruses carrying the toxins as transgenes. With these viruses, we seek to achieve stroma disruption and significant toxicity in virus-resistant cells the OAd might run into inside the tumor, so that physical barriers become one less hurdle to overcome. The designed viruses expressing these modified toxins are shown in **Figure 27**. For all cases the ICOVIR-15K platform was chosen as control backbone. In the case of the two viruses with an engineered atox from *Clostridium septicum*, the transgenes were cloned after the fiber gene under the IIIa splice acceptor activity, dependent on the MLP. The atox natural linker was substituted by a FAP-sensitive linker. In contrast, the engineered aerolysin transgene from *Aeromonas hydrophyla* was allocated under the Branch Point Splicing Acceptor (BPSA) between the E4 and RITR regions, also under the control of the MLP, and its natural linker was replaced by an MMP-9-sensitive one. This location within the Ad genome provides a more replication-restricted transgene expression, and due to the bigger distance between MLP and the transgene, BPSA, a stronger splicing acceptor than IIIa, was chosen. Also, a 6-Histidine tag was inserted at the C-terminal end of the aerolysin inhibitory domain to facilitate its detection.

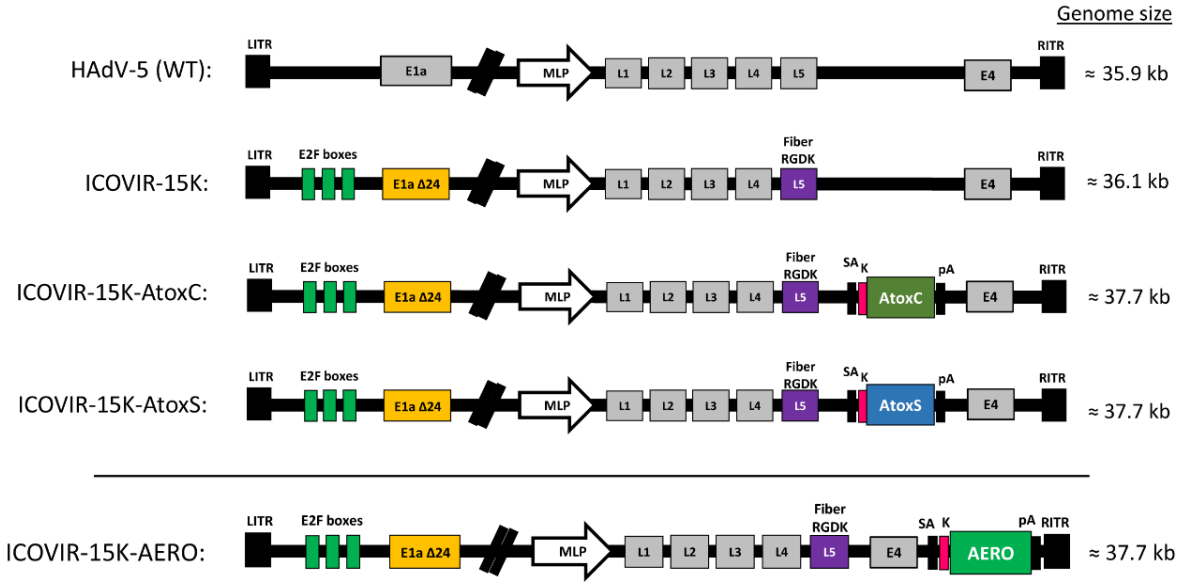

Figure 27. Stroma-activatable-expressing viruses. Schematic representation of the viruses used in this Section. ICOVIR-15K presents the already discussed oncotargeting modifications compared to HAdV-5, the wild type virus. For AtoxC and AtoxS viruses, IIIa splice acceptor and Kozak sequences were included 5' of the transgene, whereas BPSA and Kozak were chosen for the AERO virus. A stronger splice acceptor was chosen in the latter due to the increased distance from the MLP in order to guarantee efficient transgene expression. A 6-Histidine tag was inserted at the C-terminus of aerolysin to facilitate detection. For all cases, coding DNA sequences were codon-optimized towards the human-biased codon use.

The sequences of the native and modified linkers used for every case are shown in **Table 10**. Also, in **Table 11**, the reference physical and functional titers obtained after virus purification (performed as explained in Materials and Methods) are presented. All viruses, especially the ICOVIR-15K control virus and ICOVIR-15K-AERO, showed similar proper bioactivity, which enabled easy and comparable manipulation for both in vitro and in vivo assays. Atox and aerolysin viruses were seldom included together in the same assays (data not shown), since they were tested during different stages of this thesis and, more importantly, their activation is mediated by different proteases.

Virus	Natural linker	Modified linker	Sensitivity
ICOVIR-15K-AtoxC	RGKRSVDS	DRGETGPA	FAP
ICOVIR-15K-AtoxS	RGKRSVDS	GSSFSSGPVADGII	FAP
ICOVIR-15K-AERO	KVRRTR	AKGLYK	MMP-9

Table 10. Linker aminoacid sequences in engineered toxins. For Atox viruses, linkers were added through PCR procedures. For AERO, linker was included in a transgene cassette obtained from GenScript. Linkers were surrounded by two Gly residues per side in order to guarantee flexibility. Correct insertion was confirmed by DNA sequencing.

Virus	Physical titer (vp/ml)	Functional titer (TU/ml)	Ratio
ICOVIR-15K	$5,7 \cdot 10^{12}$	$5,07 \cdot 10^{11}$	11,25
ICOVIR-15K-AtoxC	$1,27 \cdot 10^{12}$	$6,37 \cdot 10^{10}$	19,89
ICOVIR-15K-AtoxS	$1,47 \cdot 10^{12}$	$7 \cdot 10^{10}$	20,42
ICOVIR-15K-AERO	$1,7 \cdot 10^{12}$	$3,15 \cdot 10^{11}$	5,41

Table 11. Physical and functional titers of toxin-expressing viruses. Ratios are expressed in vp/TU.

4.2.2 OAds expressing a stroma-targeted Alpha-toxin from *Clostridium septicum*

4.2.2.1 In vitro characterization: viral production and cytotoxicity

In order to check that the insertion of transgenes did not hamper the replicative potential of the Adenoviruses, viral production assays were performed in the virus-permissive A549 cell line. As shown in **Figure 28**, no significant differences were observed in total virus yields after 72h of infection.

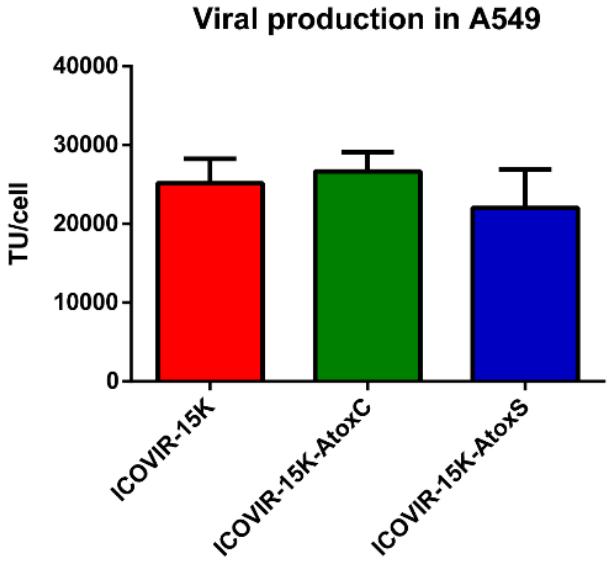

Figure 28. Viral production assays with atox-expressing viruses. As described in previous sections, A549 cells were infected at an MOI of 20 for 4h in 24-well plates, then medium was washed and fresh DMEM 10% was added, and they were left at 37ºC for 72h. Then, well content was collected, cell extracts were obtained by freeze-thawing and anti-hexon staining in 293 cells was performed to quantify the viable transducing units present for each virus. One-way ANOVA and Tukey post-hoc test were applied on these data.

In terms of cytotoxicity, viruses were tested both in FAP^- A549 cells and partially FAP^+ SW872 cells. Results are shown in **Figure 29**, and corresponding IC50 are presented in **Table 12**. Both atox viruses showed loss of potency in both cell lines. SW872 IC50 values indicate they are highly resistant to viral replication, since normal values for virus-permissive cells never reach 100 TU/ml. Altogether, this assay did not seem adequate to test the FAP-mediated toxicity in vitro, since the amount of transgene produced in these conditions is likely to be very low and their expression of FAP is variable. Of course, no advantage could be achieved by the

expression of the atox transgene in A549 cells, since it would never become activated due to the absence of FAP in target cells.

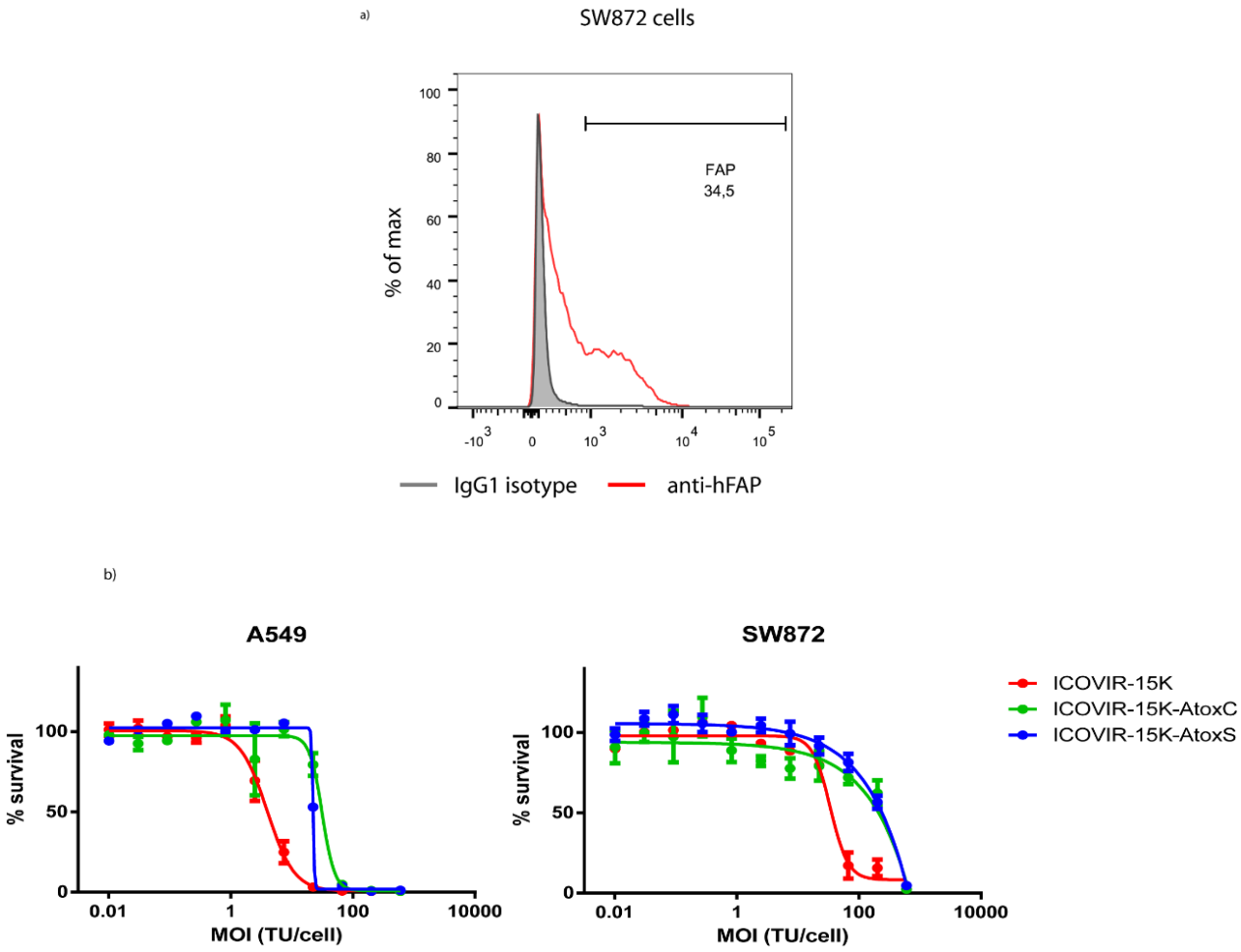

Figure 29. Cytotoxicity of atox viruses. a) FAP expression in SW872 cells was confirmed by flow cytometry. 10^4 events were acquired for analysis **b)** A549 or partially FAP$^+$ SW872 cells were infected at gradually decreasing MOIs of the different viruses, starting at 600, and incubated at 37ºC for 5-7 days. When CPE was complete in the first half of any plate, viability in all cell lines was assessed by BCA staining and absorbance was read in a plate reader at 540 nm.

Virus	IC_{50} in A549	IC_{50} in SW872	Fold vs 15K A549	Fold vs 15K SW872
ICOVIR-15K	3,95	33,95	1	1
ICOVIR-15K-AtoxC	31,37	125,08	7,94	3,68
ICOVIR-15K-AtoxS	22,24	128,54	5,63	3,79

Table 12. IC_{50} values of atox viruses in A549 and SW872. IC_{50} values are expressed in TU/ml. Fold values of <1 indicate increased potency, and vice versa.

4.2.2.2 FAP-mediated cytotoxicity

In order to discriminate the cytotoxicity mediated exclusively by FAP, concentrated supernatants from infected cultures with each virus were incubated with or without recombinant FAP and were later added to tumor cells to allow activated atox to elicit its action. In supernatants containing modified atox, recombinant FAP should cleave the linker and release the inhibitory C-terminal peptide, rendering the toxin active. Shown in **Figure 30**, a summary of the results obtained in pancreatic MiaPaCa-2 cells shows that no significantly increased toxicity was reached in the FAP^+ condition of the atox viruses compared to the control ICOVIR-15K virus. In detail, control ICOVIR-15K virus showed a FAP^+/FAP^- ratio of cell survival of 0,5, indicating that the FAP^+ condition led to increased cell death, which was unexpected for the empty virus. Both AtoxC and AtoxS viruses showed the same behavior and with notably high variability, indicating no advantage in cell death could be attributed to atox from the supernatants.

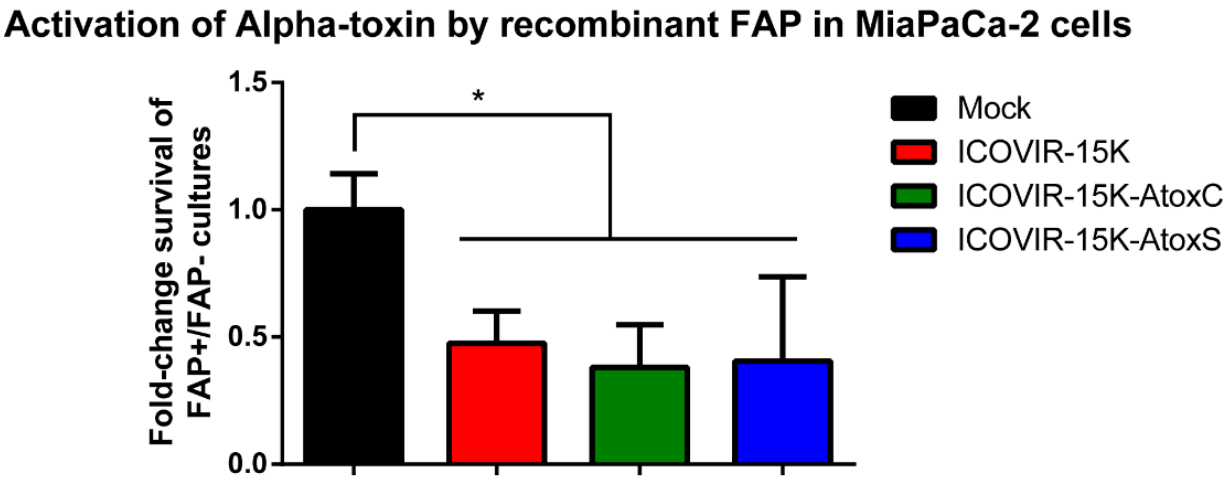

Figure 30. Cytotoxic studies with recombinant FAP. Concentrated supernatants of infected cultures with the different viruses were incubated with recombinant FAP at 37ºC for 1-2h and were added to tumor cells in 96-well plates (see Annex for more comprehensive data). After 48h, viability was assessed by standard MTT protocol. One-way ANOVA and Tukey post-hoc test was applied on these data: * $p<0,05$.

Aiming to optimize the activation potential of the engineered atox toxin, 293, 293-hFAP and 293-mFAP cells were used for further cytotoxic studies. This also allowed us to have a full FAP^+ scenario which was not possible with SW872 cells. Since PFTs are able to induce apoptosis and necrosis at early time points (Imre et al. 2012; K L Nelson, Brodsky, and Buckley 1999), cells were treated with concentrated supernatants from infected cultures and apoptosis induction was assessed 24h post-infection in order to minimize virus-induced apoptosis, which should more representative in later time points. Results shown in **Figure 31** revealed a significant

increase in apoptotic cell count with the atox virus (only AtoxC was tested since it showed a consistent tendency of higher potency than AtoxS) versus the control virus only in FAP-expressing cell lines, initially pointing at ongoing atox-mediated toxicity. However, atox toxicity was only significant in the mFAP cell line versus the FAP^- cell line, and not in the hFAP cell line. Interestingly, murine FAP was shown to also activate atox, as had been predicted, and this constituted a relevant finding in the context of an in vivo preclinical setting, in which the fibroblasts are of murine origin.

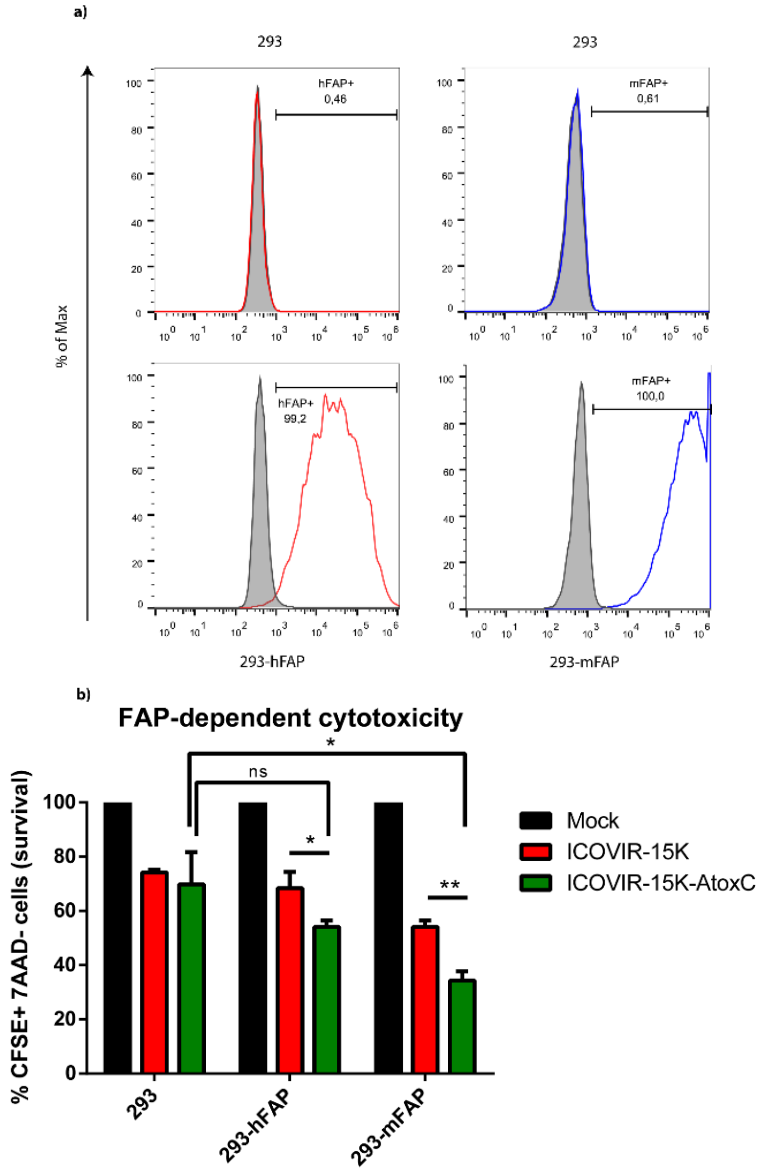

Figure 31. Atox-mediated cytotoxicity in FAP^+ cell lines. a) Human and murine FAP expression was confirmed in modified 293 cells by flow cytometry. 10^4 total events per sample were acquired for analysis **b)** Concentrated supernatants from infected cultures were added to 293, 293-hFAP and 293-mFAP cells in 96-well plates and incubated 24h at 37ºC. Then, cells were stained with the apoptotic marker 7-AAD and apoptosis induction was assessed by flow cytometry. 10^4 events per sample were acquired for analysis. Two-way ANOVA and Tukey post-hoc test were applied on these data: * p<0,05, ** p<0,01.

4.2.2.3 ICOVIR-15K-AtoxC in an orthotopic pancreatic model

Once atox-mediated toxicity had been detected in vitro, ICOVIR-15K-AtoxC was put to test in a stroma-rich pancreatic orthotopic model termed TP5 derived from a ductal adenocarcinoma patient. Hence, orthotopic tumors were implanted in nude athymic mice and tumor size was monitored after systemic treatment with the different viruses, as shown in **Figure 32**. No significant antitumoral effect was observed in tumors treated with the atox-expressing virus, even though a non-significant improvement was detected. The same applies for the survival curve, in which no significant survival enhancement was observed with ICOVIR-15K-AtoxC. In order to maximize the cytotoxic potential of a stroma-targeted toxin, an aerolysin-expressing virus inherited the goal from the atox-expressing viruses.

a)

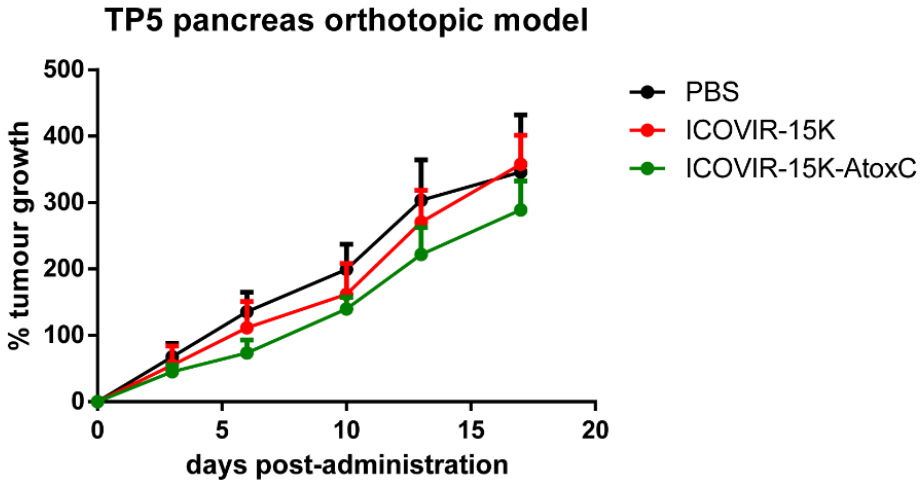

b)

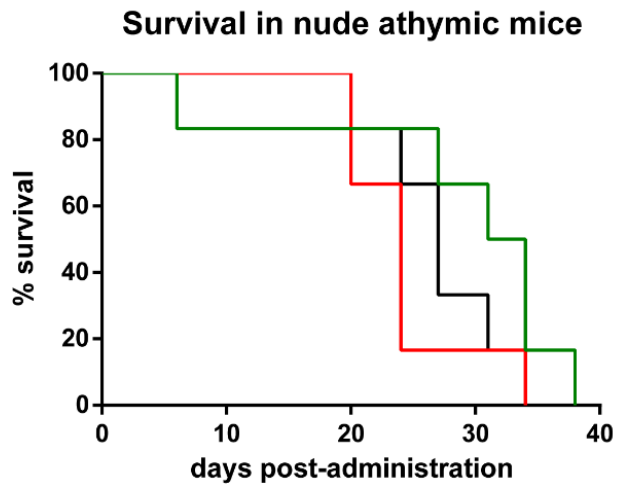

Figure 32. Antitumor efficacy study in a pancreatic orthtopic model. Cryopreserved TP5 fragment was implanted orthotopically in the pancreas of nude mice and passaged once to a second round of mice (n per group=7). Once tumors reached ~200 mm^3, treatment was administered i.v. and follow-up was performed every 2-3 days. One-way ANOVA with Tukey post-hoc test were applied on these data.

In terms of toxicity mediated by the viruses, the profiles pictured in **Figure 33** demonstrate an increased toxicity of the atox-expressing virus, with a noticeable peak at day 6, which was however not significant versus the other groups. Intriguingly, animals recovered their original weights by the end of the experiment, but tumor weights, which reached 5 g in some cases (data not shown), can also account for these complete recovery.

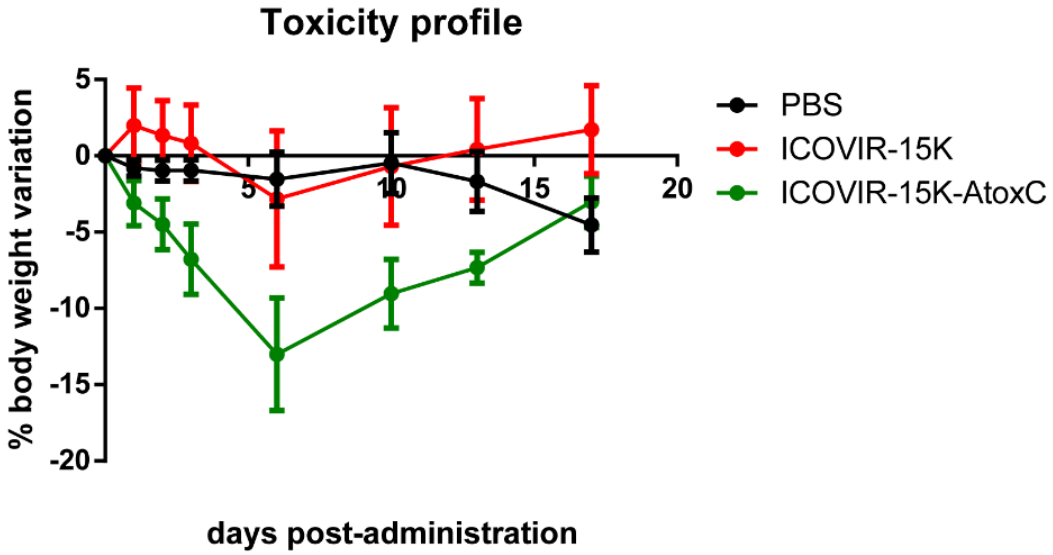

Figure 33. Body weight variation in TP5 orthotopic antitumoral efficacy assay. Animals body weight was monitored closely after virus administration (days 1, 2 and 3) to detect early toxicity and later at more separate time points. One way ANOVA and Kruskal-Wallis test were applied on these data.

4.2.3 OAds expressing a stroma-targeted Aerolysin from *Aeromonas hydrophyla*

4.2.3.1 In vitro characterization: viral production, cytotoxicity and transgene expression

The choice of combining aerolysin and a MMP-9-sensitive linker was grounded on the better understanding of the cytotoxic mechanism exerted by this toxin, its higher stability in solution thanks to dimerization (F. G. Van Der Goot et al. 1993), and its less restrictive activating cleavage, since cleavage of alpha-toxin outside of the membrane yields a wrongly-folded non-functional toxin, whereas aerolysin, even though its inhibitory peptide also acts as a chaperone and reduces oligomerization rates, does not suffer such dramatic effects upon cleavage (Iacovache et al. 2011). ICOVIR-15K-AERO was generated by homologous recombination in bacteria and further amplified in A549 cells. As results in **Figure 34** show, viral production yields after 72h infection of A549 and pancreatic HPAC cells were quantified in parallel with the ICOVIR-15K control virus. No significant differences were observed, demonstrating that no loss of replication capacity was associated with the insertion of the transgene. This was actually in line with the purification values obtained for this virus.

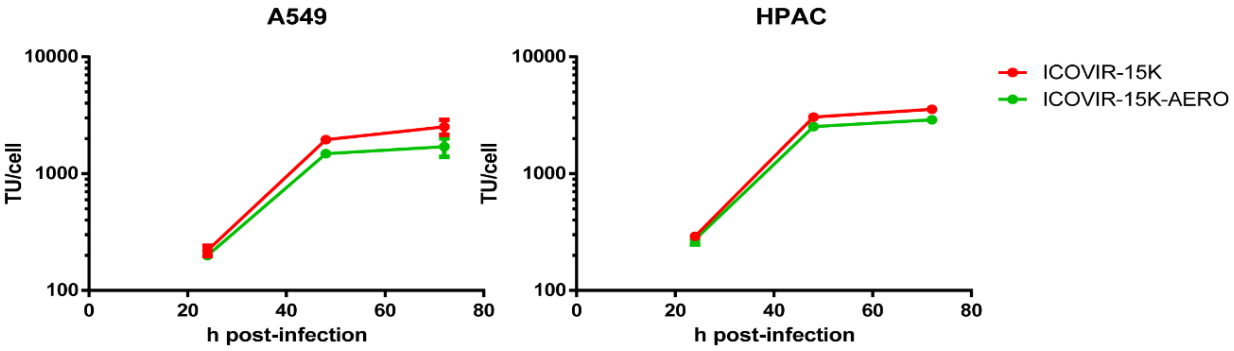

Figure 34. Viral production kinetics of an aerolysin-expressing virus in permissive cell lines. A549 and HPAC cells were infected at MOI 20 and 50, respectively, and functional viral content was quantified at 24, 48 and 72h post-infection by anti-hexon staining. T test analysis was applied on these data.

ICOVIR-15K-AERO oncolytic potential was tested in a panel of cell lines in parallel with ICOVIR-15K. Cytotoxic curves are shown in **Figure 35** and IC_{50} values are shown in **Table 13**. AERO virus cytotoxicity values in this setting are variable. In virus-permissive cell lines such as A549, HPAC or MiaPaCa-2, both viruses performed similarly, with a maximum 2,54x loss in A549 and 1,72x gain in MiaPaCa-2. In more resistant cell lines, a striking 4x gain was observed in HT1080, and also a 6,65x loss in hCAFs. In general terms, both viruses showed comparable behaviors, and further assays, shown in the following sections, were performed to shed some light on whether aerolysin-mediated toxicity could account for the biggest differences observed, since some of the tested cell lines were MMP-9^{+}, whereas others were not.

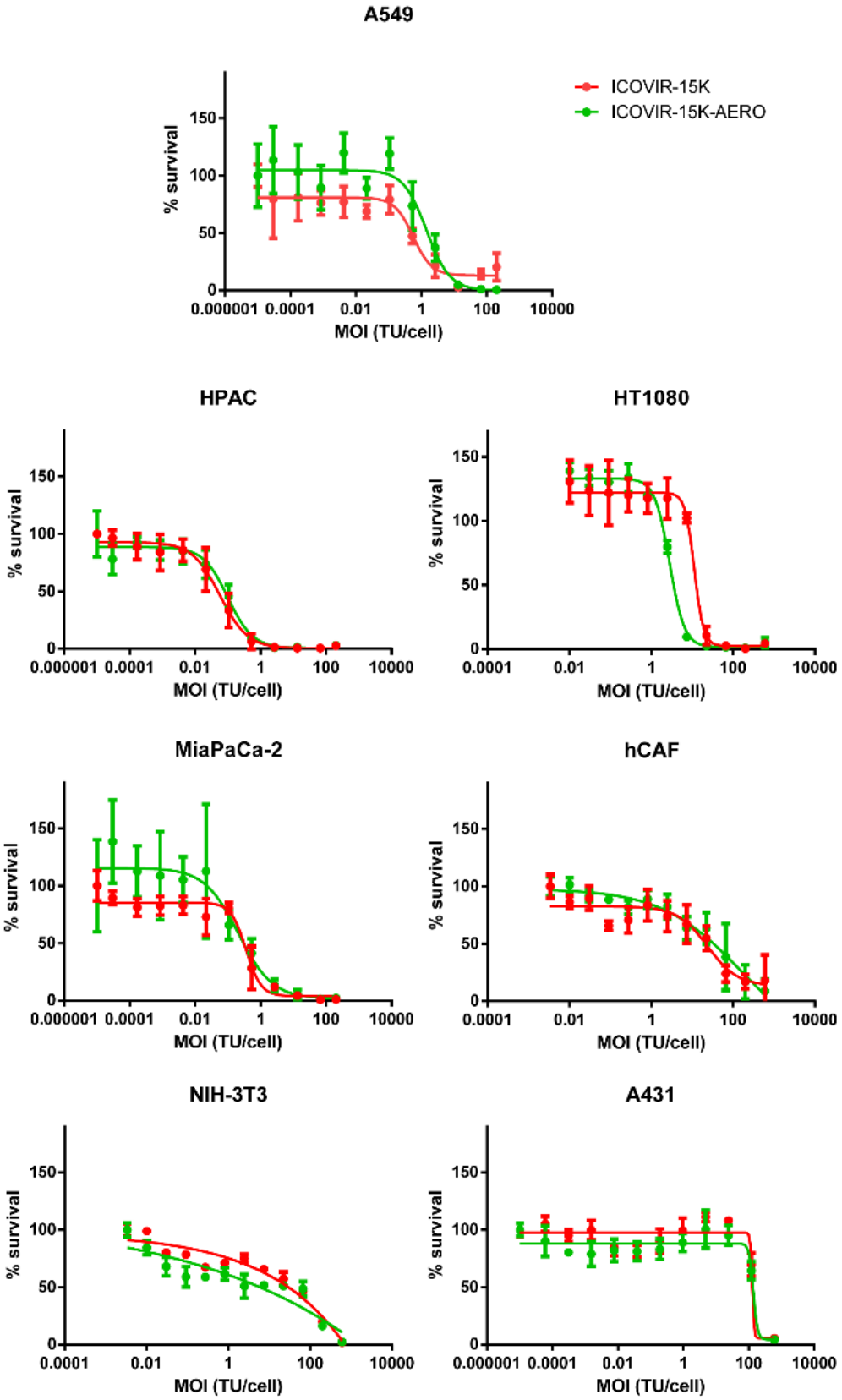

Figure 35. Cytotoxic curves of ICOVIR-15K-AERO in a panel of tumor cell lines. Cells were infected with viruses in 96-well plates at gradually decreasing MOIs, starting at 600, and viability was assessed by BCA protocol and absorbance readout after 5-7 days at 37 °C. A549, MiaPaCa-2 and HPAC cells are MMP-9^{-}, and HT1080, hCAFs, NIH-3T3 and A431 cells are MMP-9^{+} (see details in **Figure 38**).

Cell line	ICOVIR-15K	ICOVIR-15K-AERO	Fold vs 15K
A549	0,56	1,44	2,57
HPAC	0,06	0,1	1,67
HT1080	11,61	2,93	0,25
MiaPaCa-2	0,36	0,21	0,58
hCAF	23,7	157,6	6,65
NIH-3T3	109,18	60,41	0,55
A431	128,8	137,6	1,07

Table 13. IC_{50} values of ICOVIR-15K-AERO in a panel of cell lines. IC_{50} values are expressed in TU/ml. Fold values of <1 indicate increased potency, and vice versa.

Transgene expression from ICOVIR-15K-AERO was assessed through two methods. As shown in **Figure 37**, taking advantage of the Histidine tag present in the protoxin form of aerolysin, binding studies were performed with concentrated supernatants of infected cultures in cells with aerolysin-binding capacity, which had been previously screened (**Figure 36**). In addition, competition assays against a fluorescently-labelled aerolysin (FLAER) were performed to check if FLAER signal could be displaced by the aerolysin present in the supernatants.

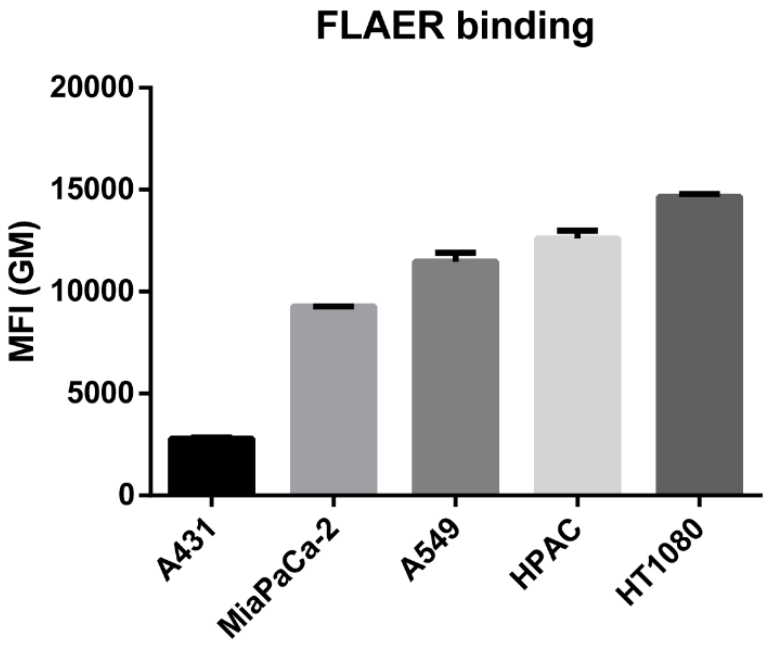

Figure 36. Aerolysin receptor expression in a panel of cell lines. A fluorescently-labelled aerolysin (FLAER) was incubated with 10^6 cells and binding capacity was measured in terms of MFI by flow cytometry (Geometric Mean shown). $2{\cdot}10^4$ events were acquired for analysis. Cell lines were chosen from cytotoxic curve performance of ICOVIR-15K-AERO, and A431 cells were added due to their MMP-9 expression (shown in **Figure 38**).

HT1080 showed the highest density of aerolysin receptors, that is, GPI-anchored proteins, and were used for the competition assays shown in **Figure 37** after FLAER titration (see Annex). A

25% reduction in FLAER signal was observed with such assays, and a 23% positive shift in His Tag binding was detected, indicating that aerolysin expressed from the virus was present in the concentrated supernatants.

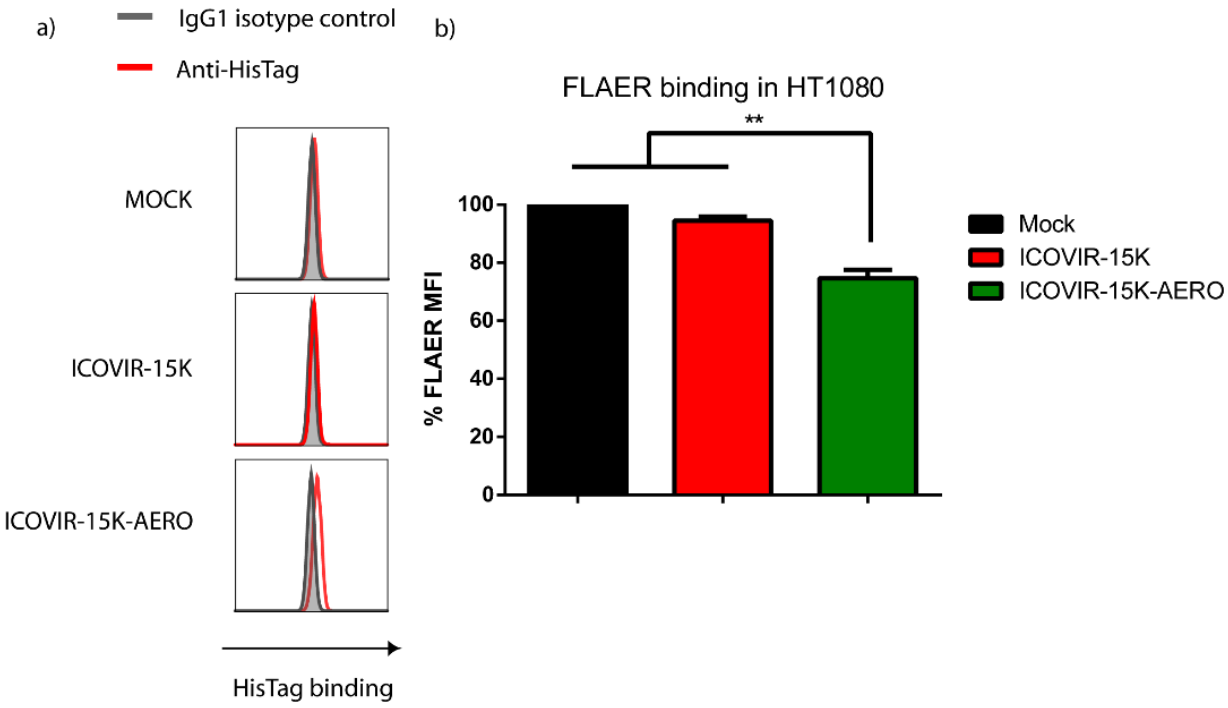

Figure 37. Detection of modified aerolysin from supernatants. a) HT1080 cells were incubated with concentrated supernatants from infected cultures for 2h. Then, His tag binding was quantified by flow cytometry. $2{\cdot}10^4$ events were acquired for analysis **b)** Concentrated supernatants from infected cultures were incubated with HT1080 cells for 2h. Then, cells were washed and FLAER was added in excess to compete for receptor binding. Afterwards, FLAER signal (Alexa 488) was quantified at the cytometer. The y axis on the graph represents % of MFI versus maximum FLAER signal (Mock). One-way ANOVA and Tukey post-hoc test were applied on these data: ** p<0,01.

4.2.3.2 MMP-9-mediated cytotoxicity

First of all, screening of MMP-9 in a panel of cell lines was performed so that the most suitable models could be chosen for further assays. As shown in **Figure 38**, HT1080 and A431 cells exhibited the highest degree of MMP-9 expression. Since these values did not correlate with cytotoxic curves shown previously, where, unlike A431, HT1080 showed sensitivity to ICOVIR-15K-AERO, assays to discriminate specific MMP-9 activation of aerolysin were designed.

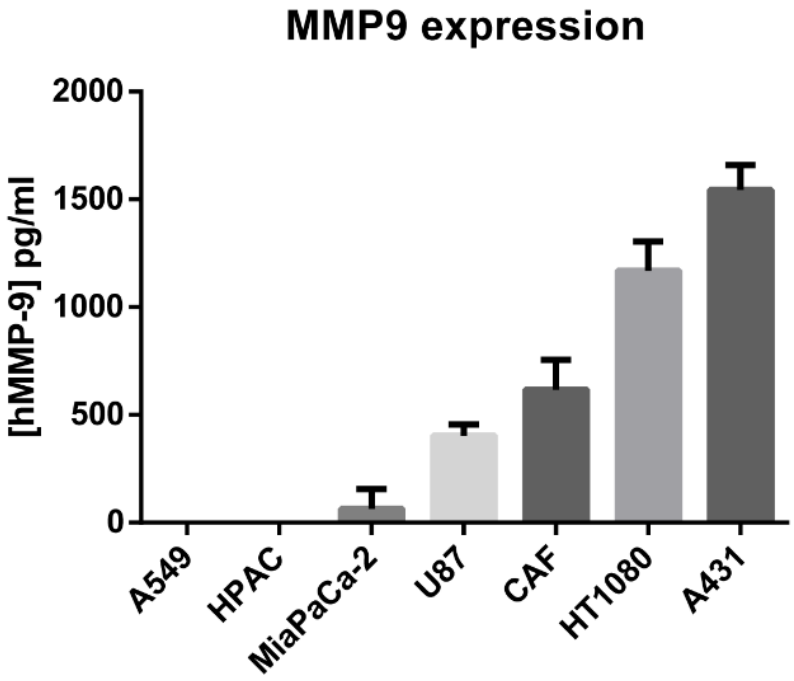

Figure 38. MMP-9 expression in a panel of cell lines. Cell supernatants were harvested after incubation at 37ºC for 3 days in confluence, and MMP-9 content was quantified by ELISA.

As it was done with FAP-sensitive toxins, cytotoxic studies to detect early-induced apoptosis by aerolysin were set up by incubating supernatants from infected cultures with recombinant MMP-9 and adding them to MMP-9$^-$ and MMP-9$^+$ cells, after which apoptosis induction was assessed. Aerolysin present in the supernatants from ICOVIR-15K-AERO should be cleaved by recombinant MMP-9 and thus become activated so that oligomerization, pore formation and subsequent engagement of apoptosis can take place. As shown in **Figure 39**, A549 turned out to be too sensitive to the virus-mediated apoptosis (supernatants cannot be completely virus-free) to yield any significant differences. Interestingly, HPAC cells, which are MMP-9$^-$, showed significantly increased toxicity exclusively when AERO supernatants were incubated with recombinant MMP-9 (gray bars). Also, MMP-9$^+$ cell lines such as hCAF, HT1080 and A431 showed significantly increased toxicity with ICOVIR-15K-AERO irrespective of the presence or absence of MMP-9 in the initial incubation. In the case of NIH-3T3 cells, they behaved like MMP-9$^+$ cells, even though expression of murine MMP-9 was not tested.

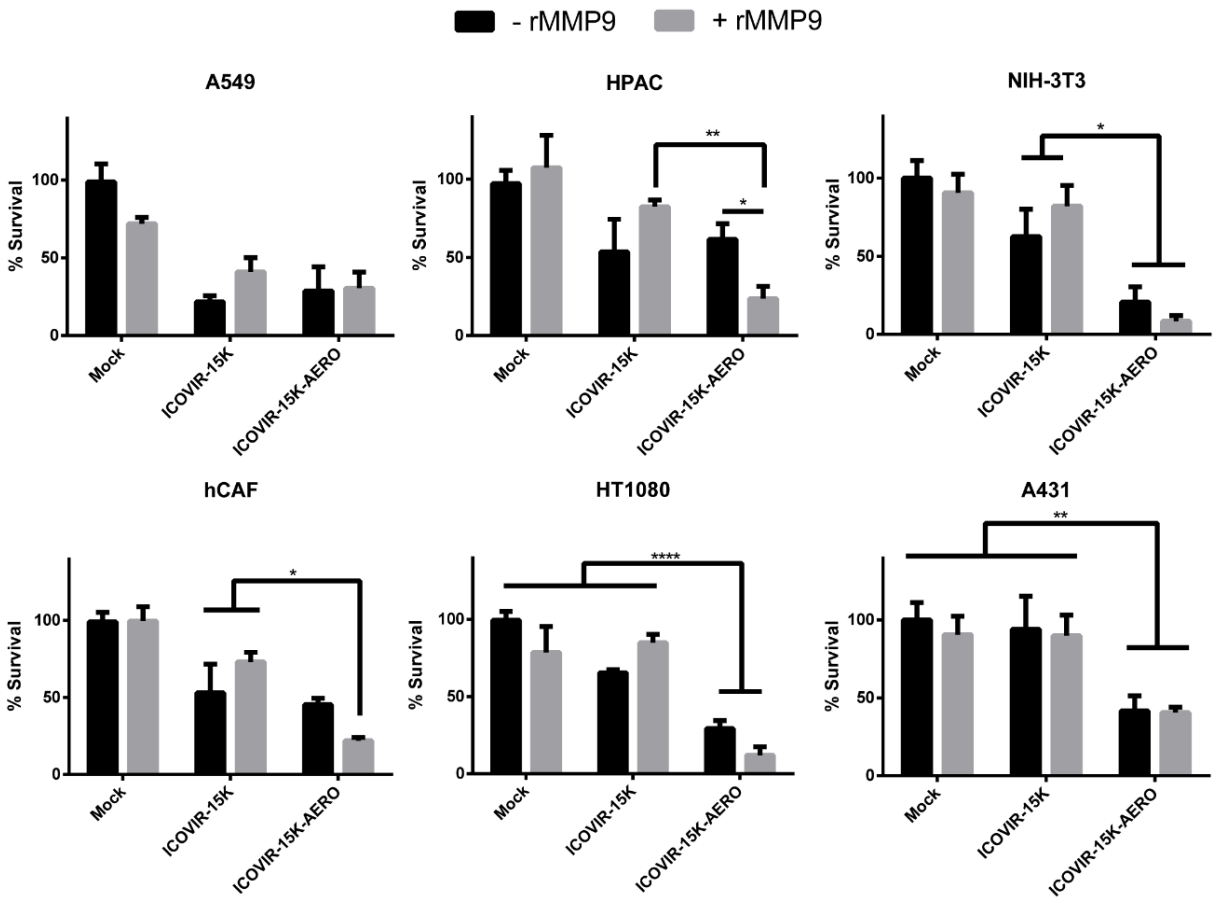

Figure 39. Aerolysin activation by recombinant MMP-9. Concentrated supernatants from infected cultures were incubated with or without 1 ng/ml rMMP-9, and these mixes were later added to cells in 96-well plates. After 24-48h, apoptosis induction was assessed by flow cytometry through 7-AAD staining. In general, 10^4 events were acquired for analysis, even though for hCAF cells this value was not always reached. Two-way ANOVA and Tukey post-hoc test were applied on these data: * p<0,05, ** p<0,01, **** p<0,0001.

Once virus-independent toxicity was demonstrated, a model to guarantee enough amounts of aerolysin to induce significantly increased toxicity in virus-resistant cells in which replication and transgene expression is defective in spite of being MMP-9^+ was performed, as A431, NIH-3T3, hCAF or even HT1080, even though IC50 values of the latter were closer to those of cell lines regarded as virus-sensitive ones.

To this purpose, cocultures comprising virus-permissive transgene-producing A549 cells and target MMP-9^- or MMP-9^+ cells were set up in order to detect a bystander effect of the aerolysin secreted by A549 cells on target MMP-9^+ cells, where aerolysin would be activated by cleavage, unlike in MMP-9^- cocultures, where the inhibitory peptide should never be removed. Results pictured in **Figure 40** show that, in HPAC, the only MMP-9^- represented in this panel, no differences were detected between viruses. This reinforced the safety and specificity of this strategy, since no unwanted leaky aerolysin activity could be detected.

Notably, significantly reduced survival was observed in MMP-9^{+} cocultures infected with ICOVIR-15K-AERO, reinforcing the demonstration of aerolysin-mediated apoptosis in vitro.

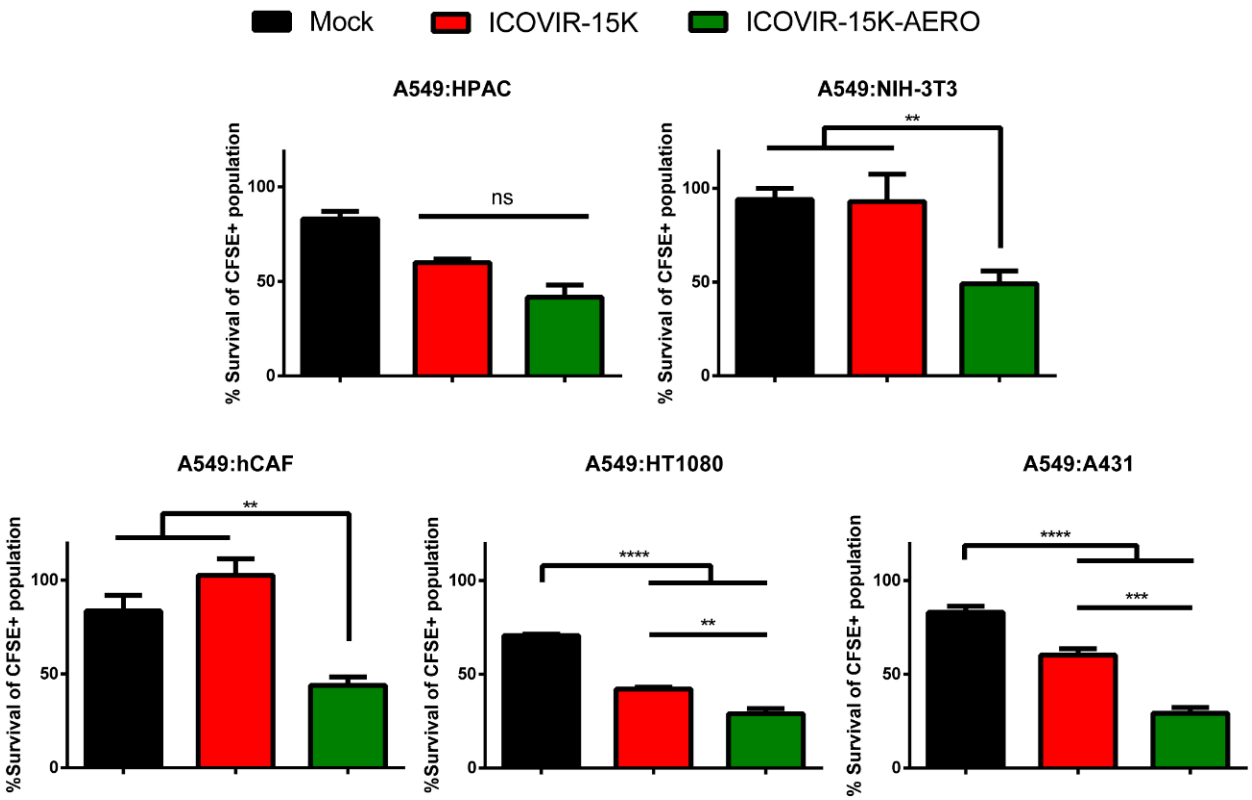

Figure 40. Bystander effect assays with ICOVIR-15K-AERO. A549 cells were infected at an MOI of 20 with the different viruses for 4h and then added to target CFSE-stained cells at a 1:1 ratio in 96-well plates. After 48-60h of incubation at 37ºC, viability was assessed by flow cytometry. $2 \cdot 10^4$ total events were acquired for analysis. One-way ANOVA and Tukey post-hoc test were applied on these data: ** p<0,01, *** p<0,001, **** p<0,0001.

4.2.3.3 *In vivo* studies with ICOVIR-15K-AERO

Taking an overall view on the in vitro data produced by ICOVIR-15K-AERO, two requirements could be concluded for further in vivo studies with this virus. Firstly, virus-permissive cells were needed to produce sufficient amounts of transgene and secondary rounds of viral infections. Secondly, expression of MMP-9 is of course mandatory to observe aerolysin-specific toxicity. Interestingly, none of the cell lines tested in vitro offered such features simultaneously, so subcutaneous tumors from a number of cell lines implanted in athymic nude mice were tested for MMP-9 expression by in situ zymography (ISZ), since the possibility that it may come from the murine stroma (we previously demonstrated sensitivity of murine fibroblasts to aerolysin) may allow the use of a virus-sensitive MMP-9^{-} cell line for in vivo approaches. Results shown in **Figure 41** demonstrated MMP-9 expression in the three cell

lines tested, and A549 and HPAC were chosen for antitumoral efficacy studies based on cytotoxic studies and aerolysin receptor quantitation.

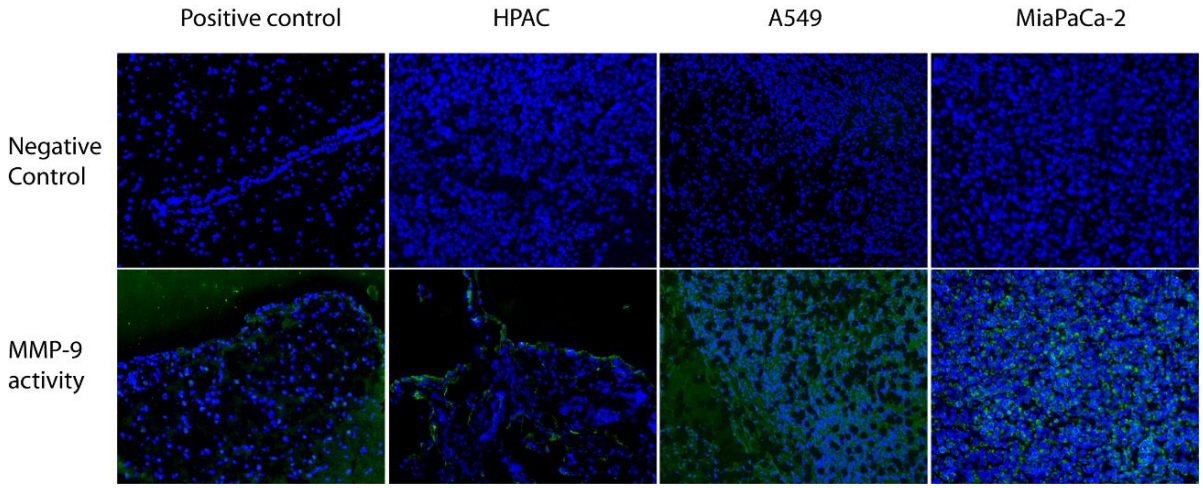

Figure 41. MMP-9 activity in subcutaneous tumors. Tumor cells (generally $3 \cdot 10^6$ cells per tumor) were implanted in both flanks of athymic nude mice and were left to grow up to 500 mm^3, moment at which animals were sacrificed and tumors were collected. Then, in situ zymography using DQ gelatin was performed in OCT slides and images (20X) were obtained at the microscope. Shown are representative images for each tumor. Positive control was obtained from human brain tissue.

Hence, subcutaneous tumors of A549 and HPAC cell lines were generated in athymic nude mice and upon virus administration tumor volume was monitored until endpoint criteria was reached. As depicted in **Figure 42**, ICOVIR-15K-AERO showed significantly reduced tumor growth in both models even from early time points (day 6) and up until the termination of the experiment, indicating a possible role of aerolysin in inducing MMP-9-activated toxicity not only in tumor cells, but also in stromal cells.

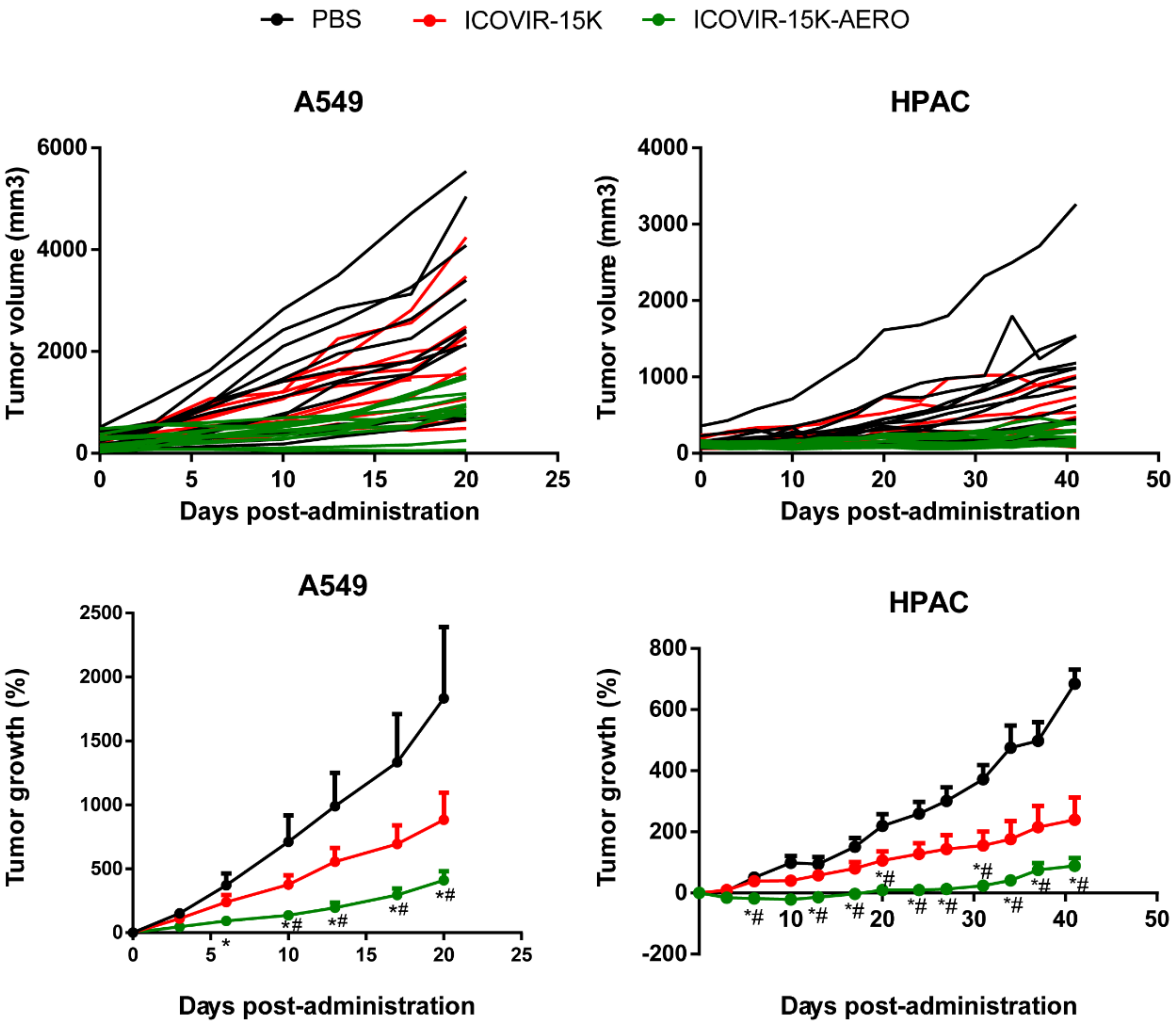

Figure 42. Antitumor efficacy studies with ICOVIR-15K-AERO. A549 or HPAC cells were implanted subcutaneously (5 and 3 million, respectively) in mice flanks and tumors were left to grow until reaching 200 or 150 mm^3, respectively, moment at which treatment was administered i.v. Tumor volume was monitored every 2-3 days. In the upper part of the panel, spider graphs of individual tumor volume values are shown. In the lower part, tumor growth percentage versus initial volumes is shown. One-way ANOVA and Kruskal-Wallis post-hoc test were applied on these data: * p<0,05 vs PBS; # p<0,05 vs ICOVIR-15K.

As for toxicity induced by the viruses, body weight follow-up was performed, and as shown in **Figure 43**, a non-significant maximum loss was consistently observed at day 6, reaching almost a 10% reduction in both models. Interestingly, in the HPAC model, mice recovered their body weights by the end of the experiment, whereas in the A549 model, even though tumor sizes did not reach very high values, loss of weight was maintained until the end of the experiment.

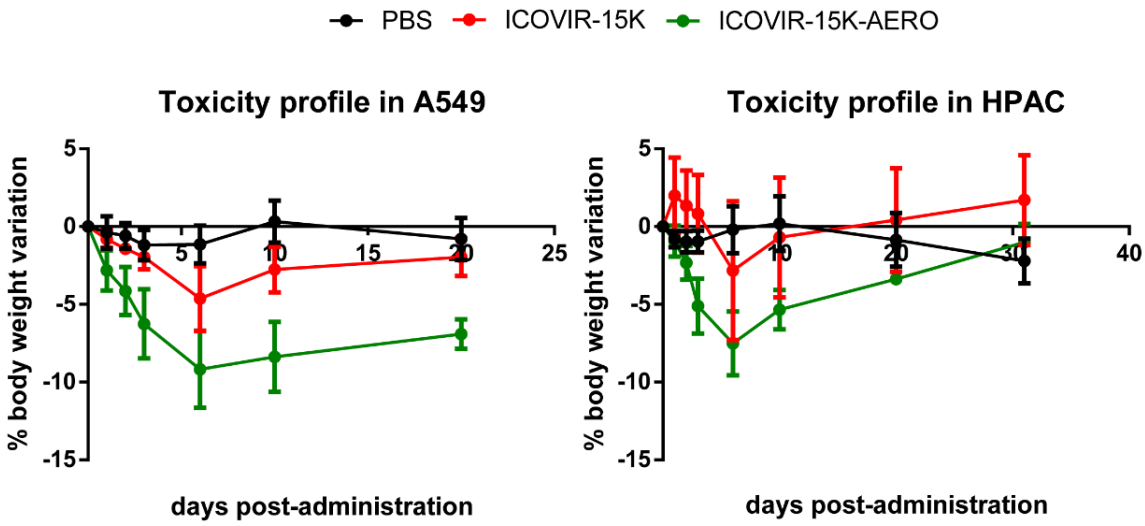

Figure 43. Body weight variation in A549 and HPAC antiumoral efficacy assays. Animals body weight was monitored closely after virus administration (days 1, 2 and 3) to detect early toxicity and later at more separate time points. One way ANOVA and Kruskal-Wallis test were applied on these data.

4.2.3.3.1 Ad5 detection in tumors

Paraffin sections from A549 and HPAC tumors were stained for Ad5 E1a protein to analyze the localization of Ad5 within the tumors. As **Figure 44** shows, virus could only be detected by this method in A549 tumors. Moreover, ICOVIR-15K treated tumors showed higher frequency of anti-E1a staining when compared to ICOVIR-15K-AERO-treated tumors, which did not correlate with antitumor efficacy values. Distribution of anti-E1a staining across the tumor is similar in all groups, with areas in which clustered cells show an intense positive signal. In general, positive cells were next to necrotic areas, suggesting Adenovirus-mediated progressive tumor oncolysis taking place inside the tumor. Fibrotic septa are observed surrounding the positive nodes in some cases.

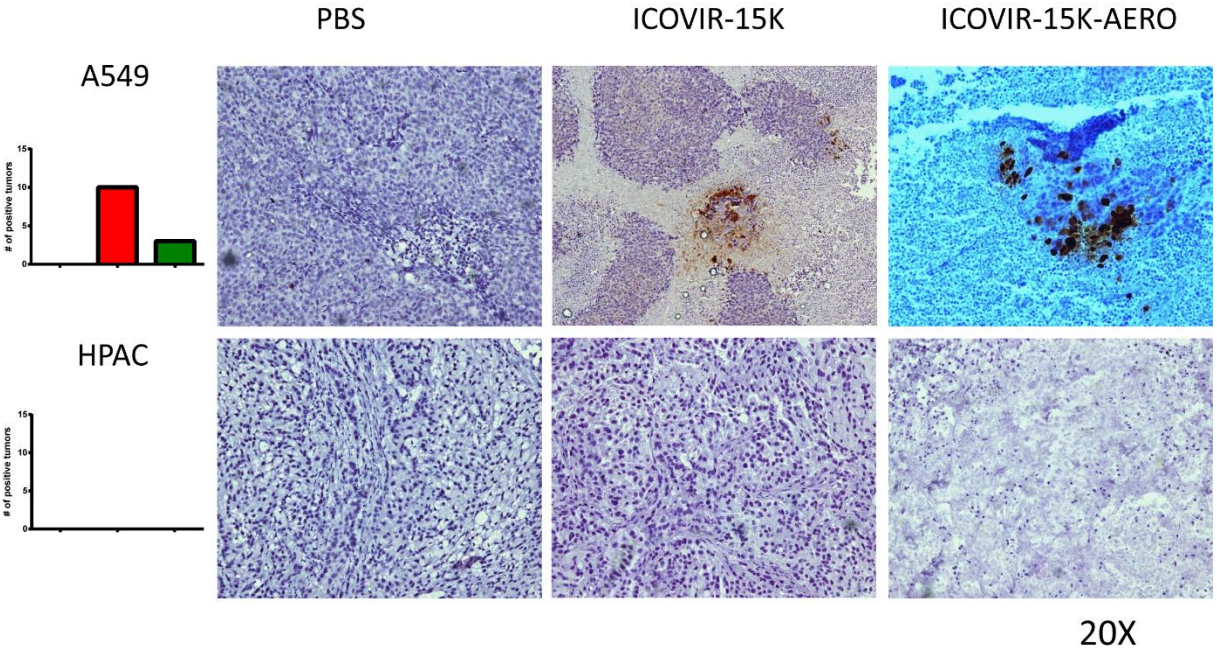

Figure 44. Ad5 staining in A549 and HPAC tumors. Paraffin-embedded sections from both models were stained for Adenoviral E1a protein (brown signal). Representative images are provided. The number of positive tumors in each group is represented in the column graphs (left). Red: ICOVIR-15K; Green: ICOVIR-15K-AERO. No positive tissue was observed in any HPAC tumor.

As a reinforcing quantitative study of the presence of Adenoviral particles within the tumors, qPCR spanning the Adenoviral hexon gene was performed in DNA samples obtained from tumor lysates. Interestingly, for both models, presence of Adenovirus was significantly higher in tumors treated with ICOVIR-15K, which once again did not correlate with the higher efficacy observed in ICOVIR-15K-AERO-treated tumors **Figure 45**. As expected, PBS-treated tumors showed negligible amounts of Ad particles.

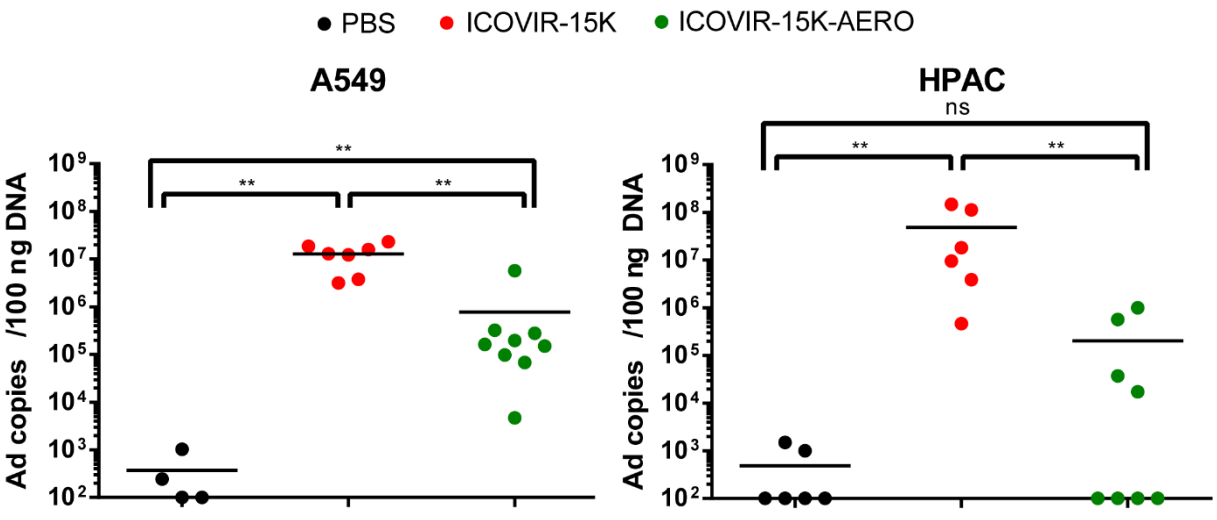

Figure 45. Ad5 detection by qPCR in A549 and HPAC tumors. DNA from tumor lysates was obtained and analyzed in triplicate for Ad5 content by a SYBR Green approach with primers spanning the hexon gene within the

Adenoviral genome in 384-well plates. A standard curve with known Ad5 concentrations was used to normalize the resulting data. Also, background values from wells containing water was substracted from samples. One way ANOVA and Kruskal-Wallis posthoc test were applied on these data. ** p<0,01.

4.2.3.3.2 Effect of ICOVIR-15K-AERO on the tumor stroma

In order to determine whether the unspecific cytotoxic activity of aerolysin was taking place within the tumor, the status of two murine stroma markers was analyzed by two different methods. Distribution of α-SMA, a marker for pericytes and, more importantly, activated fibroblasts, was studied by IHC in A549 and HPAC (not shown) tumors, and representative images are shown in **Figure 46**. No significant differences were actually observed between groups for this marker in any of the groups, which was detected mainly in fibroblast septa, even though it is also expressed by pericytes, so any blood vessel could provide a non-fibroblast positive signal.

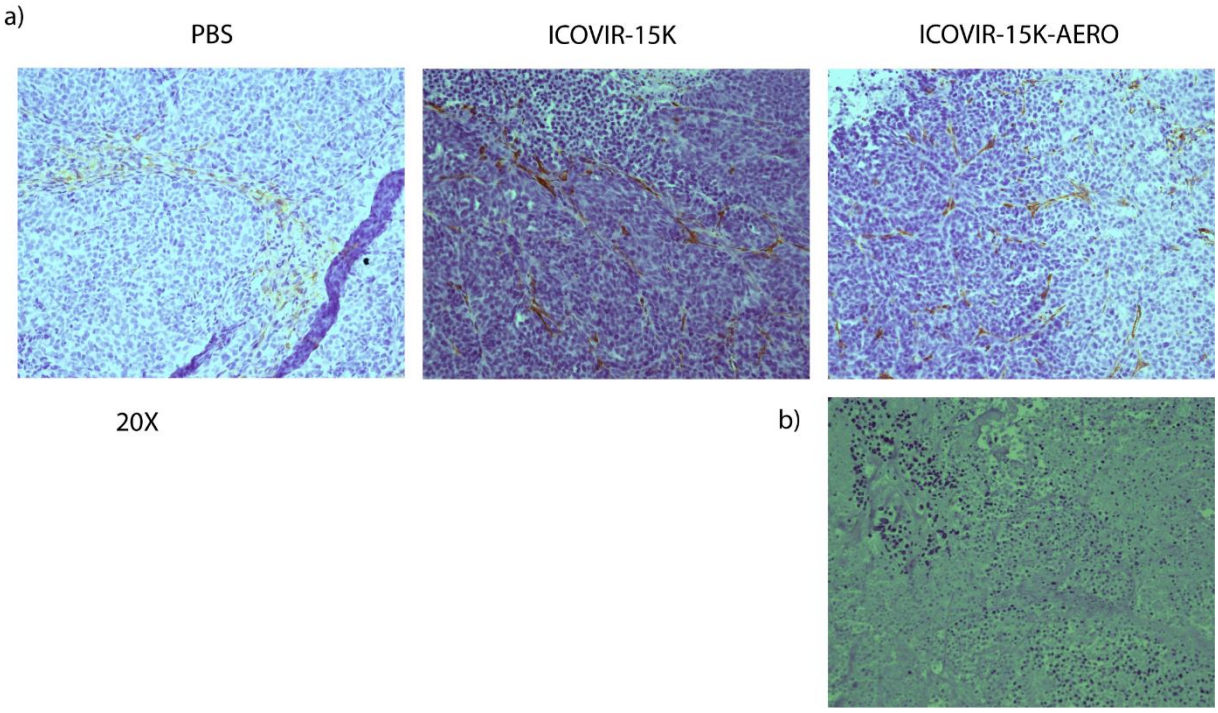

Figure 46. αSMA expression in A549 tumors. a) Paraffin-embedded sections of A549 tumors were stained for murine αSMA (brown signal). Representative images are shown for each group. Consistent and comparable degree of staining was detected in viable areas of tumors irrespective of the group they belonged to. Fibrotic nodes show a diffuse staining pattern. **b)** Wide necrotic unstained areas including dead tumor cells and dead fibrotic bundles were observed in all group. Notwithstanding, the image shown belongs to a tumor treated with ICOVIR-15K-AERO, which presented, qualitatively, higher numbers of such areas.

As a complementary tool for the analysis of the tumor stroma, murine FAP expression, which should be exclusive to tumor-associated fibroblasts, was quantified by qPCR with a TaqMan-based approach to maximize specificity, similiarly to what other groups have done in the past (Kakarla et al. 2013). Interestingly, in both A549 and HPAC models, mFAP expression was

significantly reduced in tumors treated with ICOVIR-15K-AERO (**Figure 47**), to an extent of up to 4-fold expression loss in A549 and 10-fold in HPAC when compared against PBS, which showed the highest mFAP expression in both cases, although it was not significantly higher than the one for ICOVIR-15K-treated groups in any case.

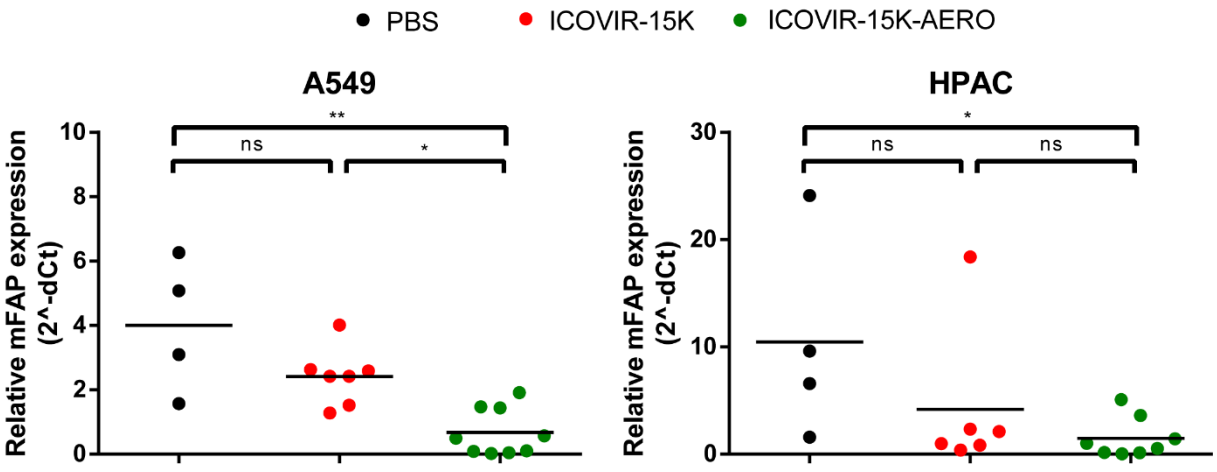

Figure 47. Murine FAP expression in A549 and HPAC tumors at endpoint. Tumors from both models were homogeneized and total mRNA was obtained by column purification. After retrotranscription of such mRNA, cDNA was obtained and was run in triplicate in qPCR assays (384-well plate) to assess the expression rate of murine FAP. Murine β-actin expression rate was used as a housekeeping reference to calculate the final relative expression of mFAP (y axis). Negative controls with water or cells expressing the human version of FAP did not amplify at all. Positive controls of cell lines expressing murine FAP were also included and amplified accordingly. One way ANOVA and Kruskal Wallis posthoc tests were applied on these data. * p<0,05; ** p<0,01.

5 DISCUSSION

5.1 Oncolytic adenoviruses carrying soluble versions of human CD200, CD200tr, the viral homolog K14 and K14tr

The human immune system is able to mount specific responses against tumor epitopes. However, research and clinical experience are highlighting a conspicuous repertoire of mechanisms tumors utilize to attenuate or even abolish such responses, rendering the cancer-specific immune effector cells anergic or causing their death. In particular, immune checkpoints are showing to play pivotal roles in maintaining immune tolerance in the tumor microenvironment of many cancer types.

CD200, formerly called OX-2, constitutes one increasingly studied immune checkpoint in the cancer immunotherapy field. Traditionally associated to maintenance of immune homeostasis in immune-privileged tissues such as the brain, it was firstly linked to tumor immunity evasion as it was shown that activating the CD200:CD200R axis translated into higher development of leukaemic tumors in mice that were otherwise resistant to such tumors. Also, in a second model, preimmunized mice expressing the costimulatory molecule CD80 were able to reject tumors, but this rejection could be suppressed by the addition of a soluble CD200 conjugate or $CD200R^+$ macrophages, and tumors were therefore developed (Gorczynski et al. 2001).

The underlying mechanism behind CD200-mediated tumor immune escape was demonstrated by MLRs in which CD200-expressing cells could down-regulate T_H1 cytokines IL-2 and IFNγ, and the levels of these cytokines could be restored in the presence of CD200R antagonists (Siva et al. 2008). Additionally, CD200 has been identified as a bad prognostic marker in Multiple Myeloma and Acute Myeloid Leukaemia (Moreaux et al. 2014; Tonks et al. 2007) and has been proposed as a marker for cancer stem cells (Kawasaki and Farrar 2008). Interestingly, a truncated CD200 splice variant (CD200tr) with antagonistic effects on CD200R was identified some years ago (Z. Chen et al. 2008).

Viral homologs of human CD200 have been discovered in many different viruses. Among them, K14 protein from Human Herpesvirus 8 (Kaposi Sarcoma-associated herpesvirus KSHV) shows identical affinity for CD200R and capability to engage CD200R downstream signaling (Foster-cuevas et al. 2004).

In this thesis, we propose the truncation of viral K14 in a parallel way as CD200tr as a way to generate a CD200R antagonist which could be considered for immunotherapy approaches. In order to test this hypothesis, oncolytic viruses carrying soluble versions of human CD200 (immunosuppressor), C200tr (immunostimulator), and viral K14 (immunosuppressor) and

K14tr (immunostimulator) as transgenes were successfully generated by homologous recombination in bacteria. All transgenes were cloned after the fiber gene in ICOVIR-15K, an oncolytic virus previously developed in our lab that allows for exogenous DNA insertion (up to ~2 kb). Amplification and purification of all viruses was performed with similar results, yielding comparable physical and functional titers. Accordingly, all viruses could be produced in virus-permissive cells after 72h infection to a comparable extent, ranging from 2000 to 12000 TU/cell, indicating that the insertion of the transgenes was not hindering the viral replication capacity.

Soluble CD200 and CD200tr could be detected successfully in supernatants from infected cultures by ELISA, achieving 400 pg/ml for C200tr and around 300 pg/ml for full-length CD200. The epitope recognized by the ELISA antibody was fully present in both proteins, which allowed detection of both secreted proteins by the same antibody.

All viruses were characterized in dose-dependent curve assays with A549 cells, which is a reference virus-permissive cell line in the Adenovirus field, and SK-Mel-28 cells, of specific interest in this chapter due to their CD200 expression. The biggest loss in cytotoxicity potential was observed for the CD200tr virus in A549 (2,18-fold loss versus control virus) and the CD200 virus in SK-Mel-28 (2,34-fold loss versus control virus). Such losses were not significant and overall, the studies demonstrated that no oncolytic potential was being lost by the expression of the transgenes.

MLRs are the most utilized means of studying the CD200:CD200R pathway, since the secretion of IL-2 and IFNγ from the myeloid cells in MLRs has resulted to be the most evident readout for CD200:CD200R signaling status. In order to guarantee that CD200R was not lost throughout DC differentiation, CD200R expression was analyzed in DCs and T cells prior to the performance of MLRs. Consistently, DCs showed almost 100% expression of this receptor, whereas it was barely detected in T cells. In contrast, around 20% CD200 expression was detected both in T cells and DCs. This is in accordance with literature describing CD200 expression to remain low in naïve lymphocytes and in myeloid cells (Caserta et al. 2012).

There are many valid MLR configurations researchers have used to study CD200:CD200R. In this work, two settings were compared. Firstly, PBMCs from different donors were simply mixed in the presence or absence of CHO-hCD200 or SK-Mel-28, two CD200-expressing cell lines previously used in the literature to study CD200 interactions (Z. Chen et al. 2008; Siva et al. 2008). Secondly, $CD14^{+}$ monocytes were differentiated into DCs and were mixed with the

non-adherent fraction of PBMCs, mainly composed by lymphocytes, from a different donor at a 10:1 ratio. In terms of IFNγ release, $CD200^+$ cells were able to reduce the levels in both settings. However, only SK-Mel-28 cells could significantly reduce IFNγ release versus the $CD200^-$ condition. Particularly, in the PBMC mix configuration, SK-Mel-28 cells could completely abolish IFNγ in supernatants, thus reproducing the results from Siva and collborators. Provided this level of inhibition, we decided to stick to the PBMC mix for further MLR assays.

In the MLRs in which the immune modulating properties of the transgenes were tested, in the absence of $CD200^+$ cells, control unmodified virus nearly doubled the IFNγ levels of the positive control. In turn, supernatant from the CD200-expressing virus could reduce IFNγ concentration up to three times versus the positive control, thus confirming its inhibitory role. Accordingly, CD200tr supernatant was able to inhibit the CD200 pathway and produced the same IFNγ levels shown by the control virus. Finally, K14 and K14tr supernatants showed similar IFNγ levels to CD200. This confirmed the ability of a soluble K14 to exhibit an immune inhibitory behavior, in line with being a CD200 homolog, but did not constitute a very encouraging result with regard to K14tr, which was our candidate to emulate CD200tr but contrarily to what we expected, the truncation of K14 did not lead to CD200R antagonism. In $SK\text{-}Mel\text{-}28^+$ samples, IFNγ levels decreased dramatically in all cases. Presumably, the degree of CD200 expression in SK-Mel-28 cells largely outnumbers the amount of soluble transgene molecules from supernatants (300-400 pg/ml), so that CD200R in the wells is mainly occupied by CD200 molecules from SK-Mel-28 cells, and immunostimulating elements can exhibit no efficient competition. In fact, this cell line showed the highest CD200 levels among 20 tumor cell lines tested, and 20 μg/ml of anti-CD200 were used to revert CD200-mediated inhibition (Siva et al. 2008).

In addition to not detecting any immunostimulating activity from K14tr, the fact that CD200tr supernatant shows comparable IFNγ levels versus the control virus indicates that no added stimulation is provided by CD200 antagonism, which is notwithstanding in concordance with results obtained with CD200tr-expressing cells in which CD200tr just restored the cytokine levels yielded by the basal allogeneic reaction (Z. Chen et al. 2008). This is presumably due to the fact that CD200 truncation does not impair binding to CD200R, but such binding does not result in CD200R downstream signaling. Hence, if the non-modified virus can already achieve the maximum level of IFNγ release, an advantage from truncated CD200 homologs, at least in terms of proinflammatory cytokine release, seems to lose strength from these first

approaches if increased immune stimulation is pursued. CD200tr might, however, promote a more proinflammatory profile within the $CD200R^+$ population, that is, leading to M1 macrophages or unfavoring MDSC, T_{reg} and M2 macrophage differentiation that might be masked in this experiment, which was read at 48, 72 or 120 hours.

In order to characterize the effect of CD200 from cells on the monocyte population, cocultures were set up with $CD14^+$ monocytes isolated from PBMCs in the presence or absence of either $CD200^-$ or $CD200^+$ tumor cells. Unfortunately, no clear preexistent immunosuppressive differentiation pattern could be observed from these experiments, since, in general, the anti-inflammatory markers analyzed showed decreased expression in coculture compared to the monocyte-only condition. In detail, M2 macrophage marker CD163 showed no significant variation throughout the days, even though a non-significant tendency towards higher expression (from day 3 to day 5) was observed in the SK-Mel-28 coculture. The MDSC marker CD33, on the other hand, was decreased in all cocultures, even though, once again, the biggest decrease was observed from days 3 and 5 in the monocyte-only condition, indicating a more long-term immunosuppressive effect taking place in cocultures, which was, in any case, independent of CD200 expression. Loss of HLA-DR expression, which indicates general MDSC differentiation, was observed in coculture, but in a CD200-independent fashion. Finally, CD200R expression in coculture, also in a CD200-independent manner. All in all, no strong evidence supporting an immunosuppressive profile promoted in monocytes by CD200 could be provided.

These results do not reinforce what is described in the literature. In detail, CD200 expression has been shown to increase CD163 and CD200R levels on M2 macrophages in 72h as part of its immunosuppressive effect (Koning et al. 2010). Also, even though CD200 signaling seems to promote MDSC differentiation (Rygiel et al. 2012), HLA-DR levels do not correlate with CD200 levels (Jenmalm et al. 2006). In the comparison between what we observed and what literature states, the only resemblance we can find is the slight tendency of CD163 induction in the monocyte:SK-Mel-28 coculture. One possible explanation could be that, unlike in the literature, in which CD200 signaling is analyzed on already maturated M1 macrophages, we decided to seed immature monocytes. Possibly, CD200:CD200R signaling was complemented by other cytokines and mechanisms throughout the experiment and was not enough to render the monocytes as pure M2 or MDSC populations. Further research on this, and also on the effect of CD200 in other cell populations, such as mast cells, in which CD200 action has also been reported (S. Zhang et al. 2004), is needed to fully understand this tricky pathway.

In this work, we tried to elucidate the effect of the different CD200-derived transgenes in antigen-specific cytotoxic lymphocyte responses against a CMV peptide by means of a previously described method involving autologous immature DCs and T cells (Eriksson et al. 2017). Unlike for Eriksson and colleagues, our goal was dual: on one hand, confirm the immunosuppressive capacity of soluble CD200 and K14, and on the other hand, study whether the truncated versions of such proteins could induce an immunostimulatory effect. Our findings were very short from our expectations, since we could only confirm the inhibitory role of CD200 and K14, which did not induce CTL proliferation at all. Intriguingly, both viruses expressing the truncated transgenes yielded the same low values as the full-length proteins (~1% reactive CTLs against CMV peptide), that is, they showed an inhibitory role, which greatly opposes what has been described for CD200tr. Such ineffectiveness could be explained by the fact that, even though DCs were infected at very high MOIs (1000), the transduction and replication efficiencies of the modified viruses were much poorer than for the control virus, which yielded a ~5% of positive cell count. CD200-expressing oncolytic viruses with a hybrid fiber combining the 5/35 serotypes would allow effective infection of DCs and probably would constitute a cleaner way to assess the effect of the transgenes. Also, using concentrated supernatants would have been a complementary way to perform this assay, but we tried to stick to the described protocol as much as possible.

Altogether, it is difficult to conclude very strongly about the possibility of a truncated K14 as an effective immunostimulator. However, our findings, apart from confirming the difficulty of dealing with the CD200:CD200R axis in terms of experiment design and readout interpretation, indicate that our truncated K14 does not collaborate to immune activation to any extent, contrarily to what we have observed for human CD200tr, at least in the $CD200^-$ MLR condition. As mentioned before, one important limitation of our approach might be that, in order to effectively modulate the CD200 pathway in the most demanding conditions ($CD200^+$ MLR, CMV-specific response), the amount of transgene generated from the modified viruses might not suffice.

The immune-balancing effects of inhibitory receptors have evolved to prevent excessive damage caused by the immune system. One of these players is the CD200–CD200R inhibitory pathway, studied in this work. In the context of anti-tumor responses, CD200:CD200R can modulate inflammation and thereby stimulate anti-tumor responses.

The mechanism of CD200:CD200R signaling pathway is notwithstanding still uncertain. However, it seems that multiple CD200- and CD200R-expressing cell populations are involved

in the inhibitory immune effects. The impact of CD200:CD200R signaling is most probably not limited to the local site of tumor growth but may systemically affect tolerance for tumor antigens. Therefore, CD200R blockade may be a highly effective anti-cancer treatment even in the case of CD200-negative tumors. In this thesis, we tried to shed some light on this matter by testing a virus-derived potential CD200R antagonist, which unfortunately did not behave as such.

5.2 Oncolytic adenoviruses expressing stroma-activatable toxins

Oncolytic viruses encounter a relevant hurdle when facing the stromal barriers of solid tumors. Firstly, the ECM constitutes a wall through which the Adenovirus will barely escape. Secondly, stromal fibroblasts are very resistant to virus replication and will not be affected by oncolysis at all. As mentioned in previous sections, multiple strategies have been adopted from many groups in the field to tackle this issue. In our own group, ECM-degrading viruses have been successfully developed (Guedan et al. 2010; Rodríguez-García et al. 2015). All strategies offer a number of advantages, but most of them render the stromal fibroblasts unaffected, or at least, no significant improvement in fibroblast toxicity has been achieved to date.

Bacterial-derived toxins have experimented increasingly high interest in tumor treatment due to their potent and unspecific toxicity. Such unspecificity, however, can constitute a disadvantage for inaccessible tumors that require systemic delivery. Pore-forming toxins like atox from *Clostridium septicum* or aerolysin from *Aeromonas hydrophyla* offer a solution to this concern, since they have an inhibitory domain that prevents their premature action. Such domain is released upon the cleavage of a linker sequence by a protease (G. van der Goot 2001). A simple substitution of such linker by a tumor-specific protease sensitive sequence allows for oncotargeting of these toxins (Brennen et al. 2012).

In this work, we proposed the combination of drug targeting and oncolytic virotherapy by generating oncolytic Adenoviruses expressing modified stroma-targeted toxins. In detail, we substituted atox and aerolysin natural linkers by FAP- and MMP-9-sensitive linkers. These two proteases are expressed almost exclusively in the tumor stroma and very rarely in healthy tissues, thereby ensuring that the cytotoxic effects will affect tumor and stromal cells only. In the case of atox, two different linkers were utilized, thereby generating ICOVIR-15K-AtoxC and ICOVIR-15K-AtoxS viruses, whereas only one MMP-9 linker was chosen for the modified aerolysin-expressing virus, ICOVIR-15K-AERO.

Generation of these viruses by homologous recombination in bacteria and further amplification in eukaryotic cells allowed effective purification of all viruses and yielded excellent physical/functional ratios, reaching an outstanding value of 5,41 for AERO when, in general, ratios between 20 and 50 are considered acceptable. Therefore, all viruses resulted to be viable.

Regarding atox viruses, they produced very similar TU/cell values in viral production assays compared to the control unmodified virus ICOVIR-15K, thus confirming their viability in virus-

permissive cells such as A549. As for their cytotoxic profile in FAP^- and FAP^+ cells, both viruses performed worse than the control virus, even though their loss was less dramatic in SW872, the FAP^+ cell line (3,68-fold loss for AtoxC and 3,79 for AtoxS versus 7,94 and 5,63 in the FAP^- cell line in terms of IC_{50} values), indicating a possible FAP-mediated gain in cytotoxicity which cannot happen in the A549 culture, where atox will never be activated. In any case, a slight loss in oncolytic potential due to the presence of the transgenes was clearly noted. Importantly, SW872 cells were shown to be resistant to all viruses, as their elevated IC_{50} values indicate (maximum of 128,54 TU/ml). This adds interest to the fact that atox viruses showed reduced losses in this cell line, since they might eventually provide an advantage in virus-resistant cells if there is enough transgene synthesized from virus-permissive cells, which would be the ideal scenario within the tumor.

In order to better discern FAP-mediated cytotoxicity, concentrated supernatants containing atox were incubated with recombinant FAP and added to target cells afterwards. Since atox is supposed to induce cell necrosis in a fairly fast fashion, viability was assessed at no longer than 48h with an MTT readout. **Figure 30** shows a representative data set obtained in all cell lines tested, in which atox-containing supernatants show comparable cytotoxicity values to the control unmodified virus, with a slight tendency for AtoxC virus to induce higher toxicity. This assay prompted us to look for a more realistic approach for two connected reasons: firstly, atox dramatically loses its water solubility upon cleavage of the inhibitory peptide, which also exerts a crucial chaperone role. This means that most atox molecules might become non-functional upon their cleavage in solution. Secondly, FAP is located at the membrane of target cells, and its action on atox is quickly followed by oligomerization and pore formation. Thus, the use of the modified 293-hFAP and –mFAP cell lines allowed a more elegant experiment set up, in which concentrated supernatants were directly added to target cells and incubated for 24h, after which early apoptosis and necrosis could be assessed by means of 7-AAD uptake by dying cells at the flow cytometer. Whilst no differences in survival were observed between viruses at the non-modified 293 cell line, a significant yet not dramatic decrease in survival was reported for both FAP-expressing cell lines with the atox-containing supernatants (based on previous data, we left AtoxS on hold). Interestingly, the biggest fall in cell survival with AtoxC supernatant was observed in the cell line expressing the murine FAP, which encouraged us to make a step forward and test the AtoxC virus in an in vivo model where murine stroma would provide murine FAP to activate atox.

Consequently, and in collaboration with Mireia Morell from IDIBELL, a stroma-rich clone was selected to engage an orthotopic pancreatic model in athymic nude mice. After two passages and once tumors reached the appropriate volume, treatment was administered intravenously and tumor volume was monitored. After 17 days, the experiment was ended because tumors met the endpoint criteria. Unexpectedly, no significant differences were detected between AtoxC and the control unmodified virus, not even against the PBS group, both for tumor growth and survival values. This indicates that atox could not become successfully activated in order to make a difference from the oncolytic intrinsic effect, but the non-significance versus the PBS group also highlighted the difficulty of dealing with orthotopic models, which are not the main source of data in our group, although was chosen in this case in order to maximize the tumor stromal content, which was what we considered the best case scenario for the atox-expressing viruses. In terms of toxicity, AtoxC virus caused the most severe weight loss in animals, with a maximum loss on day 6 after treatment, but by the end of the experiment, all mice had recovered their weight. Interestingly, the PBS group started a progressive fall on weight on day 10 no seen in the other 2 groups, probably indicating that, had the experiment continued, differences in tumor growth might have been observed between groups. However, this is mere speculation.

Even though further studies could have been conducted with the atox-expressing viruses, overlapping encouraging results obtained with the aerolysin-expressing virus, discussed in the following lines, prompted us put the atox approach on hold and focus on the aerolysin project.

There were a number of reasons to swap our toxin of interest and the activating mechanism. First of all, there is much more knowledge accumulated on aerolysin in the literature than for atox regarding all the steps of their mediated cytotoxicity. Also, as mentioned before, atox is more sensitive to wrong folding in solution, whereas aerolysin rapidly dimerizes and forms a stable water-soluble complex (F. G. Van Der Goot et al. 1993). Moreover, it has been demonstrated that cleavage of aerolysin in solution can still render the toxin active, even though it reduces its speed of action (Abrami et al. 1998; Howard and Buckley 1985). This also allowed to change the linker for another sensitive to MMP-9, a soluble matrix-degrading enzyme overexpressed in tumor stroma. This constituted a qualitative improvement, since the cytotoxic action of aerolysin upon activation in solution would affect surrounding cells unspecifically in a bystander effect fashion, unlike the targeted FAP approach, restricted mainly to the FAP^+ population and therefore more vulnerable to tumor escaping mechanisms such as antigen loss. Notwithstanding, expression of MMP-9 in non-target tissues might be

more frequent than FAP expression. This led us to clone the aerolysin gene in a more replication-restricted location within the Adenoviral genome, more specifically, between the E4 and the RITR regions (**Figure 27**). In order to compensate for this further location, the stronger splicing acceptor BPSA was chosen to precede the aerolysin gene, as other groups had previously published for other transgenes (Fernández-Ulibarri et al. 2015; Jin, Kretschmer, and Hermiston 2005).

ICOVIR-15K-AERO was successfully generated and purified, as mentioned before, and its in vitro characterization in terms of viral production indicated that no significant loss of replication capacity was taking place by the insertion of the transgene. Results shown in **Figure 34** include A549 and HPAC cell lines, and similar viral yields were consistent for both. These two cell lines would later be used for in vivo studies.

The cytotoxic profile of ICOVIR-15K-AERO was determined in a panel of cell lines in terms of IC_{50} values compared to the control ICOVIR-15K virus. AERO virus performed better than ICOVIR-15K in HT1080, MiaPaCa-2 and NIH-3T3 cells, ranging from 4-fold gain in HT1080 cells to a 1,72-fold gain in MiaPaCa-2 cells. Among all cell lines included in this screening, with **Figure 35** as reference, HT1080 is the top MMP-9^+ cell line, indicating a possible aerolysin-mediated cytotoxic advantage taking place in this cell line. However, in other MMP-9^+ cells like hCAFs or A431, AERO virus either performed worse than the control (hCAF) or did not show an advantage (A431). Notably, these cells showed high resistance to the virus, with IC_{50} values reaching 157,6 TU/ml in the case of AERO in the hCAFs. Therefore, we hypothesize not enough transgene can be generated in such conditions so that a difference can be made in favor of AERO, specially taking into account its location within the genome (between E4 and RITR), which should render transgene expression highly dependent on replication, something which does not happen in other configurations, in which transgenes regulated by the MLP are expressed in non-permissive cell lines. In A549 and HPAC cells, which are MMP-9^- and chosen for the in vivo (this apparent paradox will be explained later), AERO performed slightly worse than ICOVIR-15K, with 2,57- and 1,67-fold losses, respectively. Lastly, the modest improvement seen in MiaPaCa-2 and NIH-3T3 could be explained by the low expression of MMP-9 in the former and the expression of murine MMP-9 from the latter, something which was not tested. Theoretically, however, the MMP-9 cleavage site was shared between the MMP-9 of both species.

A panel of cell lines were characterized for their expression of aerolysin receptors by means of a fluorescently-labelled aerolysin (FLAER), which can bind the receptors but does not

oligomerizes or forms pores. HT1080 cells presented the highest density of aerolysin receptors, so this cell line was chosen to detect aerolysin from supernatants obtained from infected cultures. A549 and HPAC were the following lines with most receptor density.

Two methods were chosen to detect aerolysin from supernatants. Firstly, taking advantage of the 6 Histidine tag inserted at the C-terminus of the catalytic domain of aerolysin, we studied binding of aerolysin from supernatants to HT1080 cells. A shift in the histogram can be observed for AERO, corresponding to ~20% positive cells for bound HisTag. In order to reinforce these data, a competition assay between FLAER and the aerolysin from supernatants was set up, yielding a 25% loss of FLAER signal, which presumably corresponds to the bound aerolysin from supernatants. Taken together, these data confirmed the expression of the modified aerolysin, even though the low amount of transgene produced, coupled with the fact that 7 molecules of aerolysin are needed to form a single pore, slightly compromised the viability of this approach. In order to clarify this, further assays were performed to discern aerolysin-mediated cytotoxicity.

In a parallel way to the atox project, supernatants from infected cultures were incubated with recombinant MMP-9 in order to activate aerolysin, and were later added to target cells. In this case, this approach resulted more realistic than the one applied for the previously mentioned recombinant FAP, since MMP-9 is present in a soluble form in the extracellular compartment, so the best case scenario was being emulated. Moreover, such assays were reported in other publications (José et al. 2014), and we stuck to their protocols as much as possible, also based on the evidence that aerolysin-mediated apoptosis can be detected after 24h incubation (Imre et al. 2012).

This assays were performed in a panel of either MMP-9^{+} or MMP-9^{-} cell lines. In A549 cells (MMP-9^{-}), both 15K and AERO viruses showed low survival values irrespective of the preincubation performed, probably due to the cell line intrinsic sensitivity to the virus. Interestingly, in HPAC cells, which are also negative for MMP-9 expression, the AERO supernatant preincubated with recombinant MMP-9 provoked significantly reduced survival rates (approximately 3-fold reduction) compared to both 15K supernatant preincubated with rMMP-9 and the AERO supernatant preincubated without rMMP-9. Thus, a rMMP-9-specific cytotoxic activity was described in these cells in the presence of supernatants from AERO-infected cultures, which led us to think aerolysin was effectively being activated by rMMP-9 and inducing cell death. In HT1080 and A431, the cell lines expressing highest amounts of MMP-9, AERO supernatants yielded significantly reduced survival values irrespective of the

preincubation setting, which indicates that aerolysin was also being activated by the endogenous MMP-9 from these cells. It is worth noting that HT1080 and A431, as virus-resistant cell lines (**Table 13**), showed the most striking differences between ICOVIR-15K-AERO and ICOVIR-15K, since the ICOVIR-15K survival values were barely diminished in comparison with the mock at the time points at which experiments were read. This reinforces the fact that the observed 7-AAD staining was due exclusively to the activated aerolysin. This same effect could be observed in the murine cell line NIH-3T3, with very low survival rates with AERO supernatants compared to the control virus irrespective of the presence of rMMP-9 in the preincubation. Lastly, in the case of hCAFs, which express intermediate levels of MMP-9, significantly decreased survival against ICOVIR-15K was only observed with AERO supernatants preincubated with rMMP-9, with an approximate 3-fold reduction in live cell count. Very importantly, these results also indicated that no leaky activity of aerolysin from AERO supernatants was taking place in MMP-9$^-$ conditions, which constitutes a very relevant issue in the context of a systemic administration of oncolytic Adenoviruses that will be uptaken not only by the tumor, but also by healthy tissues where no aerolysin action is wanted.

In order to advance to a more realistic scenario for ICOVIR-15K-AERO, bystander effect assays were set up with cocultures involving virus- and transgene-producing A549 cells and target MMP-9$^+$ or MMP-9$^-$ cells. Aiming to guarantee sufficient transgene expression but also to minimize oncolysis, readout times were set to 48-60h, just short of a full viral cycle. In HPAC MMP-9$^-$ cells, no significant differences were observed between viruses, which correlates to their MMP-9 negativity, since there was no way for aerolysin to become active in those cocultures. This reinforces the restricted targeting of aerolysin, since no leaky activity was detected. In all remaining cell lines, which were MMP-9$^+$, AERO cocultures showed significantly decreased survival values compared to both the uninfected and unmodified ICOVIR-15K conditions, hence confirming a cytotoxic role for the aerolysin expressed from the virus and the viability of a bystander effect approach. It is worth mentioning that ICOVIR-15K survival values were, unlike for NIH-3T3 and hCAFs, surprisingly low in HT1080 and A431 cells, which had also shown to be resistant to the virus at low MOIs, as is the case of this experiment, in which, moreover, A549 cells are initially infected with viruses separately from target cells and are then washed and added to target cells, thus minimizing the virus liable to infect non-A549 cells. These variable values between cell lines might be due to the processing steps performed on them, since Mock values are in some cases also unexpectedly low (HT1080).

Even though we had demonstrated aerolysin-mediated cytotoxicity in two different approaches with higher consistency than what had been observed for atox viruses, we were lacking an adequate model to move in vivo because we needed it to be both virus permissive and MMP-9^{+} to both produce enough amounts of aerolysin molecules and to ensure it would become activated, respectively. NIH-3T3 were initially ruled out due to their murine origin, which implies very reduced replication from Ad5. HT1080, A431 and hCAFs were also ruled out because of their high IC_{50} values for AERO, combined with the fact that there was no previous experience in the group with tumors formed with these cell lines. HPAC and A549 cells are MMP-9^{-}, so they did not constitute theoretical feasible options. Generation of modified A549 and HPAC MMP-9-expressing cells was taken into consideration. However, since murine MMP-9 from the murine tumor stroma can also activate aerolysin from ICOVIR-15K-AERO, mMMP-9 expression through in situ zymography (ISZ) was assessed in subcutaneous tumors from A549, HPAC and MiaPaCa-2 cells, which are virus-permissive cells broadly used in our group for in vivo studies. Hence, MMP-9 expression was confirmed in all three tumors, thus validating the use of these models to test ICOVIR-15K-AERO in an antitumor efficacy assay. MMP-9 distribution within tumors proved to be ubiquitous, even though for HPAC tumors it was more clearly localized at the invasion front, in line with its role in invasion and ECM degradation.

According to the data obtained, A549 and HPAC cells were chosen for in vivo assays in nude athymic mice. In both models, significant reduced tumor growth in AERO-treated mice was observed from fairly early time points (6 days) versus ICOVIR-15K. As can be seen in spider graphs shown in **Figure 42**, AERO-treated group shows less variability than PBS or ICOVIR-15K groups in both models, even though it is clearer for A549. Importantly, the A549 assay was terminated on day 20 due to meeting the endpoint criteria in PBS mice, whereas the HPAC assay was ended on day 41 in order to analyze the tumors, but no endpoint criteria was met. A549 tumors showed a very aggressive phenotype compared to HPAC tumors, which barely grew beyond 1000 mm^3 after 40 days. Probably due to this fact, regression of AERO-treated tumors could be observed in HPAC tumors until day 13, point from which tumors from all groups showed positive growth rates, and such rates were maintained until the end of the experiments. These results indicate that an aerolysin-expressing virus can improve the performance of ICOVIR-15K in MMP-9^{+} models from early time points, probably because MMP-9 expression is engaged also at early stages of tumor progression, although no effective tumor regression can be achieved eventually. It also confirmed the ability of murine MMP-9 to effectively cleave the AKGLYK linker in aerolysin, something which had only been hinted by

the in vitro results in NIH-3T3 cells. Finally, these results validate the cloning of transgenes between the E4 and RITR regions within the Ad5 genome, something unprecedented in our group, where after-fiber transgenes had been the choice up to date.

Adenoviral content in tumors at endpoint shown in **Figure 44** and **Figure 45** showed varying patterns in each model. Firstly, the absence of E1a staining in HPAC tumors in any of the groups, coupled with the values observed in qPCR quantification for Ad copies, may indicate that by day 40 (when HPAC in vivo experiment was terminated) all viable viral particles might have been cleared from the tumor, even though non-functional virus can still be detected by qPCR. This could easily be elucidated by using total RNA as the template for Ad detection instead of DNA, as was performed in this thesis. In any case, we hypothesize that due to the initial action of the viruses, tumors would not grow in an uncontrolled fashion even though no viable viruses were present at the end. We considered the possibility that HPAC cells would be worse virus producers than A549 cells and thus provide a lower staining, but viral production values demonstrated this was not the case (**Figure 34).** In the case of A549 tumors, harvested on day 21, active viral replication could be detected by E1a staining.

There was, however, a consistent pattern in Ad detection, both at the IHC of A549 tumors and at qPCR results, which constituted a potential paradox. As can be observed in these data, ICOVIR-15K-AERO content values are in all cases significantly lower than ICOVIR-15K values, even though the former presented higher antitumor efficacy than the latter. This lack of correlation between adenovirus content and antitumor efficacy is not unprecedented in our group. We hypothesize that both viruses can effectively reach tumors in their first rounds of infection. Then, whereas ICOVIR-15K-AERO is able to better control tumor growth due to its effect on the tumor stroma (discussed in the following paragraph), ICOVIR-15K cannot bypass the stroma barriers and is therefore encaged in tumor nodes, in which several rounds of replication and lysis might still take place until virus is cleared. Our explanation for the final number of copies found of each virus is that, due to the smaller size of ICOVIR-15K-AERO-treated tumors, the virus can be cleared more easily than in larger ICOVIR-15K-treated tumors, where, moreover, the stroma is adding consistency and is reducing the permeability of the tumor. Therefore, the total amount of virus is higher in less controlled ICOVIR-15K-treated tumors. It is also likely that by the strong early control of the tumor ICOVIR-15K-AERO is exerting, the number of available tumor cells for subsequent rounds of replication might be a limitation factor for ICOVIR-15K-AERO and not for ICOVIR-15K, whose tumor-killing speed is overtaken by the tumor growth rate. Notably, up to four ICOVIR-15K-AERO-treated HPAC

tumors, the model where tumor control was strongest, presented negligible values of Ad copies. In spite of all this, we cannot rule out the possibility that, even though aerolysin might be killing fibroblasts and thus helping the wider spread of the virus, it may also, due its unspecific activity, impair the efficient development of the viral cycle by also killing recently infected cells, thereby reducing the yields of viral particles that will be generated for subsequent rounds of infection. This has not been satisfactorily elucidated by production and cytotoxicity in vitro assays performed, and probably a viral production assay in MMP-9^{+} conditions would give some hints in this direction. Also, analyzing the apoptosis rates of A549 virus-producing cells in bystander effect assays (**Figure 40**) would have provided valuable information about this issue.

In terms of toxicity profiles, ICOVIR-15K-AERO induced the biggest weight loss in both models, with maximum values on day 6 after treatment. In the case of A549, loss of weight in the AERO group was consistent throughout all the experiment, whereas mice in HPAC model finally recovered their weights, and also showed not so severe losses in weight. This is in accordance to the high aggressiveness shown by A549 tumors, which probably added up to the treatment to induce higher toxicity. No lethal toxicity was observed in any model.

After observing this significant reduction in tumor growth in AERO-treated mice, we were prompted to correlate this improvement to the effects of aerolysin within the tumor, and more specifically, on stromal cells. The choice of the tumor stroma marker to assess was a tough one, since there is a lot of controversy in the field about which are reliable CAF-specific markers. Thus, we combined the IHC analysis of αSMA and the quantitative analysis of murine FAP expression, which is a tricky target for IHC and also because another group had reported robust data by analyzing it through qPCR (Kakarla et al. 2013) after targeting the tumor stroma.

IHC assessment of αSMA did not reveal any particular advantage provided by the expression of aerolysin. Total positive staining was qualitatively comparable between groups in both models. It is possible that this marker, which is also expressed in pericytes and smooth muscle cells, both reasonably present in the tumors, was not the best candidate to discern about the killing of CAFs. Our most promising results come from the qPCR analysis of murine FAP (**Figure 47**), in which, for both models, significantly reduced expression rates were observed in ICOVIR-15K-AERO-treated tumors, providing strong evidence of the cytotoxic activity of aerolysin on the tumor stroma. In particular, ICOVIR-15K-AERO-treated A549 tumors showed significantly reduced mFAP expression compared either versus PBS or ICOVIR-15K-treated tumors. In the

case of HPAC tumors, however, mFAP expression in ICOVIR-15K-AERO tumors was only significantly lower than PBS-treated tumors but not than ICOVIR-15K-treated ones, even though a clear tendency was observed. We hypothesize that, due to the reduced tumor size of HPAC tumors, finding significant differences constituted a more challenging goal than for A549. It is possible that, had we not stopped the experiment, these differences would have become greater with time, but we cannot be sure about this, especially considering that the virus seems to be cleared by day 40 and thus aerolysin expression might stop irreversibly. The possibility of rechallenging tumors with a second round of virus treatment could also answer this question in a robust way. Interestingly, PBS tumors show the highest rates of mFAP expression. This indicates that, at least in these models, the fibrotic replacement of tumor cells killed by oncolysis mediated by ICOVIR-15K is not more active than the intrinsic generation of tumor stromal barriers associated with normal tumor progression.

All in all, we believe that these promising results should not be overlooked, although further studies must be performed with this virus and deeper analysis of the effect of aerolysin in the stroma of the tumors and infected cells should be addressed to firmly consider it as a clinical candidate with a special value in stroma-rich malignancies, which are more resistant to traditional treatments.

6 CONCLUSIONS

Oncolytic adenoviruses carrying soluble versions of human CD200, CD200tr, the viral homolog K14 and K14tr

1. Oncolytic Adenoviruses expressing soluble versions of human CD200 and CD200tr proteins and their orthologues from HHV-8 K14 and K14tr proteins retain oncolytic potency and *in vitro* features of a non-modified virus.
2. Soluble CD200 and K14 proteins expressed from oncolytic Adenoviruses retain their agonistic role on CD200R, and CD200tr retains its antagonistic role, even though it does not increase immune activation when compared to a control virus.
3. A truncated version of K14 does not behave as a homolog of CD200tr and therefore is not able to antagonize CD200R.
4. In CD200-positive cultures, immune inhibition could not be reverted by any of the transgenes expressed from the viruses.

Oncolytic adenoviruses expressing stroma-activatable toxins

5. Oncolytic Adenoviruses expressing bacterial-derived toxins atox and aerolysin modified to render them activatable in the tumor stroma retain oncolytic potency and *in vitro* features of a non-modified virus.
6. Supernatants from cultures infected with toxin-expressing viruses induce increased cytotoxicity compared to supernatants from cultures infected with a control virus after incubation with recombinant versions of the stroma-specific proteases FAP or MMP-9.
7. ICOVIR-15K-AERO shows a bystander effect in cocultures of virus-permissive MMP-9^{-} and resistant MMP-9^{+} cells by inducing higher cytotoxicity than a control virus.
8. ICOVIR-15K-AtoxC does not perform better than an unmodified virus in terms of antitumor efficacy *in vivo.*
9. ICOVIR-15K-AERO can improve *in vivo* antitumor efficacy of ICOVIR-15K in subcutaneous MMP-9^{+} tumors without causing irreversible toxicity. Such antitumor activity does not correlate with total virus yields in tumors at endpoint between ICOVIR-15K and ICOVIR-15K-AERO-treated groups.
10. ICOVIR-15K-AERO-treated tumors show significantly reduced expression of the tumor stroma marker murine FAP, showing evidence of the unspecific cytotoxic activity exerted by recombinant aerolysin in cancer-associated fibroblasts.

7 REFERENCES

Abrami, Laurence et al. 1998. “The Pore-Forming Toxin Proaerolysin Is Activated by Furin.” *Journal of Biological Chemistry* 273(49): 32656–61.

Abrami, Laurence, Marc Fivaz, and F. Gisou Van Der Goot. 2000. “Adventures of a Pore-Forming Toxin at the Target Cell Surface.” *Trends in Microbiology* 8(4): 168–72.

Aggarwal, Saurabh et al. 2008. “Fibroblast Activation Protein Peptide Substrates Identified from Human Collagen I Derived Gelatin Cleavage Sites Fibroblast Activation Protein Peptide Substrates Identified from Human Collagen I Derived Gelatin Cleavage Sites †.” *Cloning*: 1076–86.

Akkaya, Munir, Marie Laure Aknin, Billur Akkaya, and A. Neil Barclay. 2013. “Dissection of Agonistic and Blocking Effects of CD200 Receptor Antibodies.” *PLoS ONE* 8(5).

Akkaya, Munir, and A. Neil Barclay. 2013. “How Do Pathogens Drive the Evolution of Paired Receptors?” *European Journal of Immunology* 43(2): 303–13.

Alemany, R. 2013. “Viruses in Cancer Treatment.” *Clinical and Translational Oncology* 15(3): 182–88.

Alemany, R., K. Suzuki, and D. T. Curiel. 2000. “Blood Clearance Rates of Adenovirus Type 5 in Mice.” *Journal of General Virology* 81(11): 2605–9.

Alemany, Ramon, and Manel Cascallo. 2009. “Oncolytic Viruses from the Perspective of the Immune System.” *Future microbiology* 4(5): 527–36.

Allavena, P., and A. Mantovani. 2012. “Immunology in the Clinic Review Series; Focus on Cancer: Tumour-Associated Macrophages: Undisputed Stars of the Inflammatory Tumour Microenvironment.” *Clinical and Experimental Immunology* 167(2): 195–205.

Altomonte, Jennifer et al. 2009. “Enhanced Oncolytic Potency of Vesicular Stomatitis Virus via Vector-Mediated Inhibition of NK and NKT Cells.” *Cancer Gene Therapy* 16(3): 266–78.

Andtbacka, Robert H I et al. 2015. “Talimogene Laherparepvec Improves Durable Response Rate in Patients with Advanced Melanoma.” *Journal of Clinical Oncology* 33(25): 2780–88.

Aruga, a et al. 1997. “Type 1 versus Type 2 Cytokine Release by Vbeta T Cell Subpopulations Determines in Vivo Antitumor Reactivity: IL-10 Mediates a Suppressive Role.” *Journal of immunology (Baltimore, Md. : 1950)* 159(2): 664–73.

Ballard, J, a Bryant, D Stevens, and R K Twetenl. 1992. “Purification and Characterization of the Lethal Toxin (Alpha-Toxin) of Clostnidium Septicum.” 60(3): 784–90.

Barclay, A N. 1981. “Different Reticular Elements in Rat Lymphoid Tissue Identified by Localization of Ia, Thy-1 and MRC OX 2 Antigens.” *Immunology* 44(4): 727–36. http://www.pubmedcentral.nih.gov/articlerender.fcgi?artid=1555004&tool=pmcentrez&rendertype=abstract.

Bartlett, David L et al. 2013. “Oncolytic Viruses as Therapeutic Cancer Vaccines.” *Molecular cancer* 12(1): 103. http://www.molecular-cancer.com/content/12/1/103.

Bauerschmitz, Gerd J et al. 2002. “Advances in Brief Treatment of Ovarian Cancer with a Tropism Modified Oncolytic Adenovirus 1.” *Cancer Research* 10(3): 1266–70.

Bayo-Puxan, Neus et al. 2006. “Role of the Putative Heparan Sulfate Glycosaminoglycan-Binding Site of the Adenovirus Type 5 Fiber Shaft on Liver Detargeting and Knob-Mediated Retargeting.” *Journal of General Virology* 87(9): 2487–95.

Bayo-puxan, Neus, Marta Gimenez-alejandre, Sergio Lavilla-alonso, and Alena Gros. 2009. “Heparan Sulfate Proteoglycan-Binding Domain.” 1221(October): 1214–21.

Belkin, Daniel a et al. 2013. “CD200 Upregulation in Vascular Endothelium Surrounding Cutaneous Squamous Cell Carcinoma.” *JAMA dermatology* 149: 178–86. http://www.ncbi.nlm.nih.gov/pubmed/23560298.

Belousova, Natalya, Valentina Krendelchtchikova, David T Curiel, and Victor Krasnykh. 2002. “Modulation of Adenovirus Vector Tropism via Incorporation of Polypeptide Ligands into the Fiber Protein.” *Journal of virology* 76(17): 8621–31. http://www.pubmedcentral.nih.gov/articlerender.fcgi?artid=136983&tool=pmcentrez&rendertype=abstract.

Bergers, Gabriele et al. 2000. “Matrix Metalloproteinase-9 Triggers the Angiogenic Switch during Carcinogenesis.” *Nature Cell Biology* 2(10): 737–44.

Berk, Arnold J. 1986. “Adenovirus Promoters and Eia Transactivation.” *Annu. Rev. Genet.* 20: 45–79. file:///Users/winghang/Documents/Library.papers3/Articles/1986/Berk/Annu. Rev. Genet. 1986 Berk.pdf%5Cnpapers3://publication/uuid/727E98F5-13D1-43B3-89CF-A32039CBBEB8.

Bimboim, H. C., and J. Doly. 1979. “A Rapid Alkaline Extraction Procedure for Screening Recombinant Plasmid DNA.” *Nucleic Acids Research* 7(6): 1513–23.

Bischoff, JR et al. 1996. “An Adenovirus Mutant That Replicates Selectively in p53-Deficient Human Tumor Cells.” *Science* 274(5286): 373–76.

Borriello, Frank, Richard Tizard, Elizabeth Rue, and Roger Reeves. 1998. “Murine Homolog of the Rat MRC OX-2 Membrane Glycoprotein.” 118: 114–18.

Brennen, W. Nathaniel et al. 2012. “Targeting Carcinoma-Associated Fibroblasts within the Tumor Stroma with a Fibroblast Activation Protein-Activated Prodrug.” *Journal of the National Cancer Institute* 104(17): 1320–34.

———. 2014. “Pharmacokinetics and Toxicology of a Fibroblast Activation Protein (FAP)-Activated Prodrug in Murine Xenograft Models of Human Cancer.” *Prostate* 74(13): 1308–19.

Brodsky, Robert A et al. 2000. “Improved Detection and Characterization of Paroxysmal Nocturnal Hemoglobinuria Using Fluorescent Aerolysin.” *American journal of clinical pathology* 114(3): 459–66. http://www.pubmedcentral.nih.gov/articlerender.fcgi?artid=3128433&tool=pmcentrez&rendertype=abstract%5Cnhttp://www.pubmedcentral.nih.gov/articlerender.fcgi?artid

=4124633&tool=pmcentrez&rendertype=abstract.

Bunuales, Maria et al. 2012. “Evaluation of Monocytes as Carriers for Armed Oncolytic Adenoviruses in Murine and Syrian Hamster Models of Cancer.” *Human Gene Therapy* 23(12): 121026084136009. http://www.pubmedcentral.nih.gov/articlerender.fcgi?artid=3523252&tool=pmcentrez&rendertype=abstract.

Burke, James M. et al. 2012. “A First in Human Phase 1 Study of CG0070, a GM-CSF Expressing Oncolytic Adenovirus, for the Treatment of Nonmuscle Invasive Bladder Cancer.” *Journal of Urology* 188(6): 2391–97. http://dx.doi.org/10.1016/j.juro.2012.07.097.

Burnet, Sir Macfarlane. 1957. “Cancer - A Biological Approach. I. The Processes of Control.” *British Medical Journal* 1(5022): 779–86.

Cameron, Cheryl M et al. 2005. “Myxoma Virus M141R Expresses a Viral CD200 (vOX-2) That Is Responsible for down-Regulation of Macrophage and T-Cell Activation in Vivo.” *Journal of virology* 79(10): 6052–67.

Capasso, Cristian et al. 2016. “Oncolytic Adenoviruses Coated with MHC-I Tumor Epitopes Increase the Antitumor Immunity and Efficacy against Melanoma.” *OncoImmunology* 5(4): e1105429. https://www.tandfonline.com/doi/full/10.1080/2162402X.2015.1105429.

Cascallo, Manel et al. 2006. “Oncolytic Adenoviruses.” 940(September): 929–40.

———. 2007. “Systemic Toxicity-Efficacy Profile of ICOVIR-5, a Potent and Selective Oncolytic Adenovirus Based on the pRB Pathway.” *Molecular therapy : the journal of the American Society of Gene Therapy* 15(9): 1607–15.

Cascalló, Manel, Gabriel Capellà, Adela Mazo, and Ramon Alemany. 2003. “Ras-Dependent Oncolysis with an Adenovirus VAI Mutant.” *Cancer Research* 63(17): 5544–50.

Caserta, Stefano et al. 2012. “Chronic Infection Drives Expression of the Inhibitory Receptor CD200R, and Its Ligand CD200, by Mouse and Human CD4 T Cells.” *PLoS ONE* 7(4).

Cerullo, V et al. 2012. “An Oncolytic Adenovirus Enhanced for Toll-like Receptor 9 Stimulation Increases Antitumor Immune Responses and Tumor Clearance.” *Mol Ther* 20(11): 2076–86. http://www.ncbi.nlm.nih.gov/pubmed/22828500.

Chang, Jianhua et al. 2009. “A Phase I Study of KH901, a Conditionally Replicating Granulocyte-Macrophage Colony-Stimulating Factor: Armed Oncolytic Adenovirus for the Treatment of Head and Neck Cancers.” *Cancer biology & therapy* 8(8): 676–82. http://www.ncbi.nlm.nih.gov/pubmed/19242097.

Chen, Dang Xiao, Hao He, and Reg M. Gorczynski. 2005. “Synthetic Peptides from the N-Terminal Regions of CD200 and CD200R1 Modulate Immunosuppressive and Anti-Inflammatory Effects of CD200-CD200R1 Interaction.” *International Immunology* 17(3): 289–96.

Chen, H, R Vinnakota, and S J Flint. 1994. “Intragenic Activating and Repressing Elements Control Transcription from the Adenovirus IVa2 Initiator.” *Mol Cell Biol* 14(1): 676–85. http://www.ncbi.nlm.nih.gov/entrez/query.fcgi?cmd=Retrieve&db=PubMed&dopt=Citation&list_uids=8264636.

Chen, Ren-Fu et al. 2015. “Novel Oncolytic Adenovirus Sensitizes Renal Cell Carcinoma Cells to Radiotherapy via Mitochondrial Apoptotic Cell Death.” *Molecular medicine reports* 11(3): 2141–46. http://www.spandidos-publications.com/10.3892/mmr.2014.2987%0Ahttp://www.ncbi.nlm.nih.gov/pubmed/25411768.

Chen, Zhiqi et al. 2008. “Identification of an Expressed Truncated Form of CD200, CD200tr, Which Is a Physiologic Antagonist of CD200-Induced Suppression.” *Transplantation* 86(8): 1116–24. http://www.ncbi.nlm.nih.gov/pubmed/18946351.

———. 2010. “Alternative Splicing of CD200 Is Regulated by an Exonic Splicing Enhancer and SF2/ASF.” *Nucleic Acids Research* 38(19): 6684–96.

Choi, I-K et al. 2011. “Oncolytic Adenovirus Co-Expressing IL-12 and IL-18 Improves Tumor-Specific Immunity via Differentiation of T Cells Expressing IL-12Rβ(2) or IL-18Rα.” *Gene therapy* 18(9): 898–909. http://dx.doi.org/10.1038/gt.2011.37.

Choi, K-J et al. 2006. “Concurrent Delivery of GM-CSF and B7-1 Using an Oncolytic Adenovirus Elicits Potent Antitumor Effect.” *Gene therapy* 13(13): 1010–20. http://www.ncbi.nlm.nih.gov/pubmed/16525479.

———. 2012. “Strengthening of Antitumor Immune Memory and Prevention of Thymic Atrophy Mediated by Adenovirus Expressing IL-12 and GM-CSF.” *Gene Therapy* 19(7): 711–23. http://dx.doi.org/10.1038/gt.2011.125.

Chung, Young-Hwa et al. 2002. “Kaposi’s Sarcoma-Associated Herpesvirus OX2 Glycoprotein Activates Myeloid-Lineage Cells to Induce Inflammatory Cytokine Production.” *Journal of virology* 76(10): 4688–98.

Cody, James J, and Joanne T Douglas. 2009. “NIH Public Access.” *Cancer* 16(6): 473–88.

Coles, S J et al. 2011. “CD200 Expression Suppresses Natural Killer Cell Function and Directly Inhibits Patient Anti-Tumor Response in Acute Myeloid Leukemia.” *Leukemia* 25(5): 792–99. http://www.pubmedcentral.nih.gov/articlerender.fcgi?artid=3093357&tool=pmcentrez&rendertype=abstract.

———. 2015. “The Immunosuppressive Ligands PD-L1 and CD200 Are Linked in AML T Cell Immunosuppression: Identification of a New Immunotherapeutic Synapse.” *Leukemia* 1(March): 1–12. http://www.nature.com/doifinder/10.1038/leu.2015.62.

Colmont, Chantal S et al. 2013. “CD200-Expressing Human Basal Cell Carcinoma Cells Initiate Tumor Growth.” *Proceedings of the National Academy of Sciences of the United States of America* 110(4): 1434–39. http://www.pubmedcentral.nih.gov/articlerender.fcgi?artid=3557049&tool=pmcentrez

&rendertype=abstract%5Cnhttp://www.ncbi.nlm.nih.gov/pubmed/23292936%5Cnhttp://www.pubmedcentral.nih.gov/articlerender.fcgi?artid=PMC3557049.

Conticello, Concetta et al. 2013. "CD200 Expression in Patients with Multiple Myeloma: Another Piece of the Puzzle." *Leukemia Research* 37(12): 1616–21. http://dx.doi.org/10.1016/j.leukres.2013.08.006.

Coughlan, Lynda et al. 2010. "Tropism-Modification Strategies for Targeted Gene Delivery Using Adenoviral Vectors." *Viruses* 2(10): 2290–2355.

Curry, Anna et al. 2017. "Importance of CD200 Expression by Tumor or Host Cells to Regulation of Immunotherapy in a Mouse Breast Cancer Model." *Plos One* 12(2): e0171586. http://www.ncbi.nlm.nih.gov/pubmed/28234914%0Ahttp://dx.plos.org/10.1371/journal.pone.0171586.

Dahmani, Abdelmalek, Herv?? Roudot, Florence Cymbalista, and R??mi Letestu. 2016. "Evaluation of Fluorescently Labeled Aerolysin as a New Kind of Reagent for Flow Cytometry Tests: Optimization of Use of FLAER, Hints, and Limits." *American Journal of Clinical Pathology* 145(3): 407–17.

Daily, O. P. et al. 1981. "Association of Aeromonas Sobria with Human Infection." *Journal of Clinical Microbiology* 13(4): 769–77.

Dechecchi, M C et al. 2001. "Heparan Sulfate Glycosaminoglycans Are Receptors Sufficient to Mediate the Initial Binding of Adenovirus Types 2 and 5." *Journal of virology* 75(18): 8772–80. http://www.pubmedcentral.nih.gov/articlerender.fcgi?artid=115122&tool=pmcentrez&rendertype=abstract.

Denmeade, Samuel R, and John T Isaacs. 2012. "Engineering Enzymatically Activated ' Molecular Grenades ' for Cancer." 3(7): 666–67.

DePace, N. G. 1912. "Sulla Scomparsa Di Un Enorme Cancro Vegetante Del Collo Dell'utero Senza Cura Chirurgica." *Ginecologia* 9: 82–89.

Dias, J D et al. 2012. "Targeted Cancer Immunotherapy with Oncolytic Adenovirus Coding for a Fully Human Monoclonal Antibody Specific for CTLA-4." *Gene Therapy* 19(10): 988–98. http://www.nature.com/doifinder/10.1038/gt.2011.176.

Dighe, a S, E Richards, L J Old, and R D Schreiber. 1994. "Enhanced in Vivo Growth and Resistance to Rejection of Tumor Cells Expressing Dominant Negative IFN Gamma Receptors." *Immunity* 1(6): 447–56. http://www.ncbi.nlm.nih.gov/pubmed/7895156.

Dock, G. 1904. "The Influence of Complicating Diseases upon Leukaemia." *American Journal of the Medical Sciences* 127: 563–92.

Dong, Haidong et al. 2002. "Tumor-Associated B7-H1 Promotes T-Cell Apoptosis: A Potential Mechanism of Immune Evasion." *Nature medicine* 8(8): 793–800. http://www.ncbi.nlm.nih.gov/pubmed/12091876.

Dubowchik, Gene M, and Michael A Walker. 1999. “Receptor-Mediated and Enzyme-Dependent Targeting of Cytotoxic Anticancer Drugs.” 83: 67–123.

Dunn, G P et al. 2002. “Cancer Immunoediting: From Immunosurveillance to Tumor Escape.” *Nat Immunol* 3(11): 991–98. http://www.ncbi.nlm.nih.gov/pubmed/12407406%5Cnhttp://www.nature.com/ni/journal/v3/n11/pdf/ni1102-991.pdf.

Dunn, Gavin P, Catherine M Koebel, and Robert D Schreiber. 2006. “Interferons, Immunity and Cancer Immunoediting.” *Nature reviews. Immunology* 6(11): 836–48. http://www.ncbi.nlm.nih.gov/pubmed/17063185.

Eikenes, L et al. 2005. “Hyaluronidase Induces a Transcapillary Pressure Gradient and Improves the Distribution and Uptake of Liposomal Doxorubicin (Caelyx) in Human Osteosarcoma Xenografts.” *British journal of cancer* 93(1): 81–88.

Eriksson, E et al. 2017. “Activation of Myeloid and Endothelial Cells by CD40L Gene Therapy Supports T-Cell Expansion and Migration into the Tumor Microenvironment.” *Nature Publishing Group* 24(2): 92–103. http://dx.doi.org/10.1038/gt.2016.80.

Eriksson, Emma et al. 2017. “Shaping the Tumor Stroma and Sparking Immune Activation by CD40 and 4-1BB Signaling Induced by an Armed Oncolytic Virus.” *Clinical Cancer Research*: clincanres.0285.2017. http://www.ncbi.nlm.nih.gov/pubmed/28536305%0Ahttp://clincancerres.aacrjournals.org/lookup/doi/10.1158/1078-0432.CCR-17-0285.

Estep, R. D. et al. 2014. “The Rhesus Rhadinovirus CD200 Homologue Affects Immune Responses and Viral Loads during In Vivo Infection.” *Journal of Virology* 88(18): 10635–54. http://jvi.asm.org/cgi/doi/10.1128/JVI.01276-14.

F.L. Graham, J. Smiley. 1977. “Characteristics of a Human Cell Line Transformed by D N A from Human Adenovirus Type 5.” *J.gen.Virol* 36(2977): 59–72.

Fajardo, Carlos Alberto et al. 2017. “Oncolytic Adenoviral Delivery of an EGFR-Targeting T-Cell Engager Improves Antitumor Ef Fi Cacy.” 77(16): 2052–64.

Farré, Domènec, Pablo Martínez-Vicente, Pablo Engel, and Ana Angulo. 2017. “Immunoglobulin Superfamily Members Encoded by Viruses and Their Multiple Roles in Immune Evasion.” *European Journal of Immunology*: 1–47. http://www.ncbi.nlm.nih.gov/pubmed/28383780%0Ahttp://doi.wiley.com/10.1002/eji.201746984.

Fernández-Ulibarri, Inés et al. 2015. “Genetic Delivery of an Immuno RNAse by an Oncolytic Adenovirus Enhances Anticancer Activity.” *International Journal of Cancer* 136(9): 2228–40.

Foster-cuevas, Mildred et al. 2004. “Human Herpesvirus 8 K14 Protein Mimics CD200 in Down-Regulating Macrophage Activation through CD200 Receptor.” 78(14): 7667–76.

Foster-Cuevas, Mildred et al. 2011. “Cytomegalovirus e127 Protein Interacts with the

Inhibitory CD200 Receptor." *Journal of virology* 85(12): 6055–59.

Freytag, Svend O. et al. 2003. "Phase I Study of Replication-Competent Adenovirus-Mediated Double-Suicide Gene Therapy in Combination with Conventional-Dose Three-Dimensional Conformal Radiation Therapy for the Treatment of Newly Diagnosed, Intermediate- to High-Risk Prostate Cancer." *Cancer Res.* 63(21): 7497–7506. http://cancerres.aacrjournals.org/content/63/21/7497.short.

Fueyo, J et al. 2000. "A Mutant Oncolytic Adenovirus Targeting the Rb Pathway Produces Anti-Glioma Effect in Vivo." *Oncogene* 19(1): 2–12.

Gabrilovich, Dmitry I, Tadao Ishida, Sorena Nadaf, and Dendritic Cell Function. 1999. "Antibodies to Vascular Endothelial Growth Factor Enhance the Efficacy of Cancer Immunotherapy by Improving Endogenous Dendritic Cell Function Antibodies to Vascular Endothelial Growth Factor Enhance the Efficacy of Cancer Immunotherapy by Improving Endoge." 5(October): 2963–70.

Galon, Jerome et al. 2006. "Type, Density, and Location of Immune Cells Within Human Colorectal Tumors Predict Clinical Outcome." *Science Reports* 313(September): 1960–64.

Ganesh, Shanthi et al. 2007. "Relaxin-Expressing, Fiber Chimeric Oncolytic Adenovirus Prolongs Survival of Tumor-Bearing Mice." *Cancer Research* 67(9): 4399–4407.

Garin-Chesa, Pilar, Lloyd J Oldt, and Wolfgang J Rettigt. 1990. "Cell Surface Glycoprotein of Reactive Stromal Fibroblasts as a Potential Antibody Target in Human Epithelial Cancers." *Pnas* 87(September): 7235–39.

Van Der Goot, F. Gisou et al. 1993. "Dimerization Stabilizes the Pore-Forming Toxin Aerolysin in Solution." *Journal of Biological Chemistry* 268(24): 18272–79.

van der Goot, G. 2001. Current topics in microbiology and immunology *Pore-Forming Toxins*.

Gorczynski, R. M. et al. 2001. "Evidence of a Role for CD200 in Regulation of Immune Rejection of Leukaemic Tumour Cells in C57BL/6 Mice." *Clinical and Experimental Immunology* 126(2): 220–29.

Gorczynski, R M et al. 1999. "An Immunoadhesin Incorporating the Molecule OX-2 Is a Potent Immunosuppressant That Prolongs Allo- and Xenograft Survival." *Journal of immunology (Baltimore, Md. : 1950)* 163(3): 1654–60.

Gorczynski, Reg, Ivo Boudakov, and Ismat Khatri. 2008. "Peptides of CD200 Modulate LPS-Induced TNF-?? Induction and Mortality In Vivo." *Journal of Surgical Research* 145(1): 87–96.

Gorczynski, Reginald et al. 2004. "CD200 Is a Ligand for All Members of the CD200R Family of Immunoregulatory Molecules." *The Journal of Immunology* 172: 7744–49.

Gorczynski, Reginald M. 2012. "CD200 : CD200R-Mediated Regulation of Immunity." 2012.

Guedan, S et al. 2012. "GALV Expression Enhances the Therapeutic Efficacy of an Oncolytic Adenovirus by Inducing Cell Fusion and Enhancing Virus Distribution." *Gene therapy*

19(11): 1048–57. http://www.ncbi.nlm.nih.gov/pubmed/22113313.

Guedan, Sonia et al. 2010. “Hyaluronidase Expression by an Oncolytic Adenovirus Enhances Its Intratumoral Spread and Suppresses Tumor Growth.” *Molecular therapy : the journal of the American Society of Gene Therapy* 18(7): 1275–83. http://dx.doi.org/10.1038/mt.2010.79.

Hamson, Elizabeth J. et al. 2014. “Understanding Fibroblast Activation Protein (FAP): Substrates, Activities, Expression and Targeting for Cancer Therapy.” *Proteomics - Clinical Applications* 8(5–6): 454–63.

Haralambieva, I et al. 2007. “Engineering Oncolytic Measles Virus to Circumvent the Intracellular Innate Immune Response.” *Molecular Therapy* 15(3): 588–97.

Hartman, Zachary C, Daniel M Appledorn, and Andrea Amalfitano. 2008. “Adenovirus Vector Induced Innate Immune Responses: Impact upon Efficacy and Toxicity in Gene Therapy and Vaccine Applications.” *Virus Research* 132(0): 1–14.

Hedley, Susan J. et al. 2006. “Targeted and Shielded Adenovectors for Cancer Therapy.” *Cancer Immunology, Immunotherapy* 55(11): 1412–19.

Heise, C et al. 2000. “An Adenovirus E1A Mutant That Demonstrates Potent and Selective Systemic Anti-Tumoral Efficacy.” *Nature medicine* 6(10): 1134–39.

Hemminki, Akseli. 2014. “Oncolytic Immunotherapy: Where Are We Clinically?” *Scientifica* 2014: 1–7. http://www.hindawi.com/journals/scientifica/2014/862925/.

Hernandez-Alcoceba, R, M Pihalja, D Qian, and M F Clarke. 2002. “New Oncolytic Adenoviruses with Hypoxia- and Estrogen Receptor-Regulated Replication.” *Hum Gene Ther* 13(14): 1737–50. http://www.ncbi.nlm.nih.gov/pubmed/12396626.

Hirvinen, Mari et al. 2015. “Immunological Effects of a TNF-Alpha Armed Oncolytic Adenovirus.” *Human gene therapy*: 1–38. http://www.ncbi.nlm.nih.gov/pubmed/25557131.

Hofmann, U B et al. 1999. “Matrix Metalloproteinases in Human Melanoma Cell Lines and Xenografts: Increased Expression of Activated Matrix Metalloproteinase-2 (MMP-2) Correlates with Melanoma Progression.” *British journal of cancer* 81(5): 774–82.

Hofmann, Uta B. et al. 2000. “Expression and Activation of Matrix Metalloproteinase-2 (MMP-2) and Its Co-Localization with Membrane-Type 1 Matrix Metalloproteinase (MT1-MMP) Correlate with Melanoma Progression.” *The Journal of Pathology* 191(3): 245–256. http://onlinelibrary.wiley.com/doi/10.1002/1096-9896(2000)9999:9999%3C::AID-PATH632%3E3.0.CO;2-#/abstract%5Cnhttp://onlinelibrary.wiley.com/doi/10.1002/1096-9896(2000)9999:9999%3C::AID-PATH632%3E3.0.CO;2-%23/full.

Holmannová, Drahomíra et al. 2012. “CD200/CD200R Paired Potent Inhibitory Molecules Regulating Immune and Inflammatory Responses; Part I: CD200/CD200R Structure, Activation, and Function.” *Acta medica (Hradec Králové) / Universitas Carolina, Facultas*

Medica Hradec Králové 55(1): 12–17. http://www.ncbi.nlm.nih.gov/pubmed/22696929.

Howard, S Peter, and J Thomas Buckley. 1985. "Activation of the Hole-Forming Toxin Aerolysin by Extracellular Processing." 163(1): 336–40.

Huang, Bo et al. 2006. "Gr-1+CD115+ Immature Myeloid Suppressor Cells Mediate the Development of Tumor-Induced T Regulatory Cells and T-Cell Anergy in Tumor-Bearing Host." *Cancer Research* 66(2): 1123–31.

Huang, Chih Hsiang et al. 2011. "Cleavage-Site Specificity of Prolyl Endopeptidase FAP Investigated with a Full-Length Protein Substrate." *Journal of Biochemistry* 149(6): 685–92.

Huang, Jiaoti, and Robert J. Schneider. 1991. "Adenovirus Inhibition of Cellular Protein Synthesis Involves Inactivation of Cap-Binding Protein." *Cell* 65(2): 271–80.

Huang, Jing-Hua et al. 2010. "Therapeutic and Tumor-Specific Immunity Induced by Combination of Dendritic Cells and Oncolytic Adenovirus Expressing IL-12 and 4-1BBL." *Molecular therapy : the journal of the American Society of Gene Therapy* 18(2): 264–74. http://dx.doi.org/10.1038/mt.2009.205%5Cnhttp://www.ncbi.nlm.nih.gov/pubmed/19738604%5Cnhttp://www.pubmedcentral.nih.gov/articlerender.fcgi?artid=PMC2839296.

Huang, Pearl S, and Allen Oliff. 2001. "Drug-Targeting Strategies in Cancer Therapy." *Current Opinion in Genetics & Development* 11(1): 104–10.

Huang, Xue F. et al. 2003. "A Broadly Applicable, Personalized Heat Shock Protein-Mediated Oncolytic Tumor Vaccine." *Cancer Research* 63(21): 7321–29.

Huber, M A et al. 2003. "Fibroblast Activation Protein: Differential Expression and Serine Protease Activity in Reactive Stromal Fibroblasts of Melanocytic Skin Tumors, J." *Invest. Dermatol.* 120: 182–88.

Hunter-Craig, I, K A Newton, G Westbury, and B W Lacey. 1970. "Use of Vaccinia Virus in the Treatment of Metastatic Malignant Melanoma." *Br Med J* 2(5708): 512–15.

Iacovache, Ioan et al. 2011. "Dual Chaperone Role of the c-Terminal Propeptide in Folding and Oligomerization of the Pore-Forming Toxin Aerolysin." *PLoS Pathogens* 7(7).

———. 2016. "Cryo-EM Structure of Aerolysin Variants Reveals a Novel Protein Fold and the Pore-Formation Process." *Nature Communications* 7(May): 12062. http://www.nature.com/doifinder/10.1038/ncomms12062.

Iacovache, Ioan, F. Gisou van der Goot, and Lucile Pernot. 2008. "Pore Formation: An Ancient yet Complex Form of Attack." *Biochimica et Biophysica Acta - Biomembranes* 1778(7–8): 1611–23.

Ilkow, Carolina S et al. 2015. "Reciprocal Cellular Cross-Talk within the Tumor Microenvironment Promotes Oncolytic Virus Activity." *Nature Medicine* 21(5): 530–36. http://www.nature.com/doifinder/10.1038/nm.3848.

Imre, Gergely et al. 2012. “Caspase-2 Is an Initiator Caspase Responsible for Pore-Forming Toxin-Mediated Apoptosis.” *The EMBO journal* 31(11): 2615–28. http://www.ncbi.nlm.nih.gov/pubmed/22531785.

Jenmalm, Maria C et al. 2006. “Regulation of Myeloid Cell Function through the CD200 Receptor.” *Journal of immunology (Baltimore, Md. : 1950)* 176(1): 191–99.

Jin, Fang, Peter J. Kretschmer, and Terry W. Hermiston. 2005. “Identification of Novel Insertion Sites in the Ad5 Genome That Utilize the Ad Splicing Machinery for Therapeutic Gene Expression.” *Molecular Therapy* 12(6): 1052–63.

Johnson, Leisa et al. 2002. “Selectively Replicating Adenoviruses Targeting Deregulated E2F Activity Are Potent, Systemic Antitumor Agents.” *Cancer Cell* 1(4): 325–37.

José, Anabel et al. 2014. “A Genetic Fiber Modification to Achieve Matrix-Metalloprotease-Activated Infectivity of Oncolytic Adenovirus.” *Journal of Controlled Release* 192: 148–56.

Kakarla, Sunitha et al. 2013. “Antitumor Effects of Chimeric Receptor Engineered Human T Cells Directed to Tumor Stroma.” *Mol Ther* 21(8): 1611–20.

Kaplan, Daniel H et al. 1998. “Demonstration of an Interferon □-Dependent Tumor Surveillance System in Immunocompetent Mice.” *Immunology* 95(June): 7556–61.

Karlseder, J, H Rotheneder, and E Wintersberger. 1996. “Interaction of Sp1 with the Growth- and Cell Cycle-Regulated Transcription Factor E2F.” *Molecular and cellular biology* 16(4): 1659–67.

Kataoka, T et al. 1998. “FLIP Prevents Apoptosis Induced by Death Receptors but Not by Perforin/granzyme B, Chemotherapeutic Drugs, and Gamma Irradiation.” *Journal of immunology (Baltimore, Md. : 1950)* 161(8): 3936–42.

Kawasaki, Brian T., and William L. Farrar. 2008. “Cancer Stem Cells, CD200 and Immunoevasion.” *Trends in Immunology* 29(10): 464–68.

Kelly, Elizabeth, and Stephen J Russell. 2007. “History of Oncolytic Viruses: Genesis to Genetic Engineering.” *Molecular therapy : The Journal of the American Society of Gene Therapy* 15(4): 651–59. http://dx.doi.org/10.1038/sj.mt.6300108.

Kim, Joo Hang et al. 2006. “Relaxin Expression from Tumor-Targeting Adenoviruses and Its Intratumoral Spread, Apoptosis Induction, and Efficacy.” *Journal of the National Cancer Institute* 98(20): 1482–93.

KIM, Wonwoo et al. 2011. “A Novel Combination Treatment of Armed Oncolytic Adenovirus Expressing IL-12 and GM-CSF with Radiotherapy in Murine Hepatocarcinoma.” *Journal of Radiation Research* 52(5): 646–54. https://academic.oup.com/jrr/article-lookup/doi/10.1269/jrr.10185.

Kirshner, J R et al. 1999. “Expression of the Open Reading Frame 74 (G-Protein-Coupled Receptor) Gene of Kaposi’s Sarcoma (KS)-Associated Herpesvirus: Implications for KS Pathogenesis.” *Journal of virology* 73(7): 6006–14.

http://www.pubmedcentral.nih.gov/articlerender.fcgi?artid=112661&tool=pmcentrez&rendertype=abstract.

Knapp, Oliver et al. 2010. “Clostridium Septicum Alpha-Toxin Forms Pores and Induces Rapid Cell Necrosis.” *Toxicon* 55(1): 61–72. http://dx.doi.org/10.1016/j.toxicon.2009.06.037.

Knapp, Oliver, Bradley Stiles, and Michel R. Popoff. 2010. “The Aerolysin-Like Toxin Family of Cytolytic, Pore-Forming Toxins.” *The Open Toxinology Journal* 3: 53–68.

Koebel, C M et al. 2007. “Adaptive Immunity Maintains Occult Cancer in an Equilibrium State.” *Nature* 450(7171): 903–7. http://www.ncbi.nlm.nih.gov/pubmed/18026089%5Cnhttp://www.nature.com/nature/journal/v450/n7171/pdf/nature06309.pdf.

Koning, Nathalie et al. 2010. “Expression of the Inhibitory CD200 Receptor Is Associated with Alternative Macrophage Activation.” *Journal of Innate Immunity* 2(2): 195–200.

Kretz-rommel, Anke et al. 2007. “CD200 Expression on Tumor Cells Suppresses Antitumor Immunity: New Approaches to Cancer Immunotherapy.” *Journal of immunology* 178: 5595–5605.

Kritz, Angelika B et al. 2007. “Adenovirus 5 Fibers Mutated at the Putative HSPG-Binding Site Show Restricted Retargeting with Targeting Peptides in the HI Loop.” *Molecular therapy : the journal of the American Society of Gene Therapy* 15(4): 741–49. http://www.ncbi.nlm.nih.gov/entrez/query.fcgi?cmd=Retrieve&db=PubMed&dopt=Citation&list_uids=17245351.

LeBeau, Aaron M, W Nathaniel Brennen, Saurabh Aggarwal, and Samuel R Denmeade. 2009. “Targeting the Cancer Stroma with a Fibroblast Activation Protein-Activated Promelittin Protoxin.” *Molecular cancer therapeutics* 8(5): 1378–86.

Lee, L., J. Liu, J. Manuel, and R. M. Gorczynski. 2006. “A Role for the Immunomodulatory Molecules CD200 and CD200R in Regulating Bone Formation.” *Immunology Letters* 105(2): 150–58.

Lee, Young Sook et al. 2006. “Enhanced Antitumor Effect of Oncolytic Adenovirus Expressing Interleukin-12 and B7-1 in an Immunocompetent Murine Model.” *Clinical Cancer Research* 12(19): 5859–68.

Leone, Patrizia et al. 2013. “MHC Class I Antigen Processing and Presenting Machinery: Organization, Function, and Defects in Tumor Cells.” *Journal of the National Cancer Institute* 105(16): 1172–87.

Liebert, Mary Ann et al. 1999. “A Novel Tumor-Specific Replication-Restricted Adenoviral.” 1733: 1721–33.

Liebert, Mary Ann, John J Rux, and Roger M Burnett. 2004. “JOHN J. RUX and ROGER M. BURNETT.” *Human Gene Therapy* 1176(December): 1167–76.

Lopez, M Veronica et al. 2012. “A Tumor-Stroma Targeted Oncolytic Adenovirus Replicated in

Human Ovary Cancer Samples and Inhibited Growth of Disseminated Solid Tumors in Mice." *Molecular therapy : the journal of the American Society of Gene Therapy* 20(12): 2222–33. http://dx.doi.org/10.1038/mt.2012.147.

Lorvik, Kristina Berg et al. 2013. "Molecular Profiling of Tumor-Specific TH1 Cells Activated in Vivo." *Oncoimmunology* 2(5): e24383. http://www.pubmedcentral.nih.gov/articlerender.fcgi?artid=3667914&tool=pmcentrez&rendertype=abstract.

Lu, Wei et al. 2004. "Intra-Tumor Injection of H101, a Recombinant Adenovirus, in Combination with Chemotherapy in Patients with Advanced Cancers: A Pilot Phase II Clinical Trial." *World journal of gastroenterology : WJG* 10(24): 3634–38.

Mannello, F, G Tonti, and S Papa. 2005. "Matrix Metalloproteinase Inhibitors as Anticancer Agents." *Current Cancer Drug Targets* 5: 285–98. http://www.ncbi.nlm.nih.gov/pubmed/18164645.

Martuza, RL et al. 1991. "Experimental Therapy of Human Glioma by Means of a Genetically Engineered Virus Mutant." *Science* 252: 854–56.

Mcconnell, Michael J, and Michael J Imperiale. 2004. "Biology of Adenovirus and Its Use as a Vector for Gene Therapy." *Human Gene Therapy* 15(November): 1022–33.

Meier, Oliver et al. 2002. "Adenovirus Triggers Macropinocytosis and Endosomal Leakage Together with Its Clathrin-Mediated Uptake." *Journal of Cell Biology* 158(6): 1119–31.

Mellman, Ira, George Coukos, and Glenn Dranoff. 2014. "Cancer Immunotherapy Comes of Age." *Nature* 480(7378): 480–89.

Merelli, Barbara, Daniela Massi, Laura Cattaneo, and Mario Mandalà. 2014. "Targeting the PD1/PD-L1 Axis in Melanoma: Biological Rationale, Clinical Challenges and Opportunities." *Critical Reviews in Oncology/Hematology* 89(1): 140–65. http://dx.doi.org/10.1016/j.critrevonc.2013.08.002.

Minas, Konstantinos, and Janet Liversidge. 2008. "Is The CD200 / CD200 Receptor Interaction More Than Just a Myeloid Cell Inhibitory Signal?" *Critical reviews in immunology* 26(3): 213–30.

Moertel, Christopher L et al. 2014. "CD200 in CNS Tumor-Induced Immunosuppression: The Role for CD200 Pathway Blockade in Targeted Immunotherapy." *Journal for immunotherapy of cancer* 2(1): 46. http://www.immunotherapyofcancer.org/content/2/1/46%5Cnpapers3://publication/doi/10.1186/s40425-014-0046-9.

Moreaux, Jerome et al. 2014. "CD200 Is a New Prognostic Factor in Multiple Myeloma." *Blood* 108(13): 4194–98.

Mosmann, Tim. 1983. "Rapid Colorimetric Assay for Cellular Growth and Survival: Application to Proliferation and Cytotoxicity Assays." *Journal of Immunological Methods* 65(1–2): 55–63.

Nagaraj, Srinivas et al. 2008. “Tolerance in Cancer.” *Nat Med.* 13(7): 828–35.

Nakashima, Hiroshi, Balveen Kaur, and E. A. Chiocca. 2010. “Directing Systemic Oncolytic Viral Delivery to Tumors via Carrier Cells.” *Cytokine and Growth Factor Reviews* 21(2–3): 119–26.

Nelson, K L, R a Brodsky, and J T Buckley. 1999. “Channels Formed by Subnanomolar Concentrations of the Toxin Aerolysin Trigger Apoptosis of T Lymphomas.” *Cellular microbiology* 1: 69–74.

Nelson, Kim L., Srikumar M. Raja, and J. Thomas Buckley. 1997. “The Glycosylphosphatidylinositol-Anchored Surface Glycoprotein Thy-1 Is a Receptor for the Channel-Forming Toxin Aerolysin.” *Journal of Biological Chemistry* 272(18): 12170–74.

Nicol, Campbell G. et al. 2004. “Effect of Adenovirus Serotype 5 Fiber and Penton Modifications on in Vivo Tropism in Rats.” *Molecular Therapy* 10(2): 344–54. http://dx.doi.org/10.1016/j.ymthe.2004.05.020.

Pages, Franck et al. 2005. “Effector Memory T Cells, Early Metastasis, and Survival in Colorectal Cancer.” *The New England journal of medicine* 353(25): 2654–66. http://www.sciencedirect.com/science/article/pii/S0090367108702295.

Parato, Kelley A, Donna Senger, Peter A J Forsyth, and John C Bell. 2005. “Recent Progress in the Battle between Oncolytic Viruses and Tumours.” *Nature reviews. Cancer* 5(12): 965–76. http://dx.doi.org/10.1038/nrc1750.

Parker, M W et al. 1994. “Structure of the Aeromonas Toxin Proaerolysin in Its Water-Soluble and Membrane-Channel States.” *Nature* 367(6460): 292–95.

Pillwein, K et al. 1998. “Hyaluronidase Additional to Standard Chemotherapy Improves Outcome for Children with Malignant Brain Tumors.” *Cancer letters* 131: 101–8.

Popoff, MR, and P Bouvet. 2009. “Clostridial Toxins.” *Future microbiology* 4(8): 1021–64.

Puig-Saus, C et al. 2014. “The Combination of I-Leader Truncation and Gemcitabine Improves Oncolytic Adenovirus Efficacy in an Immunocompetent Model.” *Cancer gene therapy* 21(2): 68–73. http://www.ncbi.nlm.nih.gov/pubmed/24434571.

Puig-Saus, Cristina, Alena Gros, Ramon Alemany, and Manel Cascalló. 2012. “Adenovirus I-Leader Truncation Bioselected against Cancer-Associated Fibroblasts to Overcome Tumor Stromal Barriers.” *Molecular therapy : the journal of the American Society of Gene Therapy* 20(1): 54–62. http://www.pubmedcentral.nih.gov/articlerender.fcgi?artid=3255593&tool=pmcentrez&rendertype=abstract.

Quirin, C et al. 2011. “Selectivity and Efficiency of Late Transgene Expression by Transcriptionally Targeted Oncolytic Adenoviruses Are Dependent on the Transgene Insertion Strategy.” *Hum Gene Ther* 22(4): 389–404.

Ranuncolo, Stella Maris et al. 2003. “Plasma MMP-9 (92 kDa-MMP) Activity Is Useful in the

Follow-up and in the Assessment of Prognosis in Breast Cancer Patients." *International Journal of Cancer* 106(5): 745–51.

Reid, Tony, Robert Warren, and David Kirn. 2002. "Intravascular Adenoviral Agents in Cancer Patients: Lessons from Clinical Trials." *Cancer gene therapy* 9(12): 979–86.

Rittner, K, V Schreiber, P Erbs, and M Lusky. 2007. "Targeting of Adenovirus Vectors Carrying a Tumor Cell-Specific Peptide: In Vitro and in Vivo Studies." *Cancer gene therapy* 14(5): 509–18. http://www.ncbi.nlm.nih.gov/pubmed/17318198.

Rodriguez-Garcia, A et al. 2015. "Insertion of Exogenous Epitopes in the E3-19K of Oncolytic Adenoviruses to Enhance TAP-Independent Presentation and Immunogenicity." *Gene therapy* 22(7): 596–601.

Rodríguez-García, Alba et al. 2015. "Safety and Efficacy of VCN-01, an Oncolytic Adenovirus Combining Fiber HSG-Binding Domain Replacement with RGD and Hyaluronidase Expression." *Clinical Cancer Research* 21(6): 1406–18.

Rodriguez, Ron et al. 1997. "Prostate Attenuated Replication Competent Adenovirus (ARCA) CN706: A Selective Cytotoxic for Prostate-Specific Antigen-Positive Prostate Cancer Cells." *Cancer Research* 57(13): 2559–63.

Rojas-Martínez, Augusto et al. 2013. "Intraprostatic Distribution and Long Term Follow-up after AdV-Tk Immunotherapy as Neoadjuvant to Surgery in Patients with Prostatic Cancer." *Cancer gene therapy* 20(11): 642–49.

Rojas, J J et al. 2009. "A Modified E2F-1 Promoter Improves the Efficacy to Toxicity Ratio of Oncolytic Adenoviruses." *Gene therapy* 16(12): 1441–51. http://www.ncbi.nlm.nih.gov/pubmed/19710704.

———. 2012. "Improved Systemic Antitumor Therapy with Oncolytic Adenoviruses by Replacing the Fiber Shaft HSG-Binding Domain with RGD." *Gene Ther* 19(4): 453–57. http://www.ncbi.nlm.nih.gov/pubmed/21776023.

Rojas, Juan J et al. 2010. "Minimal RB-Responsive E1A Promoter Modification to Attain Potency, Selectivity, and Transgene-Arming Capacity in Oncolytic Adenoviruses." *Molecular therapy : the journal of the American Society of Gene Therapy* 18(11): 1960–71.
http://www.pubmedcentral.nih.gov/articlerender.fcgi?artid=2990517&tool=pmcentrez&rendertype=abstract.

Rojas, Luis Alfonso et al. 2016. "Albumin-Binding Adenoviruses Circumvent Pre-Existing Neutralizing Antibodies upon Systemic Delivery." *Journal of Controlled Release* 237: 78–88. http://dx.doi.org/10.1016/j.jconrel.2016.07.004.

Rosewell Shaw, Amanda, and Masataka Suzuki. 2016. "Recent Advances in Oncolytic Adenovirus Therapies for Cancer." *Current Opinion in Virology* 21: 9–15. http://dx.doi.org/10.1016/j.coviro.2016.06.009.

Rowe, WP et al. 1953. "Isolation of a Cytopathogenic Agent from Human Adenoids Undergoing

Spontaneous Degeneration in Tissue Culture." *Proc Soc Exp Biol Med* 84: 570–73.

Rubinstein, Natalia et al. 2004. "Targeted Inhibition of Galectin-1 Gene Expression in Tumor Cells Results in Heightened T Cell-Mediated Rejection: A Potential Mechanism of Tumor-Immune Privilege." *Cancer Cell* 5(3): 241–51.

Russell, Stephen J., Kah-whye Peng, and John C Bell. 2012. "Oncolytic Virotherapy." *Nature biotechnology* 30(7): 658–70.

Rygiel, T P et al. 2012. "CD200-CD200R Signaling Suppresses Anti-Tumor Responses Independently of CD200 Expression on the Tumor." *Oncogene* 31(24): 2979–88. http://dx.doi.org/10.1038/onc.2011.477.

Savontaus, M J, B V Sauter, T-G Huang, and S L C Woo. 2002. "Transcriptional Targeting of Conditionally Replicating Adenovirus to Dividing Endothelial Cells." *Gene therapy* 9(14): 972–79. http://www.ncbi.nlm.nih.gov/pubmed/12085246.

Schneider, R M et al. 2003. "Directed Evolution of Retroviruses Activatable by Tumour-Associated Matrix Metalloproteases." *Gene therapy* 10(16): 1370–80.

Schreiber, Robert D, Lloyd J Old, and Mark J Smyth. 2011. "Cancer Immunoediting: Integrating Immunity's Roles in Cancer Suppression and Promotion." *Science* 331(6024): 1565–70. http://www.sciencemag.org/content/331/6024/1565.abstract.

Sellman, B. R., and R. K. Tweten. 1997. "The Propeptide of Clostridium Septicum Alpha Toxin Functions as an Intramolecular Chaperone and Is a Potent Inhibitor of Alpha Toxin-Dependent Cytolysis." *Molecular microbiology* 25(3): 429–40.

Senzer, Neil N. et al. 2009. "Phase II Clinical Trial of a Granulocyte-Macrophage Colony-Stimulating Factor-Encoding, Second-Generation Oncolytic Herpesvirus in Patients with Unresectable Metastatic Melanoma." *Journal of Clinical Oncology* 27(34): 5763–71.

Shankaran, V et al. 2001. "IFNγ and Lymphocytes Prevent Primary Tumour Development and Shape Tumour Immunogenicity." *Nature* 410(6832): 1107–11.

Shashkova, Elena V, Jacqueline F Spencer, William S M Wold, and Konstantin Doronin. 2007. "Targeting Interferon-Alpha Increases Antitumor Efficacy and Reduces Hepatotoxicity of E1A-Mutated Spread-Enhanced Oncolytic Adenovirus." *Molecular therapy : the journal of the American Society of Gene Therapy* 15(3): 598–607. http://www.ncbi.nlm.nih.gov/pubmed/17191072.

Shin, M S et al. 2001. "Mutations of Tumor Necrosis Factor-Related Apoptosis-Inducing Ligand Receptor 1 (TRAIL-R1) and Receptor 2 (TRAIL-R2) Genes in Metastatic Breast Cancers." *Cancer Res* 61(13): 4942–46. http://www.ncbi.nlm.nih.gov/pubmed/11431320.

Sinkovics, J, and J Horvath. 1993. "New Developments in the Virus Therapy of Cancer: A Historical Review." *Intervirology* 36: 193–214.

Siva, A. et al. 2008. "Immune Modulation by Melanoma and Ovarian Tumor Cells through Expression of the Immunosuppressive Molecule CD200." *Cancer Immunology,*

Immunotherapy 57(7): 987–96.

Smith, J et al. 2008. “Interaction of Systemically Delivered Adenovirus Vectors with Kupffer Cells in Mouse Liver.” *Human Gene Therapy* 19(5): 547–54.

Smith, K. J., H. G. Skelton, G. Turiansky, and K. F. Wagner. 1997. “Hyaluronidase Enhances the Therapeutic Effect of Vinblastine in Intralesional Treatment of Kaposi’s Sarcoma.” *Journal of the American Academy of Dermatology* 36(2): 239–42.

Smith, R, J Huebner, P Rowe, and B Thomas. 1956. “Studies on the Use of Viruses in the Treatment of Carcinoma of the Cervix.” *Cancer* 9(6): 1211–1128.

Smith, Theodore A G et al. 2003. “Receptor Interactions Involved in Adenoviral-Mediated Gene Delivery after Systemic Administration in Non-Human Primates.” *Human gene therapy* 14(17): 1595–1604. http://www.ncbi.nlm.nih.gov/pubmed/14633402.

Southam, CM, and AE Moore. 1952. “Clinical Studies of Viruses as Antineoplastic Agents with Particular Reference to Egypt 101 Virus.” *Cancer* 5: 1025–34.

Srivastava, Minu K et al. 2010. “Myeloid-Derived Suppressor Cells Inhibit T Cell Activation by Depleting Cystine and Cysteine.” *Cancer Research* 70(1): 68–77.

Stern-Ginossar, Noam et al. 2008. “Human microRNAs Regulate Stress-Induced Immune Responses Mediated by the Receptor NKG2D.” *Nature immunology* 9(9): 1065–73. http://www.ncbi.nlm.nih.gov/pubmed/18677316.

Stewart, Phoebe L. et al. 1997. “Cryo-EM Visualization of an Exposed RGD Epitope on Adenovirus That Escapes Antibody Neutralization.” *EMBO Journal* 16(6): 1189–98.

Stumpfova, Magda et al. 2010. “The Immunosuppressive Surface Ligand CD200 Augments the Metastatic Capacity of Squamous Cell Carcinoma.” *Cancer Research* 70(7): 2962–72.

Su, Changqing et al. 2006. “Immune Gene-Viral Therapy with Triplex Efficacy Mediated by Oncolytic Adenovirus Carrying an Interferon-?? Gene Yields Efficient Antitumor Activity in Immunodeficient and Immunocompetent Mice.” *Molecular Therapy* 13(5): 918–27.

Szécsi, Judit et al. 2006. “Targeted Retroviral Vectors Displaying a Cleavage Site-Engineered Hemagglutinin (HA) through HA-Protease Interactions.” *Molecular Therapy* 14(5): 735–44.

Takahashi, Hidenobu et al. 2006. “FAS Death Domain Deletions and Cellular FADD-like Interleukin 1β Converting Enzyme Inhibitory Protein (Long) Overexpression: Alternative Mechanisms for Deregulating the Extrinsic Apoptotic Pathway in Diffuse Large B-Cell Lymphoma Subtypes.” *Clinical Cancer Research* 12(11 I): 3265–71.

Talbot, S J, R a Weiss, P Kellam, and C Boshoff. 1999. “Transcriptional Analysis of Human Herpesvirus-8 Open Reading Frames 71, 72, 73, K14, and 74 in a Primary Effusion Lymphoma Cell Line.” *Virology* 257(1): 84–94.

Täuber, B, and T Dobner. 2001. “Adenovirus Early E4 Genes in Viral Oncogenesis.” *Oncogene* 20(54): 7847–54. http://www.ncbi.nlm.nih.gov/pubmed/11753667.

Terabe, Masaki, and Jay A. Berzofsky. 2004. “Immunoregulatory T Cells in Tumor Immunity.” *Current Opinion in Immunology* 16(2): 157–62.

Tollefson, A E, A Scaria, et al. 1996. “The Adenovirus Death Protein (E3-11.6K) Is Required at Very Late Stages of Infection for Efficient Cell Lysis and Release of Adenovirus from Infected Cells.” *Journal of virology* 70(4): 2296–2306. http://www.ncbi.nlm.nih.gov/pubmed/8642656%5Cnhttp://www.pubmedcentral.nih.gov/articlerender.fcgi?artid=PMC190071.

Tollefson, A E, J S Ryerse, et al. 1996. “The E3-11.6-kDa Adenovirus Death Protein (ADP) Is Required for Efficient Cell Death: Characterization of Cells Infected with Adp Mutants.” *Virology* 220(1): 152–62. http://www.ncbi.nlm.nih.gov/pubmed/8659107%5Cnhttp://ac.els-cdn.com/S0042682296902950/1-s2.0-S0042682296902950-main.pdf?_tid=7f580c96-0107-11e5-b1d0-00000aab0f6b&acdnat=1432356921_760e4bc199518c2f3e247fe87070a53e.

Tonks, A et al. 2007. “CD200 as a Prognostic Factor in Acute Myeloid Leukaemia.” *Leukemia* 21(3): 566–68. http://www.nature.com/doifinder/10.1038/sj.leu.2404559.

Tsukuda, Kazunori et al. 2002. “An E2F-Responsive Replication-Selective Adenovirus Targeted to the Defective Cell Cycle in Cancer Cells: Potent Antitumoral Efficacy but No Toxicity to Normal Cell.” *Cancer Research* 62(12): 3438–47.

Tucker, Alec D., Michael W. Parker, Demetrius Tsernoglou, and J. Thomas Buckley. 1990. “Crystallization of a Proform of Aerolysin, a Hole-Forming Toxin from Aeromonas Hydrophila.” *Journal of Molecular Biology* 212(4): 561–62.

Uyttenhove, Catherine et al. 2003. “Evidence for a Tumoral Immune Resistance Mechanism Based on Tryptophan Degradation by Indoleamine 2,3-Dioxygenase.” *Nature medicine* 9(10): 1269–74.

Verma, Inder M., and Matthew D. Weitzman. 2005. “GENE THERAPY: Twenty-First Century Medicine.” *Annual Review of Biochemistry* 74(1): 711–38.

Verma, Rajeshwar P., and Corwin Hansch. 2007. “Matrix Metalloproteinases (MMPs): Chemical-Biological Functions and (Q)SARs.” *Bioorganic and Medicinal Chemistry* 15(6): 2223–68.

Waddington, Simon N. et al. 2008. “Adenovirus Serotype 5 Hexon Mediates Liver Gene Transfer.” *Cell* 132(3): 397–409.

Wang, T et al. 2004. “Regulation of the Innate and Adaptive Immune Responses by Stat-3 Signaling in Tumor Cells.” *Nat Med* 10(1): 48–54. http://www.ncbi.nlm.nih.gov/entrez/query.fcgi?cmd=Retrieve&db=PubMed&dopt=Citation&list_uids=14702634.

Wickham, Thomas J., Patricia Mathias, David A. Cheresh, and Glen R. Nemerow. 1993. “Integrins ??v??3 and ??v??5 Promote Adenovirus Internalization but Not Virus Attachment.” *Cell* 73(2): 309–19.

Williams, Simon A. et al. 2007. “A Prostate-Specific Antigen-Activated Channel-Forming Toxin as Therapy for Prostatic Disease.” *Journal of the National Cancer Institute* 99(5): 376–85.

Woller, Norman et al. 2015. “Viral Infection of Tumors Overcomes Resistance to PD-1-Immunotherapy by Broadening Neoantigenome-Directed T-Cell Responses.” *Molecular Therapy* 23(10): 1630–40. http://linkinghub.elsevier.com/retrieve/pii/S1525001616302945.

Wong, Karrie K et al. 2010. “The Role of CD200 in Immunity to B Cell Lymphoma.” *Journal of leukocyte biology* 88(2): 361–72.

Wright, G J et al. 2000. “Lymphoid/neuronal Cell Surface OX2 Glycoprotein Recognizes a Novel Receptor on Macrophages Implicated in the Control of Their Function.” *Immunity* 13: 233–42.

Wright, Gavin J et al. 2003. “Characterization of the CD200 Receptor Family in Mice and Humans and Their Interactions with CD200.” *Journal of immunology (Baltimore, Md. : 1950)* 171(6): 3034–46.

Wrzesinski, Stephen H., Yisong Y. Wan, and Richard A. Flavell. 2007. “Transforming Growth Factor-?? And the Immune Response: Implications for Anticancer Therapy.” *Clinical Cancer Research* 13(18): 5262–70.

Xia, ZJ et al. 2004. “Phase III Randomized Clinical Trial of Intratumoral Injection of E1B Gene-Deleted Adenovirus (H101) Combined with Cisplatin-Based Chemotherapy in Treating Squamous Cell Cancer of Head and Neck or Esophagus.” *Aizheng* 23(12): 1666–70.

Zhang, Jun et al. 2005. “Kaposi ’ S Sarcoma-Associated Herpesvirus / Human Herpesvirus 8 Replication and Transcription Activator Regulates Viral and Cellular Genes via Interferon-Stimulated Response Elements.” *Society* 79(9): 5640–52.

Zhang, Shuli, Holly Cherwinski, Jonathon D Sedgwick, and Joseph H Phillips. 2004. “Molecular Mechanisms of CD200 Inhibition of Mast Cell Activation.” *Journal of immunology (Baltimore, Md. : 1950)* 173(11): 6786–93.

Zhang, W, J A Low, J B Christensen, and M J Imperiale. 2001. “Role for the Adenovirus IVa2 Protein in Packaging of Viral DNA.” *Journal of virology* 75(21): 10446–54. http://www.pubmedcentral.nih.gov/articlerender.fcgi?artid=114618&tool=pmcentrez&rendertype=abstract.

Zhang, Yuanming, and Jeffrey M Bergelson. 2005. “Adenovirus Receptors.” *Journal of Virology* 79(19): 12125–31. http://jvi.asm.org/content/79/19/12125.full%5Cnpapers3://publication/doi/10.1128/JVI.79.19.12125-12131.2005.

Zheng, J-N et al. 2010. “Oncolytic Adenovirus Expressing Interleukin-18 Induces Significant Antitumor Effects against Melanoma in Mice through Inhibition of Angiogenesis.” *Cancer gene therapy* 17: 28–36.

8 ANNEX

DNA and protein sequences used in this thesis:

hCD200: http://www.ncbi.nlm.nih.gov/nuccore/390154945?report=fasta

DNA

AATATTTTTCAATTGGTACTAAGCGGTGATGTTTCTGATCAGCCACCATGGAGAGGCTGGTGATCAG
GATGCCCTTCTCTCATCTCTCCTCCTACAGCCTGGTTTGGGTCATGGCAGCAGTGGTGCTGTGCACAG
CACAAGTGCAAGTGGTGACCCAGGATGAAAGAGAGCAGCTGTACACACCTGCTTCCTTAAAATGCTC
TCTGCAAAATGCCCAGGAAGCCCTCATTGTGACATGGCAGAAAAAGAAAGCTGTAAGCCCAGAAAA
CATGGTCACCTTCAGCGAGAACCATGGGGTGGTGATCCAGCCTGCCTATAAGGACAAGATAAACATT
ACCCAGCTGGGACTCCAAAACTCAACCATCACCTTCTGGAATATCACCCTGGAGGATGAAGGGTGTT
ACATGTGTCTCTTCAATACCTTTGGTTTTGGGAAGATCTCAGGAACGGCCTGCCTCACCGTCTATGTA
CAGCCCATAGTATCCCTTCACTACAAATTCTCTGAAGACCACCTAAATATCACTTGCTCTGCCACTGCC
CGCCCAGCCCCCATGGTCTTCTGGAAGGTCCCTCGGTCAGGGATTGAAAATAGTACAGTGACTCTGT
CTCACCCAAATGGGACCACGTCTGTTACCAGCATCCTCCATATCAAAGACCCTAAGAATCAGGTGGG
GAAGGAGGTGATCTGCCAGGTGCTGCACCTGGGGACTGTGACCGACTTTAAGCAAACCGTCAACAA
AGGATATTGGTTTTCAGTTCCGCTATTGCTAAGCATTGTTTCCCTGGTAATTCTTCTCATCCTAATCTCA
ATCTTACTGTACTGGAAACGTCACCGGAATCAGGACCGAGGTGAATTGTCACAGGGAGTTCAAAAAA
TGACAGATTACAAGGACGACGACGACAAGTAATAAACTTTATTTTTCAATTGCAGAAAATTTCAAGTC
ATTTTTCATTCAGTAGTATAGCGCT

Protein

MERLVIRMPFSHLSTYSLVWVMAAVVLCTAQVQVVTQDEREQLYTPASLKCSLQNAQEALIVTWQKKK
AVSPENMVTFSENHGVVIQPAYKDKINITQLGLQNSTITFWNITLEDEGCYMCLFNTFGFGKISGTACLTV
YVQPIVSLHYKFSEDHLNITCSATARPAPMVFWKVPRSGIENSTVTLSHPNGTTSVTSILHIKDPKNQVGKE
VICQVLHLGTVTDFKQTVNKGYWFSVPLLLSIVSLVILLVLISILLYWKRHRNQDRGELSQGVQKMT

hCD200tr

DNA

AATATTTTTCAATTGGTACTAAGCGGTGATGTTTCTGATCAGCCACCATGGAGAGGCTGGTGATCAG
GATGCCCTTCTCTCATCTCTCCTCCTACAGCCTGGTTTGGGTCATGGCAGCAGTGGTGCTGTGCACAG
CAGAAAACATGGTCACCTTCAGCGAGAACCATGGGGTGGTGATCCAGCCTGCCTATAAGGACAAGA
TAAACATTACCCAGCTGGGACTCCAAAACTCAACCATCACCTTCTGGAATATCACCCTGGAGGATGAA
GGGTGTTACATGTGTCTCTTCAATACCTTTGGTTTTGGGAAGATCTCAGGAACGGCCTGCCTCACCGT
CTATGTACAGCCCATAGTATCCCTTCACTACAAATTCTCTGAAGACCACCTAAATATCACTTGCTCTGC
CACTGCCCGCCCAGCCCCCATGGTCTTCTGGAAGGTCCCTCGGTCAGGGATTGAAAATAGTACAGTG
ACTCTGTCTCACCCAAATGGGACCACGTCTGTTACCAGCATCCTCCATATCAAAGACCCTAAGAATCA
GGTGGGGAAGGAGGTGATCTGCCAGGTGCTGCACCTGGGGACTGTGACCGACTTTAAGCAAACCGT
CAACAAAGGATATTGGTTTTCAGTTCCGCTATTGCTAAGCATTGTTTCCCTGGTAATTCTTCTCATCCT
AATCTCAATCTTACTGTACTGGAAACGTCACCGGAATCAGGACCGAGGTGAATTGTCACAGGGAGTT
CAAAAAATGACAGATTACAAGGACGACGACGACAAGTAATAAACTTTATTTTTCAATTGCAGAAAAT
TTCAAGTCATTTTTCATTCAGTAGTATAGCGCT

Protein

MERLVIRMPFSHLSTYSLVWVMAAVVLCTAENMVTFSENHGVVIQPAYKDKINITQLGLQNSTITFWNIT
LEDEGCYMCLFNTFGFGKISGTACLTVYVQPIVSLHYKFSEDHLNITCSATARPAPMVFWKVPRSGIENST
VTLSHPNGTTSVTSILHIKDPKNQVGKEVICQVLHLGTVTDFKQTVNKGYWFSVPLLLSIVSLVILLVLISILLY
WKRHRNQDRGELSQGVQKMT

HHV-8 K14: http://www.ncbi.nlm.nih.gov/nuccore/U75698 (ORF K14)

DNA

AATATTTTTCAATTGGTACTAAGCGGTGATGTTTCTGATCAGCCACCATGTCTAGCCTCTTCATTTCAT
TACCTTGGGTGGCGTTCATCTGGCTAGCCCTCCTTGGCGCGGTTGGGGGTGCCCGCGTTCAGGGGCC
CATGCGGGGCTCTGCTGCCCTCACCTGCGCCATCACGCCCCGTGCTGACATAGTTAGCGTTACCTGGC
AAAAAAGGCAGCTCCCCGGTCCCGTAAACGTCGCCACGTACAGCCATTCATATGGGGTGGTGGTTCA
GACCCAGTACCGCCACAAGGCAAATATAACCTGTCCTGGGCTTTGGAACTCTACCCTTGTTATCCATA
ACCTTGCAGTGGATGATGAGGGCTGTTACCTGTGTATCTTTAACTCATTTGGTGGCCGGCAGGTGTC
ATGCACAGCCTGCCTGGAAGTGACATCTCCCCCTACTGGACACGTGCAGGTAAATAGCACAGAAGAC
GCAGACACCGTCACCTGTTTGGCAACTGGTCGCCCACCCCCCAATGTCACCTGGGCCGCACCCTGGA
ACAACGCCTCTTCTACCCAGGAGCAGTTCACTGACAGTGATGGTCTTACAGTTGCGTGGAGGACCGT
GAGGCTGCCGCGTGGGGATAATACCACCCCAAGTGAGGGAATATGTCTCATCACCTGGGGAAATGA
GAGCATATCAATCCCGGCTTCTATTCAAGGCCCCTTGGCCCATGACCTTCCCGCGGCCCAGGGAACTC
TTGCCGGGGTTGCCATTACTCTGGTGGGCCTATTTGGGATATTCGCATTACATCATTGCCGCCGCAAG
CAGGGCGGTGCATCACCTACTTCAGATGACATGGACCCCCTATCCACCCAGGATTACAAGGACGACG
ACGACAAGTAATAAACTTTATTTTTCAATTGCAGAAAATTTCAAGTCATTTTTCATTCAGTAGTATAGC
GCT

Prot

MSSLFISLPWVAFIWLALLGAVGGARVQGPMRGSAALTCAITPRADIVSVTWQKRQLPGPVNVATYSHS
YGVVVQTQYRHKANITCPGLWNSTLVIHNLAVDDEGCYLCIFNSFGGRQVSCTACLEVTSPPTGHVQVNS
TEDADTVTCLATGRPPPNVTWAAPWNNASSTQEQFTDSDGLTVAWRTVRLPRGDNTTPSEGICLITWG
NESISIPASIQGPLAHDLPAAQGTLAGVAITLVGLFGIFALHHCRRKQGGASPTSDDMDPLSTQ

HHV-8 K14tr

DNA

AATATTTTTCAATTGGTACTAAGCGGTGATGTTTCTGATCAGCCACCATGTCTAGCCTCTTCATTTCAT
TACCTTGGGTGGCGTTCATCTGGCTAGCCCTCCTTGGCGCGGTTGGGGGTGTAAACGTCGCCACGTA
CAGCCATTCATATGGGGTGGTGGTTCAGACCCAGTACCGCCACAAGGCAAATATAACCTGTCCTGGG

CTTTGGAACTCTACCCTTGTTATCCATAACCTTGCAGTGGATGATGAGGGCTGTTACCTGTGTATCTTT
AACTCATTTGGTGGCCGGCAGGTGTCATGCACAGCCTGCCTGGAAGTGACATCTCCCCCTACTGGAC
ACGTGCAGGTAAATAGCACAGAAGACGCAGACACCGTCACCTGTTTGGCAACTGGTCGCCCACCCCC
CAATGTCACCTGGGCCGCACCCTGGAACAACGCCTCTTCTACCCAGGAGCAGTTCACTGACAGTGAT
GGTCTTACAGTTGCGTGGAGGACCGTGAGGCTGCCGCGTGGGGATAATACCACCCCAAGTGAGGGA
ATATGTCTCATCACCTGGGGAAATGAGAGCATATCAATCCCGGCTTCTATTCAAGGCCCCTTGGCCCA
TGACCTTCCCGCGGCCCAGGGAACTCTTGCCGGGGTTGCCATTACTCTGGTGGGCCTATTTGGGATA
TTCGCATTACATCATTGCCGCCGCAAGCAGGGCGGTGCATCACCTACTTCAGATGACATGGACCCCCT
ATCCACCCAGGATTACAAGGACGACGACGACAAGTAATAAACTTTATTTTTCAATTGCAGAAAATTTC
AAGTCATTTTTCATTCAGTAGTATAGCGCT

Prot

MSSLFISLPWVAFIWLALLGAVGGVNVATYSHSYGVVVQTQYRHKANITCPGLWNSTLVIHNLAVDDEG
CYLCIFNSFGGRQVSCTACLEVTSPPTGHVQVNSTEDADTVTCLATGRPPPNVTWAAPWNNASSTQEQF
TDSDGLTVAWRTVRLPRGDNTTPSEGICLITWGNESISIPASIQGPLAHDLPAAQGTLAGVAITLVGLFGIF
ALHHCRRKQGGASPTSDDMDPLSTQ

AtoxC

DNA

CTCTTACACTTTTTCATACATTGCCCAAGAATAAAGAATCGTTTGTGTTATGTTTCAACGTGTTTATTTT
TCAATTGGTACTAAGCGGTGATGTTTCTGATCAGCCACCATGGGATGGTCCTGTATTATTCTGTTTCT
GGTCGCAACTGCTACTGGGGTGCATTCACTGACTAACCTGGAAGAGGGAGGGTATGCCAACCACAA
CAATGCCAGCTCCATCAAGATTTTCGGCTACGAGGACAATGAAGATCTGAAGGCTAAAATCATTCAG
GACCCTGAGTTCATCCGAAACTGGGCAAATGTGGCCCATTCTCTGGGATTTGGATGGTGCGGAGGA
ACCGCAAACCCAAATGTCGGACAGGGCTTCGAGTTTAAGCGCGAAGTGGGGGCTGGAGGCAAAGT
CTCCTACCTGCTGTCTGCACGATATAACCCAAATGACCCCTACGCCTCTGGCTATAGGGCTAAGGATC
GCCTGAGTATGAAAATCTCAAACGTGCGCTTTGTCATCGACAATGATAGTATTAAGCTGGGCACCCCT
AAAGTGAAGAAACTGGCACCACTGAACTCTGCCAGTTTCGATCTGATTAATGAGAGCAAGACAGAAT
CAAAGCTGAGCAAAACTTTTAACTACACCACAAGCAAGACCGTGAGCAAAACCGACAATTTCAAGTT
TGGAGAAAAAATCGGCGTGAAGACTTCCTTCAAAGTCGGACTGGAGGCCATTGCTGATTCAAAGGT
CGAGACCAGCTTCGAGTTCAACGCAGAGCAGGGCTGGTCTAACACTAATAGTACTACCGAAACCAAA
CAGGAGAGTACAACTTATACCGCCACAGTGTCACCCCAGACCAAGAAGCGGCTGTTCCTGGACGTGC
TGGGATCTCAGATCGATATTCCTTACGAGGGCAAGATCTACATGGAATATGACATTGAGCTGATGGG
GTTCCTGCGATATACTGGAAACGCTCGGGAAGACCACACAGAGGATCGCCCCACTGTGAAGCTGAA
ATTTGGGAAGAATGGAATGAGCGCCGAGGAACACCTGAAGGACCTGTACAGCCATAAAAACATCAA
TGGCTATTCCGAATGGGACTGGAAGTGGGTGGATGAGAAATTCGGGTACCTGTTTAAGAACTCCTAT
GATGCCCTGACCTCTCGGAAGCTGGGGGGAATCATCAAGGGCAGCTTCACCAACATCAATGGGACA
AAGATCGTGATTAGAGAGGGCAAAGAAATTCCCCTGCCTGACAAGAAAGACAGAGGCGAGACCGG
CCCCTCAGTAGATTCTCTGGACGCAAGACTGCAGAACGAGGGGATCAGGATTGAGAATATCGAAAC
CCAGGATGTGCCCGGCTTCCGGCTGAACTCCATTACATACAACGACAAGAAGCTGATCCTGATTAAC
AACATCTAATAAACTTTATTTTTCAATTGCAGAAAATTTCAAGTCATTTTTCATTCAGTAGTATAGCCCC
ACCACCACATAGCTTATACA

Protein

MGWSCIILFLVATATGVHSLTNLEEGGYANHNNASSIKIFGYEDNEDLKAKIIQDPEFIRNWANVAHSLGF
GWCGGTANPNVGQGFEFKREVGAGGKVSYLLSARYNPNDPYASGYRAKDRLSMKISNVRFVIDNDSIKL
GTPKVKKLAPLNSASFDLINESKTESKLSKTFNYTTSKTVSKTDNFKFGEKIGVKTSFKVGLEAIADSKVETSF
EFNAEQGWSNTNSTTETKQESTTYTATVSPQTKKRLFLDVLGSQIDIPYEGKIYMEYDIELMGFLRYTGNA
REDHTEDRPTVKLKFGKNGMSAEEHLKDLYSHKNINGYSEWDWKWVDEKFGYLFKNSYDALTSRKLGGI
IKGSFTNINGTKIVIREGKEIPLPDKKDRGETGPSVDSLDARLQNEGIRIENIETQDVPGFRLNSITYNDKKLIL
INNI

AtoxS

DNA

CAATTGGTACTAAGCGGTGATGTTTCTGATCAGCCACCATGGGATGGTCCTGTATTATTCTGTTTCTG
GTCGCAACTGCTACTGGGGTGCATTCACTGACTAACCTGGAAGAGGGAGGGTATGCCAACCACAAC
AATGCCAGCTCCATCAAGATTTTCGGCTACGAGGACAATGAAGATCTGAAGGCTAAAATCATTCAGG
ACCCTGAGTTCATCCGAAACTGGGCAAATGTGGCCCATTCTCTGGGATTTGGATGGTGCGGAGGAAC
CGCAAACCCAAATGTCGGACAGGGCTTCGAGTTTAAGCGCGAAGTGGGGGCTGGAGGCAAAGTCTC
CTACCTGCTGTCTGCACGATATAACCCAAATGACCCCTACGCCTCTGGCTATAGGGCTAAGGATCGCC
TGAGTATGAAAATCTCAAACGTGCGCTTTGTCATCGACAATGATAGTATTAAGCTGGGCACCCCTAA
AGTGAAGAAACTGGCACCACTGAACTCTGCCAGTTTCGATCTGATTAATGAGAGCAAGACAGAATCA
AAGCTGAGCAAAACTTTTAACTACACCACAAGCAAGACCGTGAGCAAAACCGACAATTTCAAGTTTG
GAGAAAAAATCGGCGTGAAGACTTCCTTCAAAGTCGGACTGGAGGCCATTGCTGATTCAAAGGTCG
AGACCAGCTTCGAGTTCAACGCAGAGCAGGGCTGGTCTAACACTAATAGTACTACCGAAACCAAACA
GGAGAGTACAACTTATACCGCCACAGTGTCACCCCAGACCAAGAAGCGGCTGTTCCTGGACGTGCTG
GGATCTCAGATCGATATTCCTTACGAGGGCAAGATCTACATGGAATATGACATTGAGCTGATGGGGT
TCCTGCGATATACTGGAAACGCTCGGGAAGACCACACAGAGGATCGCCCCACTGTGAAGCTGAAATT
TGGGAAGAATGGAATGAGCGCCGAGGAACACCTGAAGGACCTGTACAGCCATAAAAACATCAATGG
CTATTCCGAATGGGACTGGAAGTGGGTGGATGAGAAATTCGGGTACCTGTTTAAGAACTCCTATGAT
GCCCTGACCTCTCGGAAGCTGGGGGGAATCATCAAGGGCAGCTTCACCAACATCAATGGGACAAAG
ATCGTGATTAGAGAGGGCAAAGAAATTCCCCTGCCTGACAAGAAAGGCTCCTCCTTTTCCTCCGGCC
CCTCAGTAGATTCTCTGGACGCAAGACTGCAGAACGAGGGGATCAGGATTGAGAATATCGAAACCC
AGGATGTGCCCGGCTTCCGGCTGAACTCCATTACATACAACGACAAGAAGCTGATCCTGATTAACAA
CATCTAATAAACTTTATTTTTCAATTGCAGAAAATTTCAAGTC

Protein

MGWSCIILFLVATATGVHSLTNLEEGGYANHNNASSIKIFGYEDNEDLKAKIIQDPEFIRNWANVAHSLGF
GWCGGTANPNVGQGFEFKREVGAGGKVSYLLSARYNPNDPYASGYRAKDRLSMKISNVRFVIDNDSIKL
GTPKVKKLAPLNSASFDLINESKTESKLSKTFNYTTSKTVSKTDNFKFGEKIGVKTSFKVGLEAIADSKVETSF
EFNAEQGWSNTNSTTETKQESTTYTATVSPQTKKRLFLDVLGSQIDIPYEGKIYMEYDIELMGFLRYTGNA
REDHTEDRPTVKLKFGKNGMSAEEHLKDLYSHKNINGYSEWDWKWVDEKFGYLFKNSYDALTSRKLGGI
IKGSFTNINGTKIVIREGKEIPLPDKKGSSFSSGPSVDSLDARLQNEGIRIENIETQDVPGFRLNSITYNDKKLI
LINNI

AERO

DNA

TTCCTCAAATCGTCACTTCCGTTTTCCCACGTTACGTCACTGCTAATCTTCCTTTCTCTCTTCAGCCACCA
TGGGATGGTCATGTATTATTCTGTTTCTGGTCGCAACCGCAACCGGGGTCCACTCACAGAAGCTGAA
GATCACCGGCCTGAGCCTGATCATCAGCGGCCTGCTGATGGCCCAGGCCCACGCCGCCGAGCCCGT
GTACCCCGACCAGCTGAGACTGTTCAGCCTGGGCCAGGAGGTGTGCGGCGACAAGTACAGACCCAT
CACCAGAGAGGAGGCCCAGAGCGTGAAGAGCAACATCGTGAACATGATGGGCCAGTGGCAGATCA
GCGGCCTGGCCAACGGCTGGGTGATCATGGGCCCCGGCTACAACGGCGAGATCAAGCCCGGCACCG
CCAGCAACACCTGGTGCTACCCCACCAACCCCGTGACCGGCGAGATCCCCACCCTGAGCGCCCTGGA
CATCCCCGACGGCGACGAGGTGGACGTGCAGTGGAGACTGGTGCACGACAGCGCCAACTTCATCAA
GCCCACCAGCTACCTGGCCCACTACCTGGGCTACGCCTGGGTGGGCGGCAACCACAGCCAGTACGT
GGGCGAGGACATGGACGTGACCAGAGACGGCGACGGCTGGGTGATCAGAGGCAACAACGACGGC
GGCTGCGAGGGCTACAGATGCGGCGAGAAGACCGCCATCAAGGTGAGCAACTTCGCCTACAACCTG
GACCCCGACAGCTTCAAGCACGGCGACGTGACCCAGAGCGACAGACAGCTGGTGAAGACCGTGGTG
GGCTGGGCCATCAACGACAGCGACACCCCCCAGAGCGGCTACGACGTGACCCTGAGATACGACACC
GCCACCAACTGGAGCAAGACCAACACCTACGGCCTGAGCGAGAAGGTGACCACCAAGAACAAGTTC
AAGTGGCCCCTGGTGGGCGAGACCGAGCTGAGCATCGAGATCGCCGCCAACCAGAGCTGGGCCAG
CCAGAACGGCGGCAGCACCACCACCAGCCTGAGCCAGAGCGTGAGACCCACCGTGCCCGCCAGAAG
CAAGATCCCCGTGAAGATCGAGCTGTACAAGGCCGACATCAGCTACCCCTACGAGTTCAAGGCCGAC
GTGAGCTACGACCTGACCCTGAGCGGCTTCCTGAGATGGGGCGGCAACGCCTGGTACACCCACCCC
GACAACAGACCCAACTGGAACCACACCTTCGTGATCGGCCCCTACAAGGACAAGGCCAGCAGCATCA
GATACCAGTGGGACAAGAGATACATCCCCGGCGAGGTGAAGTGGTGGGACTGGAACTGGACCATC
CAGCAGAACGGCCTGAGCACCATGCAGAACAACCTGGCCAGAGTGCTGAGACCCGTGAGAGCCGGC
ATCACCGGCGACTTCAGCGCCGAGAGCCAGTTCGCCGGCAACATCGAGATCGGCGCCCCCGTGCCCC
TGGCCGCCGACAGCGGCGGCGCCAAGGGCCTGTACAAGGGCGGCAGCGTGGACGGCGCCGGCCAG
GGCCTGAGACTGGAGATCCCCCTGGACGCCCAGGAGCTGAGCGGCCTGGGCTTCAGCAACGTGAGC
CTGAGCGTGACCCCCGCCGCCAACCAGCACCACCACCACCACCACTAATAAACATTTTAAGAAAACTA
CAATTCCCAACACATACAAGTTACTC

Protein

MAQAHAAEPVYPDQLRLFSLGQEVCGDKYRPITREEAQSVKSNIVNMMGQWQISGLANGWVIMGPG
YNGEIKPGTASNTWCYPTNPVTGEIPTLSALDIPDGDEVDVQWRLVHDSANFIKPTSYLAHYLGYAWVG
GNHSQYVGEDMDVTRDGDGWVIRGNNDGGCEGYRCGEKTAIKVSNFAYNLDPDSFKHGDVTQSDRQ
LVKTVVGWAINDSDTPQSGYDVTLRYDTATNWSKTNTYGLSEKVTTKNKFKWPLVGETELSIEIAANQS
WASQNGGSTTTSLSQSVRPTVPARSKIPVKIELYKADISYPYEFKADVSYDLTLSGFLRWGGNAWYTHPD
NRPNWNHTFVIGPYKDKASSIRYQWDKRYIPGEVKWWDWNWTIQQNGLSTMQNNLARVLRPVRAGI
TGDFSAESQFAGNIEIGAPVPLAADSGGAKGLYKGGSVDGAGQGLRLEIPLDAQELSGLGFSNVSLSVTPA
ANQHHHHHH

Histidine Tag: CACCACCACCACCACCAC

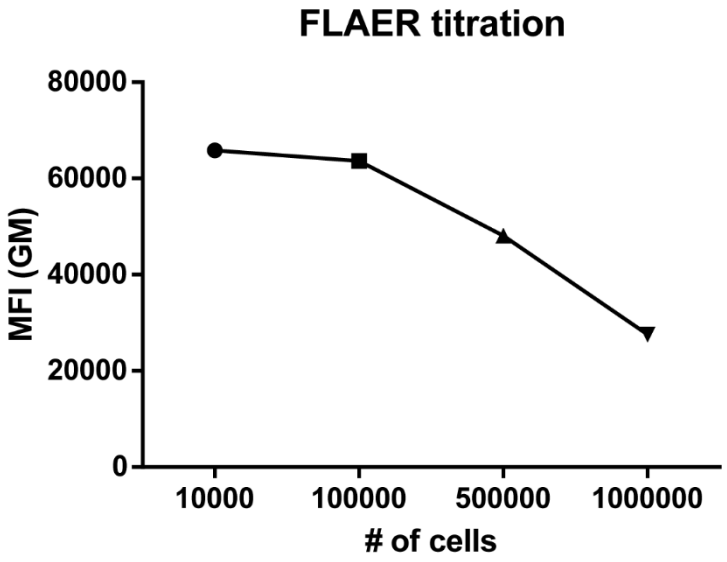
FLAER titration
80000
60000
40000
20000
0
MFI (GM)
10000
100000
500000
1000000
# of cells